THE ROLE OF POWER-TO-X TECHNOLOGIES IN DECENTRALISED MULTI-ENERGY SYSTEMS

A dissertation submitted to
ETH ZURICH

for the degree of
DOCTOR OF SCIENCES

presented by
PORTIA MURRAY
Master of Applied Science (Queen's University)
born 25 August 1990
citizen of Canada

accepted on the recommendation of
Prof. Dr. Jan Carmeliet, examiner
Prof. Dr. Martin Patel, co-examiner
Prof. Dr. Giovanni Sansavini, co-examiner
Dr. Kristina Orehounig, co-examiner

2020

Perfect is the enemy of the good.

Voltaire

ABSTRACT

In order to support energy self-reliance within countries, decrease greenhouse gas emissions, and reduce dependence on a declining fossil fuel supply, renewable energy sources are planned to replace a large percentage of fossil fuel electricity generation by 2050. With the replacement of centralised plants with decentralised solar photovoltaics or wind technologies, the future's energy system may rely on partial shifts from centralised energy generation to distributed energy generation. In order to support an increasing penetration of renewable generation in Switzerland, both short and long-term storage technologies will be required to mitigate the temporal mismatch of fluctuating renewable production and end-user demand.

Power-to-X is one group of storage pathways that are capable of both being installed in decentralised settings and storing energy long-term. Some of the relevant pathways for decentralised cases include Power-to-Hydrogen, Power-to-Methane, Power-to-CHP (combined heat and power), Power-to-Heat, and Power-to-Mobility. In this dissertation, the economic feasibility and emission reduction potential of several different Power-to-X pathways are investigated from 2015 until 2050. In order to test these pathways, this thesis has main three objectives: (1) to develop a multi-objective optimisation model that is capable of investigating Power-to-Gas pathways in multi-energy systems including long-term storage, (2) to incorporate personal transport energy demands and Power-to-Mobility pathways into the optimisation framework, and (3) to assess the uncertainties and sensitivities of these pathways from 2015 until 2050.

The model in this work uses multi-objective optimisation that minimises both total annual cost and total emissions of the system. According to these objectives, the optimisation model selects the capacity of conversion technologies (photovoltaics, fuel cells, electrolysers, methanation, heat pumps, and gas boilers) and storage technologies (batteries, compressed natural gas storage, hydrogen storage, and thermal storage). Reduced order approximations for the part-load efficiencies, ramping limitations, temporal reduction techniques for long-term storage, and export constraints are used to reflect the performance and operational

limitations. This model is tested using several scenarios in two case studies: one rural and one urban. It is found that the rural case study has high renewable potential and uses both batteries and Power-to-Heat (e.g., heat pumps and thermal storage) for short-term storage needs. Long-term Power-to-CHP storage is also used in cases that required deep decarbonisation. For the urban case study, there is not enough renewable potential to meet the energy targets or to significantly utilise storage systems.

After testing these two case studies, the model is then expanded to simulate personal transport demands of the building occupants. The model expansion includes the selection of different vehicle technologies. These include internal combustion engine vehicles with gasoline, internal combustion engine vehicles with natural gas, battery electric vehicles (BEV), plug-in hybrid vehicles, and fuel cell electric vehicles (FCEV).

This model is then applied to a suburban case study. The results show that BEVs are the preferred vehicle technology and that FCEVs are not predicted to be optimal due to their high costs and lower efficiencies. In order to assess the future performance of the system, an uncertainty analysis is performed using a Monte Carlo simulation and Latin Hypercube Sampling. Finally, a sensitivity analysis is performed on the optimisation model using Monte Carlo Filtering. This method specifically looks at the most important parameters that influence the selection of Power-to-CHP, Power-to-Methane, Power-to-Mobility with FCEVs, and at solutions that are able to achieve lower costs while still meeting emissions targets.

In the uncertainty analysis, the most popular pathways are Power-to-Mobility with BEVs and Power-to-Heat. These pathways are used in 100% of the Monte Carlo simulations that met the emissions targets. Batteries and Power-to-CHP are the next most popular storage methods and are used in 84% and 19.2% of Monte Carlo samples respectively. The least popular pathways are Power-to-Methane and Power-to-Mobility with FCEVs, both representing less than 5% of samples. From these results, we can conclude that heat pumps, solar PV, and BEVs are three of the most important technologies for reducing emissions in both our buildings and transport sectors. Long-term storage may also be a valuable asset in certain case studies with sufficient renewable deployment, particularly if deep decarbonisation targets are required.

ZUSAMMENFASSUNG

Um die Eigenständigkeit der Energieversorgung innerhalb der Länder zu unterstützen, die Treibhausgasemissionen zu senken und die Abhängigkeit von einer abnehmenden Versorgung mit fossilen Brennstoffen zu verringern, sollen erneuerbare Energiequellen bis 2050 einen großen Teil der Stromerzeugung aus fossilen Brennstoffen ersetzen. Mit dem Ablösen von zentralen Anlagen durch dezentrale Solar-Photovoltaik oder Windtechnologien kann sich das Energiesystem der Zukunft auf eine teilweise Verlagerung von der zentralen Energieerzeugung zur dezentralen Energieerzeugung stützen. Um eine zunehmende Verbreitung der erneuerbaren Energieerzeugung in der Schweiz zu unterstützen, werden sowohl kurz- als auch langfristige Speichertechnologien benötigt, um das zeitliche Ungleichgewicht zwischen schwankender erneuerbarer Produktion und dem Endverbraucherbedarf zu mindern.

Power-to-X ist eine Gruppe von Speicherpfaden, die sowohl dezentral installiert als auch langfristig Energie speichern können. Einige der relevanten Wege für dezentrale Fälle sind Power-to-Hydrogen, Power-to-Methane, Power-to-CHP (Kraft-Wärme-Kopplung), Power-to-Heat und Power-to-Mobility. In dieser Arbeit werden die wirtschaftliche Machbarkeit und das Emissionsreduktionspotenzial mehrerer verschiedener Power-to-X-Pfade von 2015 bis 2050 untersucht. Um diese Wege zu testen, hat diese Arbeit drei Hauptziele: (1) ein mehrkriterielles Optimierungsmodell zu entwickeln, das in der Lage ist, Power-to-Gas-Pfade in Multi-Energiesystemen einschließlich Langzeitspeicherung zu untersuchen, (2) den persönlichen Energiebedarf und Power-to-Mobility-Pfade in den Optimierungsrahmen zu integrieren und (3) die Unsicherheiten und Sensitivitäten dieser Pfade von 2015 bis 2050 zu bewerten.

Das Modell in dieser Arbeit verwendet eine mehrkriterielle Optimierung, die sowohl die jährlichen Gesamtkosten als auch die Gesamtemissionen des Systems minimiert. Gemäß diesen Zielen wählt das Optimierungsmodell die Kapazität der Umwandlungstechnologien (Photovoltaik, Brennstoffzellen, Elektrolyseure, Methanierung, Wärmepumpen und Gaskessel) und der Speichertechnologien (Batterien, komprimierte Erdgasspeicher, Wasserstoffspeicher und thermische Speicher)

aus. Lineare Annäherungen für die Teillastwirkungsgrade, Anlaufbeschränkungen, zeitliche Reduzierungstechniken für die Langzeitlagerung und Exportbeschränkungen werden verwendet, um die Leistung und die Betriebsgrenzen widerzuspiegeln. Dieses Modell wird anhand mehrerer Szenarien in zwei Fallstudien getestet: einer ländlichen und einer städtischen. Es wird festgestellt, dass die ländliche Fallstudie ein hohes Potenzial an erneuerbaren Energien hat und sowohl Batterien als auch Power-to-Heat (z.B. Wärmepumpen und thermische Speicher) für den kurzfristigen Speicherbedarf verwendet. Langfristige Power-to-CHP-Speicher werden auch dann eingesetzt, wenn eine weitreichende Entkarbonisierung erforderlich ist. Für die städtische Fallstudie gibt es nicht ausreichend erneuerbares Potenzial, um die Energieziele zu erreichen oder Speichersysteme signifikant zu nutzen. Nach dem Testen dieser beiden Fallstudien wird das Modell erweitert, um die persönlichen Transportanforderungen der Gebäudenutzer zu simulieren. Die Modellerweiterung umfasst die Auswahl verschiedener Fahrzeugtechnologien. Dazu gehören Fahrzeuge mit Verbrennungsmotor mit Benzin, Fahrzeuge mit Verbrennungsmotor mit Erdgas, Elektrofahrzeuge mit Batterie, Plug-in-Hybridfahrzeuge und Elektrofahrzeuge mit Brennstoffzelle.

Dieses Modell wird dann auf eine vorstädtische Fallstudie angewendet. Die Ergebnisse zeigen, dass batteriebetriebene Elektrofahrzeuge die bevorzugte Fahrzeugtechnologie sind und dass Brennstoffzellenfahrzeuge aufgrund ihrer hohen Kosten und niedrigeren Wirkungsgrade nicht als optimal eingestuft werden. Um die zukünftige Leistungsfähigkeit des Systems zu beurteilen, wird eine Unsicherheitsanalyse mit Hilfe einer Monte Carlo Simulation und Latin Hypercube Sampling Methode durchgeführt. Abschließend wird eine Sensitivitätsanalyse des Optimierungsmodells mit Monte Carlo Filtering durchgeführt. Diese Methode untersucht insbesondere die wichtigsten Parameter, die die Auswahl von Power-to-CHP, Power-to-Methane, Power-to-Mobility mit Brennstoffzellenfahrzeugen beeinflussen, und Lösungen, die in der Lage sind, niedrigere Kosten bei gleichzeitiger Einhaltung der Emissionsziele zu erreichen.

In der Unsicherheitsanalyse sind die beliebtesten Wege Power-to-Mobility mit Batteriefahrzeugen und Power-to-Heat. Diese Wege werden in 100% der Monte Carlo Simulationen verwendet, die die Emissionsziele erfüllen. Batterien und Power-to-CHP sind die nächstbeliebtesten Speichermethoden und werden in 84% bzw. 19,2% der Monte

Carlo Stichproben verwendet. Die am wenigsten verbreiteten Wege sind Power-to-Methane und Power-to-Mobility mit Brennstoffzellenfahrzeugen, die beide weniger als 5% der Fälle ausmachen. Aus diesen Ergebnissen können wir schließen, dass Wärmepumpen, PV- und Batterie-Elektrofahrzeuge drei der wichtigsten Technologien zur Emissionsreduzierung sowohl in unseren Gebäuden als auch im Verkehrssektor sind. Die Langzeitspeicherung kann auch in bestimmten Fallstudien mit ausreichendem Einsatz erneuerbarer Energien ein wertvoller Vorteil sein, insbesondere wenn weitgehende Dekarbonisierungsziele erforderlich sind.

ACKNOWLEDGMENTS

direction of this thesis.

I would also like to give a special thanks to Prof. Dr. Adam Rysanek, my supervisor at the Singapore ETH Centre. Your support over my year and two months in Singapore truly motivated me towards doing my PhD and I am certain that I would not be finishing if it were not for you. Your moral support and belief in me is always something I will appreciate.

I also give a heartfelt thanks to Prof. Dr. Stephen Harrison at Queen's University. You were my biggest supporter and motivator during my time at Queen's and I would never have gotten involved with my position in Singapore if it were not for your recommendation. I will always fondly remember the times I spent working in your lab and the discussions we had for the solar decathlon project and then my Master Thesis. You were the one who inspired me to firstly get involved in solar energy and buildings, as well as academia.

Next, I must express my sincerest gratitude towards my colleagues in the Urban Energy Systems Laboratory at Empa. Thank you to Dr. Georgios Mavromatidis, Dr. Julien Marquant, Dr. Marc Hoffmann, Dr. Christoph Waibel, Dr. Somil Miglani, and Dr. Boran Morvaj for teaching me so much about optimisation throughout my PhD. The lessons I learned from you all in this regard were invaluable. I was truly lucky to have done my PhD at a time when I could learn the ropes from all of you. It doesn't hurt that you are all fantastic friends and some of my biggest supporters too. Thank you also very much to Danhong Wang, Cristina Dominguez Hernandez, Emmanouil Thrampoulidis, and Felix Bünning for the discussions and the support, especially towards the end of my PhD.

Thank you to my parents and my brother for giving me constant moral support throughout this process. Lastly, I must express my sincerest love and thanks to my partner and constant supporter, Arne Meeuw.

Portia Murray
Zürich, October 2019

NOTATION

SUBSCRIPTS

SUBSCRIPT	DESCRIPTION
a	Segment in a Piecewise approximation
b	Building
c	Cars
d	Driving cycle
EE	Embodied Emissions
$export$	Energy exported from an energy system
MES	Multi-energy system
f	Energy carrier
h	Reduced hourly time step
i	Full horizon time step
$import$	Energy imported to an energy system
inv	Investment costs
n	Number of Pareto optimal solutions
OMF	Fixed operating and maintenance costs
OMV	Variable operating and maintenance costs
ref	Reference
s	Storage technology
t	Conversion technology
v	Vehicle technology

SUPERSCRIPTS

SUPERSCRIPT	DESCRIPTION
$building$	Variable specific to the building level
cap	Technology capacity installed
ch	Storage charging
$comp$	Compressor
dch	Storage discharging
$decay$	Hourly storage losses
$demand$	Building demand (kWh)
DI	Direct injection
$district$	Variable at the district level
$export$	Energy exported from a district to the centralised grid
FIT	Feed-in tariff
$fixed$	Fixed capital cost or embodied emission
$home$	Charging at home
$import$	Energy imported into a district
in	The consumption energy of a conversion technology
inv	Investment cost
$linear$	Linear capital cost or embodied emission per unit
max	The constrained upper limit of a decision variable
min	The constrained lower limit of a decision variable
MP	Electric market price
on/off	Binary variable to indicate a technology's on/off state
out	The production energy of a conversion technology
$public$	Public charging station
$regen$	Regeneration
$retail$	Electric retail price
$sell$	Non-renewable selling price
$sellR$	Renewable selling price
SOC	State of charge of the storage
$solar$	Solar radiation
$surplus$	Electricity surplus binary
$trac$	Traction
$transit$	Binary to indicate if a vehicle is in transit
$vcap$	Vehicle storage energy capacity
vch	Vehicle charging
$vdch$	Vehicle discharging

vdemand	Vehicle demand (km)
vdriving	Power discharged to meet driving demand
vehicles	Variable specific to vehicles
WLTP	Worldwide lightweight vehicle test procedure

MATHEMATICAL NOTATION

SYMBOL	MEANING
$A_{v,d}$	1st parametrisation constant for traction vehicle energy
$A'_{v,d}$	1st parametrisation constant for regenerative vehicle energy
$A_{v,f}$	Frontal area of a vehicle
A	Area in m2 (either rooftop or floor area)
a	Probability distribution function lower bound
$B_{v,d}$	2nd parametrisation constant for traction vehicle energy
$B'_{v,d}$	2nd parametrisation constant for regenerative vehicle energy
b	Probability distribution function upper bound
$C_{v,d}$	3rd parametrisation constant for traction vehicle energy
$C'_{v,d}$	3rd parametrisation constant for regenerative vehicle energy
c_{ar}	Aerodynamic resistance
c_d	Drag area (vehicle)
c_p	Specific heat capacity at constant pressure
c_r	Rolling resistance
c_v	Specific heat capacity at constant volume
$Cost_{carriers}$	Net annual cost of purchased and sold energy carriers
$Cost_{inv}$	Net annual investment or capital cost
$Cost_{OMF}$	Net annual fixed operations and maintenance costs
$Cost_{OMV}$	Net annual variable operations and maintenance costs
$Cost_{total}$	Net annual costs for the energy system
$CO2_{total}$	Net annual CO_2 emissions
$CO2_{EE}$	Net annual CO_2 embodied emissions
$CO2_{carriers}$	Net annual CO_2 emissions from purchased carriers
CRF	Capital recovery factor
$d_{n,\bar{n}}$	Distance between behavioural and non-behavioural CDFs
$Days$	Typical/representative days
E	Energy stored
EC	Energy consumption of vehicles
f	Volume fraction
$F_{x_i|y_b}$	Cumulative distribution function for the behavioural subset
$F_{x_i|y_{\bar{b}}}$	Cumulative distribution function for the non-behavioural subset
H	Pressure head of water
$LCOE$	Levelised cost of energy

$LCO2$	Levelised CO_2 emissions
$Lifetime$	Assumed lifetime of the technology
M	Arbitrary large number (Big-M constraint)
m_{es}	Mass of vehicle energy storage system
m_{gl}	Mass of vehicle glider
m_{pt}	Mass of powertrain
$\dot{m}$	Mass flow rate
OMF	Fixed operation and maintenance cost
OMV	Variable operation and maintenance cost
P-value	Measure of rejection of null hypothesis in K-S test
P	Power
PL	Part-load fraction
Pr	Pressure
$Price$	Price per unit
Q	Volumetric flow rate
R	Ideal gas constant
r	Discount rate
SD	Shut-down binary
SU	Start-up binary
T	Temperature
u	Wind speed
W_{ideal}	Ideal compression energy
Y_b	Behavioural subset (Monte Carlo Filtering)
$Y_{\bar{b}}$	Non-behavioural subset (Monte Carlo Filtering)
z	Height above ground
$\overline{Z}$	Compressibility factor
α	Beta distribution shape parameter
α_{wind}	Coefficient of the wind speed increase with height
β	Beta distribution shape parameter
γ	Specific heat ratio of a gas
ΔT	Timestep
δ	binary variable
η	Efficiency
$\eta_{isentropic}$	Isentropic efficiency
η_{mech}	Mechanical efficiency
κ	Fraction of regenerative vs. friction in braking
μ	Mean
ρ	Density
σ	Standard deviation

Φ	Cumulative distribution function value
χ	Factor for additional support for powertrain

ACRONYMS

AFV	Alternative fuel vehicles
BAU	Business as usual
BEV	Battery Electric Vehicle
BTES	Borehole Thermal Energy Storage
CAES	Compressed Air Energy Storage
CD	Charge Depleting
CDF	Cumulative distribution function
CHF	Swiss Francs
CHP	Combined Heat and Power
CM	Conventional Markets
CMR	Catalytic Methane Reactor
CNG	Compressed Natural Gas
CNGS	Compressed Natural Gas Storage
COP	Coefficient of Performance
CRF	Capital Recovery Factor
CS	Charge Sustaining
DES	Decentralised Energy Systems
DHW	Domestic Hot Water
DI	Direct Injection
EU	European Union
EV	Electric Vehicle

FCEV	Fuel Cell Electric Vehicle
FCHEV	Fuel Cell Hybrid Electric Vehicle
FIT	Feed-in Tariff
GIS	Geographical Information System
GSD	Global Sustainable Development
GWR	Buildings and apartment registry
ICE	Internal Combustion Engine
ICEV	Internal Combustion Engine Vehicle
ICEV-g	Internal combustion engine gasoline vehicle
ICEV-cng	Internal combustion engine compressed natural gas vehicle
IPCC	Intergovernmental Panel on Climate Change
HEV	Hybrid Electric Vehicle
HP	Heat pump
H2S	Hydrogen storage
LCA	Life cycle assessment
LCOE	Levelised Cost of Energy
LCO2	Levelised CO_2 Emissions
LiDAR	Light Detection and Ranging
LHS	Latin Hypercube Sampling
LHV	Lower Heating Value
MC	Monte carlo
MCF	Monte Carlo Filtering
MES	Multi-Energy Systems
MFH	Multi-family house

MGT	Micro-Gas Turbine
MILP	Mixed Integer Linear Programming
NEP	New energy policy
NG	Natural gas
OMF	Fixed Operation and Maintenance costs
OMV	Variable Operation and Maintenance costs
PDF	Probability density function
PEM	Polymer Electrolyte Membrane
PEMFC	Polymer Electrolyte Membrane Fuel Cell
PEME	Polymer Electrolyte Membrane Electrolyser
PHEV	Plug-in Hybrid Electric Vehicle
pkm	Passenger kilometre
P2CHP	Power-to-CHP
P2G	Power-to-Gas
P2H	Power-to-Hydrogen
P2M	Power-to-Methane
P2L	Power-to-Liquid
P2P	Power-to-Power
P2X	Power-to-X
PV	Photovoltaics
PWA	Piecewise Affine
RES	Renewable Energy Sources
RSD	Regional Sustainable Development
SA	Sensitivity Analysis

SD   Shut-down

SFH   Single-family house

SIA   Swiss Society of Engineers and Architects

SNG   Synthetic Natural Gas

SOFC   Solid-Oxide Fuel Cell

SRES   Special Report on Emissions Scenarios

SU   Start-up

TES   Thermal Energy Storage

UA   Uncertainty Analysis

vkm   Vehicle kilometre

V2B   Vehicle-to-Building

V2G   Vehicle-to-Grid

WLTP   Worldwide Harmonised Light Vehicle Test Procedure

CONTENTS

1

INTRODUCTION

1.1 BACKGROUND AND CONTEXT

For countries worldwide to meet their emission reduction targets, the share of renewable energy sources in the electricity, heating, and transportation sectors must increase. Most countries have promised to aggressively cut fossil fuel based energy consumption and replace it with renewable energy. Globally, the energy consumption sectors with the highest emissions are industry (37%), followed by buildings (27%), and transport (25%) (International Energy Agency 2018a). The total energy consumption in these sectors is also predicted to increase dramatically due to increases in population, globalisation, consumerism, and industrialisation of developing countries. At the writing of this thesis in the summer of 2019, it is clear that the combustion of fossil fuels in our atmosphere is having detrimental effects on Earth's natural ecosystems that will be long-lasting and devastating to the biodiversity that is unique to this planet. To prevent the worst effects of climate change, the CO_2 intensity in these sectors must be reduced dramatically as soon as possible to limit these emissions, thus many countries are implementing plans for decarbonisation. To first investigate solutions to the current crisis, a brief overlook of the historical context that lead to this environmental crisis is overviewed.

1.2 HISTORICAL USE OF DIFFERENT ENERGY CARRIERS

The historical sources for our global energy generation has changed vastly in the past 150 years. Until the mid-nineteenth century, the vast majority of the energy for society and the economy was generated from wood and other traditional biomass products (Allen 2009). This can be seen in Fig. 1.1. The first energy transition came with the coming of the industrial revolution from 1860 until 1950.

In this Figure, it is clear that biomass dominated as the primary
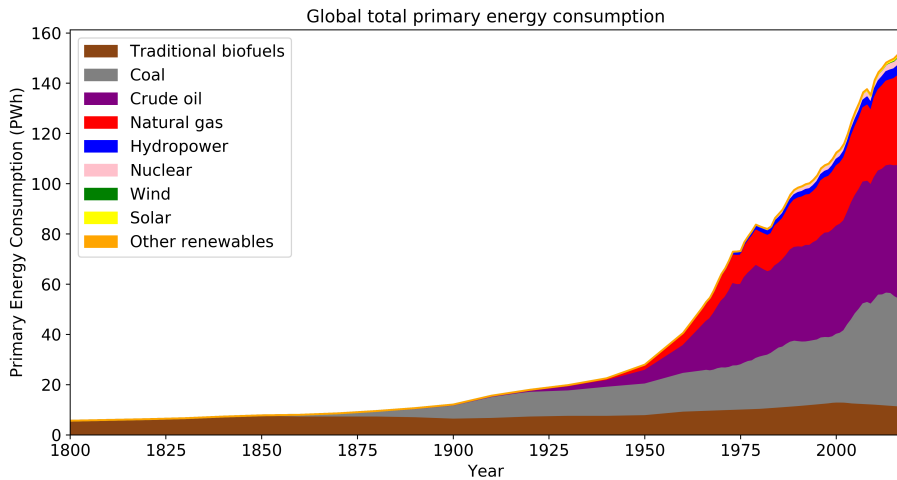
Figure 1.1.: Global primary energy consumption by energy carrier from 1800-2017 (*BP Statistical Review of World Energy* 2019).

source of energy until around 1880, when coal begins to be utilised for industry, heating, and electricity generation. Coal replaces biomass as the major energy carrier between 1890 and 1925. This represents the use of coal driving the second industrial revolution. Towards the end of this period, oil began being refined and used for heating and vehicles. Natural gas was also simultaneously being extracted during this time as it is a byproduct of oil extraction and can be used for heating and lighting. It is also around 1950 that the total energy demand starts rapidly increasing, which coincided with the post-war industrial era. Around 1970, oil replaced gasoline as the major energy source which is increasing rapidly due to the massive increase in energy demand for transportation. Hydropower and nuclear both play a major role in terms of electricity generation, but when compared to total energy consumption (which includes transportation, heating, agriculture, industry, and other relevant energy carriers) we see that they actually contribute to a small fraction of this total primary energy consumption. Our energy demands today remain massively dependant on fossil fuels from oil, coal, and natural gas.

ELECTRICITY

The first electricity grids were established in the 1880s and were supported from coal thermal plants (Borbely et al. 2019). At the beginning

of the 20th century, many small hydro stations were constructed and quickly expanded by the 1950s (O'Connor et al. 2014). After the 1957s, nuclear power was also introduced as a major generator of electricity. Natural gas, which was originally only a byproduct of petroleum production, began to be used in electricity production plants. In the 21st century, natural gas has recently begun to replace coal electricity generation due to two reasons. Firstly, because natural gas became very cheap after the fracking boom after 2010, and secondly, because natural gas plants can respond extremely quickly to changes in load and thus are excellent at providing grid services, such as frequency regulation and spinning reserve. These coal and natural gas plants still comprise approximately 46% of all European electricity production (International Energy Agency 2018a). Despite the tremendous uptake in solar and wind installations in the 21st century, these renewable sources both comprise only about 16% of total European electricity production. Thermal power plants are very difficult to get rid of because they are the most flexible utilities available to grid providers and can be turned on and off quickly to meet peak demands, which makes them very difficult to replace entirely.

HEATING

At the beginning of the 20th century, the heating energy carrier of choice switched from wood to coal (O'Connor et al. 2014). By the mid 1920s, oil burners increased in popularity and replaced coal as the major heating fuel. This was then followed by an uptick in installed natural gas systems for heating, but use was limited to buildings that were connected to gas grids (Nagengast 2001). This switch from coal to much cleaner burning fuels was an advantage for air quality, both in homes and in cities. Cities in the industrial revolution were infamous for their poor air quality due to the burning of coal in cities for industry and heating, and in this modern day, there are still 4.3 million premature deaths per year attributed to indoor air pollutions from using solid fuels for heating or cooking in developing countries (World Health Organisation 2014). Over 75% of energy used for heating in Europe today still comes from fossil fuels (EU Commission 2015). District heating systems supplied by waste heat from thermal power plants are also increasing, however the penetration of heat pumps and biomass based systems is still less than 19% of all heating energy (EU Commission

2015).

TRANSPORT

Personal transport is a sector that was dominated by animal labour (O'Connor et al. 2014) until the mass production and commercialisation of the Internal Combustion Engine Vehicle (ICEV) by Henry Ford in 1913. Once the ICEV was inexpensive enough for the masses to own and the road and gasoline fuelling infrastructure was in place, they became common place in nearly all homes of all income classes by the 21st century. Although the automobile has changed much in design and efficiency over the years, gasoline or diesel fuelled vehicles still represent over 99% of all vehicles globally (Gorner et al. 2019). The electrification of vehicles is underway, but has not been nearly as successful as the electrification of trains or, to a lesser extent, busses.

SUMMARY

From this history, we can observe that the industrial revolutions brought about an energy transition towards fossil fuels in the electricity, the heating, and in the personal transport sectors. With the early low cost, high energy density, and high abundance of these fuels, our demand of these fuels expanded exponentially, thus allowing our economies to expand and flourish. Now, with the awareness of a diminishing fossil fuel supply, as well as the consequences of climate change that have resulted from the exploiting these fuels, we are now forced to seek new technologies and new renewable and sustainable energy carriers to supply these demands. Not only do we have to pursue new technologies, we must also reduce our energy consumption. This can be done by either increasing our energy efficiency or by reducing our consumption needs. Each of these steps must be pursued if we wish to reduce our dependancy on fossil fuels.

1.3 ENERGY TRANSITION IN THE 21ST CENTURY

According to the Swiss Energy Strategy 2050 (Prognos AG 2013), Switzerland has proposed to reduce both its dependence on fossil fuels, eliminate nuclear power by 2035, and replace this generation with primarily hydro-power, photovoltaics, wind energy, geothermal energy,

biomass, and biogas by 2050. Currently, 35% of electricity generation in Switzerland is currently provided by four ageing nuclear stations that are predicted to be shut-down between 2020 and 2035. The remaining share of electricity in Switzerland is composed of 57% hydro, 5% biofuel and waste, and 2% solar and wind, and 1% natural gas (International Energy Agency 2018a).

Hydro, biofuels, and waste have already been extensively exploited and do not have large potentials for further expansion. Photovoltaics (PV), and to a lesser extent wind, have the largest potential for expansion. According to the work of Assouline et al. (2017), the potential for generation on decentralised rooftop photovoltaic systems alone could be as high as 17.87 TWh in 2015, with the total electricity consumption being 57 TWh (Zünd 2019), and this could be further expanded with the additional buildings that will be erected between 2015 and 2050. This transition will also rely on partial conversions from centralised power plants to decentralised renewable sources and from centralised generation to a decentralised structure of smart grids or microgrids that are based around communities of prosumers. This shift from an energy system based on centralised production to a system based on decentralised production is demonstrated in Fig. 1.2.

The current representation of the grid in Switzerland includes many large generating stations, such as nuclear, hydro plants, and waste incineration plants. These large centralised plants use vast electricity supply networks, complete with high, medium, and low voltage lines, to deliver electricity from the centralised station to the consumer over great distances. Electricity in former centralised networks flowed in one direction: from the centralised production plant to the consumer. The nuclear generation plants currently represent 35% of this energy and would be replaced with solar production, wind production, and and other distributed energy resources which are installed within the communities that were formally only energy consumers. These grids must also support an increasing penetration of intermittent renewable generation that fluctuates with variability in weather conditions, thus communities of prosumers must be appropriately designed to manage their own energy production and consumption to minimise impact on the centralised grid and increase their own self-sufficiency. To do this, the design of many of these systems will need to change to provide flexibility and to meet loads due to electrification.

The adaptation of vehicle charging within Multi-Energy Systems
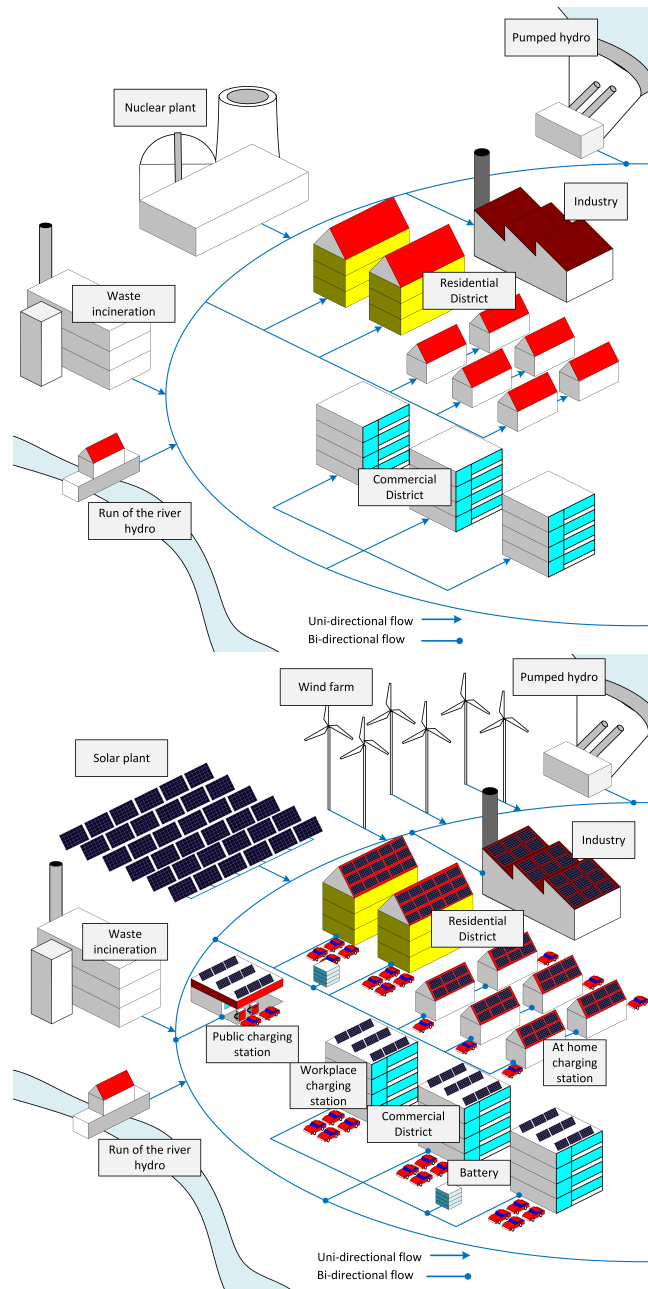
Figure 1.2.: (Top): A representation of centralised generation in Switzerland, (Bottom): A representation of what decentralised generation system in Switzerland might look like.

(MES) is also shown in Fig. 1.2 since a shift to Alternative fuel vehicles (AFV) for a large portion of the current vehicle stock would represent a significant amount of energy that now must be sourced from renewable energy. In Switzerland, although nearly 28% of the total end use energy demand in 2015 came from residential building usage, another 26% of this energy came from road based passenger transportation (Raubel et al. 2017), thus these vehicle charging loads would be significant and would have to be factored into the future energy system design.

1.4 DECENTRALISED MULTI-ENERGY SYSTEMS

Buildings in Switzerland (e.g. residential, commercial, and industrial) still represent approximately 25% percent of the total emissions and approximately 40% of the total energy consumption in the country. Building systems have a large potential for reducing emissions, particularly since the heating systems of many buildings are still reliant on fossil fuel boilers. In Switzerland, currently over 39% of the buildings use oil heating and another 21% of the buildings use natural gas heating (Bundesamt für Statistik 2017). The percentage of buildings using heat pumps is growing, however adoption rates are low as they typically require a building envelope retrofit and have higher associated installation costs than boilers.

In addition, rooftop PV systems also have the potential to produce a significant portion of a building's energy needs, thus strongly reducing dependency on the electricity grid and thus on centralised generation. These rooftop PV systems can also be combined with conversion and storage technologies to exploit synergies and increase overall system efficiency. This is more effective when done in groups of buildings, rather than individual buildings, due to different buildings' loads flattening out demand curves and lowering overall costs.

To reduce dependence on fossil fuels for energy demands within urban areas, modern communities may install decentralised systems of renewable energy to provide households energy demands with conversion technologies powered by renewable energy. Typically used conversion technologies today include biomass boilers, natural gas boilers, oil boilers, and heat pumps. Additionally, novel technologies such as micro-gas turbines, electrolyers, and fuel cells. These devices bear the potential to efficiently convert energy between electricity, heating,

hydrogen, and natural gas, which can lead to better technical, economic, or environmental performance than if these grids operate independently of each other (Mancarella 2014).

To design the best system for the energy needs of a community, grids can be designed to interact with each other and can rely on multiple energy carriers, resulting in the integrated design of MES. As described by Mancarella (2014), "*MES are systems whereby electricity, heat, cooling, fuels, transport, and so on interact with each other at various levels*". Integrated energy carriers also allow distributed energy resources such as PV, small-hydro, or wind production to extend beyond electrical demands to heating or mobility demands, thus resulting in a higher local energy self-sufficiency factor and lower per capita emissions.

In a traditional energy system context, building electricity and heating demands are the main focus, however in future energy systems vehicle charging may also become an important building energy load. CO_2 emissions in both of these sectors are continually rising due to the increasing population, number of buildings, and increasing mobility, thus it is critical to implement strong decarbonisation initiatives for these sectors as soon as possible and to design energy systems that are able to support all local demands with as much renewable energy as possible.

The utilisation of renewables in MES can be further increased with the use of storage systems for multiple energy carriers. Although there are many different storage systems available, not all are suited for decentralised cases. Decentralised energy systems typically require smaller capacity storage systems compared to centralised applications for large grid-scale renewable installations, but still require storage to manage the mismatch in local supply and demand and the duration and energy carrier of the storage are typically dependant on the local demand requirements. If the full potential of distributed energy resources in communities is realised, distributed storage could represent a significant portion of the storage capacity within the country.

1.5   LONG-TERM STORAGE

To support the renewable energy transition within Switzerland and world-wide, we must face the issues associated with a growing penetration of intermittent renewable technology. With this percentage of renewables growing, we often see surpluses of renewable energy corre-

sponding with low or sometimes negative electricity prices in the spot market. Currently, overproduction of PV or wind energy is managed with curtailment. This is the most cost effective method of surplus management when infrequently used, but this use of curtailment is likely to increase significantly once additional renewable capacity is installed, since even more energy will be curtailed at times of peak renewable output, resulting in lower capacity factors for renewable energy and an increase in the Levelised Cost of Energy (LCOE). Storage can be used to prevent this curtailment, thus increasing the capacity factor for renewables once again. In principle, storage sounds like a simple solution for this problem, but in application, storage systems can be expensive to install and operate and inefficient if designed improperly or for the wrong application.

Batteries are the most common storage technology currently utilised. Batteries show great potential for storage capacity on short-time scales, due to their high efficiency and fast reaction times, but they are rarely used for storage durations longer than a day. Unfortunately, there is not only a daytime overproduction of renewable energy, but PV also produces much more energy in summer than in winter. In countries where heating is the dominant energy demand in buildings, this results in not only a daytime to night time incongruity but also a seasonal one. Both of these production and demand offsets are demonstrated in Fig. 1.3.

In this Figure, the plot on the left shows a time period of two days and the daytime demands, typically in the morning and late evening, exceeding the local energy production. The renewable production is at its maximum in the middle of the day when solar radiation is at its peak.

The annual plot on the right shows that demand is at is peak in the winter when heating is at its peak. Renewable production is simultaneously at a minimum due to low river flow rates and low solar radiation. In summer, the only heat requirements are Domestic Hot Water (DHW) demands, but both hydro and PV production are at a maximum. Since PV is typically the only distributed energy resource available for urban or suburban communities, this seasonal surplus and deficit are typical for most communities in heating dominated climates. To shift the energy from renewable surpluses to later demand, storage is required. The duration for the shift is directly correlated with the size of storage considered, thus different types of storage are
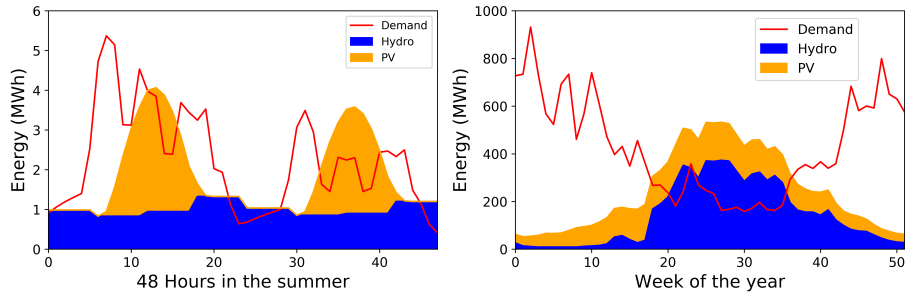
Figure 1.3.: Diurnal (Left) vs. seasonal (Right) storage offsets between supply and demand for 300 buildings in a small village in a mountainous area of Switzerland (Zernez). Demand here includes both heating and electricity demand. The hydro production here is run-of-the-river thus it also decreases due to the flow rate of the river in winter. This case study will be further discussed in Section 1.7.2.1.

suited for different storage durations. This is demonstrated in Fig. 1.4. Please note that no thermal storages are included in this Figure. It is designed to compare storages with reference to the electrical energy carrier. In this Figure, it is seen that short duration electricity storages and capacities include flywheels and batteries. Batteries, with the exception of redox flow batteries, are an example of a storage technology where both power and total stored energy are coupled together. Storage technologies that are designed for longer durations will be required to support a high energy storage capacity and a smaller power capacity. Such technologies require large energy storage reservoirs. The storages can be further compared by their round-trip efficiencies, as shown in Table 1.1. In this Table, short-term duration technologies, such as flywheels, lead-acid batteries, sodium-sulphur batteries, Li-ion batteries, and short-term thermal storage tanks are all highlighted by their discharge times from a few minutes to a few days at maximum, and relatively high round-trip efficiencies. Out of these technologies, Li-ion batteries are the best performing for electrical energy storage, and short-term thermal storage is also effective for heat loads. For long-term storage, the round-trip efficiencies are significantly lower, but can be used over longer periods of time.

There are currently several front-runner categories for long-term energy storage that are emerging as possible long-term storage solu-
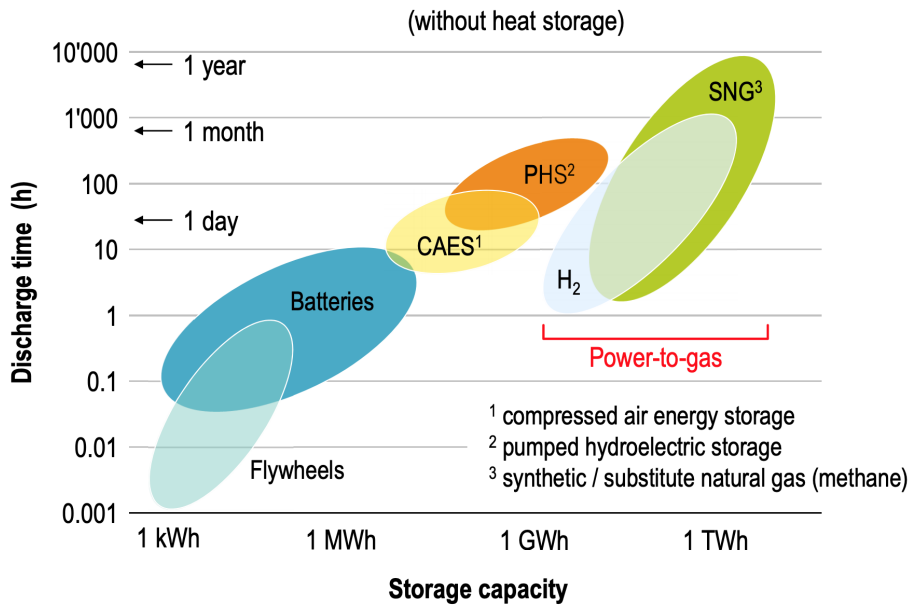
Figure 1.4.: A comparison of storage systems according to their typical capacity and duration. This Figure is adapted from Sterner et al. (2014).

Table 1.1.: Description of different storage technologies, their typical round trip efficiency ranges, power capacities, storage durations, and the scale of storage.

Storage	Efficiency	Capacity Rating (MW)	Storage Duration	Scale
Flywheel	85-95%	0.2-20	Seconds - Minutes	Centralised/ Decentralised
Short-term thermal	94-98%	0.01-200	Minutes - Days	Centralised (District Heating)/ Decentralised
Lead-acid battery	70-80%	0.05-40	Minutes - Days	Centralised/ Decentralised
Sodium-sulphur battery	75-85%	0.05-35	Minutes - Days	Centralised/ Decentralised
Li-ion battery	80-90%	0.1-50	Minutes - Days	Centralised/ Decentralised
Vanadium redox battery	65-85%	0.2-10	Hours - Months	Centralised/ Decentralised
Compressed air	70-75%	50-300	Hours - Months	Centralised
Pumped hydro	70-85%	1-5,000	Hours - Months	Centralised
Borehole thermal	36-41%	1-100	Hours - Months	Centralised (District heating)/Decentralised
Power-to-Gas	30-75%	0.01-1,000	Minutes - Months	Centralised/ Decentralised
Power-to-Liquid	10-50%	10-1,000	Days - Months	Centralised/ Decentralised

tions: Compressed Air Energy Storage (CAES), pumped hydro storage, Borehole Thermal Energy Storage (BTES), Vanadium redox batteries, and Power-to-Gas (P2G) storages. Out of these options, only pumped hydro is currently widely used. CAES and pumped hydro both have limitations due to the availability of geographically applicable sites. Pumped hydro storage requires two large water reservoirs and a height differential of typically a hundred metres between them. These are often built in mountainous regions or valleys and sometimes in retired mining sites. This type of storage typically requires large amounts of land to be flooded, and thus is sometimes controversial due to the disruption of ecosystems and destruction of protected land. It is also only well suited for centralised grid services as its economics only make sense for very large scale applications.

CAES currently requires an underground reservoir (for constant volume storage) or underwater tank (for constant pressure storage) at a depth of hundreds of metres to store compressed air. For constant volume storage, geographical formations such as mined caverns, pressure vessels, or aquifers are required. Due to the scale of these sites, it is also not suited for decentralised storage.

Borehole thermal energy storage, in which solar thermal energy collected in summer is stored in underground boreholes for later winter heating demand, has been used successfully in several sites in Canada, Germany, and Scandinavian countries (Gao et al. 2015), however it can only be used for the heating energy carrier and often has large time dependant losses due to heat losses to the surroundings. Such installations are often done in suburban or rural communities in locations with large enough areas to supply the number of boreholes required, which can be as many as a few hundred to several thousand. Boreholes are typically required to be spaced a minimum distance of 10 meters apart from each other, thus this type of installation requires a significant amount of land area, which is not usually feasible for urban cases.

Vanadium redox batteries are a type of flow battery. This type of battery uses tanks of positive and negative electrolytes which can be pumped to the electrodes of the battery cells to charge or discharge the battery. Storage of the electrolytes in tanks allows this type of battery to decouple power from stored energy, thus making it suitable for larger energy storage capacities and longer storage durations. Its round-trip efficiency is also quite good in comparison to the other long-term storage types suited for decentralised cases. The large disadvantage of flow

batteries is the low energy storage density, which can be highlighted in
Fig. 1.5.

In this Figure, it is shown that there is a large difference in the vol-
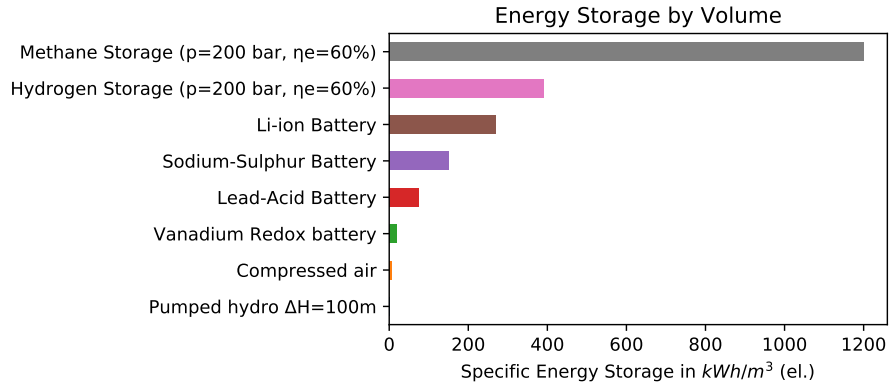
Figure 1.5.: Comparison of the volumetric energy density of different
storage types.

ume required for energy storage depending on the technology. Pumped
hydro and compressed air both have very low energy densities, thus
they require large geographical reservoirs for installation and are only
used in centralised contexts. Vanadium redox batteries also require
large storage volumes for the electrolyte solution, thus they would
require extremely large tanks to store enough energy for long durations.
Li-ion batteries are the most energy dense of the batteries, thus they
are used in vehicles where space is confined. It is also observed that
compressed hydrogen and methane far exceed the energy density of
other types of storages and is only exceeded by liquid fuels such as
gasoline ($8977\ kWh/m^3$). These higher energy densities allow for the
storing of a large amount of energy. Since long-term storage involves
storing very large amount of energy, high energy densities are more
likely to make the concept feasible to reduce the amount of physical
space the system requires. Lower round-trip efficiency is sacrificed
for this, although methane and hydrogen storage also have the ad-
vantage of having almost negligible time dependant losses since they
are a form of chemical energy storage and are therefore preferable for
long durations compared to storages that have high time dependant
losses (e.g., batteries or thermal storages). Methane and Hydrogen

storage are a section of P2G technologies which are a sub-category of Power-to-X (P2X).

1.6 POWER-TO-X

P2X is the last category of long-term energy storages, which includes P2G and several different energy conversion and storage pathways. Generally speaking, P2X refers to a series of energy storage pathways that usually fall under the category of chemical energy storage. Chemical energy storage has the benefit of having no time dependant losses, which makes them particularly suited for long-term storage. The individual pathways of storages are firstly overviewed with their efficiencies in Table 1.2 and then are described in more detail in the following sections.

POWER-TO-GAS

P2G refers to the use of electrolysis to split water into hydrogen and oxygen gas. This reaction is shown in (1.1). The efficiency for this process depends on the method of electrolysis (which will be discussed further in Chapter 3), but is currently approximately 60-70% efficient. Future developments hope to bring this efficiency above 75% by 2050. This hydrogen can then be used a variety of ways, thus the term P2G is a category of several different gaseous P2X pathways, which include Power-to-Hydrogen (P2H), Power-to-Methane (P2M), and also include Power-to-Ammonia and Power-to-Syngas. These will be individually described in the next sections.

$$H_2O\,(l) \longrightarrow H_2(g) + 0.5\,O_2(g) \tag{1.1}$$
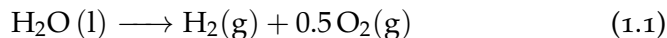
POWER-TO-HYDROGEN

P2H refers to the collection of hydrogen after water electrolysis for use in two ways: (1) either directly injecting hydrogen into the natural gas grid or (2) using the hydrogen as a chemical feedstock for industry. Direct injection into the natural gas grid is permitted until certain volume concentrations. Depending on the country, percentages in Europe are allowed between 2-10% (Altfeld et al. 2013). These limitations are due the differences in operation of several natural gas conversion technologies, such as gas boilers or gas turbines. Since hydrogen gas has different combustion dynamics than natural gas, too high of a

Table 1.2.: Description of various P2X pathways and the corresponding efficiencies.

P2X Type	Path	Efficiency	Conditions
P2H	Electricity ->H_2 (No compression)	64-77%	Electrolysis only
P2H	Electricity ->H_2 (80 bar)	57-73%	Pressure required for grid injection
P2H	Electricity ->H_2 (200 bar)	54-72%	Pressure for compressed storage
P2H	Electricity ->H_2 (700 bar)	50-65%	Pressure required for FCEV charging
P2M	Electricity ->H_2 + CO_2 ->Methane (80 bar)	51-65%	Pressure required for grid injection
P2M	Electricity ->Methane (200 bar)	49-64%	Pressure for compressed storage
P2L	Electricity ->Liquid fuels	35-50%	Methanol synthesis or Fischer-Tropsch
Power-to Ammonia	Electricity ->H_2 ->Ammonia	11-19%	Haber-Bosch Process
Power-to Syngas	CO_2 + H_2O ->CO + H_2	44-60%	Co-electrolysis to produce CO and H_2 (syngas)
P2P	Electricity ->Hydrogen (80 bar) ->Electricity	34-44%	Fuel cell for electricity
P2P	Electricity ->Methane (80 bar) ->Electricity	30-38%	Gas turbine for electricity
P2CHP	Electricity ->Hydrogen (80 bar) ->CHP	48-62%	Fuel cell for heat and electricity
P2CHP	Electricity ->Methane (80 bar) ->CHP	43-54%	Gas turbine for heat and electricity
P2Mobility	Electricity ->BEV	73-77%	BEV charging
P2Mobility	Electricity ->Hydrogen (700 bar) ->FCEV	18-25%	FCEV charging
P2Mobility	Electricity ->Methane (200 bar) ->ICEV-cng	15-20%	ICEV charging with CNG
P2Mobility	Electricity ->Gasoline ->ICEV-g	10-15%	ICEV charging with methanol
P2Heat	Electricity ->Heat	60-300%	Assuming thermal storage losses of 20-50%

concentration could cause conversion technologies, such as turbines or boilers, to malfunction.

There are several industries that use hydrogen as a feedstock. 54% of all produced hydrogen for the chemical industry is used to make ammonia, which is then most commonly used as a feedstock for fertilisers

and other nitrogen compounds. Ammonia is created from hydrogen using the Haber-Bosch synthesis reaction, shown in (1.2). Nitrogen gas is required for this reaction.

$$N_2(g) + 3\,H_2\,(g) \longrightarrow 2\,NH_3\,(g) \tag{1.2}$$

H_2 is also used in the chemical industry for refining uses such as hydro-cracking, in the electronics industry, the metal and glass industry, and lastly in the food industry. Uses for ammonia, hydrogen, and some of the other products of P2X processes used in the in the chemical industry are often also referred to broadly as Power-to-Chemicals. Currently, only 4% of the hydrogen that is supplied as a feedstock for industry is produced via electrolysis. The majority of the hydrogen is produced from natural gas via steam-methane reforming, from oil via oil reform-ing or from coal via coal gasification. The methods that derive H_2 from fossil fuels emit a significant amount of CO_2 into the atmosphere but are very low cost in comparison to electrolysis.

As the cost of electrolysis decreases, it is anticipated that the large amount of curtailed renewable energy could be used to run electroly-sers to produce this H_2 for industry instead of deriving H_2 from fossil fuels.

The hydrogen produced via electrolysis can also be stored for uses in other pathways, such as Power-to-Methane, Power-to-Power, Power-to-CHP, or Power-to-Mobility. Hydrogen is typically compressed for storage somewhere between 80-700 bar. 700 bar is required for mobility use of hydrogen. Compressing hydrogen until this pressure consumes a significant amount of electrical energy (this will be covered in more detail in Section 3.5). This can be as much as 10% of the total energy content of the hydrogen itself when compressing to 700 bar, thus com-pressing hydrogen to high pressures is best avoided if possible. This is difficult to avoid for Power-to-Mobility applications with hydrogen vehicles since the tanks for these applications are usually at 700 bar to get a comparable energy density to gasoline or diesel.

POWER-TO-METHANE

P2M refers to the use of methanation to synthesise methane (CH_4) or Synthetic Natural Gas (SNG) from H_2 and CO_2. Methanation is based on the Sabatier reaction, which was discovered in 1902 and is described in (1.3).

$$CO_2\,(g) + 3\,H_2 \longleftrightarrow CH_4\,(g) + 2\,H_2O\,(g) \tag{1.3}$$
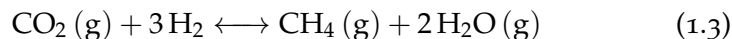
Hydrogen can, of course, be sourced from electrolysis, and CO_2 for this reaction must also be sourced prior to methanation. It can be sourced from different methods, including extraction from the atmosphere, biogas processing, from coal power plants, or from cement production exhaust. Depending on the method, this extraction can be quite energy intensive, particularly CO_2 extraction from the air. Extraction from the air uses adsorbents, such as amine or hydroxide, to adsorb CO_2 from the air. Electrical energy is required to provide airflow via fans and heating energy is required to drive off the CO_2 from the absorbents. This heating energy demand can be decreased if waste heat from an industrial process is utilised. This process is also less energy intensive when the CO2 concentration is higher, such as in the emissions of a cement or a coal power plant operation. Although this capture process is not accounted for in this work, life-cycle emissions values per kilogram of CO_2 are used to account for the emissions from the high energy usage and the CO_2 price is adjusted according to the capture method.

The methanation reaction occurs in catalytic or biological reactors (discussed further in Section 2.3.1) at temperatures as high as 700°C, therefore high temperature heat can be used for other reactions. The produced SNG can be injected into the natural gas grid without concentration limitations, or used in place of natural gas as fuel in gas boilers, gas turbines, and Internal Combustion Engines. Combustion of this SNG is now carbon neutral, as CO_2 was extracted from the air to produce it thus making it net zero in terms of CO_2 emissions. The process of methanation is, by itself, around 80% efficient (Lehner et al. 2014), therefore after electrolysis the efficiency of this pathway is between 30-50%.

The large advantage of P2M is that it can be injected into the natural gas grid without concentration limitations, thus allowing the extensive network of natural gas grid infrastructure to be exploited as storage. This could result in potentially huge storage capacity potentials on national scales. When combined with biogas, it could contribute to decarbonising the natural gas grid. Another advantage of SNG is that it is easier to compress and store than hydrogen due to its higher density. The volumetric energy density at specific pressures for methane and hydrogen are compared in Table 1.3 and it is seen that, at high pressures, the energy density of methane is significantly higher, thus would

occupy significantly less space to store the same amount of energy as hydrogen.

Table 1.3.: Comparison of the density, the LHV, and volumetric energy density of hydrogen and methane at standard storage pressures. The lower heating value is the amount of heat released by the combustion of a material without recovering the heat of vaporisation. 80 bar typically required for grid injection, 200 bar is standard for compressed methane, and 700 bar is required for hydrogen vehicle charging.

Temp. 25 °C	Density (kg/m3)		LHV (kWh/kg)		Volumetric Energy Density (kWh/m3)	
Pressure	H_2	CH_4	H_2	CH_4	H_2	CH_4
1.01 bar	0.09	0.67	33.3	13.9	2.99	9.29
80 bar	6.54	59.0	33.3	13.9	218	820
200 bar	15.6	180	33.3	13.9	519	2503
700 bar	39.5	301	33.3	13.9	1299	4183

POWER-TO-LIQUID

Power-to-Liquid (P2L), which is often also called Power-to-Fuel, includes the development of pathways to use renewably produced hydrogen derived from electrolysis to create synthetic liquid fuels, such as methanol, heating oil, diesel, gasoline, and kerosene. Methanol (CH_3OH) is synthesised using the methanol synthesis reaction, which is shown in (1.4). The efficiency of this reaction is generally above 60-65% efficient.

$$CO_2\,(g) + 3\,H_2\,(g) \longrightarrow CH_3OH\,(g) + H_2O\,(l) \qquad (1.4)$$
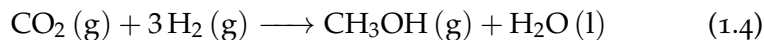
The remainder of the fuels are synthesised with the Fischer Tropsch processes, which require carbon monoxide. The water-gas shift, shown in (1.5), reaction must first be used to produce carbon monoxide from carbon dioxide (sourced from CO2 capture, as was done with methane) and hydrogen (sourced from electrolysis), and then synthesis of liquid fuels can be performed using the Fischer-Tropsch process in (1.6). These

processes are generally between 25-50% (Blanco et al. 2018) efficient depending on the fuel being processes.

$$CO_2\,(g) + H_2\,(g) \longrightarrow CO\,(g) + H_2O\,(l) \tag{1.5}$$

$$CO\,(g) + H_2\,(g) \longrightarrow CxHyOH + H_2O\,(l) \tag{1.6}$$
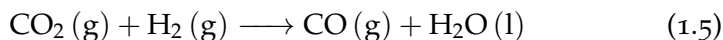
These series of reactions are able of producing liquid fuels such as gasoline, diesel, kerosene, and others, which are the standard fuels used in transportation. Since CO_2 is extracted from the atmosphere or industrial exhaust streams for these reactions, the combustion of these liquid fuels is again CO_2 neutral as with methane. This is important for sectors like aviation, where the energy density in the liquid fuels cannot yet be replaced with less dense fuels or batteries.

POWER-TO-SYNGAS AND CO-ELECTROLYSIS

Power-to-Syngas is also directly related to the Fischer Tropsch processes, but rather than electrolysing hydrogen and then separately producing carbon monoxide for the reaction, there is an alternate process which requires the production of syngas (the mixture of hydrogen gas and carbon monoxide). There are currently three types of water electrolysis, which will be discussed in more detail in Chapter 2: alkaline electrolysis, Polymer Electrolyte Membrane (PEM) electrolysis, and solid-oxide electrolysis. Both alkaline and PEM electrolysis are commercialised processes that occur at low temperatures, but solid-oxide electrolysis is a newer, and potentially more efficient type of electrolysis that occurs at high temperatures (700-900 °C). At these high temperatures, both CO_2 and H_2O can be used to create syngas, a mixture of carbon monoxide and hydrogen, which can then be used to make a variety of liquid fuels using the Fischer Tropsch processes. Using co-electrolysis eliminates the need for an extra step with the water-gas shift reaction, thus potentially making the synthesis of these fuels more efficient. The development of co-electrolysis is still in the research and development phase, but is one potential pathway which can make renewable liquid fuels for aviation and heavy duty transport, where fossil fuels are difficult to replace. To ensure that such fuels would truly be renewable, the energy and emissions that goes into their processing must also be accounted for. The energy for this co-electrolysis should also be renewable and the CO_2 obtained for co-electrolysis must be also obtained using renewable electricity. Much work is still to be done

in this sector to make this pathway carbon neutral from a life-cycle standpoint.

POWER-TO-POWER

Power-to-Power refers to the re-electrification of either hydrogen or methane after it has been produced and stored. The re-electrification of hydrogen typically involves using hydrogen as a fuel for a fuel cell. With methane, this re-electrification can include using methane as the fuel for either a fuel cell or a gas-turbine. If using a fuel cell, it is more efficient to use hydrogen directly, as the reformation step is not required, however hydrogen fuel cells do not have the convenience of using the local natural gas grid in case of short supply renewable fuel.

Power-to-Power is rightfully criticised due to its low round-trip efficiencies. Typically, production of hydrogen and compression for storage is already between 40-60% efficient, depending on the efficiency of the electrolyser and the pressure of the storage, and fuel cells have an electrical efficiency of approximately 50-65%, resulting in round trip efficiencies of 30-40%. With SNG and a gas turbine, this further decreases to about 10-20%.

POWER-TO-CHP

Both fuel cells and gas turbines can also operate as Combined Heat and Power (CHP) units, thus increasing their efficiencies through the use of waste heat utilised for a heating system. Power-to-CHP, for the fuel cell and gas turbine operating as CHP units respectively, can increase the round-trip efficiency of these two to approximately 48-62%. Within a decentralised community, this heat is in high demand in winter and thus can be readily utilised especially when renewable electricity supply is low and heating demand is required.

POWER-TO-MOBILITY

Power-to-Mobility includes the pathway of using renewable electricity for vehicle charging. There are four potential pathways, depending on the vehicle powertrain and type of fuel used. The first method uses electrical energy to charge Battery Electric Vehicle (BEV) or Plug-in Hybrid Electric Vehicle (PHEV). This is the most efficient method of Power-to-Mobility, as BEVs have an efficiency of 73-77% from electricity

to wheel propulsion. If the electricity used to drive the BEV is 100% renewable, then this method has no operational emissions.

The second method is with a Fuel Cell Electric Vehicle (FCEV), which requires hydrogen compressed to 700 bar for charging. The advantage of a FCEV over a BEV is that they have higher travelling ranges, due to the higher energy density of compressed hydrogen compared to batteries, and they charge much more quickly than BEVs. If the hydrogen used for charging is derived from electrolysis, then the efficiency of this pathway is 18-25% from electricity to wheel propulsion. Although this efficiency is lower than with BEVs, if renewable energy is used to drive electrolysis then this method can also have no operational emissions.

Thirdly, ICEV with compressed SNG as a fuel can also be included as a potential pathway, however the efficiency from electricity to propulsion is only around 15-20%. ICEV vehicles are significantly less efficient than electric vehicles, thus the losses using this method are significantly lower.

Lastly, ICEVs fuel by gasoline or diesel can use fuel synthesised through P2L. This is the least preferable pathway, due to the significant energy losses in the pathway, resulting in an approximate efficiency of 10-15%.

POWER-TO-HEAT

Power-to-Heat is a different form of P2X as it stores energy in the form of heat, rather than chemical or electrical energy storage. Power-to-Heat involves the use of heat pumps, which are highly efficient devices, to generate heat at times of peak production of renewables, and then store this heat for later use. Although heat pumps are very efficient devices, heat storage typically has high time dependant losses, therefore it is often difficult to store heat energy for long periods of time. Nevertheless, heat storage is very inexpensive compared to many of the other Power-to-X pathways and can be quite efficient if stored over shorter periods of time.

POWER-TO-X PATHWAY OVERVIEW

To demonstrate the different P2X pathways, the potential deployment scenarios and services they are able to provide are shown in Fig. 1.6. This Figure gives an overview of the various pathways discussed in this Section. Many require large capital investments for the equipment required, especially the Power-to-Chemical and Power-to-Liquid path-
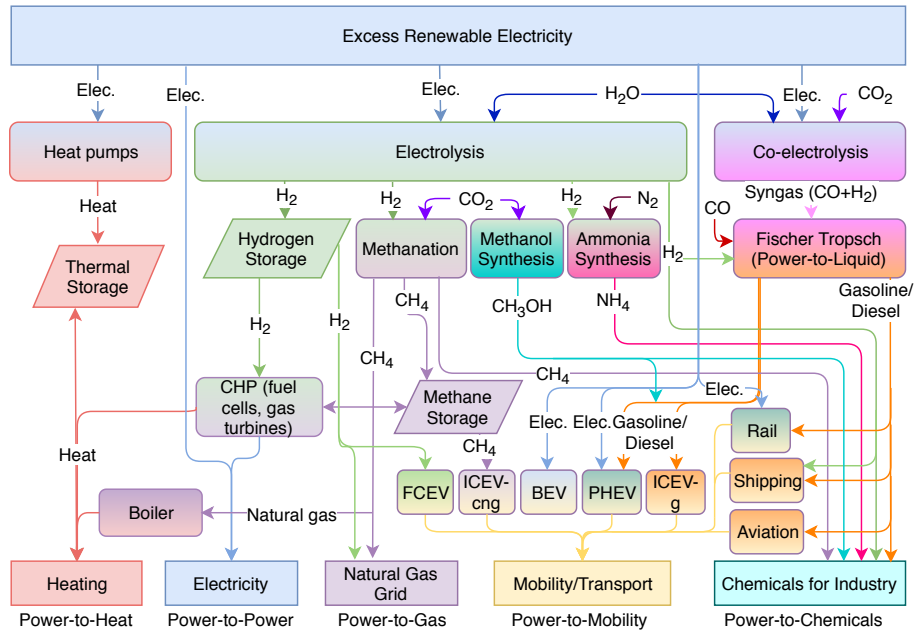
Figure 1.6.: Potential P2X deployment scenarios and the services they are able to provide by transforming renewable electricity.

ways. Some of these pathways are more feasible in centralised case studies than in decentralised case studies. Many also require several conversion steps, resulting in high energy losses, thus making the pathways expensive to implement for little return. Referring back to Table 1.2, it is shown that the pathways with the least conversion steps and least compression are the most efficient, therefore further processing and compression is best avoided if possible. Due to the low round-trip efficiencies of Power-to-Power, Power-to-CHP is a better alternative if the waste heat can be exploited for building heating. In addition, the Power-to-Mobility pathways with electric vehicles (BEV and FCEVs) are much higher than for ICEVs. Inclusion of a Power-to-Mobility pathway with EVs is a logical step to reduce emissions in personal transport, however incorporating the necessary charging for these vehicles into MES is not a straight forward task and will require a well-designed system to ensure that the level of renewable energy is stabilised and managed sufficiently to make an improvement.

Since many communities are also connected to natural gas grids, P2G is a logical connection for interaction as it can be used to import and

export the energy connected to the system. In addition, the synthesis reactions for methane are more efficient than those for the liquid fuels in the P2L pathways, thus this route has higher round trip efficiencies.

The main advantage of P2L is that liquid fuels have high energy densities that are difficult to replace in heavy duty transportation and they can be shipped more easily. The production of these fuels is better suited for large industrial facilities due to the large amount of renewable energy required and the industrial scale of applications. Since the synthesis efficiencies for these processes are lower than for hydrogen or methane and transportation of fuels is not a large concern within a decentralised MES (since energy will be stored on-site), P2L and Power-to-Syngas are not evaluated in this work as natural gas is already the preferred fuel within the building sector and P2M is a more efficient pathway. In addition, the Power-to-Chemical pathways, such as Power-to-Ammonia, are not considered as they are also best suited for large centralised renewable operations to minimise the cost of chemical feedstocks.

With these considerations, this thesis will limit the investigations of P2X pathways for use as storage in MES to P2H, P2M, P2CHP, Power-to-Mobility, and Power-to-Heat.

1.7 THESIS OBJECTIVE AND SCOPE

This research began as part of the "Integrated Multi-Energy-hub Systems" or IMES project from the Energy Science Centre at ETH Zürich. This is a NRP 70 Energy Turnaround funded project from the Swiss National Science Centre. The aim of this project was to address four of the major challenges that are predicted to arise with the phase-out of nuclear power in Switzerland: i) the handling of the transient nature of both loads and decentralised energy resources, ii) maintaining system stability, iii) integrating decentralised energy production, and iv) reducing the daily and seasonal load and generation imbalances in the system. To do this, it was determined that the investigation of long-term storage technologies should be investigated for distributed generation alongside short-term storage technologies.

Most Power-to-X pathways include chemical energy storage, which do not have time dependant losses. The absence of time dependant losses in chemical energy storage makes P2X an attractive concept for long-term storage. Currently, most Power-to-X papers target applica-

tions on the centralised scale and its potential as a distributed storage technology has not been investigated in much detail. After further investigation, the specific pathways of Power-to-Hydrogen, Power-to-Methane, Power-to-CHP, Power-to-Mobility, and Power-to-Heat were focused on. The potential of these different pathways were proposed to be investigated for application in decentralised cases. It is also of interest to compare the different pathways and to investigate whether it is better to apply certain combinations of storage types. An optimisation modelling approach was then selected that would optimise for the best configuration of the technologies, to evaluate them in an unbiased way. This model can evaluate the best pathways for certain case studies and to do this from the years of 2015-2050. A sample decentralised MES with many of the required conversion and storage technologies can be seen in Fig 1.7.

1.7.1 *Optimisation as a Design Tool*

When considering the potential design of a MES for a group of buildings with different energy loads, the decisions leading to the best performing solutions are not always obvious, especially when there are several objectives in mind. In this case, the goals are not only concerned with the performance and cost of the model, but also the ability of the system to meet emission targets for buildings and personal transport. With so many different pathways to evaluate, multi-objective optimisation is a particularly effective method of selecting the most affordable system that can still meet the loads of a community and the emissions targets.

For these reasons, the models in this work are developed to select the configuration and capacities of different technologies used in energy systems, and their annual operation, to select the best system according to a certain objective function. The objective is to find the best performing solution that is able to meet the loads of the community, is able to meet emissions targets, and also has low net annual costs. Some other limitations also exist, such as policy changes, planning timelines, the current available infrastructure, and acceptance of society. Many of these other factors can also be formulated as objectives. With these goals in mind, this thesis uses a multi-objective function which minimises both total annual costs of the system, as well as the annual emissions. The techno-economic model built in this work is
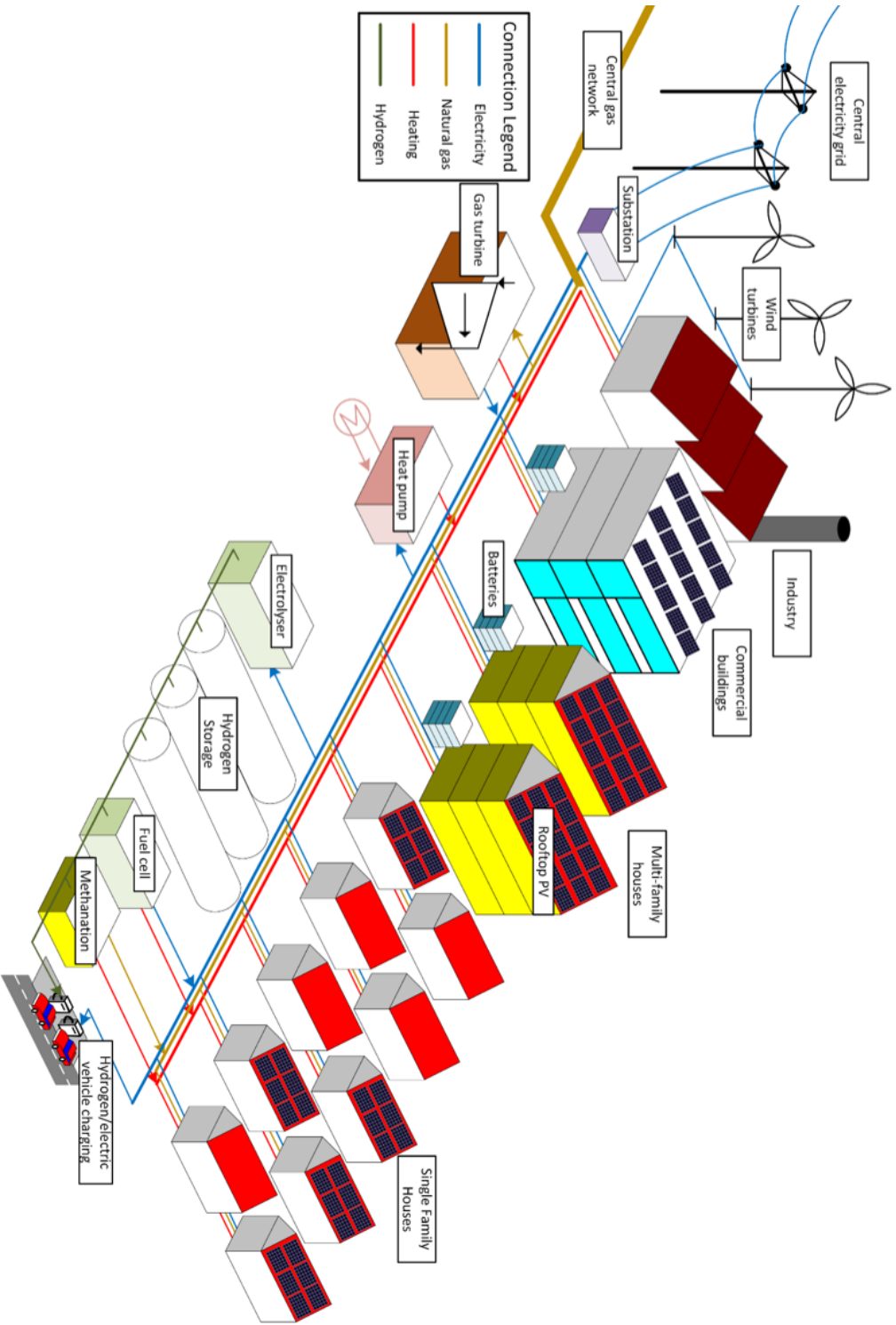
Figure 1.7.: A depiction of a decentralised multi-energy system with an option of several conversion and storage technologies for the implementation of different P2X pathways.

based on a MES optimisation model structured using the energy hub approach. The Energy Hub model was first mentioned in literature in Geidl and Andersson (2006) and is based on mathematical programming principles. In their definition paper, Energy Hubs are described as a *"system, where multiple energy carriers can be converted, conditioned, and stored to satisfy a set of demands"*. Technologies are defined as energy converters that can transfer energy from one carrier to another at a certain efficiency or can be stored. The model uses optimisation to select the configuration, sizing, and the operation of the system. Using this optimisation framework, the selection of a series of conversion technologies and storage technologies can be evaluated.

1.7.2   *Application to Multiple Case Studies*

The purpose of this thesis is to evaluate the potential of P2X technology in decentralised MESs. An MES is a system that provides the energy needs for multiple energy carriers for an urban setting. In this thesis, this includes the energy (i.e., heating and cooling) demands of a group of buildings and potentially the transport demands of the occupants in those buildings. In this context, a MES must be specifically tailored to a set of loads, or in this case, a specific group of buildings. To appropriately apply the methodologies developed in this thesis, several case studies are used to test the model in different contexts. Three locations in Switzerland are chosen, each of which is representative of a different type of Swiss community. These three contexts include a rural case study, a suburban case study, and an urban case study. These case studies will be further described in the following sections and the exact details of the building ages and types can be found in Appendix A.

1.7.2.1   *The rural case study: Zernez*

Zernez is a rural alpine village in Canton Graubünden in the Swiss Alps with approximately 1150 people inhabiting 308 buildings. The building stock consists of mostly single-family homes, multi-family homes, shops, hotels, and agricultural buildings. The total building floor area is estimated to be 79,047 m^2. The building stock is comprised of a mix of old, but well-kept buildings, and a group of new buildings. The current heating demand is supplied by a mix of biomass, electric

boilers, and heating oil. It is located at an altitude of 1475 m resulting in a cold climate with an average temperature of 4.7°C.

Although the village has a large number of protected buildings, there are many rooftops that are available for installation of PV panels. It is possible that up to 60 small-wind turbines can be installed in the immediate area, although the wind speeds in the area are typically between 2 and 4 m/s. There is also a river passing by the community which is planned for a small 2.3 MW micro-hydro station. Flow rates from this river over a one-year period have also been recorded to approximate the power that this station could produce. The case study is shown in Fig. 1.8.

Figure 1.8.: A GIS depiction of the 308 buildings in Zernez.

1.8 THE URBAN CASE STUDY: ALTSTETTEN

Altstetten is a populated and primarily residential quarter in the city of Zürich in Switzerland. A section of 77 buildings in Altstetten is chosen as it was scaled to nearly the same total annual demand as Zernez, as these two case studies will later be used for comparison. These buildings consist of primarily multi-family homes and mixed-use buildings with residential units and shops. The overall population

is estimated to be 1,784 inhabitants. The total estimated floor area is 166,315 m^2. With this population and floor area, it has a much higher population density than Zernez. Currently all of the buildings are connected to the natural gas grid for heating and the buildings were mostly built before the 1960s. As it lies in a city, small wind and hydro are not available and only rooftop PV systems are available for renewable resources.

Figure 1.9.: A GIS depiction of the 77 buildings in Altstetten.

1.9 THE SUBURBAN CASE STUDY: ZUCHWIL

Zuchwil is a municipality in the district of Wasseramt in Canton Solothurn. This case study is chosen, as it is in the proximity of a current P2M project, run by Regio Energie Solothurn (Graf 2019). This site is within close proximity to the natural gas grid for direct injection and the water network for supplying the electrolyser with water. A group of 52 buildings are selected from this municipality for analysis. These buildings consist of four multi-family houses, 28 attached houses and 20 detached single-family houses. There are 168 people located in these 52 buildings. The total area of these buildings is estimated to be 13,846 m^2. The layout of the buildings can be seen in Figure 1.10. The houses were mostly built between 1980-1994 and are not retrofitted at this time. The age of construction, energy carrier, building type, and number of occupants were taken from the Swiss Buildings and Apartment Registry (Bundesamt für Statistik 2012). Similar to the Altstetten case study, only solar PV on rooftops is available as renewable potential, however since this case study consists of mostly single family homes,

Figure 1.10.: A GIS depiction of the 52 buildings of Zuchwil (shown in red).

the amount of PV production per capita is higher than for the Altstetten case study. This case study is chosen to be smaller than the others, as it is planned for implementation of the optimisation that considers both buildings and mobility. To do this, more decision variables are required which mean limiting the case study's size.

1.9.1   *Uncertainty and Sensitivity Analysis*

Another aspect of the design of these systems, which is often neglected in the MES optimisation models, is the parameter uncertainty. These models for urban energy systems are based on many assumptions, particularly regarding economic, efficiency, and environmental variables. When trying to predict prices, efficiencies, and CO_2 emissions in the future, uncertainty plays an even larger factor and can significantly impact the outcome of the model. Since several P2X scenarios are being evaluated, it is difficult to predict what the prices and efficiencies for these technologies may be in the future, especially considering the ongoing research and development with many of the hydrogen based technologies.

To address this uncertainty, a global sensitivity analysis is conducted

to evaluate the most sensitive parameters for the feasibility of different P2X pathways. This analysis will build on the deterministic optimisation model that includes both building and mobility demands. With this analysis, the most common solutions among the sensitivity analysis can be identified as being robust solutions and the most sensitive parameters can be identified for the reference of decision makers, thus allowing them to make informed decisions on the best pathways to choose depending of the future realisation of parameter value assumptions. This sensitivity analysis can also allow for evaluation of the effect of these parameters on the range of total cost and emissions that certain pathways are likely to have. The end goal of this work is to identify the most robust, affordable, and environmental P2X pathways and what role they may play in allowing us to meet our targets in MES. The recommendations of this thesis will not only apply to Switzerland, but the conclusions of the sensitivity analysis can provide recommendations for applications to any decentralised multi-energy system in Europe. However, the results will be specific to decentralised systems. In addition, we can determine the role short-term and long-term storage could play in the design of MES. This can include trying to increase the deployment of distributed energy resources or the self-sufficiency factor in these communities so that they can become more self-reliant and less dependent both on fossil fuels and the centralised grid without having to sacrifice comfort in the home or their personal mobility.

1.10 RESEARCH QUESTIONS

With the scope and overarching methodology defined, the main research questions for this thesis can be summarised as follows:

1. To what extent can local renewable sources be used to provide energy for both building and mobility demands? Does coupling of these sectors in a MES further reduce costs and emissions?

2. Is the use of long-term energy storage required for decentralised energy systems to meet their energy targets in the case studies? Is it only suitable for deep decarbonisation?

3. Is it feasible to design decentralised energy systems to support the charging of a fleet of vehicles with local renewable energy sources? Which storages are required to do so?

4. Which P2X pathways are the most cost and emissions effective to implement in decentralised MES? Under which assumptions are these pathways optimal?

5. Which P2X pathways have the highest potential to help us meet our emissions targets?

1.11 OUTLINE

With the goals of this thesis stated, the thesis is structured into eight Chapters:

1. Chapter 2: Power-to-X in Multi-Energy Systems: State-of-the-Art

2. Chapter 3: MES Optimisation Development with P2X

3. Chapter 4: Future Scenarios in P2X for Two Decentralised Cases

4. Chapter 5: Optimisation of Personal Vehicle Charging

5. Chapter 6: Application of Power-to-Mobility Optimisation

6. Chapter 7: Uncertainty and Sensitivity Analysis

7. Chapter 8: Conclusions and Outlook

Chapter 2 provides a state-of-the-art review of MES optimisation models using long-term storage and models that consider different P2X pathways. Additionally, papers that look into sensitivity analysis in MES optimisation models are also included.

Chapter 3 presents the methodology of building an optimisation model to consider P2X pathways within a decentralised energy system. This begins with the calculation of building demand and renewable potential. After this, the MES model is built in an optimisation framework, including the construction of these P2X pathways for both short and long-term storage horizons.

Chapter 4 shows the application of the model developed in Chapter 3 to two different districts (Zernez and Altstetten as described in Section 1.7.2) and in several different scenarios from 2015 to 2050. These different scenarios are constructed based on scenarios in an Intergovernmental Panel on Climate Change (IPCC) report.

Chapter 5 extends the development of the optimisation model in

Chapter 3 to include the modelling of vehicle ownership and personal transport demands. A series of vehicle technologies are defined, their efficiencies are evaluated at different driving cycles, and the optimisation model is updated to include their selection and charging.

Chapter 6 shows the application of the model developed in Chapter 5. It is applied to the Zuchwil case study described in 1.7.2 and the optimisation assessed is applied for the years of 2015 to 2050. The results of the effect of the inclusion of Power-to-Mobility are discussed.

Chapter 7 applies an uncertainty and sensitivity analysis to the model developed in Chapter 5. The uncertainty characterisation of uncertain parameters is performed, the Uncertainty Analysis (UA) and Sensitivity Analysis (SA) methodologies are described, and the results of the analysis are presented and discussed.

Chapter 8 summarises the conclusions of this thesis and provides recommendations for the feasibility of P2X as an energy storage for MES, as well as discussing the economic feasibility, effect on emissions, and finally giving recommendations for the potential role of P2X in decentralised MESs until 2050.

1.12 SUMMARY AND OUTLOOK

In this Chapter, we have first discussed how the historical adoption of fossil fuels during the 20th century in the electricity, heating, and transport sectors led to the current energy and climate crisis while over 90% of our primary energy consumption still comes from fossil fuels. This resulted in the structure of the current centralised energy system, where electricity is produced in large centralised plants and is then transported through the electricity grid to the consumer. The rising installations of distributed renewable sources, such as PV and wind, are enabling a shift towards decentralised multi-energy systems that are based on decentralised renewable generation.

To balance the fluctuating nature of renewable energy from wind and solar, both short-term and long-term storage systems within decentralised MESs are required. There are options for short-term energy storage with high deployment rates and efficiencies, such as batteries and thermal storage, but the options for long-term storage are generally associated with low round-trip efficiencies or, like pumped hydro and compressed air energy storage, are not available for decentralised applications due to their large size and requirement of certain geological

sites. Due to these limitations, Power-to-X is proposed for decentralised long-term storage.

Power-to-X includes many separate storage pathways, such as Power-to-Gas, Power-to-Hydrogen, Power-to-Methane, Power-to-Liquid, Power-to-Syngas, Power-to-Power, Power-to-CHP, Power-to-Mobility, and Power-to-Heat. The pros, cons, and efficiencies for each pathway are compared and Power-to-Liquid and Power-to-Syngas are ruled out for consideration in decentralised systems due to their suitability for the industrial sector and the lack of need for liquid fuels in decentralised systems for buildings. Power-to-Hydrogen, Power-to-Methane, Power-to-Power, Power-to-CHP, Power-to-Mobility, and Power-to-Heat are recommended for further investigation in decentralised multi-energy systems.

With these pathways defined, optimisation is proposed to select the best pathways for a multi-energy system by optimising for the best technology according to certain objective functions. Multi-objective optimisation, minimising both net annual costs and net annual emissions, is proposed to select the most economical and environmental pathways. Three case studies are introduced for testing the optimisation model within rural, suburban, and urban municipalities.

The goals of this thesis are to firstly find the extent to which local renewables can be used to meet building and personal transport demands. Secondly, it is investigated whether long-term storage is required to meet the energy targets in Switzerland or if P2X is only suitable for deep decarbonisation. Thirdly, we will investigate whether multi-energy systems are able to support a fleet of vehicle charging with local resources. Fourthly, the P2X pathways that have the highest potential for meeting energy targets at the lowest cost should be identified. The last goal is to propose which P2X pathways are the most likely to be implemented.

With these research questions, the Chapter structure of the thesis is presented, starting with an analysis of the state-of-the-art and ending with the final conclusions and outlook.

POWER-TO-X IN MULTI-ENERGY SYSTEMS: STATE OF THE ART

In this Chapter, the state of the-art papers in the field of MES optimisation will be reviewed with a specific focus on work that includes Power-to-Hydrogen, Power-to-Methane, Power-to-Mobility, and Power-to-Heat. In addition, the state of the art in water electrolysis, fuel cells, and methanation are also reviewed. Lastly, the handling of uncertainty analysis in the reviewed papers and the state of the art in MES optimisation sensitivity and uncertainty analysis are discussed.

2.1 MULTI-ENERGY SYSTEMS IN LITERATURE

There is a wide array of literature dedicated to the design and analysis of multi-energy systems. These papers vary in several different aspects, such as scale of the system (from the building level, to the district, and city level), the energy carriers of the demands considered, the selection of technologies considered, and their methodologies. Due to the large number of publications, papers that have a focus on P2X and have applications for building electricity, building heat, or mobility demands are primarily considered in this review.

Several of the publications on MES are based on optimisation from the Energy Hub concept that was defined by Geidl and Andersson (2006). In this definition paper, energy hubs are described as "a system, where multiple energy carriers can be converted, conditioned, and stored" to satisfy a set of demands. Technologies are defined as energy converters that can transfer energy from one carrier to another at a certain efficiency. Storage technologies allow energy to be charged at a certain time step, and then released at a later time step. There has been a wide array of literature focusing on different aspect of the Energy Hub model, however most papers consider a conventional set of technologies in the mix. These typically include, but are not limited to boilers (natural gas, biomass, or oil), PV, heat pumps, CHP technology, batteries, and thermal storage. However, the focus of this work is

on energy storage using different P2X pathways, therefore work that has been identified to use the identified pathways of interest, namely Power-to-Hydrogen, Power-to-Methane, Power-to-Mobility, and Power-to-Heat, are covered in this literature review. In addition, a review of the state of the art for sensitivity analysis in MES design is included.

2.2   POWER-TO-HYDROGEN

2.2.1   *Water Electrolysis*

The central process that enables hydrogen and oxygen to be produced from electricity and water is water electrolysis. In this Section, the state of the art in water electrolysis is reviewed prior to the applications of P2H. Before exploring the different types, the thermodynamics are overviewed. The chemical reaction of electrolysis, that was described in (1.1) can be further described in (2.1).

$$\Delta H(T) = \Delta G(T) + T\Delta S(T) \tag{2.1}$$

Here, $\Delta H(T)$ is the total enthalpy supplied to an electrolysis cell, $\Delta G(T)$ is the change in Gibbs free energy or the amount of electrical energy, T is the temperature, and $\Delta S(T)$ is the change in entropy. $T\Delta S(T)$ represents the amount of heat to be supplied to the electrolysis cell to drive the reaction. The reversible voltage, or the minimum voltage that has to be applied to the cell to initiate the reaction, is found in Eq. (2.2)

$$V_{rev} = \frac{\Delta G}{nF} = 1.23V \, (P = \ 1bar, T = 298K) \tag{2.2}$$

Here, n is the number of moles and F is the Faraday constant. The thermoneutral voltage can be calculated with Eq. (2.3).

$$V_{th} = \frac{\Delta H}{nF} = \frac{\Delta G}{nF} + \frac{T\Delta S}{nF} = 1.48V \tag{2.3}$$

If the voltage applied to the electrolysis cell (E_{cell}) is less than V_{th}, but higher than V_{rev} the reaction takes place while absorbing heat from the environment. If E_{cell} is more than V_{th}, the electrolysis cell produces surplus heat and the reaction needs to be cooled to reduce degradation on the system. The operating pressure and temperature also strongly

effects the system. This effect can be described with the Nernst Equation in Eq. (2.4).

$$\Delta V = V - V^0 = \frac{RT}{nF} ln \frac{1}{\sqrt{P}}$$ (2.4)

Here, V^0 is the cell voltage at 298 K and 1 bar, R is the ideal gas constant, T is the temperature in Kelvin, and P is the pressure in Pascals. This shows that an increase in the cell pressure or temperature correlates to an increase in cell voltage. The electrical efficiency (η_{el}) of the overall electrolyser system can be described in Eq. (2.5).

$$\eta_{el} = \eta_V \cdot \eta_F = \frac{V_{th}}{V_{app}} \cdot \frac{n_{meas}}{n_{th}} - > \eta_V$$ (2.5)

Here, η_V is the voltage efficiency, η_F is the current efficiency, V_{app} is the applied voltage, n_{meas} is the measured amount of produced hydrogen, and n_{th} is the theoretical amount of produced hydrogen according to Faraday's Law. The losses in efficiency are due to several overvoltages, including activation losses V_{act}, ohmic losses V_{ohm}, and concentration losses V_{conc}. The total overall voltage applied to the cell is calculated with Eq. (2.6).

$$V = V_{ref} + V_{act} + V_{ohm} + V_{conc}$$ (2.6)

The activation losses are attributed to kinetic losses in the charge transfer at the electrode interfaces and are typically lower at higher current densities. Ohmic losses are generally attributed to resistances in the electric currents, hindering the flow of charge passing through the cells. Lastly, concentration losses are attributed to the restricted rate of mass transfer that is ongoing in the cell which hinders the flow of ions. With the reaction mechanics discussed, we can now evaluate the advantages and disadvantages of the different types of electrolysis.

ALKALINE ELECTROLYSIS

Alkaline Electrolysis is the oldest and most mature form of electrolysis. It uses a liquid electrolyte solution of potassium hydroxide (KOH) or sodium hydroxide (NaOH), which results in the two half-cell reactions:

$$Cathode : 2\,H_2O + 2\,e^- \longrightarrow H_2 + 2\,OH^-$$ (2.7)

$$Anode : 2\,OH^- \longrightarrow \frac{1}{2}\,O_2 + H_2O + 2\,e^-$$ (2.8)
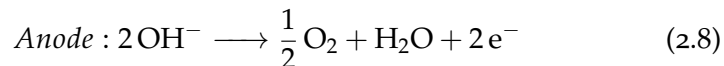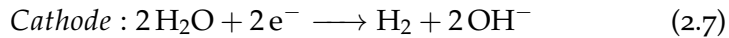
The operating temperature of these cells is typically from 70-90 °C. The systems can be pressurised, but usually only up to 15 bars. Alkaline electrolyser cells can be stacked commercially usually with 30-300 cells and can produce industrial quantities of hydrogen at a high purity (+99.5%). They can be operated at part-load conditions between 20-100% but operate with a lower purity and efficiency at the lower end of the range. Electrical efficiencies usually lie between 60-80%. In addition, they take typically 15 minutes for start-up and shut-down and the cells degrade at a more rapid rate when frequently cycled. Generally, the lifetime of alkaline electrolsyers is stated to be 40,000 operating hours (Lehner et al. 2014). Their major advantage is the low costs of this technology, particularly on the industrial scale. Their main disadvantage is their lack of dynamic operation, which can make them unsuitable for responding to dynamic renewable electricity surpluses, such as peaks in PV or wind production due to quick changes in the solar radiation or wind speeds (Lehner et al. 2014).

POLYMER ELECTROLYTE MEMBRANE ELECTROLYSIS
The second most popular type of electrolyser is the Polymer Electrolyte Membrane (PEM). Although this type of electrolyser is commercialised, it is generally used for smaller scale applications. This cell uses a micrometer thin proton conducting membrane as solid polymer electrolyte, rather than the liquid electrolytes used in alkaline electrolysis. The half-cell reactions are described below:

$$Cathode : 2\,H^+ + 2\,e^- \longrightarrow H_2 \tag{2.9}$$

$$Anode : H_2O \longrightarrow \frac{1}{2}O_2 + 2\,H^+ + 2\,e^- \tag{2.10}$$
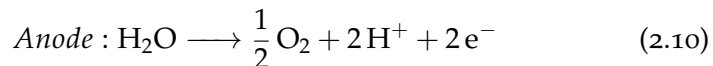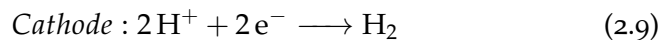
These single cells are connected forming a stack. The lack of a liquid, and associated equipment such as pumps and gas separation, allows for a more compact system. Polymer Electrolyte Membrane Electrolysers (PEMEs) are associated with a current density about four times higher than that of alkaline electrolysers. Electrical efficiencies usually lie between 60-70% and can produce pressurised hydrogen at 30-60 bars. They typically operate at 60-80°C and produce very pure hydrogen (+99.99%). Their operating lifetime is generally assumed to be between 60,000-80,000 operating hours, which is significantly longer than an alkaline electrolyser due to less degradation (Körner et al. 2015). Most

importantly, PEMEs can be operated in a highly dynamic fashion from 0-100% part load conditions. They can also respond very quickly to power fluctuations and have start-up and shut-down times typically under 5 minutes. This is beneficial when the system is required to respond to fluctuations in renewable surplus output that changes quickly with weather conditions.

SOLID OXIDE ELECTROLYTE ELECTROLYSIS
Solid oxide electrolysers are the least developed type of electrolysis and are still in the research stage of development. According to an investigation of current P2G systems by Gahleitner (2013), there were no current installations that used solid oxide electrolysers. The major difference with solid oxide electrolysis is operation at high temperatures of 700-1000 °C. The electrolyser has a dense solid oxide layer that becomes conductive at high temperatures and can be used as an electrolyte. The half-cell reactions are shown below:

$$Cathode : H_2O + 2\,e^- \longrightarrow H_2 + O_2^- \tag{2.11}$$

$$Anode : O_2^- \longrightarrow \frac{1}{2}\,O_2 + 2\,e^- \tag{2.12}$$
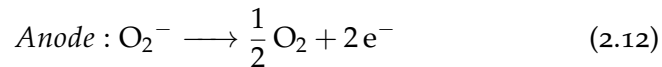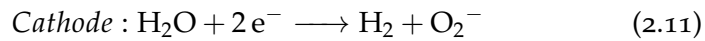
These high temperatures are beneficial for reducing thermodynamic and kinetic overvoltages, resulting in higher efficiencies (70-80% theoretically), but the high heat also quickly degrades components and the efficiency along with it (Lehner et al. 2014). Due to the high heat of operation, the system is not flexible to changes in load and takes as long as 30-45 minutes to start-up and shut-down. This delayed start, slow response rates to changes in load, and its high degradation make it unsuitable for dynamic renewable energy applications at this time. In addition, its early state of development also correlates to the highest electrolyser capital costs at this time.

As was reported in Section 1.6, this system can be used for co-electrolysis of both CO_2 and H_2 to produce syngas (a mix of H_2 and CO) which can be used for making liquid fuels, thus the potentials for this technology are strongest for applications in the industrial sector.

2.2.1.1 *Electrolyser Summary*

Out of the three electrolyser technologies, each has their advantages and disadvantages. Alkaline electrolysis has reasonably high efficiencies,

low costs, and can be installed in large capacities, but it degrades quickly and is slow to respond to changes in loads. PEME has higher costs, can respond quickly to changes in load, and can run at low part loads. It does have higher costs, lower efficiencies, and is only available in smaller sizes, but this is suitable for our applications in decentralised cases for fluctuating renewable loads. Solid oxide electrolysers are currently unsuitable for our applications due to their degradation under inflexible loads, high costs, and long start-up and shut-down times.

2.2.2 *Fuel Cells*

In this Section, Power-to-Power and Power-to-CHP pathways that are enabled with a hydrogen powered fuel cell are included, therefore the available fuel cell technologies will be overviewed in the same fashion as the electrolysers.

Fuel cells are electrochemical cells that convert a fuel, in this case hydrogen, and an oxidising agent, in this case oxygen, into electricity. There are two main types of fuel cells that are used in buildings: PEM fuel cells and solid oxide fuel cells. Both are based on the same technology as their similarly named electrolyser counterparts. The calculation of cell voltage in fuel cells is described in Eq. (2.13).

$$V = V_{ref} - V_{act} - V_{ohm} - V_{conc} \tag{2.13}$$

The same activation, ohmic, and concentration losses that were associated with additional electricity supply in electrolysers now decrease the electric output in fuel cells.

POLYMER ELECTROLYTE MEMBRANE FUEL CELLS
Polymer Electrolyte Membrane Fuel Cells (PEMFCs) are devices that take hydrogen and oxygen gas and produce electricity. They operate under the reverse half-cell reactions described in (2.9) and (2.10). These devices are popular for the same advantages and disadvantages as the electrolysers. They can cope with quick changes in loads, and since they do not have liquid electrolytes and are quite compact, they can be used in mobile applications. They also operate at high efficiencies under part-load operation. PEMFCs operate with temperatures of 60-80°C, therefore they can be used in low temperature heating applications. Their electrical efficiency is typically between 50-65%, but their total efficiency can go up until 95% if their waste heat is utilised. Since

their production has increased for transport applications, the costs for these units has dropped. They are also available in small capacities for individual homes, or in larger capacities for districts.

SOLID OXIDE FUEL CELLS

Solid oxide fuel cells are similar to their electrolyser counterparts and operate under the reverse half-cell reactions described in (2.11) and (2.12). These fuel cells also operate at temperatures of 700-1000 °C. Compared to other CHP technologies, solid-oxide fuel cells have the highest electrical efficiencies. They have higher electrical efficiencies compared to PEMFCs, but can have the same overall efficiency of 95% if the waste heat is used for other heating applications. Since this heat is at a higher temperature, it can be suitable for high temperature applications, but less heat is produce than with a PEMFC due to the higher electrical efficiency. These units, unlike the electrolysers, have been commercialised and actually comprise over 10% of the micro-CHP market (Dodds, Staffell, et al. 2015). Due to the high temperature, these fuel cells take a long time to start-up and shut-down and do not respond quickly to changes in the output, thus are not very dynamic devices. Like the electrolyser, they are prone to more rapid degradation than PEM fuel cells, especially when cycled. Their costs are also higher than those for PEMFCs.

2.2.2.1 *Fuel Cell Summary*

Due to the dynamic operation, high overall efficiency, and lower cost, PEMFCs are found to be preferred for dynamic building loads. Since the overall efficiency of both fuel cells are the same, and most buildings have higher heating demand than electrical demands, the lower electrical efficiency of PEMFCs is not a disadvantage unless the device is used in the summer. Many countries, such as Japan and Korea, advocate for the use of solid oxide fuel cells, but their lack of dynamic behaviour is a strong disadvantage for this work.

2.2.3 *Papers using P2H*

In this section, the review of literature is limited to those articles which use hydrogen as an energy carrier in the design of an optimal MES, but do not use the methanation stage of P2G.

The oldest paper reviewed in this space is by Vosen et al. (1999) who used optimisation to design for a hybrid hydrogen and battery storage system for off-grid energy supply. This paper looked into the design and control of a system that would use a battery for day shifting and the combination of an electrolyser, hydrogen storage, and a fuel cell for seasonal load shifting. The cost of the hybrid system was found to be lower than the cost of a stand-alone battery or stand-alone hydrogen system. This is one of the first proposals of using hydrogen as an energy carrier for long-term storage, and since the costs of these technologies have strongly decreased since 1999, particularly with PV and batteries, the current feasibility of these systems is likely to not only be advantageous for off-grid systems.

The second oldest paper reviewed to include hydrogen was the original publication of the Energy Hub model by Geidl, Gaudenz, et al. (2007), where hydrogen is included as an energy carrier in optimal power flow of MES. In this model, hydrogen is only mentioned as a possible energy carrier that can be produced via electrolysis and used for re-electrification.

This use of hydrogen in an Energy Hub was expanded by Hajimiragha et al. (2007). The authors further developed an optimal power flow model with additional hydrogen energy considerations, such as fuel cell vehicle charging infrastructure. Their optimisation model used hydrogen converters as well as district heat, natural gas, hydrogen, and electricity. Building energy demand and fuel cell vehicle demand, in the form of hydrogen, were included in the model.

A similar method using Energy Hubs was also developed by Maroufmashat, Fowler, et al. (2016). The authors created a Mixed Integer Linear Programming (MILP) model for four pre-defined urban districts over a year of operation. The optimisation included the design of hydrogen charging facilities within four urban districts.

Several other papers reviewed the design and optimisation of hydrogen storage systems for applications of on-site renewable facilities, such as wind farms or large solar installations in rural areas. X. Zhang et al. (2015) used a genetic algorithm to design a PV-Battery-Hydrogen system using a multi-objective analysis that minimised costs and maximised self-sufficiency. It was found that under pessimistic costs, batteries were a cheaper option, however under optimistic costs, hydrogen storage was competitive with batteries and performed better when accounting for grid power fluctuations. The heating energy carrier was not addressed

in this system.

Bernal-Agustín et al. (2010) created a techno-economical optimisation of PV-Wind systems with a grid connection. The model focused on power feed-in to the grid and selling of hydrogen. It was found that the selling price of hydrogen would have to be high to recover the capital costs for the system in 10 years (Bernal-Agustín et al. 2010).

Similarly, Korpas et al. (2006) developed an operation planning model for a wind-hydrogen model participating in power markets. When wind electricity production was in excess, hydrogen was produced via an electrolyser and stored. Electricity was then later produced via hydrogen in a fuel cell and was then sold back to the electricity grid on the spot market. Alternatively, hydrogen was also used directly for fuel cell vehicle charging. They used linear optimisation to determine the operational set points of an electrolyser and fuel cell using a receding horizon control strategy and participated in arbitrage to maximise profits. It was found that electricity prices must have a large variability for the fuel cell to be used, since the overall efficiency of the system is relatively low for electricity production. The authors recommended combining the scheduling model with an investment cost model and a long time horizon to estimate cost reductions and efficiency improvements over time in different power systems.

Petruschke et al. (2014) used a combination of a heuristic and linear optimisation structure to separate the optimisations for system configuration, technology sizing, and operation for a PV-Wind-Hydrogen system on an island. This paper states that it was able to reduce simulation time due to the separation of the sizing and operations optimisation which represents a multi-layer simulation approach. The paper investigated different percentages of renewable shares for the electric grid (heat demand was not considered) and found that the size of the hydrogen system was increased as the renewable share increased. Batteries and thermal storage were not considered in the model.

Li et al. (2017) used a bi-level optimisation for a stand-alone microgrid capable of providing electric power, cooling, heating, and hydrogen demands. This bi-level strategy applied a MILP to simulate the operation and a genetic algorithm to size the component decision variables. Uncertainties were taken into account using a Minimax robust optimisation approach. They also considered degradation of the storage technologies in the model and found that fuel cells, batteries, and electrolysers were sized larger when degradation was accounted for. The

uncertainty analysis found that higher levels of uncertainty resulted in larger sizes of storage to buffer the uncertainty in the demand and in the renewable forecasts.

Dufo-López et al. (2008) performed a triple-objective optimisation for the design of a PV-wind-diesel-hydrogen-battery system in Spain using a genetic algorithm. The three optimisations represented minimisation of costs, minimisation of emissions, and minimisation of unmet demand in kWh/year. The authors found that "Due to the high costs of the hydrogen components, energy storage in most solutions is done only using batteries".

Yang et al. (2016) investigated the optimal operation of residential, commercial, and industrial prosumers in a MES and found that the active participation of the prosumers played an important role in better response to time of use electricity prices and that peak shaving could be better managed for the community as a whole. Electricity, cooling, plug-in hybrid vehicles, and heating demands were all considered in this model, however only the dispatch was optimised, as opposed to the full design and operation of the system. In addition, only short-term storage with batteries and thermal storage were considered by Yang et al. (2016).

A major shortcoming of the assessed literature, with the exception of Dufo-López et al. (2008) and Yang Zhang et al. (2017), is the storage duration considered. One of the main benefits of P2H storage is its long storage cycle durations over months, thus it is able to store seasonal variations without time dependent losses.

One paper that considers seasonal hydrogen storage is that by Gabrielli, Flamm, et al. (2016). This paper compares two different horizon reduction methods for designing for a seasonal storage system with hydrogen (using an electrolyser, compressed hydrogen storage, and a variety of CHP engines). A multi-objective approach is used for this model, but the focus of this paper is on the horizon reduction methodology rather than benchmarking the cost-effectiveness and efficiency of the hydrogen storage.

Multiple studies exist that have used optimisation in the context of future energy systems to identify and assess strategies for reducing emissions. In Lunz et al. (2016), a methodological approach using Germany in 2050 was used with multi-objective optimisation for 29 scenarios selected from previous studies. This work focused on analysis at the national level (i.e., Germany) instead of MES at the neighbourhood

or district scale.

To assess the future feasibility of P2H systems, the MARKAL/ TIMES model (Simoes et al. 2017), which used linear optimisation to model future energy scenarios from a policy perspective, was applied to hydrogen technologies and power-to-gas in Sgobbi et al. (2016). In this study, the model was run for two pre-defined policy scenarios for the years of 2020, 2030, 2040, and 2050 for the EU. The results showed that hydrogen technologies were relevant for meeting long-term emission reduction targets and indicated that they might become economically feasible by 2040, particularly in the industrial sector.

SUMMARY OF P2H PAPERS

There is a large amount of literature that has been dedicated to P2H. Drawing upon the reviewed publications, the existing applications for multi-energy systems generally focus on larger energy systems, with many being on the national scale (Lunz et al. 2016; Simoes et al. 2017). Many of these large case studies are too simplified to consider long-term storage and are not well suited to assess the potential of distributed resources and storage, thus it is also important to investigate applications on decentralised neighbourhoods or districts. Other applications are limited to large renewable installations; such as wind farms or PV plants. These scenarios often only include the electrical energy carrier for demands and ignore the heating energy carrier.

After reviewing the papers in this section, we can identify that there is a gap of research in which the future evolution and planning of long-term P2H systems and short-term storage systems is not yet assessed in a decentralised multi-energy context. In this thesis, an optimisation model will be built in Chapter 3 and applied in Chapter 4 to evaluate the potential of long-term energy storage in multi-energy systems for two different case studies. This model will include both the heating and electrical energy carriers and integration with the natural gas grid. The model allows for coupling of both short-term and long-term storage technologies.

2.3 POWER-TO-METHANE

2.3.1 *Overview of Methanation Technology*

Before discussing the applications of P2M the state of the art in methanation technology will be discussed. As previously mentioned, methanation is based on the Sabatier reaction, which was shown in (1.3). This reaction requires both hydrogen, produced via electrolysis, as well as carbon dioxide which can be derived from several different sources. The Sabatier reaction is highly exothermic and an equilibrium reaction. The equilibrium constants depend strongly on temperature. Low temperatures have unfavourable reaction kinetics, therefore high temperatures and catalysts are used. These catalysts are typically Nickel catalysts, but Cobalt and Iron type catalysts can also be used (Lehner et al. 2014). There are two main categories of methanation: catalytic and biological.

CATALYTIC METHANATION
 Catalytic methanation has been used since 1902, but its applications for P2G are recent. It has been previously used in the oil and gas industry as a substitute for producing natural gas and was originally only used in industrial applications. It typically occurs at temperatures between 250-500°C. Due to how exothermic this reaction is, it is ideal for installation in locations where the high temperature waste heat can be used for other processes. There are several different reactor concepts that have been developed, but the most popular are the fixed bed reactors, fluidised bed reactors, and bubble column reactors. Fixed and fluidised bed reactors are the most used in practice.
Fixed bed reactors use catalysts that are placed in the bottom of the reactor forming a homogenous, solid, and static catalyst bed. A series of reactors are connected in a cascade, with intermittent gas cooling, gas recycling, and reaction heat removal between each reactor step. Temperature control is required to manage temperature peaks that can occur within the reactors.
Fluidised bed reactors are designed for an isothermal temperature profile in the reactor to prevent the hot spots that occur in the fixed bed reactors. This is achieved by the fluidisation of the catalyst particles. The movement of this fluid catalyst causes abrasion within the reactor. Due to the fluid isothermal temperature profile, the heat in the reactor is better managed and several reactors are not required. The result is a

design that is easier to control.

Bubble column reactors use a liquid heat transfer medium to try and achieve isothermal process conditions and to allow for better heat removal. This is similar to the design goal of the fluidised bed reactor, but the abrasion is reduced in this design. This design has typically three phases between the solid catalysts, the liquid heat transfer medium and the gaseous educts, thus the reaction kinetics and hydraulic operation are complex.

Each of these reactor types have been used for decades, but there is still continuous research works to improve the design due to difficulties with the catalysts, heat management, abrasion, and optimising reaction kinetics.

BIOLOGICAL METHANATION

As opposed to using the chemical catalyst route described above, bio-catalysts or enzymes can be used in a biological methanation system. Methanogenic bacteria produce these enzymes. The resulting reactions are described in (2.14) and (2.15)

$$CH_3COOH(g) \longleftrightarrow CH_4g + CO_2 \ \Delta G_R^0 = -33.0 kJ/mol \quad (2.14)$$

$$CO_2(g) + 4 H_2(g) \longleftrightarrow CH_4(g) + 2 H_2O(g) \ \Delta G_R^0 = -135.0 kJ/mol \quad (2.15)$$
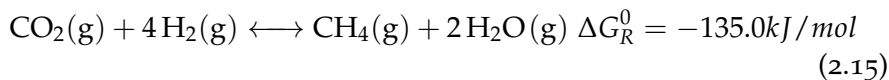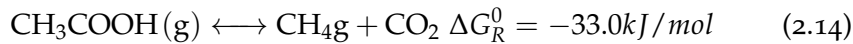
Reaction (2.14) is common in the decomposition of biomass, whereas (2.15) is used in certain biogas plants. In actual processes, this approach can be used in biogas plants or in separate reactors with different reactor designs. The advantage of biological methanation is that high temperatures are not required, thus the heat removal and control that is problematic with catalytic methanation is not a problem. The major problem is delivering the hydrogen adequately to the microbes to sustain a high reaction rate. Ultimately, biological methanation has never been used in large scale applications and is primarily used in the laboratory and in pilot plants. Although it is a promising advancement, it is not yet commercialised but is anticipated to have lower costs than catalytic methanation when developed.

2.3.2 *Papers using Power-to-Methane*

There are significantly fewer papers that look at P2M in this step, as it is best suited for natural gas grid injection and has lower round-trip

efficiencies, especially for decentralised systems. P2M is usually recommended on centralised grid scale applications for direct injection on the mass scale (e.g. Garmsiri et al. (2014)).

The first paper that looked into methanation as a pathway in a MES was the original Energy Hub paper by Geidl and Andersson (2006), where methanation is included as a conversion step in which the waste heat can be used for heating and methane can be used for cogeneration.

Simonis et al. (2017) investigated P2M for wind plants in Emden, Germany, as a method of utilising excess renewable energy and transferring it to the natural gas grid or local biogas-CHP plants. It was found that a 17 MW plant could absorb 68% of excess renewable energy in the area and could contribute to the decarbonisation of the natural gas grid.

Collet et al. (2017) performed both a techno-economic and life-cycle assessment of P2M upgrading technologies. It was found that P2M generates more emissions than direct injection with hydrogen and renewable electricity must be used to reduce the emissions further. It was also found that P2M had a higher environmental impact than biogas upgrading.

Reiter et al. (2015) performed a Life cycle assessment (LCA) of Power-to-Hydrogen and Power-to-Methane. It was found that the electric grid CO_2 intensity used had to be under 190 g CO_2/kWh to lower the global warming potential. It was also found that P2M had higher emission than P2H. The authors recommended utilising H_2 and CH_4 in the industrial and transport sectors.

Garmsiri et al. (2014) used a parametric analysis to determine the feasibility and size of P2H and P2M systems for a wind farm in Canada to inject H_2 and CH_4 into the natural gas grid.

Devlin et al. (2017) developed an economic dispatch model with an optimal gas flow model for the interconnected energy systems of Great Britain and Ireland. Surplus wind energy was considered for production of SNG to inject into the gas grid. Extreme weather conditions were assessed and it was determined that the gas system could withstand these extreme conditions.

Parra et al. (2017) looked into a comparison of the life-cycle for both P2H and P2M and assessed their potentials for providing six services: renewable premium for deep decarbonisation (100% renewable energy), hydrogen supply into industry, heat supply, oxygen supply, frequency control, a CO_2 levy. It was found that P2H was economically profitable

for all of these sectors, but P2M was found only to be profitable when using biomass gasification for 4 of these services and none when using CO_2 extracted from the air. The increased costs of the CO_2 captured from air and the lower efficiency with the methanation step made this pathways infeasible for all of the services mentioned.

There are few other papers that review the use of P2M for non-industrial applications. Much of the work in this area simply recommends injecting hydrogen into the natural gas grid directly, rather than converting to methane, and then managing the gas grid with higher fractions of hydrogen in it, even up to 17-20%. This is recommended in both Clegg et al. (2016) and Qadrdan et al. (2015).

SUMMARY OF P2M PAPERS

Out of the papers that have been collected that apply P2M in energy systems, none look specifically at decentralised energy cases or mobility applications. There are many papers that look at P2M in theory, such as in Power-to-Gas review papers, but all of the application papers are on the regional to national scale. Due to this research gap, P2M will be included in the P2X optimisation model in comparison to other pathways, such as Power-to-Hydrogen and Power-to-CHP in Chapter 5 and 6. The extension of producing SNG for the charging of natural gas internal combustion engine vehicles will also be investigated.

2.4 POWER-TO-MOBILITY

There are many studies in recent years that look into the diffusion or integration of Alternative fuel vehicles (AFV) technologies into the transport sector, however many of the models are based on different methodologies, have different system boundaries, and different scopes. As a result, they differ significantly in their findings.

One category of these models focuses solely on decarbonising the transport sector using techno-economic modelling to compare different AFV types. This is often done on the macro-scale. One of these studies is Offer et al. (2010), who conducted a techno-economic comparison of BEVs, FCEVs, and Fuel Cell Hybrid Electric Vehicle (FCHEV) for the year of 2030. The results indicate that by 2030, FCEVs could have similar lifetime costs to ICEV gasoline vehicles, however the lifetime costs of FCHEVs and BEVs were much lower than for FCEVs. A sensitivity analysis was also conducted and indicated that the model outcome was

sensitive to powertrain capital costs.

Similarly, Contestabile et al. (2011) performed a techno-economic analysis which compared the costs of ICEVs, Hybrid Electric Vehicles (HEVs), PHEVs, BEVs, FCEVs and FCHEVs in the year of 2030 assuming optimistic and pessimistic costs for four different car segments: super-mini, medium, multi-purpose, and luxury. It was predicted that, in the short-term, ICEVs and PHEVs will play a role, but in the future BEVs and FCEVs will be the powertrain technologies of choice required to meet energy targets.

Pasaoglu et al. (2012) developed an energy policy model to investigate the integration of different vehicle types in the European Union to meet 2050 targets. They determined that alternate fuel vehicles, such as BEVs, PHEVs, and FCEVs would be necessary to meet the emissions targets for transport in the European Union (EU) and that efficiency improvements with ICEVs were insufficient. As with Offer et al. (2010), Contestabile et al. (2011) and Pasaoglu et al. (2012), the charging infrastructure and the energy system for the fuel supply are not included in the model nor is the scheduling of charging of vehicles.

Gnann et al. (2015) conducted a review on the market diffusion of AFVs and their infrastructure. Their investigation found that the current assessment of the modelling of the diffusion of cars failed to integrate the infrastructure costs or constraints in adapting to new technologies. In addition, it is stated that at the time of the writing of the article, that there were limited optimisation papers that considered infrastructure and charging for multiple types of fuels or multiple types of vehicles (Gnann et al. 2015).

The next series of papers expand on the concept of comparison of powertrains for reducing carbon, however the investment costs and coordination of the charging infrastructure is also included on a macro scale. One example of this is Shafiei et al. (2015), who compared the adoption of hydrogen, biofuel, and electric vehicles in Iceland. This included the modelling of fuel prices, fuel supply, fuel stations, and fuel demand. Four scenarios were chosen: a business as usual scenario, a biofuels scenario, a hydrogen scenario, and an EV scenario. The emissions were shown to be the lowest in the biofuels scenario, followed by the hydrogen scenario and finally the EV scenario. However, the EV scenario was the most attractive in terms of reducing the total fuel demand and the lowest fuel costs. The hydrogen scenario was the most successful at reducing fuel imports. Although these scenarios

incorporate infrastructure costs and fuel supply in the modelling, the market integration of the different vehicle types from 2015 to 2050 is assumed in preset scenarios, rather than optimising or selecting the best diffusion of vehicle types.

Onat et al. (2014) looked at both the macro-economic as well as the life-cycle emissions for BEV, HEV, PHEV, and ICEV vehicles in the United States. This also included the investigation of social and economic costs of health problems due to pollution, and income generation by expansion of new industries. They looked at two scenarios for EV charging: one that supported charging with existing renewables integration, and one including solar charging stations. They found that electric vehicles reduce health costs associated with pollution from vehicle emissions and environmental costs due to emissions as much as 35% and 45% respectively. When comparing the life-cycle stages of materials extraction, production, manufacturing, operation, and end-of-life of the vehicles, it was found that manufacturing has the strongest social-economic impact and operation is the most significant for environmental impacts. BEVs outperformed all other vehicle times in all life-cycle analysis categories except for water usage. This analysis method used in this paper for both transportation and the charging structure is simplified and neglects to include the infrastructure, however the life-cycle analysis shows many important factors that all of the other previously discussed works neglect. This emphasises that the emissions and pollution in the manufacturing and processing stages are significant to both the environment and pollution related health effects and should not be neglected.

Dodds and McDowall (2014) conducted a review of transport models and their ability to integrate the required infrastructure and energy system analysis. They stated that the shortcoming of many of the above methodologies are that they only look at the transport sector and fail to integrate the energy systems that supply the charging of these vehicles. Since the charging infrastructure and operation of the energy sector also impacts the operation of the vehicles, the necessary interaction between the transport and the energy system is missing in the majority of discussed works. A few of these studies look directly into the integration of AFV charging with building energy systems, which is important since much of the vehicle charging is done at home with electric vehicles or can be done with hydrogen in a neighbourhood. However, almost all of the works that incorporate vehicle charging infrastructure

or scheduling along with building or grid energy requirements do so only for a single energy carrier.

One example is Tanguy et al. (2016), who looked at Vehicle-to-Building (V2B) or the integration of BEV or PHEV charging into the systems within a home's building system. In this paper, an optimisation schedules the collaborative charging of Electric Vehicles (EVs) to provide demand management to the electric grid of a university campus. The resulting optimisation model shows that V2B used for peak-shaving is financially optimal for participants.

Tan et al. (2016), described a review of optimisation models and necessary constraints for unidirectional and bidirectional Vehicle-to-Grid (V2G). This includes providing services to the grid such as spinning reserve, peak shaving and valley filling, grid regulation, reactive power compensation, etc., however it only considers operation for EVs as a service back to the grid and neglects looking at the energy system as a whole in terms of decentralised energy supply and energy demand Tan et al. 2016.

For the hydrogen energy carrier, Hajimiragha et al. (2007), which was mentioned in Section 2.2 looked at FCEV charging in the energy systems of commercial building complexes. Similarly, Maroufmashat, Fowler, et al. (2016) investigated the optimal operation of a hydrogen microgrid which included buildings and charging demand for hydrogen vehicles. This paper considered multiple energy carriers for the buildings (electric and heat demand) but did not consider any other vehicle types besides FCEVs.

Papers that include V2B or V2G, such as Tan et al. (2016) or Tanguy et al. (2016), add an important layer of complexity into transport modelling since they include the building energy demands and the buildings' energy systems limitations in renewable energy supply. However, the mentioned papers only look at vehicle charging with the electric energy carrier and disregard selection of the vehicle technologies themselves. As is noted by X. Zhang et al. (2015), the current system of smart-grids typically refers to the electrical grid, but neglects to consider both the natural gas grid and potential heating grids. When dealing with conversion technologies such as fuel cells, heat pumps, and electrolysers, the synergies between these grids can be exploited for higher efficiency. X. Zhang et al. (2015) also emphasised that the role of hydrogen has been currently underplayed, as it is able to provide storage at larger scales than batteries and also fuel cells can be used for Power-to-CHP. This

paper has strong support for hydrogen technologies, however there is no modelling conducted to demonstrate that these advantages will be strong enough to support their claims that FCEVs and stationary fuel cells will play important roles in future smart grids.

From looking at Section 2.2 and 2.3, there are many papers that clearly address building energy loads while neglecting mobility loads, but one model that does incorporate personal transport with different powertrain types and with the energy system model to supply the charging with multiple energy carriers is the widely used MARKAL/ TIMES model, which is advocated by Dodds and McDowall (2014) and is used widely by organisations such as the International Energy Agency (Loulou et al. 2004). The MARKAL/ TIMES model uses MILP to model both the energy system as well as the personal transport system on a national scale. However, due to the nature of the MARKAL model, only a few days of each year are simulated and storage over longer periods of time than a day are not considered, thus long-term storage is neglected. In addition, the model is on the macro-scale and includes the entire national energy system of the UK, thus it does not consider energy demands on the building level, nor does it consider bi-directional charging of electric vehicles. This must be investigated on the decentralised system level to see the level of local storage that will be required to support the increasing electrification.

SUMMARY OF POWER-TO-MOBILITY PAPERS

Although there are a large number of studies that investigate the future impact of AFVs in the transport sector, or in some cases on the wider energy system, there is a lack of papers that incorporate the optimal selection of vehicle powertrain technologies with the local energy system's renewable energy supply and infrastructure for multiple energy carriers or fuel types. This can be observed in Table 2.1, which compares the consideration of aspects focused on in this thesis with those of the reviewed papers. Models that do, tend to look on the macro-scale for an entire nation and, as a result, fail to integrate the vehicle charging schedule with the other energy demands of local networks, such as future heat pumps requirements, and building electricity loads. Bi-directional charging has also been identified as an important tool for balancing the energy grid (Tan et al. 2016), but many papers looking at V2G only focus on the electrical energy carrier and fail to

model other vehicle types that charge with other energy carriers.

An investigation of a Power-to-Mobility optimisation will be coupled with a building energy optimisation model in Chapter 5 and 6 including charging with multiple energy carriers.

Table 2.1.: Comparison of the transport papers and models reviewed.

Authors	Year	Vehicles considered	Model Type	Buildings considered?	Embodied Emissions considered?
Offer et al.	2011	ICEV-g, HEV, BEV, FCHEV, FCEV	Techno-economic	No	No
Contestabile et al.	2011	BEV, ICEV-cng, FCHEV, FCEV	Techno-economic	No	No
Pasaloglu et al.	2015	ICEV-g, BEV, PHEV, FCEV	Scenario development	No	No
Shafiei et al.	2015	ICEV, BEV, FCEV	Scenario development	No	No
Onat et al.	2014	HEV, PHEV, BEV	Life-cycle analysis	No	Yes
Dodds and McDowell	2014	IEV, HEV, BEV, FCEV	MARKAL-TIMES	No	No
Tanguy et al.	2016	BEV, PHEV	Linear Optimisation	Yes	No
Hajimiragha et al.	2007	FCEV	Optimal Energy Flow	Yes	No
Maroushmafat et al.	2006	FCEV	Energy Hub Optimisation	Yes	No

2.5 POWER-TO-HEAT

Power-to-Heat, is an outlier as a P2X pathway, since it only provides energy to the heating energy carrier rather than to the electricity energy carrier. In addition, it relies entirely on technology that has nearly reached maturity and is associated with high round-trip efficiencies when used over short time horizons. It has two disadvantages: (1) high time dependant losses and (2) it only works for the heating energy carrier, which limits its applications.

Yilmaz et al. (2018) did a study of the potential of implementing Power-to-Heat as a form of demand response in the EU. Potentials for demand response as high as 20 GW were predicted, however it was noted that most current applications are on the industrial scale, and that the regulatory adaptations would have to take place at the local level to incentivise use of Power-to-Heat in decentralised cases.

Bloess et al. (2018) conducted a review article of papers using optimisation for Power-to-Heat. It was found that Power-to-Heat is applicable both on the building level in decentralised cases, or within district heating systems. Power-to-Heat can be done using several methods and technologies, such as electric boilers or heat pumps, phase-change materials, thermal storage, or using the buildings thermal mass themselves to store the heat. It was found that the most cost effective and one of the most efficient paths was the simple combination of heat pumps and thermal storage tanks. Using the buildings thermal mass generally did not provide enough flexibility for these systems. The electricity price was a large factor in considering the economic attractiveness of Power-to-Heat. Production from rooftop PV systems was not specifically addressed in this work.

Kirkerud et al. (2017) investigated the potential of Power-to-Heat in Northern Europe and determined that it could store as much as 19.1 TWh of electricity. It was also concluded that, when used in district heating systems, it could increase the value of surplus renewable electricity and increase system flexibility for hours to weeks. Bloess (2019) looked similarly at the potential of Power-to-Heat in Germany and specifically the effects it would have on the rest of the energy system in 2050. It was concluded that a coupling of the power and heating sectors would be necessary, since electricity is considered the optimal energy carrier for 100% of the heating demand. Battery capacity was found to decrease when heating and electricity sectors were coupled vs. a

stand-alone power system, but the opposite was true for Power-to-Gas storage. The necessity of P2G systems was significantly elevated when these sectors were coupled in 2050 due to the long-term nature of this storage and its relatively low costs per kWh of storage.

In Salpakari et al. (2016), Power-to-Heat is investigated to manage the renewable energy surplus in Helsinki, Finland to meet the city's carbon neutrality goals by 2050. The specific system used includes heat pumps and electric boilers in a district heating system with stratified thermal storage tanks. It was found that heat pumps could deliver 50% of the required heat and could increase the self-use of electricity by 60-80%. Since district heating dominates the city in this case study, this pathway is easier to implement than in a decentralised setting.

On the building level, Bee et al. (2019) investigated a system with PV, a heat pump, and a battery to evaluate self-consumption rates in single-family homes. High performance buildings were used and it was found that self-consumption rates could be as high as 90% in warm European climates, but about 20% in a climates such as Helsinki. This paper did not look at the district approach, and limited the scope to applications in individual buildings.

SUMMARY OF POWER-TO-HEAT PAPERS

Power-to-Heat, according to the literature, is an attractive solution but only functions for one of the three energy carriers of interest. In a successful MES with both electricity and mobility loads, it will have to be coupled with other forms of storage to improve the self-sufficiency for the loads of all energy carriers. Nevertheless, it is a powerful tool to reduce the emissions in the fossil fuel dominated heating sector. It is especially proposed for cities in the north, where heating demands are higher. Power-to-Heat will be considered in both of the optimisation models built in Chapter 3 and 5.

2.6   POWER-TO-X COMPARISONS AND HYBRID STORAGE SYSTEMS

There are a series of papers that specifically compare different P2X pathways. One of the most cited from this group is a paper by Sternberg et al. (2015). In this paper, the authors compare a series of P2X energy pathways as storage devices. The authors use two key performance indicators, global warming reduction and fossil fuel reduction, to test

the different pathways using a life-cycle approach. They found that Power-to-Heat using heat pumps and Power-to-Mobility with electricity charging BEVs were the best pathways according to their performance indicators. The highest environmental impact reductions were achieved with batteries, and to a lesser extent, P2H. Although the results of this paper include many important conclusions about the pathways, there is no increased value for storage depending on the intended duration of storage, nor is it used in a practical case study and tested for self-consumption rates and suitability for meeting the required loads.

In another comparison work by Maroufmashat and Fowler (2017), different P2G pathways were compared for their value as storage technologies. They similarly found that P2H and mobility applications were the best suited pathways in terms of overall efficiency, but found that long-term storage of hydrogen or methane for re-electrification had some of the lowest round-trip efficiencies. This paper did not consider a life-cycle approach and is looking for applications for the centralised grid, however the conclusions nevertheless align with those of the previous paper. The disadvantage of comparing different P2X pathways separately is that the ideal solution could likely come from a system that uses combinations of different storage pathways, particularly if storages with different cycle durations can be combined.

Lewandowska-Bernat et al. (2018) reviewed the architectures of several different P2G pathways to investigate which are viable to support long-term and large-scale storage. P2G can also be used to provide flexibility in the grid, and also as an energy source for both heating and mobility. This paper summarises many of the discussion points about the benefits of P2G, however these must be tested in real case studies to see their feasibility in application. Without applying and comparing these pathways, the proposed advantages, such as providing long-term storage, reducing CO_2 emissions, and providing fuel for mobility, and the disadvantages, such as the cost and overall efficiency, must be benchmarked by designing systems for real case studies with electricity, heating, and mobility demands.

Zerrahn et al. (2018) reviewed the economics of different electrical energy storages. They demonstrated that "electrical storage needs may decrease if the electricity sector is broadened to also include flexible additional demand, for example heating, mobility, or hydrogen production". In addition, they proposed Power-to-X conversions as a valuable addition, but that further and more detailed research into these Power-

to-X conversions would be required to evaluate their effectiveness at managing surplus electricity.

Mathiesen et al. (2015) investigated strategies for 100% renewable energy and transport systems. In this paper, the authors argued that renewable energy must be integrated into the grids for each energy carrier to achieve 100% renewable energy and that sector coupling is necessary to reach 100%. This will include biomass, electrofuels, P2G storage, electric vehicles, and district heating system which use CHPs and heat pumps for heating. The authors hypothesised that combined storage configurations could support 100% renewable energy.

SUMMARY OF P2X COMPARISON PAPERS

The discussions of these papers reiterate some of the previously mentioned points. These include that Power-to-Mobility and Power-to-Heat are likely the best applications for P2X due to high efficiencies (see Table 1.2). These are followed by P2H and lastly P2M. The literature makes it clear that the economics of these technologies are uncertain and that their potentials must be further investigated. These pathways should be applied to real case studies with three energy demands considered (i.e., building heat, building electricity, and personal transport) to evaluate the economic cost and performance of these pathways and under which assumptions the pathways are recommended with uncertainty considered (Chapter 7).

When comparing these different pathways and storage methods, one detail these papers lack is the ability to couple different types of storages together, particularly with different storage durations, to create a better performing hybrid storage system. In this thesis, storage systems will have the potential to be used together in the optimisation model built in Chapter 3, to optimise synergies. The coupling of short-term storage methods with long-term storage methods are of particular interest.

2.7   INCORPORATING UNCERTAINTY INTO A MES OPTIMISATION

2.7.1   *Future Scenario Analysis*

Several of the papers attempt to use a scenario based format to incorporate parameter uncertainty into the analysis. These scenarios are often formulated in a similar fashion to the International Energy

Agency's World Energy Outlook (International Energy Agency 2018b) or Intergovernmental Panel on Climate Change's Special Report of Emissions Scenarios (Nakicenovic et al. 2000) and often use a version of the popular "Business as Usual", "New Energy Policy", and "Sustainable Development" scenarios. It is also common to use an "Optimistic" and "Pessimistic" scenario comparison as was done in X. Zhang et al. (2015) and Contestabile et al. (2011). Scenario analyses are popular due to the importance of major climate change reports, such as those from the International Energy Agency, the Intergovernmental Panel on Climate Change, and the Energy Information Administration in the United States.

Yazdanie et al. (2017) optimised the system design using the TIMES (Integrated MARKAL-EFOM System) framework for the MES of Basel in Switzerland for the years of 2010 to 2050. The technology focus was on boilers, heat pumps, solar thermal, PV, micro-CHP, batteries, and thermal storage. A cost optimisation using emission target constraints was performed. Four scenarios were used representing a business as usual scenario, a new energy policy scenario, and a gas variant that allowed for either restricted or unrestricted national imports of natural gas. It was found that building renovations were the most cost optimal measure that could significantly decrease energy demand. In addition, carbon taxes were found to strongly promote low-emission technologies such as heat pumps, rooftop PV, small gas CHPs, and batteries.

In Han et al. (2017), a MES was designed for the island of Jeju in South Korea. The authors used optimisation and scenarios framed as conventional energy, transitional energy, and 100% renewable energy scenarios to meet thermal, electrical, and vehicle demands on the island. Although the study is framed in scenarios, the evolution of the energy system over time is not considered. In Ren et al. (2010), a MILP model was used for the integration and evaluation of MES for a campus in Japan. The model used cost minimisation to decide which technologies would be the lowest cost for the campus to meet electricity and heating demand. The sensitivity study showed that the results were the most sensitive to energy demand, energy prices, and the carbon tax rate. Although batteries and thermal storage were considered, longer term storage was neglected and it was determined that installation of distributed renewables was not cost optimal but could be optimal if a higher carbon tax was established.

McKenna et al. (2017) created a techno-economic model based on an

energy autonomous network in residential buildings for MES. This paper tested various degrees of decentralisation with the lowest level being systems within single-family homes to the largest scale of 1000 single family households. The authors developed a MILP model to maximise electrical self-sufficiency in the community by selecting the optimal configuration, sizing and operation of micro-CHPs, photovoltaics, thermal and electrical storage, and boilers. It was found that cases with larger numbers of prosumers were able to be more electrically self-sufficient and less expensive than single family homes operating as stand-alone systems supplying. Single-family homes operating as stand-alone systems could meet 30% of their electricity needs but districts with more than 560 single family homes met almost 100% of the district's electricity demand. In this work, the heating demand was not considered in the calculation for self-sufficiency and long-term storage options were neglected.

In the mobility space, Shafiei et al. (2015), which was previously mentioned in Section 2.4, had a different scenario for each energy carrier type.

This type of scenario analysis is typically used because it requires little computational time to compute a few scenarios. This type of analysis is typically done with long and complex models which cannot afford the simulation time for a sensitivity or uncertainty analysis requiring thousands of runs. However, it is also very difficult to draw conclusions about the quantification of the uncertainty or the effect of specific parameters from the outcomes of these scenarios. To specifically assess uncertainty, a full uncertainty analysis needs to be performed.

To build on the scenario analyses in the research space, we will build our own scenarios in Chapter 4.

2.7.2 *Sensitivity Analyses*

Sensitivity analysis investigates the impact of the inputs on the outputs of the simulation. A local sensitivity analysis considers the sensitivity of selected input parameters on the output individually. Several of the works used in this analysis have included local sensitivity analysis in their case studies to look at the isolated effects of selected parameters on the outcomes of the models. Examples of this are included in Parra et al. (2017), Han et al. (2017), Gabrielli, Flamm, et al. (2016), Reiter et al. (2015), Collet et al. (2017), Li et al. (2017), X. Zhang et al. (2015), and

Devlin et al. (2017).

A global sensitivity analysis is a method in which the uncertainty of uncertain parameters are all simultaneously investigated rather than individually. Global sensitivity analysis was performed in MES optimisation in the work of Mavromatidis (2017). In this work, a global sensitivity analysis is conducted with a MES optimisation, however this work does not focus on the P2X technology pathways that are the focus of this work. Mavromatidis (2017) recommends the use of both Monte Carlo Filtering, as well as well as Sobol analysis and the Method of Morris to identify or rank input parameters according to how much the output of the results are influenced by these parameters. Since the economic and environmental predictions of these case studies are highly uncertain and the predictions for some of the cost assumptions can either make or break the feasibility of several of these P2X pathways in the future, an opinion that has been clearly expressed by many of the papers reviewed in this Chapter, it is in our interest to apply a thorough assessment of all input parameters to predict which pathways are the most optimal, given the present uncertainty, and which parameters the model is the most sensitive to.

This insight could be highly informative to system designers, energy planners, and policy makers that might need to decide whether or not this technology should be used in the future. With the importance of uncertainty and sensitivity analyses highlighted, our own analysis will be conducted in Chapter 7. In this Chapter, Monte Carlo simulations will be used for the uncertainty analysis and regional sensitivity analysis with Monte Carlo Filtering will also be performed.

2.8 CONCLUSIONS AND THESIS OUTLOOK

Much of the work done in the P2X section focuses on P2H, however many of these papers focus on applications for large scale renewable installations, such as large wind or PV stations, rather than decentralised cases. In addition, there are a variety of papers that focus on hydrogen to support long-term shifts in completely off-grid storage. The work on P2M is mainly focused on applications for direct injection into the grid on the centralised level and applications in distributed cases are rare.

Alternatively, Power-to-Mobility and Power-to-Heat are both popular choices in decentralised contexts and are recommended in both P2X comparison papers. Power-to-Mobility is particularly encouraged with

BEV, however it is not often simultaneously simulated in the context of hydrogen and SNG, particularly with long-term storage potentials. Most of the Power-to-Mobility papers focus solely on the transport energy carrier and neglect that the energy systems used for charging often have to supply building electricity and heating demands as well.

Power-to-Heat papers typically ignore electricity demands in buildings entirely and focus only on the heating energy carrier. Overall, the investigation of different pathways has not been applied in a decentralised energy system with applications for vehicle charging, building electricity, and building heating. In this context, this work attempts to address gaps in literature in three steps. Firstly, a model is developed to consider the long-term potential of hydrogen storage, while simultaneously considering battery and thermal storage (Power-to-Heat) for the short-term. Secondly, mobility is integrated into the first optimisation model to support Power-to-Mobility pathways. Lastly, a Monte Carlo uncertainty analysis and a global sensitivity analysis of the second optimisation model using Monte Carlo Filtering are conducted.

MES OPTIMISATION WITH P2X TECHNOLOGY PATHWAYS

In this Chapter, the development of the MES optimisation model is presented. This first includes descriptions of the different energy carriers used in the simulation, as well as the descriptions of the conversion and storage technologies used. The multi-objective function using the epsilon-constraint method will then be described. This chapter forms the basis for the description of the optimisation framework used throughout this work, as well as the descriptions of all building energy demand calculations, renewable potentials, and stationary technologies.

3.1 BACKGROUND AND CONTEXT

In Section 2.2, it was assessed that many of the work done on P2H system neglects applications to decentralised cases, instead focussing on large renewable installations. Secondly, the long-term potential of P2H as a method of shifting demands from summer production to winter production was also not looked at. Hybrid storage systems have also been mentioned in several papers to look at the managing of short-term storage with certain technologies and long-term storage with other technologies.

With this consideration, optimisation model built in this section is used to assess the potential of both long-term (hydrogen storage) and short-term (batteries and thermal) storage systems in decentralised neighbourhoods is developed using a multi-objective optimisation approach that minimises both costs and CO_2 emissions. To evaluate the performance of long and short-term storage systems in the future, multi-objective optimisation is proposed. Multi-objective optimisation allows us to use both an economic and environmental objective. Since our ultimate objective in this work is to implement systems that would allow us to deploy renewable energy to meet energy targets, the optimal solution space that ranges from the most cost effective system to implement the most environmental system to implement is of great interest.

The long-term storage potential of P2H, in particular, is focused on for its capability to shift renewable surpluses in summer towards demand later in the year.

3.2   MODELLING METHODOLOGY

The model developed in this Chapter represents a MES with six energy carriers: electricity, heating, hydrogen, natural gas (or SNG), CO₂, and water. The model optimises for the configuration and sizing of a selection of storage technologies, conversion technologies, and renewable technologies. A schematic representation of the technologies and energy grid included in the model are shown in Fig. 3.6.

Three grids are included in the model: a natural gas grid, a heating
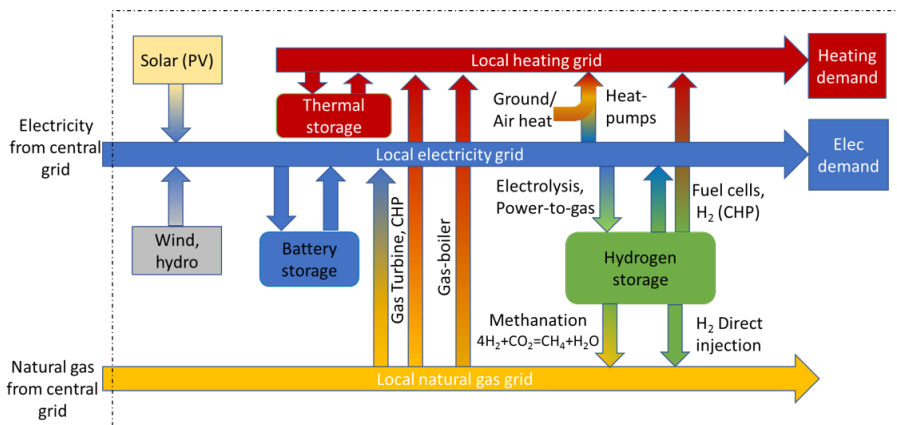
Figure 3.1.: A Schematic representation of the model with conversion technologies, storage technologies, and potential grid interactions.

grid, and an electricity grid. The renewable technologies include small-wind turbines, small-hydro, and solar PV located on the rooftops of the buildings under analysis. Conversion technologies in the model include heat pumps, electrolysers, fuel cells, gas turbines, and gas boilers. The storage technologies include battery storage, thermal storage, and hydrogen storage. From the hydrogen storage, a limited portion of hydrogen can be injected directly into the natural gas grid up to a volume concentration of 2%, as it is the upper limit in Switzerland

(Altfeld et al. 2013). The output production of these technologies must be used to meet the heating and electric demand of the neighbourhood.

The modelling of the MES can be split into three separate categories. Firstly, the buildings demand is simulated for a given set of buildings within the boundary of the defined energy system using a dynamic building model. Secondly, the renewable energy supply is simulated or real data is acquired from an existing system that is measuring total production. Lastly, a multi-objective MILP optimisation model that minimises both costs and CO_2 emissions is run for a full year with an hourly resolution. According to the objective, the optimal system configuration, sizing, and operation are selected as model outputs. These models are used in the work flow described in Fig. 5.1.

MILP is chosen as the optimisation method, as the optimisation problems are anticipated to be very large, with the number of decision variables in the millions. MILP optimisation ensures that a global optimisation can be found and is generally much faster than non-linear methods. Due to the need to linearise the dynamic operation of the technologies, binary variables are also required, thus eliminating linear optimisation.

In this work flow, the process begins with a selection of a set of buildings and a corresponding year of analysis. From the selected year, a weather file is chosen and the building geographic and statistical data are chosen. Based on the weather data of the associated case study and the building geography, the demands of the buildings are simulated. The weather file is chosen based on the case study location, the year of analysis, and the climate change scenarios, which will be further discussed in Section 4.1.1. In parallel, the renewable potentials are also simulated using weather and geographic data (Section 3.3). The outputs of these two models are the building demands and renewable energy potential profiles for the buildings over a one-year period. These profiles are then combined with the set of economic, technical, and environmental parameters that are determined based on the year of analysis and are used as inputs into the optimisation modelling (Section 3.4).
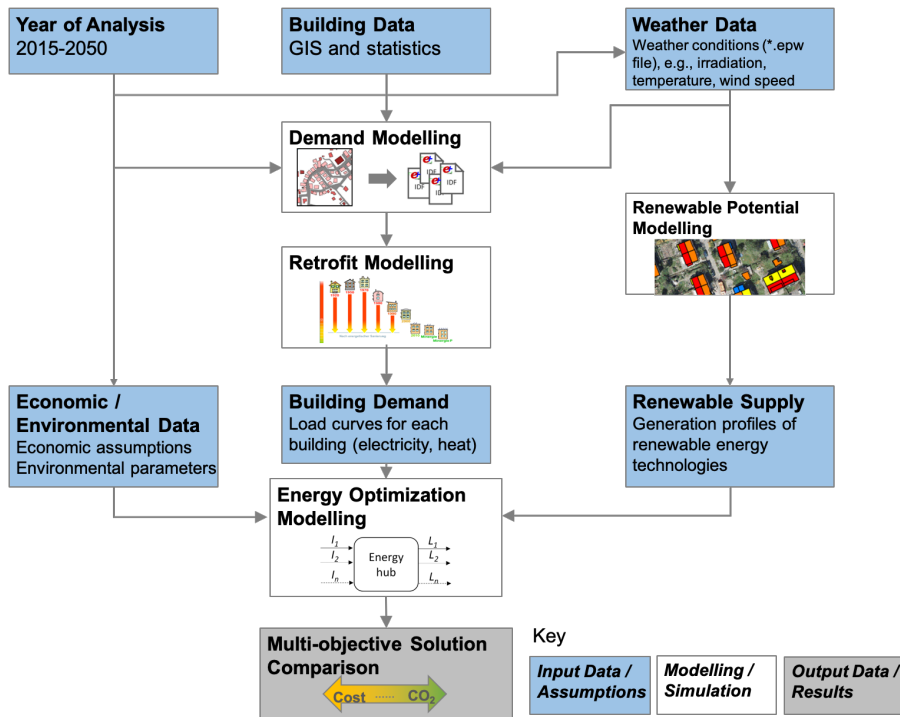
Figure 3.2.: Modelling work flow and analysis, including input data, sub-models, and output data.

3.2.1 *Building energy demand*

3.2.2 *Demand model*

To calculate the electricity and heating demand in the buildings, the dynamic building model developed in D. Wang et al. (2018) is used. The CESAR tool utilises EnergyPlus as a simulation engine to model hourly electricity, space heating, and domestic hot water demand for all buildings considered in the case studies. Using the building 2D geometry available in ArcGIS and the building height, 2.5D building geometry is constructed.

   In addition, statistics on building type, building age, and number of occupants are used to estimate both electrical and heating demand at hourly intervals for a year of operation. This data is taken from the Building and Apartment Registry (Gebäude und Wohnungregister") data from the Bundesamt für Statistik (2012). It assigns building construction, glazing ratio, and infiltration values based on building age and type. The standard U-values based on construction age can be found in Appendix B and the remaining parameters can be found in D. Wang et al. (2018). This information is combined into individual EnergyPlus building files for each building, taking neighbouring buildings as shading objects into account. The EnergyPlus files are combined with a weather file and simulated over a one-year period at hourly intervals to compute the 2015 base demand for the case studies.

3.2.3 *Retrofit modelling*

The current retrofit rate for residential buildings lies roughly between 1-2% of the building stock. The Swiss Energy Strategy 2050 has outlined retrofit rates based on building type (single or multi-family houses) and building age for the 'Weiter wie Bisher' scenario (equivalent to 'business as usual' or BAU) and the 'Neue Energiepolitik' scenario (equivalent to 'new energy policy' or NEP) which assumes at least a twofold increase in the renovation rate, relative to the BAU scenario(Prognos AG 2013). Based on these retrofit rates, buildings within the case studies are selected to be retrofitted and their constructions are updated according to the specifications in Appendix B. The future demand is then calculated for the years of 2020, 2035, and 2050 using the updated EnergyPlus files and the appropriate weather file for the location, year,

and climate change scenario. The retrofit rates applied to the building stock in 2035 and 2050 are summarised in Table 3.1. These rates are taken from both the Swiss Energy Strategy's BAU and New Energy Policy (NEP) scenarios (Prognos AG 2013).

Table 3.1.: Retrofit rate (% of buildings per year) for the years of 2015-2050 for the Swiss Energy Strategy's Business as Usual and New Energy Policy Scenarios. The rates are shown for both single and multi-family homes.

Retrofit Rate (SFH/ MFH)	Scenario	2016 - 2020	2021 - 2025	2026 - 2030	2031 - 2035	2036 - 2040	2041 - 2045	2046 - 2050
1981-1985	BAU	1.0/ 1.6	1.0/ 1.6	1.0/ 1.6	1.0/ 1.7	1.0/ 1.6	1.0/ 1.6	1.0/ 1.6
	NEP	1.5/ 2.1	1.8/ 2.5	2.1/ 2.6	2.4/ 2.7	2.6/ 2.7	2.6/ 2.6	2.4/ 2.6
1986-1990	BAU	0.7/ 1.0	0.8/ 1.2	0.9/ 1.4	0.9/ 1.5	0.9/ 1.6	1.0/ 1.6	1.0/ 1.6
	NEP	1.2/ 1.7	1.5/ 2.4	1.9/ 2.7	2.2/ 2.7	2.5/ 2.8	2.7/ 2.6	2.6/ 2.5
1991-1995	BAU	0.4/ 0.7	0.5/ 1.1	0.6/ 1.3	0.6/ 1.4	0.7/ 1.5	0.7/ 1.6	0.8/ 1.7
	NEP	0.8/ 1.2	1.3/ 2.1	1.7/ 2.5	2.0/ 2.7	2.2/ 2.8	2.6/ 2.7	2.7/ 2.6
1996-2000	BAU	0.4/0.4	0.5/ 0.8	0.6/ 1.0	0.6/ 1.1	0.7/ 1.2	0.7/ 1.3	0.8/ 1.4
	NEP	0.8/ 0.6	1.3/ 1.3	1.7/ 2.0	2.0/ 2.4	2.2/ 2.7	2.6/ 2.8	2.7/ 2.8
2001-2005	BAU	0.2/ 0.5	0.3/ 0.7	0.4/ 0.9	0.5/ 1.0	0.5/1.1	0.6/ 1.2	0.7/ 1.3
	NEP	0.4/ 0.5	0.7/ 0.9	0.9/ 1.5	1.3/ 2.0	1.6/ 2.4	1.9/ 2.8	2.2/ 2.8
2006-2010	BAU	0.1/ 0.1	0.1/ 0.3	0.2/ 0.4	0.3/ 0.5	0.4/ 0.8	0.5/ 0.9	0.5/ 1.0
	NEP	0.1/ 0.2	0.4/ 0.9	0.7/ 1.5	0.9/ 2.0	1.3/ 2.4	1.6/ 2.8	1.9/ 2.8

3.3 RENEWABLE TECHNOLOGIES

For each case study assessed in this thesis (see Section 1.7.2), the renewable potentials within the energy systems boundaries are exam-

ined. As the case studies include both rural, suburban, and urban settings, Geographical Information System (GIS) data is used to assess the amount of land on the building parcels and the natural resources in the immediate area. Light Detection and Ranging (LiDAR) data for both terrain and building elevation are acquired from Swisstopo (2014) of the area of interest to evaluate the rooftop geometry for available solar installations, as well as the shading from the terrain in the area. As decentralised renewables are the focus, wind or PV farms are not included, but rather rooftop PV, small-hydro, and small-wind potential that is suitable for installation in more populated areas.

ROOFTOP PHOTOVOLTAICS

A GIS approach based on the method developed in Mavromatidis, Orehounig, and Carmeliet 2015 is used to derive the hourly solar radiation on the rooftops, as well as to calculate the available area for solar installations. Using LiDAR data for the building elevation and digital terrain raster data from Swisstopo 2014, the rooftop slopes, aspects, area, and solar incidence on rooftop surfaces are calculated at a 2 m x 2 m resolution in ArcGIS for all non-protected buildings in the two case studies. This is demonstrated for the case studies of Zernez and Altstetten, shown in Fig. 3.3. Zernez is shown to have a total available PV installation area of $25,200m^2$ and Altstetten is shown to have $12,400m^2$.

Figure 3.3.: Solar radiation potentials of the cases with Zernez on the left and Altstetten on the right.

The temperature dependant efficiency of the PV panels is then calculated at each time interval using efficiency correlations based on the temperature of the panels. These correlations are described in Eq. (3.1) and (3.2) (Mavromatidis, Orehounig, and Carmeliet 2015).

$$T_{b,h}^{cell} = T_h^{amb} + \frac{NOCT - 20}{800} \cdot P_{b,h}^{solar} \ \forall \ b \in B, \ h \in H \qquad (3.1)$$

$$\eta_{b,h}^{PV} = \eta_{ref}^{PV} \cdot (1 - \beta_{ref} \cdot (T_{b,t}^{cell} - 25)) \ \forall \ b \in B, \ h \in H \qquad (3.2)$$

Here, B is the set of buildings with roofs under evaluation and H is the hourly time horizon of the model from 0 to 8760 hours in the year. $T_{b,h}^{cell}$ is the temperature of the rooftop PV panels, T_h^{amb} is the outdoor ambient temperature from the weather files, $NOCT$ is the nominal operating cell temperature, $P_{b,h}^{solar}$ is the hourly incident solar radiation per m^2, η_{ref}^{PV} is the reference PV cell efficiency, and $\eta_{b,h}^{PV}$ is the temperature adjusted PV cell efficiency.

3.3.1   Small-wind

Due to the low average wind speeds anticipated in the case studies (please see Chapter 4), a low speed wind turbine is proposed. The selected model is the Aventa LoWind Turbine (Aventa 2018). At a hub height of 18 m, the corrected wind speed is calculated with Eq. (3.3) and (3.4).

$$u = u_r \left(\frac{z}{z_r}\right)^{\alpha_{wind}} \qquad (3.3)$$

$$\alpha_{wind} = \frac{ln(u_2) - ln(u_2)}{ln(z_2) - ln(z_1)} \qquad (3.4)$$

Here, u represents the corrected wind speed, u_r represents the reference wind speed at a certain height, z is the height of the wind turbine, z_r is the height at which the reference wind speed is taken, and α_{wind} is a coefficient that represents the rate of wind speed increase as a function of height that can be solved with Eq. (3.4). In Eq. (3.4), u_1 and z_1 refer to the wind speed measurement and height at one height above the ground and u_2 and z_2 refer to the wind speed measurement and height at a second height. For alpha to be calculated, measurements should be taken at both heights. The power curve for the selected wind turbine

is then used to correlate hourly power production depending on the corrected wind speed, as seen in Fig: 3.4.

In this Figure, it can be seen that the turbine has a cut-in speed of
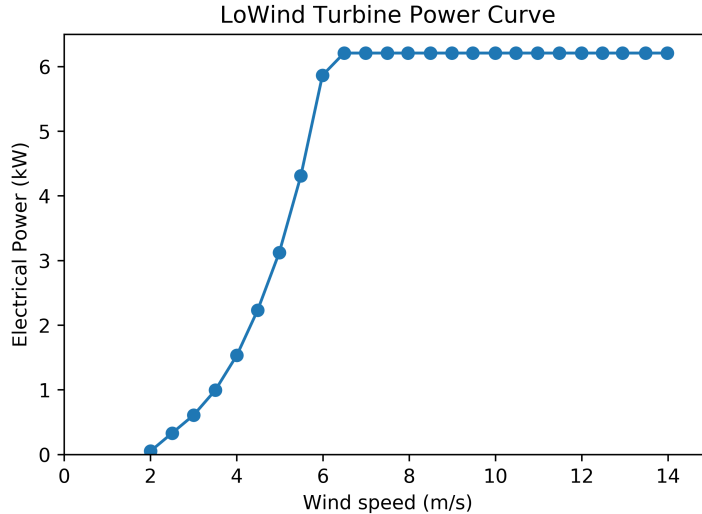
Figure 3.4.: Aventa LoWind low speed wind turbine power curve.

2 m/s and a maximum power of 6.2 kW. Additionally, the maximum wind speed of operation is 14 m/s, above which the turbine must be shut off.

3.3.2 *Small-hydro*

The potential of a 2.3 MW micro hydro plant is assessed for a river in Zernez (described in Section 1.7.2.1). Flow rates are provided for a potential site in the nearby river that is currently not utilised for hydropower. These measured volumetric flow rates are aggregated into hourly intervals to calculate the available energy potential over the year using Eq. (3.5),

$$P_{hydro,h}^{Potential} = \eta_{turbine} \rho g Q_h H \tag{3.5}$$

In Eq. (3.5), $P_{hydro_h}^{out}$ is the generated hydropower in kWh, $\eta_{turbine}$ is the turbine efficiency, g is the acceleration due to gravity, Q_h is the volumetric flow rate in m^3/s, and H is the effective pressure head of water across the turbine in meters. In this case, the turbine efficiency

is assumed to be 80%, as it is a smaller turbine in a micro-hydro plant (Paish 2002).

3.4   ENERGY OPTIMISATION MODELLING

For the MES optimisation model itself, multi-objective optimisation with MILP is used. This type of modelling is based on the 'Energy Hub' concept (Geidl and Andersson 2006), which was previously mentioned in Section 2.1. The model uses a series of constraints that represent conversion technologies, storage technologies, distribution grids, and other factors. In this type of optimisation, the decision variables represent the selection of the technology configurations, technology sizes, and operation of the technologies at hourly time steps over a one-year period (8760 hours). The model optimises the sizes of the technology units, technology performance, network performance, and operation of the system. In this model, energy must be balanced from energy potentials to energy demands while trying to optimise a certain objective function. The demands are usually energy loads for buildings or other sectors and the potentials are either renewable energy or energy carriers that can be purchased, such as electricity, natural gas, or oil. The energy carriers in this Chapter include electricity, heating, hydrogen, natural gas (or SNG), CO_2, and water. It is noted that although CO_2 and water are not typically considered energy, they are used for methanation and electrolysis to produce methane and hydrogen and are thus treated as energy carriers. Most 'Energy Hub' models try to optimise for minimal costs, but sometimes other objectives such as minimal emissions or maximisation of profit can be performed.

Rather than using the typical days or rolling horizon methods for this optimisation, a full horizon (8760 hourly time steps) is used to accurately assess the long-term storage system potential in the model. This decision results in a computationally intensive model, since the duration of the solving of the model takes significantly longer with a model with more decision variables. This is especially true when the model has binary or integer decision variables for each time step.

3.4.1 *Optimisation Selection of the renewable technologies*

ROOFTOP PV

In the optimisation model, the installed PV area on each rooftop is one of the decision variables. The maximum available area for installation on each building ($A_{PV,b}^{max}$), the hourly solar radiation on each rooftop surface ($P_{b,h}^{solar}$), and the efficiency $\eta_{b,h}^{PV}$, are used to calculate the potential solar output. The maximum solar area and the calculated solar output are calculated with Eq. (3.2) and (3.7).

$$A_{PV,b}^{cap} \leq A_{PV,b}^{max} \ \forall \ b \in B \tag{3.6}$$

$$P_{PV,b,h}^{out} = A_{PV,b}^{cap} P_{b,h}^{solar} \eta_{b,h}^{PV} \ \forall \ b \in B, \ h \in H \tag{3.7}$$

Here, $A_{PV,b}^{cap}$ is the optimised area of PV installed on each rooftop and $P_{PV,b,h}^{out}$ is the hourly power output of PV on each rooftop surface.

WIND TURBINES

In the optimisation, an integer value is used to select the optimal number of wind turbines, with the turbine number being represented as an integer decision variable. The upper limit constraint on the turbines is presented in Eq.: 3.9.

$$N_{wind,elec}^{cap} \leq N_{wind,elec}^{max} \tag{3.8}$$

$$P_{wind,elec,h}^{out} = N_{wind,elec}^{cap} \cdot f(u_h) \tag{3.9}$$

Here, $N_{wind,elec}^{cap}$ is the number of installed turbines, $N_{wind,elec}^{max}$ is the maximum number of turbines, $P_{wind,elec,h}^{out}$ is the hourly output from all the turbines to the grid, and u_h is the hourly wind speed. The $f(u_h)$ represents power curve from the turbines used to calculate the electrical output power from the wind speed shown in Fig. 3.4. Since wind turbines need to be placed at least three rotor diameters away from each other and from buildings, Zernez was determined to be the only case study with enough space to place the turbines since Zuchwil and Altstetten are surrounded by other buildings. It is approximated from a GIS analysis that 60 small-wind turbines at a hub high of 18 meters could be placed in the vicinity of Zernez with a clearance of three rotor diameters.

SMALL HYDRO

The small hydro system used in this model is of fixed capacity, depending on the project site evaluated in the Zernez case study, which will be later described in Chapter 4. This site is fixed at 2.3 MW, thus it is modelled with a binary value in the optimisation to indicating whether it is selected or not selected in the results. Its output is enforced with the constraint described in Eq. (3.10)

$$P_{hydro,h}^{Out} = P_{hydro,h}^{Potential} \cdot \delta_{Hydro} \qquad (3.10)$$

3.4.2 *Dispatchable conversion technologies*

Dispatchable conversion technologies include heat pumps, gas boilers, Micro-Gas Turbine (MGT), PEMFC, and PEME. The operation parameters of each technology are based on the sizing of the technology.

ELECTROLYSERS

Electrolysers are the first component in the P2H pathway. PEMEs are chosen for this model due to their quick responsiveness, flexibility, ability to withstand higher degrees of cycling than alkaline electrolysers, and ability to produce pressurised H_2 (Götz et al. 2016). In this model, the PEME is assumed to produce hydrogen at a pressure of 10 bar. Due to the complex part-load performance of PEMEs, a Piecewise Affine (PWA) approximation is used to model the part-load performance. This is further discussed in Section 3.4.2.1.

FUEL CELLS

Fuel cells are the second technology included in the P2H configuration. As was mentioned in Section 2.2.2, it is a CHP technology which runs on hydrogen and oxygen (from the air). As opposed to other CHP technologies, fuel cells have a higher electrical efficiency than a thermal efficiency. PEMFCs are chosen due to their increased flexibility and responsiveness as opposed to solid-oxide fuel cells (Götz et al. 2016). Solid-oxide fuel cells have higher electric efficiencies, however their high temperature operation (700-1000°C) results in a slow response to changes in load. Due to the complex performance curve of PEMFCs, PWA linear relationship is used to simulate the part-load electrical and thermal efficiency curves.

MICRO-GAS TURBINES

Micro-gas turbines are micro CHP devices that run on natural gas. They are modelled based on Capstone MGT which provides their efficiency curves for both electricity and heat for all of their MGT sizes on their website (Capstone Turbine Corporation 2017). A PWA approximation with two segments of this curve is then used for both electricity and heat.

GAS BOILERS

Gas boilers are the most common heating device in Switzerland and one of the cheapest to install and operate. They emit slightly less CO_2 than oil boilers, but are still entirely reliant on imported natural gas which is purchased from the grid. Gas boilers are modelled using a constant efficiency an efficiency of 90% and a minimum part-load restriction of 5%.

HEAT PUMPS

Heat pumps are assumed in the case studies, but due to the low temperatures in winter, a linear correlation between Coefficient of Performance (COP) and the heat source temperature from Sanner (2003) is used to model the heat pumps. This relationship is dependent on the heat source temperature and the delivered heat temperature which is assumed to be 70 °C for district heating applications. This relationship is calculated with Eq. (3.11). The minimum part-load operation is 15%.

$$COP_h^{GSHP} = 0.0567 T_h^{evap} + 2.4 \qquad (3.11)$$

The number of heat pumps installed is limited by the number of boreholes available for placement. A GIS analysis can be performed on the parcel area of a given group of buildings. Boreholes can then be placed with a minimum radius of 10 m apart from each other and from buildings. For more details on GIS borehole placement, please refer to Miglani et al. (2016).

METHANATION

It is possible to convert carbon dioxide and hydrogen to methane via methanation. This methane can be used in place of natural gas with no limitations on injection into the natural gas grid. The chemical reaction of methanation is performed in fixed-bed Catalytic Methane Reactor (CMR) and a CO_2 supply is required for the reaction. This

carbon dioxide gas must be purchased. The most common ways to source CO_2 are either by capture from the air, capture from industrial emissions (such as cement production), or capture from biogas production. Capture from air is currently expensive as it is energy intensive, and can be as expensive as 260 Swiss Francs (CHF) per ton (Parra et al. 2017). Alternately, CO_2 collected from biogas and cement production can cost on the range of 40-80 CHFs per ton. Methanation can have a delayed start-up of up to 30 minutes, therefore its output is limited on start-up due to these delays. The emissions from the energy consumption of the CO_2 are accounted for by using the life-cycle value for CO_2 production, which is assumed to be 0.74 kg CO_2-eq/kg CO_2 (Wernet et al. 2016) in Chapter 5.

3.4.2.1   *Piecewise Affine Technologies*

To properly reflect part-load operation of the PEMFC, PEME, and MGT, PWA Gabrielli, Gazzani, et al. 2018. The purpose of this work was to develop accurate reduced order models which could be used in linear optimisation. To do this, the part-load curves for PEMFCs and PEMEs are split into four segments and the MGT curve is split into two which reflect the optimised minimal error in representing the non-linear model. This method is defined with Eq. (3.12) and (3.13). For further details on the development of these reduced order models, please refer to Gabrielli, Gazzani, et al. 2018.

$$P_{t,f,n,h}^{out} = \alpha_{t,f,n} \cdot P_{t,f,n,h}^{in} + \beta_{t,f,n} \cdot S_{t,f,h}$$
$$\forall \, n \in N, \; h \in H, t \in [PEMFC, \; PEME], \; f \in [Elec, Heat, H2] \tag{3.12}$$

$$S_{t,f,h} \cdot P_{t,f,n}^{min} < P_{t,f,n,h}^{out} \leq S_{t,f,h} \cdot P_{t,f,n}^{max}$$
$$\forall \, n \in N, \; h \in H, t \in [PEMFC, \; PEME], \; f \in [Elec, Heat, H2] \tag{3.13}$$

Here, N represents the number of segments in the approximation. $P_{t,f,n,h}^{out}$ is the output of the conversion technologies (hydrogen for PEMEs and electricity for PEMFCs) and $P_{t,f,n,h}^{in}$ is the input power to the conversion technologies (electricity for PEMEs and hydrogen for PEMFCs). $\alpha_{t,f,n}$ and $\beta_{t,f,n}$ are constants of the part-load curve derived for each technology. Lastly $P_{t,f,n}^{min}$ and $P_{t,f,n}^{max}$ represent the lower and upper breakpoints of each segments respectively. These parameters for both PEMFC and PEME can be found in Table 3.2. In Eq. (3.12) and (3.13), the term $S_{t,f,h}$ represents the multiplication $P_{t,f}^{cap} \cdot \delta_{t,f,h}$. This is the multiplication

Table 3.2.: Piecewise affine approximations for PEMFC and PEME part-load performance curves.

Technology	PEME	H2- air PEMFC		MGT	
Carrier	Hydrogen	Electric	Ther-mal	Electric	Ther-mal
Alpha	{0.60, 0.56, 0.53, 0.51}	{0.59, 0.54, 0.50, 0.47}	0.39	{0.36, 0.33}	0.65
Beta	{-0.01, 0.00, 0.01, 0.03}	{-0.00, 0.02, 0.06, 0.11}	0.00	{-0.02, 0.00}	0.00
Break-points (X-axis)	{0.07, 0.09, 0.22, 0.53, 1.00}	{0.21, 0.53, 0.87, 1}	{0.00, 1.00}	{0.06, 0.66, 1.00}	{0.00, 1.00}
Break-points (Y-axis)	{0.01, 0.05, 0.12, 0.28, 0.53}	{0.12, 0.30, 0.47, 0.53}	{0.00, 0.39}	{0.01, 0.22, 0.33}	{0.04, 0.41, 0.625}

of two decision variables, thus resulting in a non-linear constraint. The product of these two variables is linearised by replacing $P_{t,f}^{cap} \cdot \delta_{t,f,h}$ with the term $S_{t,f,h}$ using the series of constraints from Eq. (3.14) - (3.16).

$$S_{t,f,h} \leq P_{t,f}^{max} \delta_{t,f,h} \ \forall \ t \in [PEMFC, \ PEME], \ f \in F, \ h \in H \qquad (3.14)$$

$$S_{t,f,h} \leq P_{t,f}^{cap} \ \forall \ t \in (PEMFC, \ PEME), \ f \in F, \ h \in H \qquad (3.15)$$

$$S_{t,f,h} \leq P_{t,f}^{cap} - \cdot P_{t,f}^{max}(1 - \delta_{t,f,h}) \ \forall \ t \in (PEMFC, \ PEME), \ f \in F, \ h \in H \qquad (3.16)$$

The approximations for both PEMEs and PEMFCs are shown in Fig. 3.5.

3.4.3 *Other Conversion Technology Constraints*

The remaining conversion technologies (i.e. gas boilers, heat pumps, and methanation) have less complex part-load operations, thus piecewise affine assumptions are not used. The remaining technologies and their constraints are described in the following section.
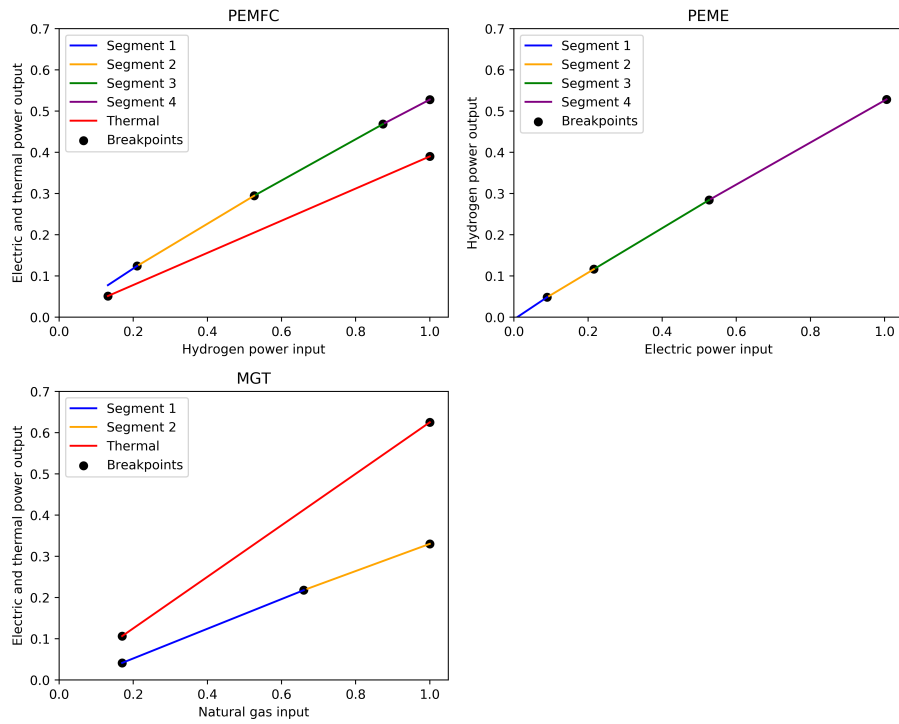
Figure 3.5.: Piecewise-affine approximations for PEMFCs, PEMEs, and MGTs.

3.4.3.1 *Constraints for Linear Conversion Technologies*

The maximum capacity for gas boilers and heat pumps are modelled with the series of constraints from Eq. (3.17) to (3.19).

$$P_{t,f}^{cap} = P_{t,f}^{max} \cdot \delta_t \ \forall \ t \in [GB, HP], f \in F \tag{3.17}$$

$$P_{f,b,h}^{out} = P_{t,h}^{in} \cdot \eta_{t,f,h} \ \forall \ t \in [GB, HP], \ f \in F, \ h \in H \tag{3.18}$$

$$P_{t,f,h}^{out} \leq P_{t,f}^{cap} \ \forall \ t \in T, \ f \in [GB, HP], \ h \in H \tag{3.19}$$

Here, F is the set representing the energy carriers included in this model (i.e., electricity, heat, hydrogen, and natural gas). In Eq. (3.17) and (3.19), P_t^{cap} refers to the installed power of each technology, $P_{t,f}^{max}$ refers to the maximum size, in kW of output, that can be installed, and δ_t is a binary variable that indicates whether a particular technology is installed. In Eq. (3.18) $P_{f,b,h}^{out}$, $P_{t,f,h}^{in}$, and $\eta_{t,f}$ refer to the output, input, and efficiency of each technology respectively.

To represent part-load operation appropriately, a minimum part-load constraint is used to ensure that the technologies are operated above their minimum operational range. This is enforced with Eq. (3.20).

$$S_{t,f}^{cap} \cdot PL_t^{min} \leq P_{t,f,h}^{out} \ \forall \ t \in T, f \in F, h \in H \tag{3.20}$$

Here, PL_t^{min} is the minimum part-load fraction and $S_{t,f}^{cap}$ represents $P_{t,f}^{Cap} \cdot \delta_{t,h}^{on/off}$ or the multiplication of the installed capacity by a binary variable which indicates whether or not the device is on or off. This in enforced again with Eq. (3.14) - (3.16).

3.4.3.2 *Start-up and Shut-down Constraints of Dispatchable Conversion Technologies*

In addition to the minimum part-load constraint, the start-up and shut-down behaviour of devices are also considered. Many devices, such as the PEMFC, PEME, and the CMR, require start-up and shut-down periods, in which they consume energy but do not output energy. These Start-up (SU) and shut-down Shut-down (SD) periods can take as long as 5 minutes for a PEMFC or as long as 30 minutes for a CMR. Both the PEMFC and the PEME can also be put in standby mode, in which they are turned on and consume energy, but do not output

energy. In this state, they can quickly respond to changes in load thus are not subjected to the start-up or shut-down period constraints. To realistically represent these technologies, two more binary variables for start-up ($\delta_{t,h}^{SU}$) and shut-down ($\delta_{t,h}^{SD}$) are used. These binary variables are controlled related to the on/off binary with Eq. (3.21).

$$\delta_{t,h}^{SU} - \delta_{t,h}^{SD} = \delta_{t,h}^{on/off} - \delta t, h - 1^{on/off} \ \forall \ t \in T, \ h \in H \tag{3.21}$$

With this constraint, $\delta_{t,h}^{SU}$ only has a value of one when the device is started and $\delta_{t,h}^{SU}$ is one when the device is shut-down. With these binaries, the operation during these states can be controlled with Eq. (3.22) and (3.23).

$$P_{t,f}^{cap} \cdot SU_t^{max} \geq P_{t,f,h}^{out} - M \cdot (1 - \delta_{t,h}^{SU}) \ \forall \ t \in T, \ h \in H \tag{3.22}$$

$$P_{t,f}^{cap} \cdot SD_t^{max} \geq P_{t,f,h}^{out} - M \cdot (1 - \delta_{t,h}^{SD}) \ \forall t \in T, \ h \in H \tag{3.23}$$

Here, SU_t^{max} is the maximum fraction of output on start-up and SD_t^{max} is the maximum fraction of output on shut-down.

3.5 STORAGE TECHNOLOGIES

HYDROGEN STORAGE

The hydrogen produced from the electrolyser is stored in compressed gaseous cylinders up to 90 bars of pressure. The compression energy is calculated with Eq. (3.24) and (3.25). The sizing of the compressor is done with Eq. (3.26).

$$W_{ideal} = \overline{Z}RT_1 \frac{\gamma}{\gamma - 1} \left[\left(\frac{Pr_2}{Pr_1} \right)^{\frac{\gamma-1}{\gamma}} - 1 \right] \tag{3.24}$$

$$P_{comp,elec,h}^{in} = \dot{n}_{H2,h} \frac{W_{ideal}}{\eta_{isentropic} \cdot \eta_{mech}} \tag{3.25}$$

$$P_{comp,elec,h}^{in} < P_{comp,elec,h}^{cap} \ \forall \ h \in H \tag{3.26}$$

In Eq. (3.24), $\overline{Z}$ is the compressibility factor of hydrogen at a certain temperature and pressure, R is the ideal gas constant in kJ/kmol-K, T_1 is the inlet temperature in Kelvin, P_1 and P_2 are the inlet and outlet pressures respectfully, and γ is the specific heat ratio of the gas (C_p/C_v). This computes the work of isentropic compression as a function of

the final pressure per unit mass. The electricity of compression is calculated with Eq. (3.25), where $n_{H2,h}$ is the hourly molar flow rate of hydrogen production, $\eta_{isentropic}$ is the isentropic efficiency of the compressor, which is assumed to be 80% (Maroufmashat, Fowler, et al. 2016) and η_{mech} is the mechanical efficiency of the electric motor, which is assumed to be 90%. The sizing of hydrogen compressors ($P_{comp,elec,h}^{cap}$) is performed based on the energy required electricity to compress the maximum hourly hydrogen production flow rate in the year. The state of charge of the hydrogen tank is calculated at each hourly time step with Eq. (3.27). The sizing of the hydrogen storage is then regulated with Eq. (3.28) and the maximum state of charge is regulated with Eq. (3.29).

$$m_{H2,h}^{SOC} = m_{H2,h-1}^{SOC} + m_{PEME,H2,h}^{out}\dot{}\Delta T - m_{PEMFC,H2,h}^{in}\dot{}\Delta T - m_{H2,h}^{\dot{DI}}\Delta T \; \forall\, h \in H \tag{3.27}$$

$$m_{H2}^{cap} \leq m_{H2}^{max} \tag{3.28}$$

$$m_{H2,h}^{SOC} \leq m_{H2}^{cap} \; \forall\, h \in H \tag{3.29}$$

In this equation, $m_{h,H2}$ is the current mass of hydrogen stored, $m_{h-1,H2}^{SOC}$ is the state of charge of the storage (in kilograms) in the last time step, $m_{P\dot{E}ME}\Delta$ is the hydrogen produced by the electrolyser, $m_{PEMFC,H2,h}^{in}\dot{}\Delta$ is the hydrogen consumed by the fuel cell, and $m_{H2,h}^{\dot{DI}}$ is the hydrogen used for direct injection into the grid. It is assumed that the decay of the storage in the tank is zero (i.e., has no leaks) and that the system has an efficiency of 99% on discharge. In addition, direct injection of natural gas into the grid is assumed to not require additional compression power as it is being injected into the low pressure part of the gas grid which is typically less than 70 bars in European gas grids compared to the 90 bar stored in the hydrogen tanks. The hydrogen storage maximum capacity is sized in kg of hydrogen. In addition, the seasonal storage component of the simulation must be included to initialise the first time step of the year to be of the same state of charge of the last time step, as is shown in Eq. (3.30).

$$m_{h=1,H2}^{SOC} = m_{h=8760,H2}^{SOC} \tag{3.30}$$

BATTERIES AND THERMAL STORAGE

Simplified battery and thermal storage models are assumed for this

work. The models are described in Eq. (3.31) - (3.33), with Eq. (3.31) describing the energy balance in both storages, Eq. (3.32) restricting the state of charge below the capacity, and Eq. (3.33) limiting the maximum discharge and charge rates.

$$
E_{s,h}^{SOC} = E_{s,h-1}^{SOC} \cdot \eta_s^{decay} + \eta_{s,h}^{ch} P_{s,h}^{ch} \Delta T -
$$
$$
\frac{1}{\eta_s^{dch}} P_{s,h}^{dch} \Delta T \ \forall \, s \in (Bat, \ TES), h \in H \tag{3.31}
$$

$$
E_{s,h}^{SOC} \leq E_s^{cap} \ \forall \, Bat, \ TES \in S, \ h \in H \tag{3.32}
$$

$$
P_{s,h}^{ch/dch} \leq E_s^{cap} f_s^{ch/dch} \ \forall \, s \in (Bat, \ TES), \ h \in H \tag{3.33}
$$

Here, E_h^{SOC} is the storage level in the battery, $P_{s,h}^{ch/dch}$ are the charge and discharge powers in kW, $\eta_s^{ch/dch}$ represents the charging and discharging efficiencies, and η_s^{decay} is the rate at which the stored energy decays in an hour. For this model, the charging and discharging efficiencies of lithium-ion batteries are assumed to both equal 92% and the decay is set to 0.1% per hour. For the thermal storage, the charging efficiency, discharging efficiency, and decay are set based on the work of Stadler et al. (2008) to 90%, 100%, and 1% per hour. $f_s^{ch/dch}$ describes the limit on the discharge and charging rates as percent of maximum capacity that can be charged or discharged within an hour. For batteries, based on a C-rate of 0.5C, this is assumed to be to 50%. For thermal storage, this is set again by Stadler et al. (2008) to be 25% .

3.5.1 *Network Losses and Direct Injection*

In the model, network grids for electricity, heating, and natural gas are included. A transformer efficiency to the low-voltage grid of 98% was assumed. The heating network is approximated with a minimum spanning tree network from the energy centre in the middle of the neighbourhood to the building centroids. A heating loss rate of 4.3% per km of heating pipe is assumed (Keirstead et al. 2012). Electric pumping power is taken to be 8.5% of the total heating demand in each time step (Weber et al. 2011).

Direct injection of hydrogen into the natural gas grid is also allowed for up to a 2% limitation by volume (the recommended value for

networks with turbines (Altfeld et al. 2013)). This condition is enforced by Eq. (3.34).

$$Q_{H2,h}^{DI} \leq (Q_{NG,h}^{import}) \cdot f^{DI,max} \ \forall \, h \in H \qquad (3.34)$$

Here, $Q_{H2,h}^{DI}$ is the volumetric flow rate of hydrogen injected into the natural gas grid, $Q_{NG,h}^{import}$ is the flow rate of the natural gas imported into the grid in each time step, and f^{DI} is the maximum volume fraction of hydrogen in the natural gas grid that is permissible by law (assumed to be 2% in this work).

The energy content of both gases can be converted using their heating values, which are approximately 39.4 and 14.5 kWh/kg for hydrogen and natural gas respectively.

In the model, the three grids are assumed and are simultaneously balanced with constraints to ensure that supply meets demand. The balance for electricity, heating, and natural gas in the network are shown in Eq. (3.35).

$$\frac{P_{f,h}^{import}}{\eta_f^{loss}} + \sum_t^T P_{t,f,h}^{out} + \sum_s^S P_{h,s}^{dch} =$$

$$\frac{P_{f,h}^{demand}}{\eta_{f,h}^{grid}} + \sum_s^S P_{s,f,h}^{ch} \sum_t^T P_{t,f,h}^{in} + P_{f,h}^{export} \ f \in F \ h \in H \qquad (3.35)$$

Here, F represents the set of energy carriers (i.e., electricity, heat, hydrogen, and natural gas), T is the set of renewable and conversion technologies (i.e., PEME, gas boilers, heat pumps, MGT, PEMFC, PV, hydro, and wind), and S is the set of storage technologies (i.e., Li-ion batteries, Thermal Energy Storage (TES), and Hydrogen storage (H2S)), $P_{f,h}^{import}$ is the energy for each energy carrier that is imported into the system on the district scale, η_f^{loss} is the import efficiency of the carrier, $P_{t,f,h}^{out}$ is the energy produced by each technology in each time step for each energy carrier, $P_{s,h}^{dch}$ is the energy discharged from each storage technology in each time step, $P_{f,h}^{Demand}$ is the hourly energy demand in the district for each energy carrier, $\eta_{f,h}^{grid}$ represent the losses of the energy carriers when transported in the local grid, $P_{t,f,h}^{in}$ is the energy consumed by each technology for each energy carrier in each hour, $P_{s,h}^{dch}$, and $P_{f,h}^{export}$ is the energy exported back to the grid for each carrier in each time step. Only electricity is able to be exported back to the grid

in this case.

In addition, the term $P_{f,h}^{export}$ which represents export of the energy back to the grid, can be split into renewable energy exported and non-renewable energy exported. This is shown in Eq. (3.36).

$$(P_{elec,h}^{sell} + P_{elec,h}^{sellR}) = P_{elec,h}^{export} \ \forall \ h \in H \tag{3.36}$$

Electricity sold from renewable technologies ($P_{elec,h}^{sellR}$) like PV, hydro, and wind, can be sold at the feed-in tariff rate. The feed-in tariff is an incentive for renewable production such as PV, small-hydro, and wind. Electricity sold from all other devices ($P_{elec,h}^{sell}$) is sold back at the market price of electricity. The market price represents the real price of electricity for either buying or selling (in this case selling), which fluctuates due to supply and demand on the national grid level. Its prices are typically two to three times lower than the retail price. Although battery storage or fuel cell output can indirectly come from renewable energy, in this model the electricity discharged from storage devices cannot be sold to the grid at the feed-in tariff rate, to ensure that only renewable energy can profit from the feed-in tariff. Since the battery can be charged with energy from any source, it is difficult to account for how much energy in the battery is renewable at a given time. Preventing the sale of electricity back to the grid from the battery at the feed-in tariff rate ensures that only renewable energy profits from the feed-in tariff. To incentive local use of renewable energy, there is a constraint to ensure that only surplus electricity from renewable devices during each time step can be sold back at the feed-in tariff price. This constraint is shown in Eq. (3.37).

$$\begin{aligned} P_t^{sellR} \leq (P_{PV,h}^{out} + P_{hydro,h}^{out} + P_{wind,h}^{out} - P_{elec,h}^{demand}) \\ \cdot \delta_h^{surplus} \forall \ h \in H \end{aligned} \tag{3.37}$$

Here, $\delta_t^{surplus}$ is a binary variable that is one if $P_{PV,h}^{out} + P_{hydro,h}^{out} + P_{wind,h}^{out} > P_{elec,h}^{demand}$ (i.e., a surplus) and zero if $P_{PV,h}^{out} + P_{hydro,h}^{out} + P_{wind,h}^{out} \leq Demand_{elec,h}$ (i.e., a deficit). This constraint ensures that electricity can only be sold back at the feed-in tariff rate if the production of renewables is greater than the electricity demand. In addition, the amount of energy that can be sold at the feed-in tariff rate is limited by the difference between the renewable production (hydro, PV, and wind) and the electric demand.

3.5.2 *Multi-objective optimisation*

Multi-objective optimisation is used to minimise both system costs and carbon emissions. The system costs are calculated using Eq. (5.26). This method of calculating carbon emissions only considers operational emissions. This is in contrast to the life-cycle method of calculating CO_2 which includes embodied emissions for all of the technologies. The life-cycle method will be used in Chapter 5 and beyond, however Chapter 3 and 4 will only account for operational emissions as detailed below.

$$Cost_{total} = Cost_{inv} + Cost_{OMF} + Cost_{OMV} + Cost_{carriers} \qquad (3.38)$$

Here, $Cost_{total}$ is the cost objective to be minimised, $Cost^{inv}$ is the equivalent annual investment cost of the technologies, $Cost^{OMF}$ is the fixed operation and maintenance costs, $Cost_{OMV}$ is the variable operations and maintenance costs, $Cost_{carriers}$ represents the combined costs of the energy carriers, including electricity and natural gas. The investment costs are calculated with Eq. (3.39).

$$Cost_{inv} = \sum_t^T (Cost_t \cdot P_{t,f}^{cap} \cdot CRF_t) + \sum_{s=1}^S (Cost_s \cdot E_s^{Cap} \cdot CRF_s) \qquad (3.39)$$

In Eq. (3.39), $Cost_{t/s}$ represents the capital cost of the technologies per unit of capacity installed, and $P_{t,f}^{cap}$ is the capacity of each technology installed. Capital Recovery Factor (CRF), or equivalent annual cost factor is calculated for each technology based on its rated lifetime in years. To calculate the CRF, Eq. (5.30) is used from Knopf (2011).

$$CRF_{t/s} = \frac{r}{\left[1 - \frac{1}{(1+r)^{Lifetime_{t/s}}}\right]} \quad \forall \, t \in T, s \in S \qquad (3.40)$$

Here, r is the discount rate, and $Lifetime$ is the expected age of the technology in years. A discount rate of 6% is used throughout this thesis (Sixth Northwest Power 2010). The lifetimes of the technologies are listed in Table 3.3.

The operations and maintenance costs are then calculated with Eq. (3.41) and (3.42).

$$Cost_{OMF} = \sum_t^T \sum_f^F (Price_{t,f}^{OMF} \cdot P_{t,f}^{cap}) + \sum_s^S (Price_s^{OMF} \cdot P_s^{cap}) \qquad (3.41)$$

Table 3.3.: Lifetimes of the technologies.

Technology	Lifetime (years)	References
PV	25	Jordan et al. 2012
Small hydro	50	Paish 2002
Small wind	25	DEA 2016
Heat pumps	20	DEA 2016
Gas boilers	20	DEA 2016
PEMFC	11	Lott et al. 2014
PEME	11	Lott et al. 2014
MGT	10	Nascimento et al. 2013
CMR	20	Lehner et al. 2014
Li-ion bat.	11.5	Battke et al. 2013
TES	17	Stadler et al. 2008
H2S	22	Amos 1998
CNGS	22	Amos 1998
Compressor	10	Lehner et al. 2014

$$Cost_{OMV} = \sum_{t}^{T}\sum_{f}^{F}(Price_{t,f}^{OMV} \cdot \sum_{h=1}^{8760} P_{t,f,h}^{out}) + \sum_{s}^{S}(Price_{s}^{OMV} \cdot \sum_{h=0}^{8760} P_{s,h}^{dch})$$

$$(3.42)$$

Fixed operations costs are calculated based on the technology sizes and variable operations costs are calculated based on the operational output of the technologies over the one-year period. For conversion technologies, this is defined by the output energy in kWh over the year ($P_{t,h}^{out}$). For storage technologies, this is defined by the discharge energy in kWh over the one-year period ($P_{s,h}^{dch}$). The last cost is the net cost of all imported and exported energy carriers, which in this case includes only natural gas and electricity costs. The calculation of the costs of energy carriers are shown in Eq. (3.43).

$$Cost_{carrier} = \sum_{h=1}^{8760}(P_{elec,h}^{import} \cdot Price_{h}^{retail}) - \sum_{h=1}^{8760}(P_{elec,h}^{sell} \cdot Price_{h}^{MP}) -$$
$$\sum_{h=1}^{8760}(P_{elec,h}^{sellR} \cdot Price_{h}^{FIT}) + \sum_{h=1}^{8760}(P_{NG,h}^{import} \cdot Price_{NG})$$

$$(3.43)$$

In Eq. (3.43), $P_{NG,h}^{import}$ represents the natural gas purchased from the grid in each time step and $Price_{NG}$ is the fuel price.

The annual CO_2 emissions, in kg CO_2/kWh are calculated with Eq. (5.34).

$$CO2_{total} = \sum_{h=1}^{8760} (P_{NG,h}^{out} \cdot CO2_{NG} + P_{elec,h}^{out} \cdot CO2_{elec}) \qquad (3.44)$$

Here, $CO2_{elec}$ and $CO2_{NG}$ are the carbon factors in kg CO_2/kWh for natural gas and the electricity intensity in the grid.

With the two objectives defined, the epsilon-constraint method is used to derive a series of points along the Pareto curve. In this case, the two objectives are individually minimised in single-objective optimisation. Then, the epsilon values for the remaining Pareto points ($N - 2$) are calculated with Eq. (3.45) and the optimisation is carried out with Eq. (3.46). In both equations, N refers to the total number of desired Pareto optimal points.

$$\epsilon_n = \frac{CO2_{total}^{CostMin} - CO2_{total}^{CO2min}}{N - 1} + CO2_{total}^{CO2min} \qquad (3.45)$$

$$\begin{aligned} &Minimise\ Cost_{total} \\ &Subject\ to:\ CO2_{total} \leq \epsilon_n \end{aligned} \qquad (3.46)$$

3.5.3 *Levelised Objectives for Case Study Comparison*

To compare the results of different case studies on a fair basis, the *Levelised Cost of Emissions* (LCOE) and *Levelised CO_2 Emissions* (LCO2) for MES will be used. The $LCOE_{MES}$ is defined as the total annual costs of the energy system (defined in Eq. (5.26)) divided by the sum of the total annual electricity and heating demand. The $LCO2_{MES}$ is defined as the total annual emissions (defined in Eq. (5.34)) divided by the sum of the total annual electricity and heating demand. The calculation of $LCOE_{MES}$ and $LCO2_{MES}$ are shown in Eq. (3.47) and (3.48) respectively.

$$LCOE_{MES} = \frac{Cost_{total}}{\sum_{h=1}^{8760}(P_{elec,h}^{demand} + P_{heat,h}^{demand})} \qquad (3.47)$$

$$LCO2_{MES} = \frac{CO2_{total}}{\sum_{h=1}^{8760}(P_{elec,h}^{demand} + P_{heat,h}^{demand})} \qquad (3.48)$$

The terms $P_{elec,h}^{demand}$ and $P_{heat,h}^{demand}$ in Eq. (3.47) and (3.48) refer to the hourly demand of all buildings.

Please note than *LCOE* can only be calculated in this manner if constant pricing over the time horizon is used. In this model, prices are considered to be constant over the single year that is optimised, but if dynamic pricing is used the alternative formulation in Blok et al. (2016) can be used.

3.5.4 *Energy Strategy Targets*

To benchmark optimal solutions against the targets of the Swiss Energy Strategy, the Kaya Identity is used. The emissions targets are not included in the optimisation but used to benchmark the solutions for the years of 2020, 2035, and 2050. The calculation of these energy targets for buildings is defined in Mavromatidis, Orehounig, Richner, et al. 2016 in reference with the Swiss Energy Strategy 2050 (Prognos AG 2013). This evaluation uses the Kaya identity to calculate the emissions targets based on Eq. (3.49).

$$CO2_{buildings} = \frac{CO2_{buildings}}{E_{buildings}} \cdot \frac{E_{buildings}}{A_{buildings}} \cdot A_{buildings} \qquad (3.49)$$

Here, $CO2_{buildings}$ refers to the total Swiss CO_2 emissions targets from buildings (in this case in $kgCO_2$), $E_{buildings}$ refers to the total energy consumption in buildings (in kWh), and $A_{buildings}$ refers to the total floor area in buildings (in m^2) at 2020, 2035, and 2050 defined in the strategy. Both the floor area for all buildings and the CO_2 targets are defined in the strategy for the years of 2020, 2035, and 2050. As the total emissions for all buildings and the floor area of all buildings are fixed in the energy strategy at each year, the $\frac{CO2_{buildings}}{E_{buildings}}$ and $\frac{E_{buildings}}{A_{buildings}}$ can both be adjusted to meet the targets. The term $\frac{CO2_{buildings}}{E_{buildings}}$ refers to the CO_2 intensity per kWh of energy produced in buildings. The value of $\frac{CO2_{buildings}}{E_{buildings}}$ decreases with an increasing percentage of renewables being used to meet energy demand and increases when the percentage using fossil fuels increases. The term $\frac{E_{buildings}}{A_{buildings}}$ refers to the energy density of buildings per unit area, which represents the energy efficiency of the building envelope and the building heating system. The more inefficient the buildings are (i.e., older building stock), the higher the energy density is. When buildings are retrofitted, their kWh/m^2 decreases, thus this value decreases from 2015 to 2050 based on increasing number of retrofitted buildings. The

model optimisation can choose the level of renewables on the system side, thus optimising the $\frac{CO2_{buildings}}{E_{buildings}}$. The resulting optimisation solutions can be compared against the official targets according to the energy strategy, to benchmark possible solutions. This is demonstrated in Fig. 3.6.
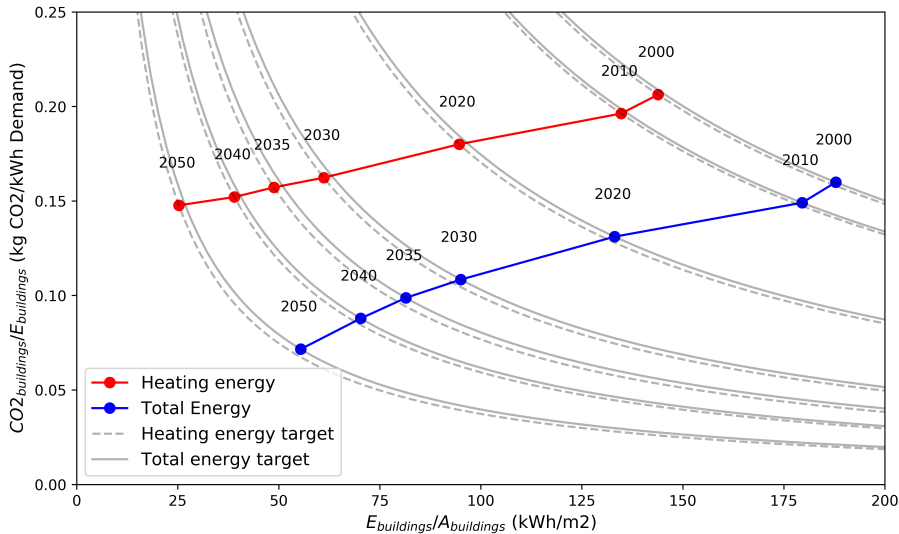
Figure 3.6.: A representation of Swiss Energy Strategy emission targets using the Kaya identity for Swiss Buildings from 2000-2050.

3.6 SUMMARY AND OUTLOOK

In this Chapter, the optimisation model has been developed to assess the long-term storage potential of hydrogen and the short-term storage potential with batteries and thermal storage has been developed. This model employs electrolysers to convert surplus renewable electricity, produced from local PV, wind, or hydro, to hydrogen for storage. This hydrogen can then be injected directly into the natural gas grid, or used to fuel hydrogen fuel cells (Power-to-CHP). Heat pumps and thermal storage are also available for a Power-to-Heat conversion.

The optimisation framework has been described, including the part-load performances of the conversion technologies, the minimum operation, the maximum capacity, the direct injection limits, the balance on the storage technologies, the import and export constraints to the

centralised natural gas and electricity grids, the losses in the grids, and lastly the energy balances for the districts. The multi-objective function using the epsilon constraint method has also been described to minimise both net annual costs and net annual carbon dioxide emissions. Lastly, two key performance indicators, the LCOE and Levelised CO_2 Emissions (LCO2) have been invoked to allow for direct comparison of case studies of different sizes.

The next steps are to test the model with a case study and to assess the performance over several years of analysis. This leads us to Chapter 4, in which the model described in this chapter is applied to two case studies of interest in two different municipalities. These case studies are applied for three different future scenarios of interest, and the results are evaluated for the years of 2015, 2020, 2035, and 2050.

FUTURE SCENARIOS IN P2X FOR TWO DECENTRALISED CASES

The purpose of this Chapter is to evaluate the potential of both long-term (hydrogen storage) and short-term (batteries and thermal) storage systems in decentralised neighbourhoods using the optimisation model developed in Chapter 3. This model is implemented in this Chapter to evaluate the performance of long and short-term storage systems until 2050. Several different future scenarios are constructed, based on the Intergovernmental Panel on Climate Change's 'Special Report on Emissions Scenarios' (Nakicenovic et al. 2000). Three future scenarios are defined and simulated for the years of 2015, 2020, 2035, and 2050 for both a rural (Zernez) and an urban (Altstetten) neighbourhood in Switzerland. Based on the scenarios, the energy demand and renewable potential projections until 2050 are simulated including retrofitted buildings and renewable potential changes in the neighbourhoods. In addition, a range of parameter assumptions (e.g., for economic variables, policy changes, environmental conditions) are used in each scenario to show the variation in the model based on different input assumptions. The long-term storage potential of hydrogen, in particular, is evaluated for its capability to shift renewable surpluses in summer towards demand later in the year.

4.1 BACKGROUND AND CONTEXT

To test the model that is presented in Chapter 3, two case studies in different contexts are used in this Chapter: one rural and one urban. The rural and urban case studies refer to Zernez and Altstetten respectively, which were first presented in Section 1.7.2. In addition, the current and future systems are also of interest for our research until 2050 to test if Power-to-Hydrogen, Power-to-Heat, Power-to-Power, or Power-to-CHP could play an increased role in the future. As was mentioned in Section 1.9.1, the variation of many optimisation inputs, such as economic, environmental, and performance variables, could vary significantly in the future. One method of accounting for this uncertainty is to use scenarios. In this Chapter, scenarios are built for the assessment of decentralised energy systems in the future and these are applied to two

case studies using the multi-objective function defined in Section 3.5.2.

4.1.1   *Development of scenarios*

Parameters and assumptions in future energy systems underlie uncertainty regarding their future development, e.g., technology trajectories (learning) and market trends (price volatility). To cope with this uncertainty (i.e., the numerous projections for individual parameters with a broad spectrum of low, medium or high values), scenarios provide a better understanding to reach decisions that are robust under a wide range of possible futures (Moss et al. 2010). Thus, scenarios are an appropriate tool to assess the alternative images of complex systems by using a consistent set of assumptions within so-called storylines or narratives used to describe the economic, global, and environmental conditions of a scenario (Nakicenovic et al. 2000).

In 2000, the IPCC published the 'Special Report on Emissions Scenarios' (SRES) (Nakicenovic et al. 2000), which contains both quantified projections and narratives ('storylines') for the future and which has been extensively used as the reference for subsequent research and for the political and societal discourse on climate change (Girod et al. 2009). In the Special Report on Emissions Scenarios (SRES), the IPCC scenarios are based on four narrative storylines that can be categorised along two major dimensions: globalisation (from more regional to more global), and sustainability (from more economic to more environmental). These dimensions, along with the resulting storylines, seem to reappear as key archetypical scenarios in a large number of recent international assessments (Vuuren et al. 2012). Figure 4.1 shows these scenarios from the original IPCC publication (Nakicenovic et al. 2000).

This study builds upon the IPCC classification and defines three scenarios that are deemed relevant for the investigation of potential future developments from the baseline year 2015 to 2020, 2035, and 2050: 1.) "Conventional Markets", 2.) "Global Sustainable Development", and 3.) "Regional Sustainable Development". These three scenarios, shown in Fig. 4.1, are considered to cover a wide range of possible futures, but certainly not all (e.g., hazardous events, disasters). Thus, they allow using consistent combinations of assumptions composed of the various projections in literature for each parameter (see subsection 4.1.3). For this analysis, the A2 scenario was omitted, as in this context it corre-

More Economic

Scenario 1:
Conventional Markets

A1

-B: balanced
-Fl: fossil-intensive
-T: non-fossil

A2

Globalization

More
Global

More
Regional

Scenario 2:
Global Sustainable
Development

B1

B2

Scenario 3:
Regional Sustainable
Development

More Environmental
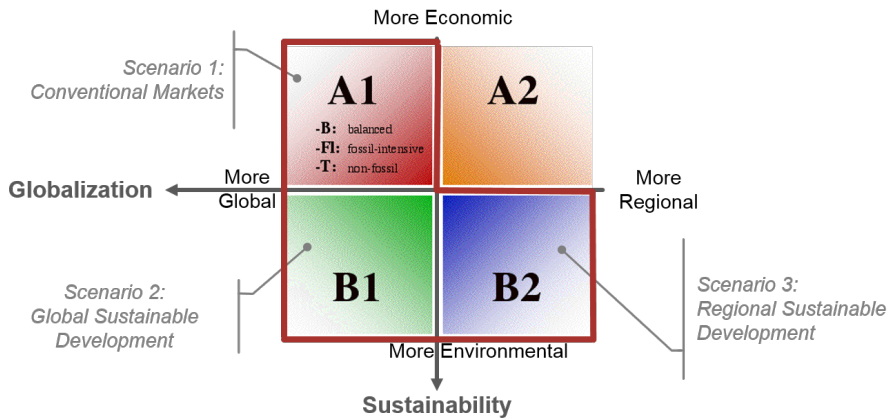
Sustainability

Figure 4.1.: IPCC *Special Report on Emission Scenarios* (2000). The red line outlines the three scenarios adapted in this Chapter (Nakicenovic et al. 2000).

sponds to transition to more decentralised solutions without a focus on sustainability. This scenario is both unlikely in the Swiss context and would not result in either cheaper nor lower emission solutions in this analysis.

4.1.2 *Description of Scenarios*

4.1.2.1 *Conventional Markets*

The Conventional Markets (CM) scenario is based on IPCC scenario A1 and assumes a world of global, well connected markets with a strong economic focus. Since the emphasis rests on fossil-based generation, the deployment of renewable energy sources remains on a low, business-as-usual level, and consequently the climate is changing more rapidly. To account for changing climate, future weather files are used (from Remund et al. (2010)) based on the IPCC's SRES scenarios.

   In the Conventional Markets scenario, the energy prices (electricity, gas, oil) are considered to increase only moderately due to high global flow rates and low trade barriers. Because of the economic focus, the feed-in remuneration is phased-out in the short-term, and both the CO_2 tax and the retrofit rate (i.e., pace of efficiency improvements in the building stock) are kept at a rather low, as-is level. As a conse-

quence, technology costs are assumed to be at a high level for renewable technologies (e.g., solar PV, wind), at a low level for fossil-based technologies (e.g., oil/gas boiler) and at a medium level for other storage or conversion technologies. For the technology performance, such as efficiencies or lifetime, the relations are inverted. For the building retrofits rate, the current retrofit rate in Switzerland is used, which is defined by the Business as Usual scenario in the Swiss Energy Strategy 2050 to be, on average (actual rates are specific to the age of buildings), 1% of buildings per year (Prognos AG 2013).

4.1.2.2 *Global Sustainable Development*

The Global Sustainable Development (GSD) scenario, resting on IPCC B1 scenario, pictures a future based on global cooperation, well connected markets but also a strong focus on environmental consciousness and protection. Global regulation puts the fossil phase-out into practice and fosters the deployment of renewable energy sources, internationally coordinated and mostly in centralised settings, which is why the global temperature increase is more limited than the other scenarios.

In the GSD scenario, the sustainability focus leads to a high tax for emitting CO_2 and a high retrofit rate. The reimbursement for feeding electricity into the grid remains high in the GSD scenario due to a strong grid infrastructure for transmission and distribution for power ex- and imports. Energy prices are expected to increase with a medium rate, as the usage and thus the flow rates for fossil fuels is limited. Since this sustainable scenario relies on the deployment of renewable energy, the cost for renewable energy sources technologies are assumed to be low, while for fossil-based technologies they remain rather high, and vice versa for their technology performances. In addition, this sustainable scenario includes an increased rate in retrofits defined by the New energy policy (NEP) scenario in the Swiss Energy Strategy 2050 of 2% of buildings, on average, per year (Prognos AG 2013).

4.1.2.3 *Regional Sustainable Development*

The Regional Sustainable Development (RSD) scenario is derived from IPCC scenario B2 and assumes a shift towards local and decentralised solutions to cope with environmental issues. Similar to the Global Sustainable Development scenario, fossil fuels are phased out, while renewable energy sources are deployed to a large extent, especially in

decentralised settings.

In the RSD scenario, there is also a sustainability focus which leads to a high tax for emitting CO_2 and a high retrofit rate. As opposed to the GSD scenario, in the RSD scenario feed-in rates are slowly phased out as the focus shifts towards self-consumption. Energy prices are expected to increase at a high rate, as the usage and thus the flow rates for fossil fuels is limited, especially in this scenario where additional restrictions (e.g., high import tariffs) hamper both their demand and supply. Since this scenario also relies on the deployment of renewable energy, the technology costs and performances are the same as with the GSD scenario. In addition, the retrofit rate are also the same as the GSD scenario.

4.1.3 *Setting of future parameters*

To set the model parameters according to the underlying logic of the above described scenarios, this study relies on projections from literature. If available, projected values were directly sourced from publications, such as in Lott et al. (2014), or are based on ranges (i.e., lower or upper projected limits) given in different sources and referring to the nature (cf. low, medium, high) of each scenarios' parameters. Appendix C includes all of the assumed values for the scenarios with references. Table C.1 shows the values set for energy carrier prices, emissions factors, and selling prices. Table C.2 shows the economic and performance parameters for renewable technologies, Table C.3 shows the parameters for the heating technologies, Table C.4 shows parameters for the hydrogen technologies, and Table C.5 shows the parameters for the storage technologies. These Tables set the parameters for the three scenarios and model-related parameters from 2015 until 2050.

Typically, with the simulation of MES, it is more accurate to use dynamic electricity prices and CO_2 emissions in the grid. Although this information is available in the present day, real-time electricity prices and grid CO_2 emissions are heavily dependant on the export and imports of Switzerland with its neighbours (i.e., France, Germany, Austria, and Italy) and the hourly CO_2 intensities of each countries respective grids. The nature of trade with these countries is something that is very difficult to predict for the future, especially at hourly intervals. For this reason, we have used constant prices and grid CO_2 emissions rather

than dynamic hourly values for this analysis although it is noted that this is a limitation of the present work.

4.1.4   *Future demand data for case studies*

To predict future demand for buildings, two factors are considered: retrofits and climatic weather changes. Based on the 2015 baseline year, the demand model (Section 3.2.2) was used to calculate individual demand for all buildings in Zernez and Altstetten. The baseline year is simulated with a typical meteorological weather file from both locations specifically. Future demand for the years of 2020, 2035, and 2050 are calculated with the retrofitting model (Section 3.2.3). Using this model, retrofits are applied and building constructions are updated at future years of consideration. In addition, weather files considering climate change in the future were obtained from Meteonorm based on the work published in Remund et al. (2010). The weather files in this work are based on the IPCC A1B and B1 scenarios. For the future demand, the CM scenario was chosen to use the Business as Usual scenario retrofit rates and the A1B weather files, the GSD scenario was chosen to use the New Energy Policy scenario retrofit rates and the B1 weather files, and the RSD scenario was chosen to use the New Energy Policy retrofit rates and the A1B weather files. Since the B2 weather files are not yet available for these locations, the A1B is used in its place as the warming predicted in the B2 scenario on average globally falls in the range predicted by the A1B scenario. A summary table of the temperatures in the weather file are shown in Table 4.1.

 The results of the aggregated demand for these case studies are shown in Fig. 4.2. In this Figure, three scenarios (which are Conventional Markets, Global Sustainable Development, and Regional Sustainable Development) are shown from 2015 to 2050. The heating demand decreases over time due to more buildings being retrofitted each year in both neighbourhoods. When these buildings are retrofitted, windows, facade, floor, and roof insulation are all added to reduce the heating demand. In addition, the electrical appliances and lighting are updated to increase their efficiency and decrease the electrical energy demand in the buildings. The GSD and RSD scenarios have an average retrofit rate 2% of buildings per year compared to the CM rate of 1%, thus they are able to retrofit twice the number of buildings, resulting in a lower demand. In addition, the buildings are simulated with the

Table 4.1.: Weather file average temperature for the future scenarios, years, and locations.

Region	Parameter	2015	2020		2035		2050	
		Base-line	A1B	B1	A1B	B1	A1B	B1
Global	Mean temp vs. 1980-1999 (Δ °C)	+0.4	+0.7	+0.5	+1.2	+1.0	+1.7	+1.3
Zernez	Max temp (°C)	25.1	24.3	24.7	27.6	26.3	27.7	26.3
	Mean temp (°C)	4.4	4.9	4.9	5.5	5.2	6.1	5.5
	Min temp (°C)	-20.0	-16.3	-15.9	-15.9	-16.6	-16.0	-16.1
Zürich	Max temp (°C)	29.9	32.3	33.0	33.0	33.8	32.9	33.3
	Mean temp (°C)	8.7	10.4	10.4	11.0	10.7	11.5	11.0
	Min temp (°C)	-10.4	-8.6	-8.2	-8.1	-9.0	-7.6	-8.1

relevant weather files, with the A1B (used by CM and RSD scenarios) scenario having higher warming than the B1 (GSD) scenario. As a result, the RSD has a lower heating demand over time compared to the GSD scenario despite having the same retrofit rate, as the RSD has a warmer average temperature and thus less heating demand than the GSD scenario.
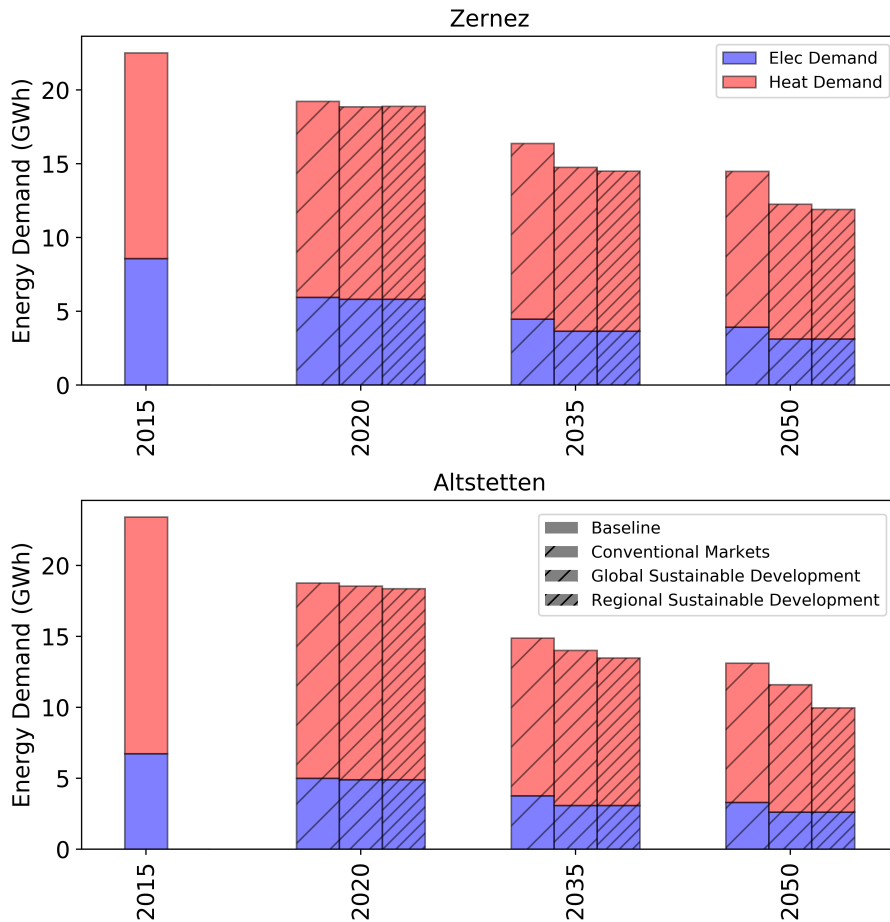
Figure 4.2.: Future building energy demand of Zernez (left) and Altstetten (right).

4.1.5   *Future renewable potential vs. demand*

In addition to the electricity and heating demand for the buildings, the renewable potentials are also calculated for the respective case studies. As the change in wind speeds and solar potential are predicted to not change significantly in the weather files, these renewable potentials are assumed to remain nearly the same over time. It is predicted that the demand decreases due to retrofits and the renewable potential remains constant. This is represented in Fig. 4.3. In this Figure, the surplus or deficit is calculated by subtracting the total energy demand in each hour from the total renewable production in each hour and then summing up the monthly totals. It can be observed that the surplus for both case studies grows over time due to the lower demand in 2050 compared to 2015. In addition, Zernez has a much higher amount of renewables, resulting in a greater surplus. It is noted that Zernez's renewable potential represents 60.9% and 94.5% of its total energy demand in 2015 and 2050 respectively. In Altstetten, the renewable potential only comprises 14.5% and 23% of the total energy demand in 2035 and 2050 respectively. This means that, even assuming perfect storage efficiencies, a 100% self-sufficient system could not be theoretically obtained in Zernez or Altstetten, even in 2050.

In Fig. 4.3, the level of surplus renewables (i.e., times of higher renewable potential than demand) increases over time, especially in the Zernez case. With extra surplus energy, the optimisation may decide to install less renewables, to install the renewables but sell production to the grid, or to use storage technology to shift the energy surplus to later energy deficit.

4.2   RESULTS AND DISCUSSION

Based on the scenarios formulated in Section 4.1.1, a series of simulations were conducted to evaluate the scenarios using the multi-objective method to find a set of Pareto optimal solutions.

4.2.1   *Pareto fronts*

Figure 4.4 shows the Pareto fronts for all scenarios, years, and objectives simulated with the $LCOE_{MES}$ on the x-axis and LCO2 on the y-axis.
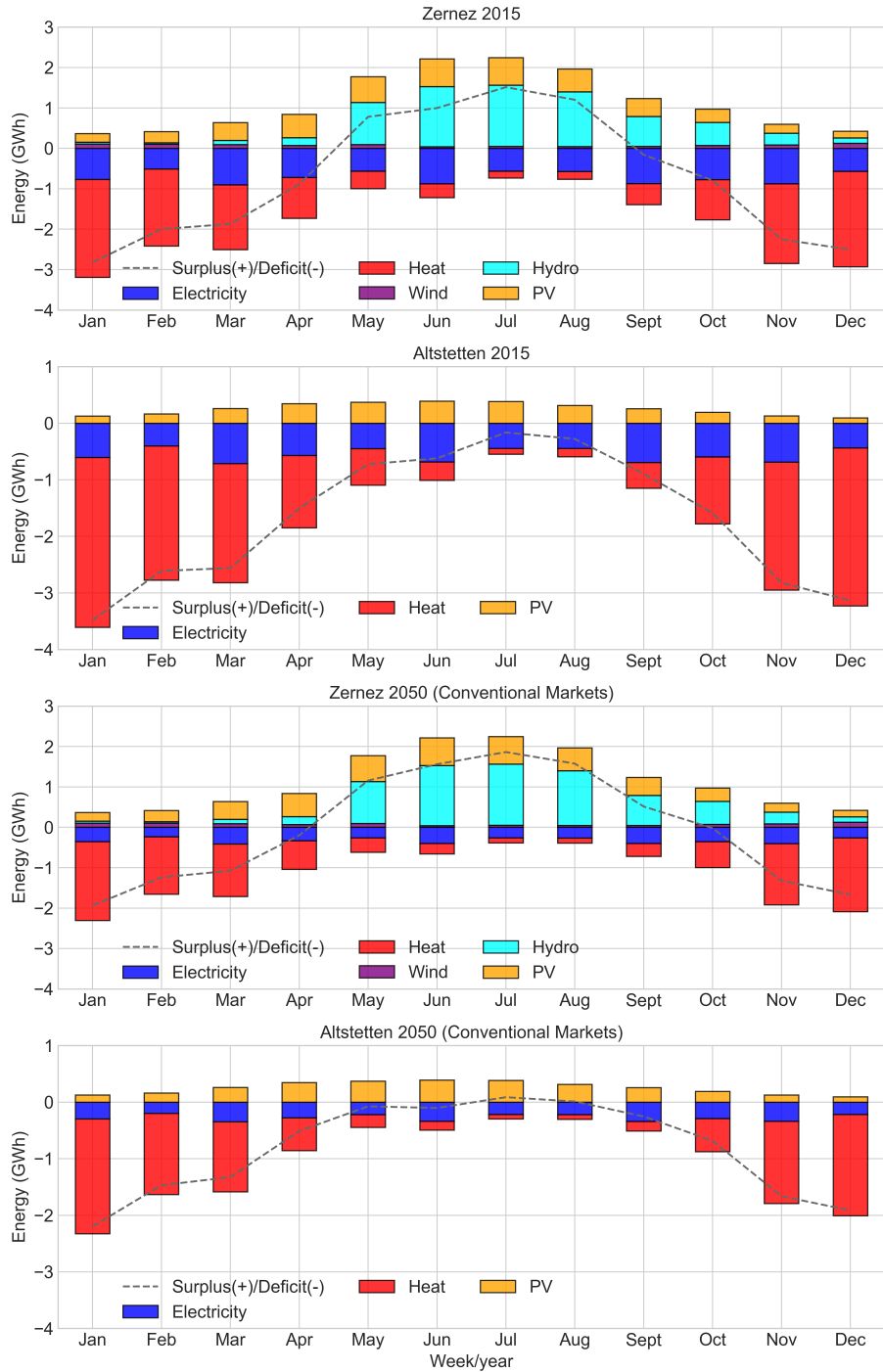
Figure 4.3.: Renewable potential (positive) and demand (negative) for Zernez and Altstetten in the 2015 Baseline year and the CM scenario in 2050.

In multi-objective optimisation, the solutions show the set of Pareto optimal solutions according to the two objectives. The energy strategy targets are included in dashed lines. Please note that the targets differ from the CM scenario to the GSD and RSD scenario due to the difference in the assumed CO_2 intensity of the electricity grid (please see Table A.1 for details). The Pareto curves, moving from upper-left
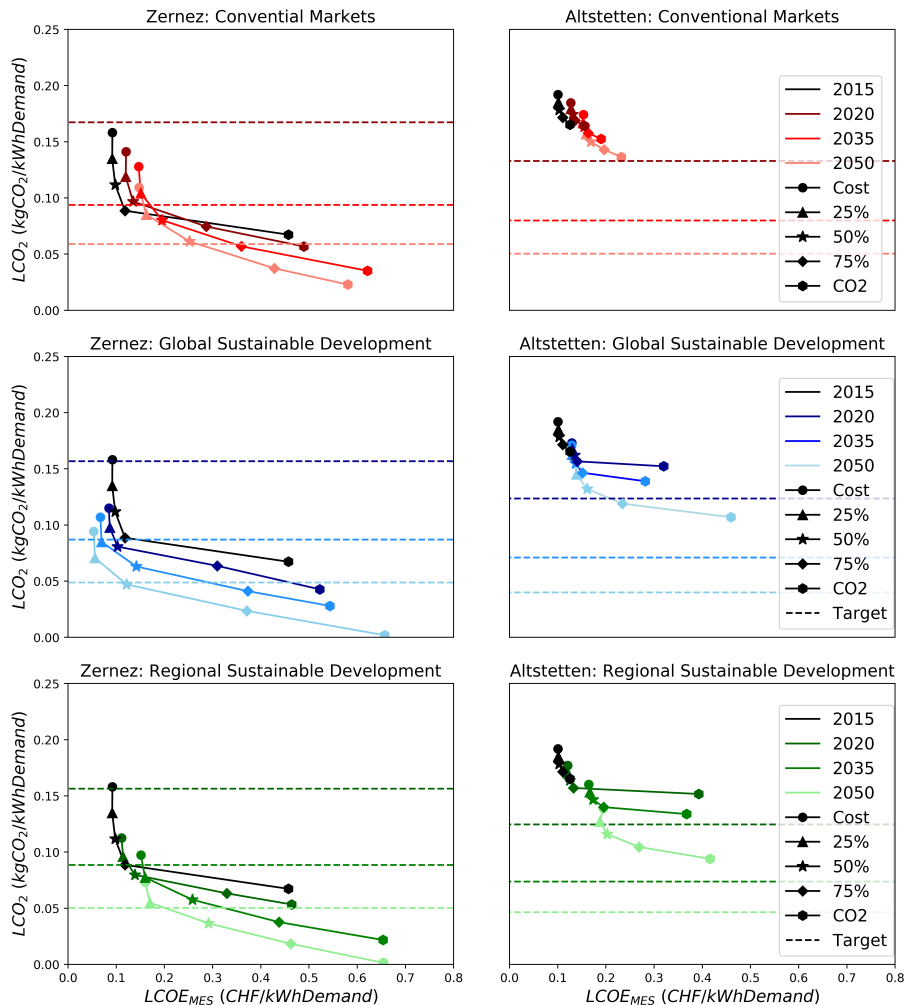
Figure 4.4.: Pareto fronts for each year and scenario. Dashed lines represent the Swiss Energy Strategy emissions targets, colours represent the year, and the point shape represents the objective.

and cost optimal to lower-right and CO_2 optimal, show five different solutions that are all on the spectrum from fully cost optimal to fully CO_2 optimal. From 2015 to 2050, the subsequent years' emissions drop lower, indicating that more renewable sources are being used to meet a higher fraction of the demand over time. In addition, many of these solutions are also dropping in cost over time as the capital costs of technologies decrease. For the Zernez case study, much larger emission reductions can be achieved due to the higher renewable potential. Emission reduction in the Altstetten case study is more restricted due to the lower renewable potential available.

For both case studies, the Pareto curves initially have a steep drop in emissions followed by shallow and rapid increase in costs. This indicates that a large portion of emissions reduction can be met without a high increase in the costs, however the costs rapidly increase above the 75% CO_2 minimisation solution. As seen in this Figure, the rapid increase in costs in the CO_2 optimal solution is mostly caused by installation of a large hydrogen storage system and the capital required to build them. It should be noted that the sizes of these large hydrogen storage systems in the CO_2 optimal solutions are most likely infeasible as it would require too much space for hydrogen storage tanks, however these solutions provide us with reference point to the minimum possible feasible emissions that can be theoretically obtained. Typically, solutions at the elbows of these curves would represent the best trade-off of emissions and cost, although ultimately it would be up to a decision maker to decide where along the Pareto front the preferred solution would lie. If the intention is to meet the energy targets, all three future scenarios are projected to be able to meet the energy targets with the 50% CO_2 objective solution in 2050 in Zernez. In Altstetten, all solutions miss the energy strategy targets.

4.2.2 *Performance of the case studies in the context of the Swiss Energy Strategy 2050*

In Fig. 4.5, the results from Fig. 4.4 have been replotted with respect to the buildings energy density ($\frac{E}{A}$ from Eq: (3.49)) on the x-axis and the system CO_2 intensity ($\frac{CO2}{E}$ from Eq: (3.49)) to benchmark the feasible options against the energy targets.

Figure 4.5 shows the energy density values decreasing (or energy efficiency of the buildings increasing) in both case studies over time
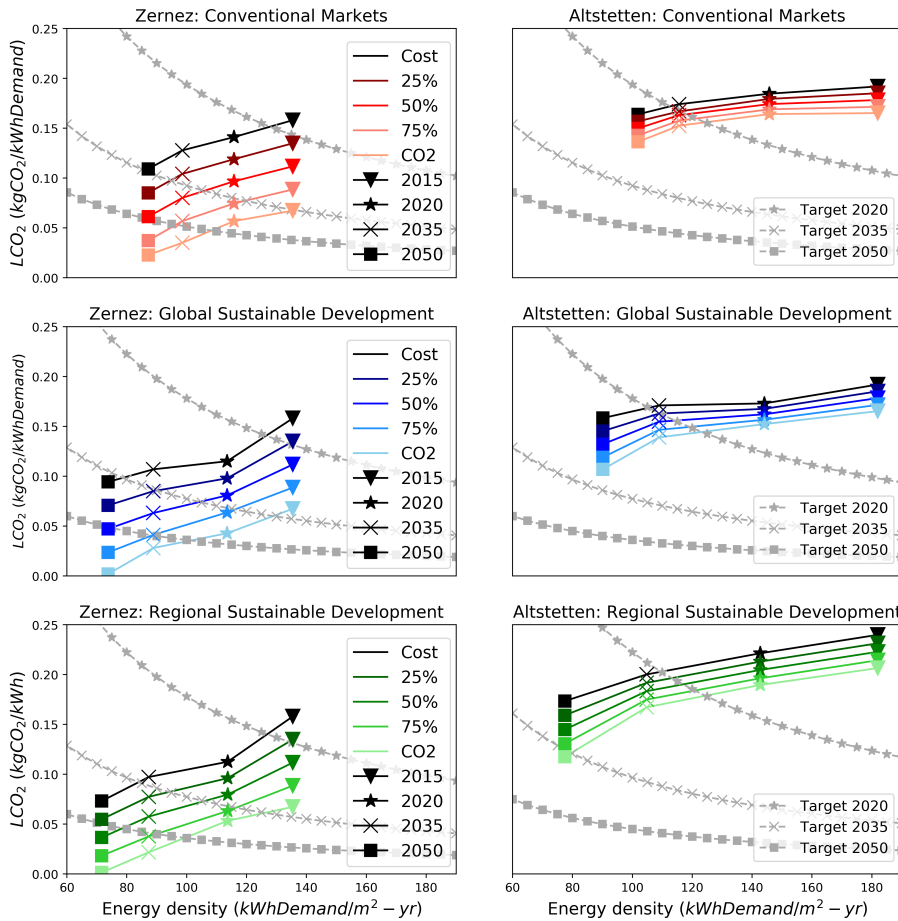
Figure 4.5.: Building total (electricity and heat) energy density vs. the LCO$_2$E for all Pareto optimal solutions. The point shape represents the year, the colour represents the objective, and the dashed lines represent the Swiss Energy Strategy emissions targets.

due to the continuous retrofit of buildings. The energy strategy targets are shown in the dashed grey lines for the years of 2020, 2035, and 2050 according to the Kaya identity calculations described in Section 4.2.2. For the Zernez case study, it is seen that the 50% CO_2 minimisation objective is able to meet the emissions targets in 2050 in all three future scenarios.

In Altstetten, it is again seen that solutions miss the targets, which implies that solutions that meeting targets is infeasible given the energy demand and renewable potentials available. This does not mean that the case study will be unable to meet its targets, but rather that it will miss the targets by solely relying on the implementation of the decentralised MES concept and the presumed retrofit rates. The building stock in Altstetten is comprised of mostly older multi-family houses, resulting in a high heating density. There is also a high ratio of heated and electrified area vs. the available area for solar installations compared to the rural case study. Due to the low renewable potential, there is not enough renewable energy generated on-site to meet the targets. To improve the buildings energy performance, a higher retrofit rate should be adopted for the neighbourhood, however even if the retrofit rates are increased, additional renewable energy would most likely still be required to meet the targets due to the shallow slope of the target curves in 2050. Renewable energy imports, such as biomass, biogas, or externally produced PV or wind would need to be imported into the MES to meet targets in this neighbourhood.

4.2.3 *Technology sizing*

The conversion and storage technology sizing associated with the 50% CO_2 minimisation solutions are shown in Fig. 4.6 and 4.7 respectively. The 50% CO_2 minimisation objective is shown, as it represents the most cost effective solution that is able to meet the energy strategy targets in 2050 in Zernez in each future scenario. The technologies are separated by conversion technologies (both dispatchable and non-dispatchable) and storage technologies.

Here, renewable technologies such as PV and HPs are both cost effective and cost optimal as they are installed in their full capacity in almost all cases. Small-wind is also installed in the same fashion but to a lesser extent due to the high costs and low output of small-wind turbines. MGTs are often installed in the year of 2015 and in many of
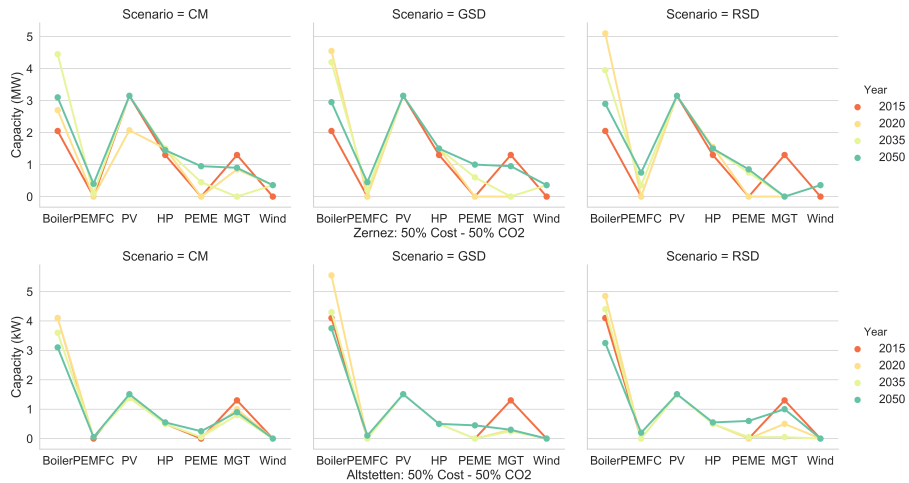
Figure 4.6.: Conversion technology sizing for the 50% CO₂ minimisation objectives for Zernez (above) and Altstetten (below).
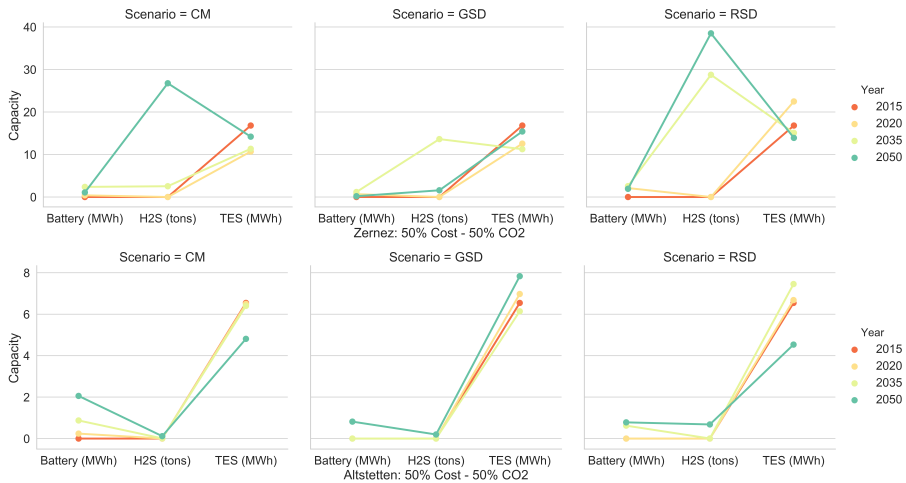
Figure 4.7.: Storage technology sizing for the 50% CO₂ minimisation objectives for Zernez (above) and Altstetten (below).

the CM solutions due to low gas prices, but are not installed when the prices increase in the GSD and RSD scenarios. Boilers are also installed in all cases as they are typically the back-up heating technology that is relied upon. Since heat demand cannot simply be purchased from a central grid in times of need, thermal storage systems and boilers are heavily relied upon due to the high heating demand of both case studies in winter.

PEMFC, H2S, and PEME represent technologies that must be installed to implement hydrogen storage systems. The size of hydrogen storage systems increases over time as the technology capital costs become cheaper, the performance of the equipment improves, there is a higher level of surplus energy, and electricity costs increase. In addition, it is seen that the largest H2S systems are installed in the RSD scenario, followed by the CM and lastly the GSD scenario. The difference is dependent on the feed-in tariff of the scenarios. The RSD and the CM scenarios both have a quick phase out of the feed-in tariff, while the GSD scenario keeps the feed-in tariff high until 2050. As a result, it is more profitable in the GSD scenario to sell surplus electricity back to the grid rather than storing it on-site. The RSD scenario has the largest hydrogen storage systems, as it has a higher level of surplus electricity than the CM scenario due it its lower demand. With a large amount of surplus electricity available, the system chooses to store this electricity rather than sell it to the grid at a low rate. The results find it is almost always optimal to install renewable technologies, as it is optimal to purchase the maximum feasible amount of renewables available for nearly all objectives.

In the Altstetten case study, small hydrogen systems are installed. Due to the lower renewable potential, the system found it is preferable to install batteries and to use hydrogen storage for storage durations longer than one day, although the storage system is not large enough to qualify as seasonal storage.

4.3   COST BREAKDOWN

The costs displayed in Fig. 4.4 are further broken down into five categories in Fig. 4.8: conversion technology capital, storage technology capital, operation and maintenance, fuel, and electricity costs.

The GSD scenario achieves the lowest cost solutions, while the CM
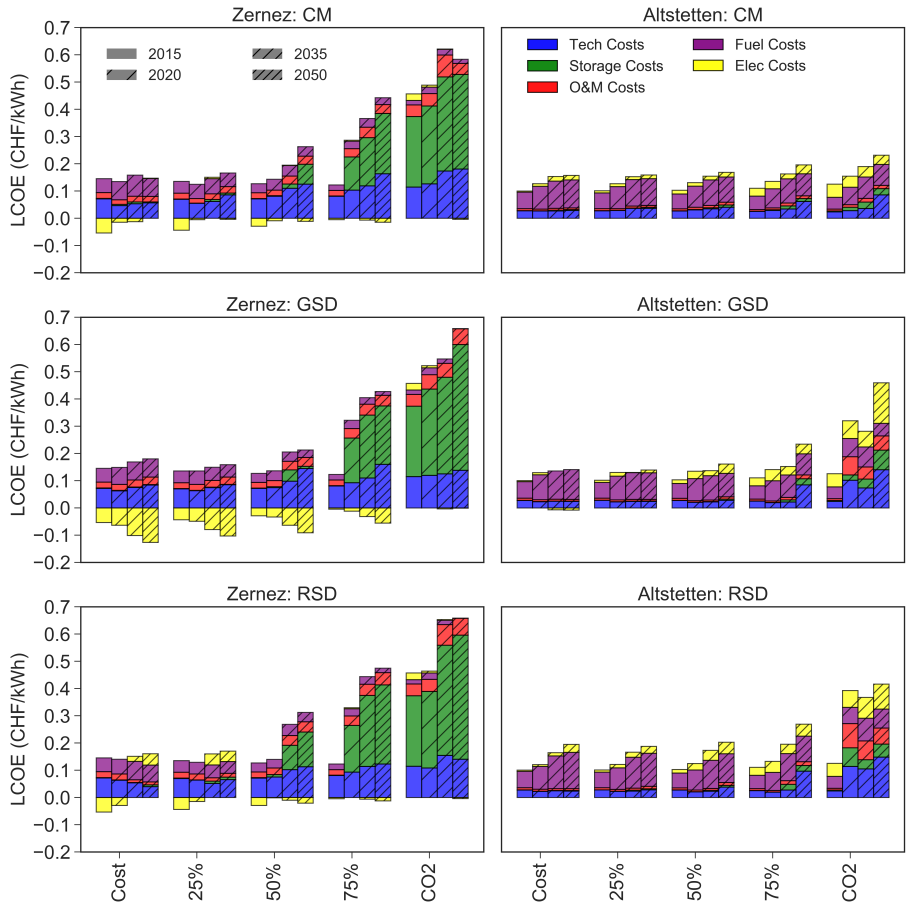
Figure 4.8.: Cost objective composition for Pareto optimal solutions broken down by conversion technology capital costs, storage technology capital costs, O&M costs, fuel costs, and electricity costs.

scenario has the highest costs. In the cost optimal solutions for the Zernez case study, there are observed negative electricity costs (profits). This is also true for the 25% and 50% solutions in the GSD scenario. These are all cases with a high feed-in tariff. In cost optimal solutions, the capital costs of storage and the conversion technologies are responsible for the majority of the costs. This is due to large hydrogen storage systems being installed. More reasonably sized systems are installed in the 50% and 75% cases. In Altstetten, the costs are dominated by natural gas as the case study is strongly dependent on gas boilers to meet its heating demand.

4.3.1   *Increase in share of renewables over time*

Each of the 100 solutions previously shown not only represents the design of the system configuration and the sizes of the technologies but also their operation. Figure 4.9 shows the technology outputs that contribute to the total annual aggregated demand of the case studies for the years of 2015 to 2050. It is split by the demand carriers of electricity and heating.

Figure 4.9 shows that heat pumps, PV, and hydro all contribute greatly to the end energy demand. As the demand decreases over time, the same output from these devices allows boilers, gas turbines, and grid electricity to be used less. Stored energy is used in greater portions in 2050 with PEMFCs and batteries playing an increasing role, especially in the RSD case. Thermal storage is also used, but its potential is already maximised in 2015 and it remains constant until 2050 as its costs begin low and are predicted to remain constant over time. It is to be noted that although the percentages of hydro and PV use in Zernez appear to decrease over time, their use is not actually decreasing, but rather more production is being used to charge the storage technologies as opposed to being used directly to meet demand (the future demand is lower due to retrofits). In addition, a higher portion of renewable energy is sold back to the grid, especially in the GSD case. In Altstetten, the demand in 2050 is still dependent on boilers, MGT, and grid electricity due to the lack of renewables.

These figures show that heat pumps and PV play a key role in both case studies. Their total potential is restricted due to available area of installation specific to each case study, but nevertheless they are
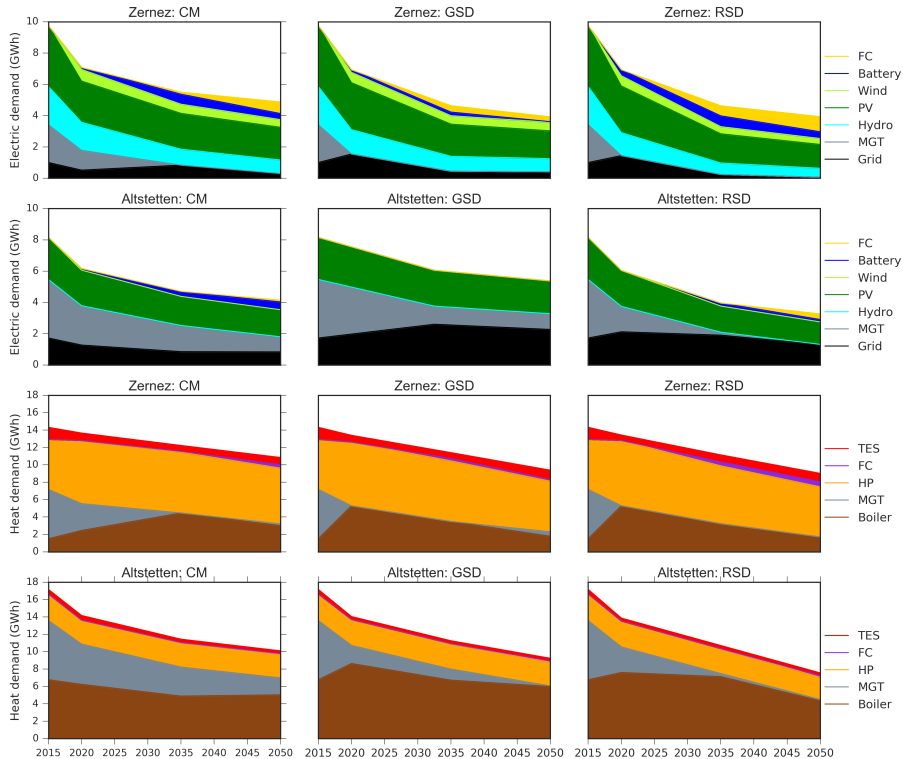
Figure 4.9.: Energy demand (electricity and heat) met by each energy source from 2015 to 2050 for the 50% CO₂ minimisation solutions. Please note that renewable technology output (i.e., PV, wind and hydro) refers to only demand that is directly met from these technologies rather than renewable energy stored in storage systems. Renewable energy from storage systems is shown as energy met from the Battery, TES, and fuel cell (which, although not a storage technology is powered by stored hydrogen gas).

predicted to be the most cost effective and low carbon technologies available for the futures of both case studies for heating and electricity demands respectively. In addition, the RSD scenario has the highest portion of storage usage by 2050. The high feed-in tariffs in the GSD case disincentives storage of renewables on-site and promotes selling electricity back to the grid. This implies that the feed-in tariff does not promote the use of on-site storage systems, and thus does not foster self-sufficiency in the local neighbourhood. A high feed-in tariff with a high penetration of renewables could cause many producers to sell their electricity back at the same time, resulting in centralised grid overloading issues. The use of on-site storage can prevent these issues by allowing neighbourhoods to store this energy rather than selling it back to the grid. This study therefore recommends a phase out of the feed-in tariff between 2020 to 2030 to incentivise the use of local storage solutions, thus promoting on-site consumption.

4.3.2 *Storage Performance*

To further compare the load shifting with the storage systems in each scenario, Fig. 4.10 shows the charging and discharging of each of the three storage systems over the full simulation year in 2050 for the 50% CO_2 minimisation solution. For hydrogen storage, charging energy is represented by the amount of electricity input into the electrolyser and the discharging energy is accounted for in two streams: hydrogen directly injected into the natural gas grid and energy (both heat and electricity) produced from the PEMFC. Both the battery and thermal storage are also shown with their charging and discharging energy.

In Zernez, the storage systems are used to a larger extent, as there is a higher renewable surplus. Although a P2H system is used in all three future scenarios in Zernez in 2050, it is used the least in the GSD case study due to the high feed-in tariff. In summer, there is only a small amount of heating demand for domestic hot water, and the electricity can be met directly from the hydro and PV resources, therefore the storage is not needed significantly in the short-term and the renewable electricity can be sold back to the grid for profit. In both the CM and RSD scenarios, the surplus is used to charge the hydrogen storage throughout the year, although predominantly in the summer, as it is no longer profitable to sell the surplus back to the grid due to the phase out of the feed-in tariff. In the RSD case, the hydrogen storage is used
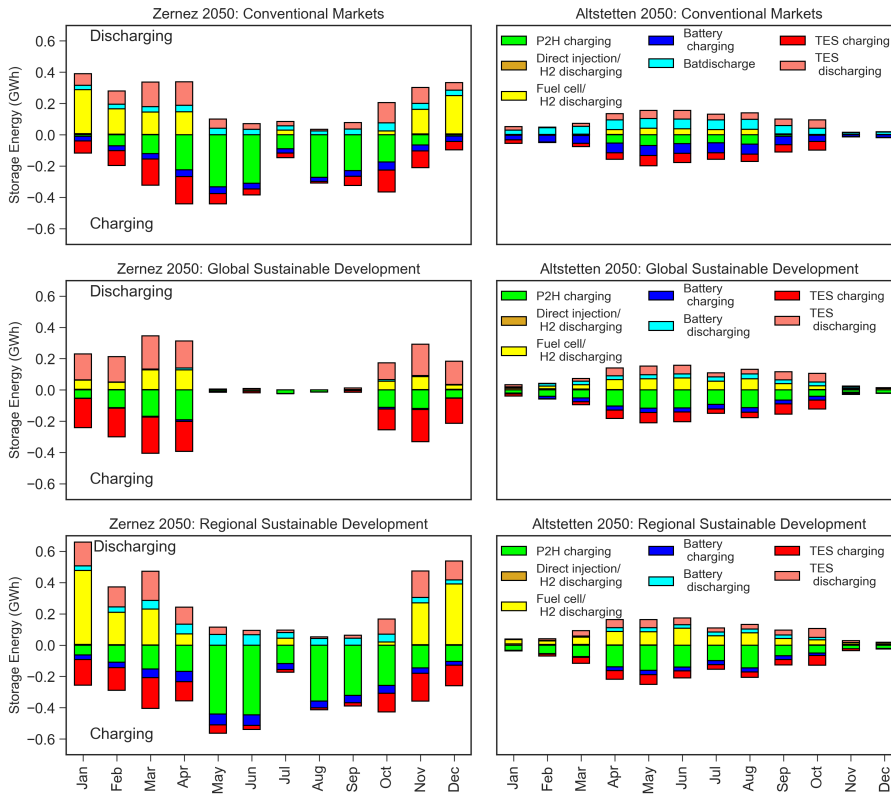
Figure 4.10.: Charging and discharging of the storage technologies for the 50% CO_2 objective minimisation solutions in 2050 for each month in 2050. Negative values indicate the charging of the storage technologies and positive values indicate the discharging of storage technologies.

to a greater extent due to the higher renewable surplus caused by the lower demands.

In Altstetten, the hydrogen system is only used in the summer when there is a renewable surplus. In the GSD and RSD scenarios, the hydrogen storage is able to shift a similar amount of energy compared to the thermal and battery storages but it does not shift the energy demand from month to month, as was done in Zernez. The CM scenario uses short-term storage more than the hydrogen storage. Due to the lower renewable surplus, short-term storage is preferable to long-term storage as it is more efficient.

When comparing the optimal storage technologies in the two cases, it is clear that hydrogen storage requires a high level of renewable surplus to be feasible as a long-term storage. In neighbourhoods where the renewable potential is too low, it will not have enough load to shift for long-term storage to be feasible. In addition, if the feed-in tariff remains high, hydrogen storage is less likely to be used as the profits of selling surplus electricity back to the grid will be higher than the value of stored energy in the hydrogen system. This is observed in the GSD scenario in both case studies, where the surplus electricity is sold to the grid rather than stored in the hydrogen system during the summer's renewable electricity surplus.

4.4 DISCUSSION OF THE P2X MODEL'S RESULTS FOR FUTURE SCENARIOS

The scenario analysis used in this Chapter highlights that use of variable input parameters can strongly impact the results of the model, but the scenario methodology gives little insight of how to quantify these changes and which parameters have the largest influence on the outcome of the model. To further investigate the impacts of input parameters, an uncertainty analysis and sensitivity analysis of this model parameters should be performed, although the computational time of the model would likely have to be reduced to conduct a proper uncertainty analysis with a Monte Carlo method. More simulations would have to be run on the uncertain parameters (i.e., feed-in tariff, electricity price, capital cost of technologies, etc.) to draw further conclusions.

Although it is difficult to draw conclusions from the scenario results, a few observations can be made. Firstly, heat pumps are clearly both a cost effective and lower emission technology than gas boilers, thus

they are installed in every Pareto solution. In addition, nearly all the renewable capacity (e.g., PV, small-wind, and small-hydro) was installed in both case studies for each year of analysis, with the exception of small-wind in Zernez in 2015. This shows that renewable potential, especially rooftop PV and small-hydro, are both cost effective and low emissions in almost every solution found. Battery systems are rarely used in the cost optimal cases, but are used frequently in both Zernez and Altstetten past the 50% minimisation cases.

Lastly, it is clear that all of the minimum CO_2 objective solutions utilise a Power-to-CHP system that uses electrolysers, hydrogen storage, and fuel cells for long-term storage. These systems are required to increase the utilisation of renewables to achieve deep decarbonisation, however they are not cost effective and actually achieve relatively little reduction in CO_2 emissions respective to the sizes of the systems and the expense. To further restrict the size, embodied emissions of the technologies will be incorporated in the calculation of the net annual CO_2 objective. Currently, large systems are being used because there is no penalty for costs in the minimum CO_2 solutions, but embodied emissions adds a CO_2 penalty with the use of large systems, therefore penalising them in the CO_2 objective function. For the remainder of this thesis, embodied emissions of technologies will be used in the calculation of the CO_2 objective function.

These additions would build strongly on the method of multi-objective optimisation for MES that is investigated in this work and would allow for the better identification of energy strategies for decarbonisation, which could be a powerful tool for meeting the climate change goals by 2050.

It is also noted that methanation was missing in the process flow of this model. This was initially not included due to the low round-trip efficiency; however this strategy might significantly reduce the amount of hydrogen available on site. Since the potential for direct injection is so low with the hydrogen concentration limitation, consideration of selling methanation without limit back to the grid might be a valuable way of storing less hydrogen on site. Methanation will henceforth be included in the optimisation, using the descriptions specified for CMRs in Section 3.4.2.

Lastly, since renewable electricity and hydrogen are both produced and stored on-site in this model, the charging of alternative fuel vehicles is a logical fit for this system. Vehicle road based transportation is also a

major source of CO_2 emissions in Switzerland and is similarly targeted by the Swiss Energy Strategy 2050. Its demand pattern is also relatively constant over the year, thus possibly reducing the need for shifting large amounts of summer production to winter at high costs. Implementation of vehicle charging with local production could significantly reducing emissions from burning gasoline in vehicles owned by the building's occupants.

4.5   SUMMARY AND OUTLOOK

In this Chapter, we have developed a methodology to assess the potential of long and short-term storage in future scenarios with a multi-objective optimisation for a decentralised MESs that evaluates the optimal configurations from 2015 to 2050. Three future scenarios, framed from the IPCC, Special Report on Emissions Scenarios, were used for evaluation for the future years of 2020, 2035, and 2050. They are titled *Conventional Markets*, representing global markets with a strong economic focus, *Global Sustainable Development* representing global markets with a strong environmental focus, and *Regional Sustainable Development* representing regional markets with a strong environmental focus. The model was evaluated with two case studies: one urban and one rural, with different amounts of renewable potential. Pareto optimal solutions are run for all combinations of future years, future scenarios, and case studies. The solutions are compared against the national future energy strategy targets. In addition, the full-year horizon directly targets the differences between long-term and short-term storage.

Separate conclusions can be made from the findings of the two case studies. For the rural case study (Zernez), the high renewable potential allows for several solutions that were able to meet the energy targets. Due to the high level of renewables, long-term storage was an asset in the design after 2035 when the feed-in tariff was phased out. The urban case study (Altstetten) could not meet the targets in any scenario due to the lack of available renewables and the remaining high level of energy demand due to the older building stock. Although the retrofit rates were the same for both case studies, the higher energy demand of the older building stock in the urban case study would have benefited more from a higher retrofit rate. Long-term storage was not feasible in this case as there was not enough renewable surplus to shift with

the storage system. Instead, short-term storage was sufficient to shift the load for this case study. From this analysis, we can conclude that long-term storage is only attractive for case studies with a sufficiently high level of renewable surplus.

In both case studies, it was found that retrofit and renewable energy integration were important in meeting the energy strategy targets. For the neighbourhood with less renewable potential and a less efficient building stock, in this case the urban case study, the importance of retrofits should be particularly emphasised. The population density in the urban case study resulted in a lower amount of rooftop space for PV relative to the energy density of the buildings. In an urban area, alternative strategies to solar technologies would be difficult to include due to the lack of available area to install other technologies. To further decrease the use of fossil fuels, external renewable energy must be imported into the neighbourhood.

The results of the three future scenarios show that storage systems were the most favoured in the RSD scenario. This was due to the lower local demand resulting in higher surplus electricity. Due to low feed-in tariffs and increasing electricity prices, it was more cost effective to install a storage system and use this energy at a later time than to sell it back to the grid at a low cost. The CM scenario also favoured storage despite having the lowest renewable surplus of all scenarios, which implies that the feed-in tariff has a strong effect on storage system selection and capacity. The GSD scenario was also effective at reducing emissions and was the most cost favourable scenario due to the feed-in tariff profits, however it chose to sell most of its surplus back to the grid which may result in stress on the centralised grid and a lower self-sufficiency ratio for the community. All three scenarios were able to meet the emissions reduction targets for the rural case study and its storage systems. This suggests that both long and short-term storage should play an important role in helping systems in rural settings meet their energy strategy targets.

When planning for the future, decision makers should consider the effects that input parameters have on the optimal system configuration and thus on their ability to contribute to emission reduction targets. Results show that feed-in tariff and the level of surplus energy (which is highly impacted by the building energy demand and the level of available renewable potential) have a high impact on the optimal system design. If the realised parameters for these values in the future

vary strongly from the predictions in this work, then the conclusions of this Chapter will differ. In such a model, uncertainty in the input parameters and their effect on the model must be considered and the effects of these future outcomes should be known before decisions are made regarding the implementation of these systems. The effect of uncertainty on the model will be investigated in more detail in Chapter 7.

INCLUSION OF POWER-TO-MOBILITY IN THE OPTIMISATION

In this Chapter, the optimisation model from Chapter 3 is adapted to include vehicle selection and charging demands supported by several energy carriers. To optimise for vehicle selection and charging, information regarding vehicle ownership in buildings and households and vehicle driving profiles and demands are required. To predict car ownership, mobility census data is collected to approximate the vehicle charging demand energy that may be required within a MES. Five vehicle technologies are then defined for selection and their efficiencies at various driving cycles are calculated for input into the optimisation model. Within the optimisation, the constraints that describe the vehicle charging, discharging, demand, storage, use of public charging stations, and use of community and building charging stations are defined. The use of embodied energy to calculate life-cycle emissions is also introduced and described to consider the total impact that urban energy systems have on the environment. Lastly, with the consideration of vehicle transport and embodied energies, new energy targets that are based on the 2000 Watt Society targets are defined.

5.1 BACKGROUND AND CONTEXT

The personal road transport sector in Switzerland, has a CO_2 reduction potential predicted to be as large as 40% by 2040 for the entire sector and more than half of the total energy saving potential for road transport overall (Raubel et al. 2017). The energy required to operate personal vehicles represents a significant contribution of greenhouse gas emissions per capita in most developed countries due to the high ownership and use of personal internal combustion engine vehicles (ICEV). The current stock of ICEVs in 2015 represents a significant energy saving potential, since ICEVs are entirely dependent on fossil fuels for energy supply and they have lower efficiencies per kilometre when compared with most alternative fuel vehicle (AFV) technologies. This predicted reduction in emissions by 2040 is mostly attributed to the future adoption of AFV technologies, most predominantly battery

electric vehicles (BEV), hybrid electric vehicles (HEVs), plug in hybrid electric vehicles (PHEVs), and (to a much lesser extent) fuel cell electric vehicles (FCEVs). AFV technologies, however, pose certain challenges that prevent their quick adoption in developed countries. Firstly, charging for BEVs in homes is a process that currently takes several hours and can thus be an inconvenience for commuters that use their vehicles frequently. Secondly, BEVs have shorter ranges, typically about 200-350 km for a mid-sized car versus approximately 700 km range for ICEVs (Hofer 2014), which can make long journeys difficult to coordinate or requiring long pauses for charging. Thirdly, the existing public infrastructure for battery charging is expanding, but still has limitations for longer trips. Lastly, if a BEV or a PHEV is charged with electricity produced from fossil fuels, its per kilometre emissions can be higher than that of ICEVs (Brennan et al. 2016). Similarly, if FCEVs are charged with hydrogen produced via steam methane reforming, their emissions can also be higher than that of an ICEVs at a much higher expense per kilometre. Thus it is important to ensure that either the electricity or hydrogen supply for charging comes from partially renewable sources to ensure a carbon reduction in comparison to the status quo with ICEVs.

To ensure BEVs emit less than ICEVs, assuming the vehicle efficiencies used in this work (please see Fig. 5.7) in 2015, the CO_2 intensity of the electric grid must be less than or equal to 0.093 kg CO_2/kWh of electricity, compared to the current Swiss life-cycle mix grid CO_2 value of 0.102 kg CO_2/kWh (Eggimann et al. 2016). This low value is due to the large portion of nuclear and hydro that emit less than ICEVs. The hydrogen used for charging can be produced in three ways: with electrolysis, with steam methane reformation, and with coal gasification. Steam methane reformation and coal gasification are quite cheap, however are inefficient and emit a large amount of CO_2. The life-cycle emissions of steam methane reforming can be considered to be as high as 9-13 kg CO_2-eq/kg H_2 (Dufour et al. 2012) which would make the FCEV's per kilometre emissions only slightly lower than an ICEV, but at a much higher cost. If electrolysis utilises renewable electricity, it has no operational emissions, although the investment cost is still relatively high in comparison to steam methane reformation.

In summer, we currently see large surpluses of renewable energy that are typically managed with curtailment. In the future, these surpluses can be managed with energy storage (including hydrogen production)

or demand response. Since personal transport demand is a load that is relatively constant from season to season, it can be used as a form of demand response to manage renewable electricity surpluses with intelligent vehicle charging. With the growing popularity of EVs and the potential for further expansion of the commercial fuel cell market and FCEVs, charging stations within communities with their own renewable energy supply can be included to further reduce greenhouse gas emissions from consumers and to extend the reach of renewable energy to the personal transportation sector.

5.2 TRANSPORT MODELLING METHODOLOGY

Multi-energy systems are capable of meeting the electric and heating demands of a group of buildings through the use of conversion and storage technologies, as was demonstrated in Chapter 3 and 4. Models are typically used to choose a selection of renewable and conventional technologies than can be installed in district energy systems, but these models are not often used to select the vehicles that are used by the occupants of these buildings and to coordinate the charging of these vehicles with the local renewable energy production. To select the best combination of both building energy and vehicle technologies according to defined objectives, optimisation can be used. In this chapter, the mixed integer linear programming model developed in Chapter 3 is extended to optimise the selection vehicle technologies in addition to conversion and storage technologies, as well as their annual operation. The optimisation returns the decision variables according to two objectives, minimum total cost or minimum carbon dioxide emissions over a period of one year.

In Chapter 3, only operation emissions were considered, but to capture the full picture, a life cycle analysis approach of calculating carbon emissions is used in this Chapter to consider the embodied emissions of conversion, storage, and vehicle technologies.

In addition to the annual energy demands for each building, the demand profiles for the vehicles owned by the residents of each building are also required as inputs into the optimisation model. To predict these profiles, a car ownership model (Section 5.2.2), the individual vehicle driving profiles (Section 5.2.3), and several updates to the optimisation model itself are required. The updates to the model of Chapter 3

are highlighted in Fig. 5.1, which shows the sub-models used in this methodology and the interaction and transition of data between the sub-models used in this Chapter. These sub-models are explained in more detail in the following sections. Since the model developed in this Chapter will be tested with the Zuchwil case study (see Section 1.7.2), the input data for car ownership and car usage profiles will be developed for the 52 buildings and 168 occupants in that case study.
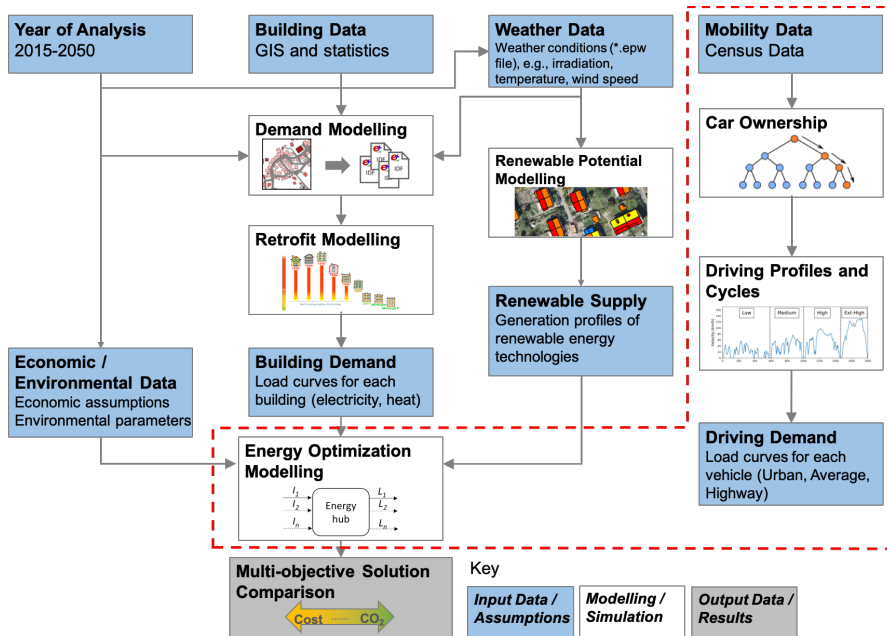
Figure 5.1.: Structure of the models and the transfer of data. The new models described in this section are contained within the red dashed line. These include the car ownership model, the assignment of driving profiles and the description of driving cycles, and the new constraints implemented in the optimisation model to described the selection and charging of vehicles.

5.2.1 *Representative Days*

Due to the computationally intensive nature of solving large optimisation problems, a long-temporal resolution can make the problem a

lengthly task. This problem is commonly addressed by reducing the temporal scale by clustering the days within the year into a smaller number of representative days. One of the downsides of modelling non-consecutive days is that storage continuity is difficult to establish for charge and discharge periods longer than 24 hours. In Chapter 3, one of the model features was to use long-term storage to evaluate the potential of hydrogen as a seasonal storage. To do this, a full annual hourly horizon from 0 to 8760 hours was used to model consecutive days and optimise for storage cycles of up to a year at maximum. This is not normally done in MES optimisation due to the computationally intensive nature of simulating a full year, particularly if binary variables for part load operation are used for each hourly time step, as is done in this work.

With the addition of decision variables due to vehicle selection and vehicle charging, the updates to the model in this Chapter have resulted in a significantly more computationally intensive model. In the interest of reducing the run time of the model, a full horizon was abandoned in this Chapter in favour of the representative days method. This is done using the typical days method used in Marquant et al. (2015). Using this method, the k-Medoids clustering algorithm is used to select a smaller selection of days that are representative of the demands of a full year. Since this method is applied to each building's demands, the error with the clustering days and the full year is minimised. These reduced time horizons can be compared with the full time horizons for the electricity and heating demand and the solar radiation potential on the rooftops in Figure 5.2. In addition to the typical days, the peak heating, electricity, and solar days are also selected to include extreme days into the design of the system for proper technology sizing. Using this method, 12 typical days (one for each month of operation) and three peak days (to represent the peak loads) were used. The most representative day for each month is chosen, to rely on continuity of the storage technologies over the full year. Each representative day is repeated for each day within the month, thus allowing storage durations longer than 24 hours. In addition to the three peak days, this results in a reduction of the horizon from 8760 hours to 360 hours. In Fig. 5.2, we observe that the reduced time horizons contain the same peaks and valleys as the full horizons. Seasonal storage is still used with this method by repeating typical days according to the number of days these represent. This will
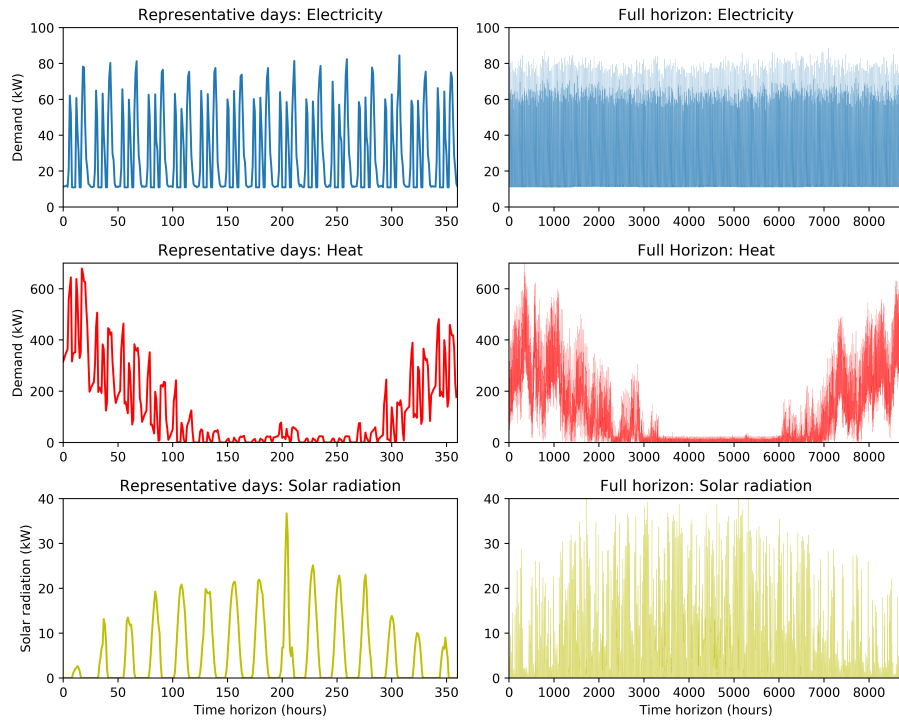
Figure 5.2.: Representative days vs. the full horizon for the electricity demand, heating demand, and the solar radiation. This data is taken from the 52 buildings in the Zuchwil case study.

be later described in Section 5.2.5.2 and Eq. (5.12).

5.2.2 *Car Ownership Model*

The first of the sub-models to be discussed is the car ownership model. In our case studies, the number of vehicles owned by the building's occupants is a required input, but the statistical data available on the exact number of vehicles per household is usually not known. In the absence of this exact data, we have obtained the Swiss mobility micro census data (Bundesamt für Statistik 2015). The Swiss mobility dataset includes a variety of mobility related information regarding vehicles, public transit, and regular driving routes of approximately 58,000 households surveyed throughout Switzerland. To predict the number of vehicles per household within the Zuchwil case study, a machine learning model can be trained using a variety of other information related to the household that is available through the mobility census data or through the Building and Apartment Registry (Bundesamt für Statistik 2012).

Paredes et al. (2017) attempted to develop machine learned based ownership models that are based on statistical data. They found that, when comparing several different machine learning methods, that random forest had the highest accuracy and lowest rate of false negative predictions. Chaudhary (2017) created appliance ownership models for the home and also found that random forest was the highest accuracy. Candanedo et al. (2017) also recommend either gradient boosting or random forest as methods of predicting ownership of home appliances. Due to these findings, a random forest model is chosen to predict the number of vehicles.

In the work of Paredes et al. (2017), building type, ethnicity, motorcycle ownership, geolocation, employment status, income level, job type, and the number of children were used to predict ownership with a 79% accuracy in Singapore. In this work, the following categories are used:

1. Household size (number of people)

2. Household income

3. Building type (single family, multi-family, etc.)

4. Number of units in the buildings (if multi-family)

5. Total number of people in the building

6. Household type (single person, couple, couple with children, single parent, etc.)

7. Canton

8. Population of town

There are 45,452 households with good quality information in all these categories. One-hot encoding was used for categorical parameters such as building and household type. The simulation set was trained on 75% of the full data set and tested on the remaining 25%. The data set was trained using Scikit-learn (Pedregosa et al. 2012) random forest function with 100,000 estimators and a minimum sample leaf of 65. The prediction accuracy of the testing data set is shown in Table 5.1.

In this Table, the testing set of 11,363 households, with the actual

Table 5.1.: Random forest model car prediction accuracy for the testing data set (11,363 households) by comparing the actual number of vehicles in the households (observations) against the number of vehicles predicted by the model (Predicted). The bold numbers represent those correctly predicted.

		Predicted			
Population = 11,363		0 Cars	1 Car	2 Cars	2 Cars +
Observations	0 Cars	**1546 (13.6%)**	650 (5.72%)	38 (0.33%)	0 (0%)
	1 Car	358 (3.15%)	**4586 (40.4%)**	898 (7.90%)	12 (0.105%)
	2 Cars	26 (0.229%)	666 (5.86%)	**1958 (17.2%)**	54 (0.475%)
	2+ Cars	0 (0%)	80 (0.704%)	417 (3.67%)	**74 (0.65%)**
		Accuracy			**0.734**

number of vehicles (observations) per household, is used to test the accuracy of the model's predicted values. The Table's bold diagonal numbers indicate the number of vehicles that are correctly predicted and the off-diagonal numbers indicate households where the number of vehicles were incorrectly predicted. It can be seen that households

with over two vehicles are the most difficult for the model to predict, however this represents a small fraction of total households. Most of the inaccuracies are over or under predicting the number of vehicles by one. The overall accuracy of this prediction is determined to be 73% on a per household basis, but the accuracy of predicting the total number of vehicles correctly in the testing data set is above 98%. Considering the diversity of households across the country, this accuracy was considered to be satisfactory for this study. The trained random forest model was then applied to the 64 households in the case study and it predicted that 77 vehicles are owned by the community's residents in Zuchwil.

5.2.3 *Driving Profiles*

With the predicted number of cars known, driving profiles are required to represent the hourly driving demand for each vehicle in the optimisation. All 77 vehicles in Zuchwil are associated with individual hourly driving profiles. The driving profiles for the vehicles have three important pieces of information that are required by the optimisation model and will be used as inputs into the optimisation:

1. The vehicles have a binary variable to indicate when they are parked at home, which is referred to as the charge availability

2. The distance driven in each hour of the day for a typical week

3. Type of roads used for driving (i.e., highways, major roads, or secondary roads)

Based on the road type, the efficiency for the vehicle is assigned according to the corresponding driving cycle. A typical driving profile for a single day is demonstrated in Fig. 5.3. The aggregated driving profiles of all 77 vehicles for each driving cycle on a typical workday is shown in Fig. 5.4.

5.2.4 *Vehicle Technologies*

There are five types of vehicles that are included in this analysis: gasoline ICEVs (ICEV-g), Compressed Natural Gas (CNG) ICEVs (ICEV-cng), PHEVs, BEVs, and FCEVs. The vehicles in this analysis are
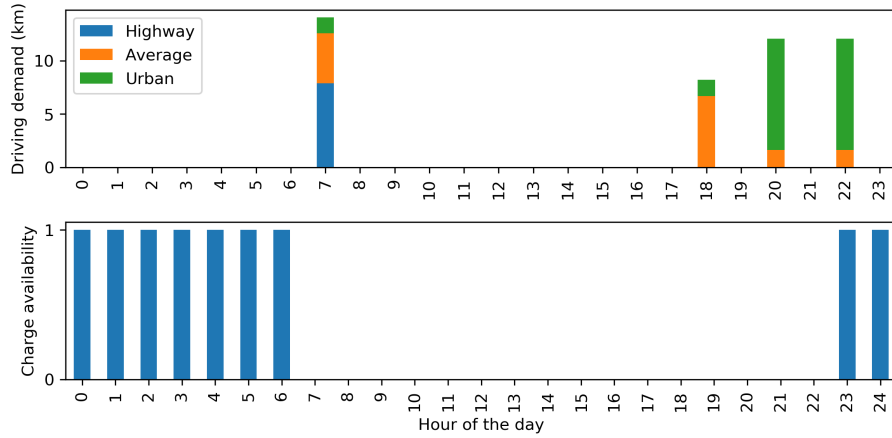
Figure 5.3.: A sample driving profile for one vehicle on a single work day.
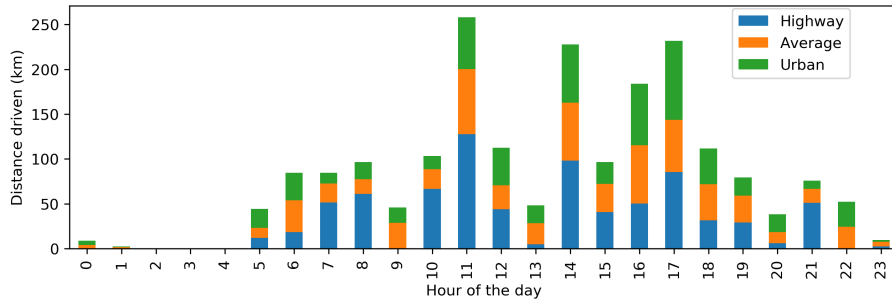
Figure 5.4.: The cumulative driving demand for a typical work day for all vehicles.

considered to be mid-size or C-segment vehicles. Although in reality, the vehicles reflect many different classes, we lack the data to know which class all owned vehicles belong to. In addition, the consideration of several different types of weight class would significantly increase the number of optimisation decision variables thus the run time of the optimisation would be too large to manage for this study. For these reasons, the most common vehicle class, mid-size vehicles, is assumed for all vehicles. The vehicles all have different powertrains, thus the efficiencies for all vehicles are standardised using the Worldwide Harmonised Light Vehicle Test Procedure (WLTP), which will be further

described in Section 5.2.4.1. A schematic of the individual vehicle powertrains is shown in Fig. 5.5.

GASOLINE AND CNG ICEV

A standard ICEV vehicle is assumed for the reference vehicle and can be chosen for a vehicle replacement. An ICEV uses an internal combustion engine, fuel by gasoline, and then a transmission with five different gear ratios to transmit the torque to velocity at the wheels. There are no regenerative devices in an ICEV, thus braking energy cannot be recovered. The mid-size vehicle assumed contains a gasoline tank, which sustains a range of approximately 700 km. ICEV charging infrastructure (petrol stations) for these vehicles is already established at no extra cost.

In addition to gasoline fuelled ICEVs, compressed natural gas (CNG) is also available as a fuel option. As opposed to a gasoline tank, a compressed tank that stores natural gas at 250 bar and has the same kilometre range as the gasoline tank.

PHEV

Plug-in hybrid vehicles contain both a small battery and an electric motor, as well as an internal combustion engine and a gasoline tank. The internal combustion engine operates similarly to the ICEV, however the electric motor contains a single speed gear. The battery in the hybrid vehicle can be charged by plugging it into an external electricity source or by normal driving. PHEVs were chosen over HEVs, since HEVs still rely solely on fossil fuels for propulsion. When driving, there are two modes: Charge Depleting (CD) or Charge Sustaining (CS). In the charge depleting mode, the ICE engine is turned off and the battery and electric motor are used. This mode can be sustained until a minimum state of charge of the battery, in this case 80% depth of discharge, and then the motor is switched to charge sustaining mode. In this mode, the engine is switched on and the state of charge of the battery is maintained. With the battery, this vehicle is able to utilise regenerative braking. Due to the fuel tank, a PHEV typically has a range as long as an ICEV, however it has a higher efficiency due to the battery and electric motor and use of regenerative braking.

BEV

Battery electric vehicles use a large battery and an electric motor

to power the vehicle. Since the battery is the only source of energy, it is much larger than the battery in a PHEV. Due to the lower energy density of batteries compared to gasoline, CNG, or compressed hydrogen, BEVs typically have lower kilometre ranges, typically around 200-300 km in 2015 for mid-sized vehicles. A range of 200 km is assumed for a mid-sized BEV in 2015 with the WLTP cycle. As battery technology improves, this energy density is assumed to increase. Due to the increased energy density, longer ranges in the future will also be possible, thus it is assumed that the range of BEVs can be extended to 300 km in 2035 and again to 500 km in 2050. These ranges are based on the calculated efficiencies using the WLTP average cycle (Section 5.2.3). Since not every consumer will require long range vehicles, lower range BEVs will also be available in the future with higher performances and lower costs. The battery allows the vehicle to utilise regenerative braking, resulting in a higher tank-to-wheel efficiency than all other vehicle types.

BEVs can be charged either at home or at high voltage public charging stations in this work. The speed of charging is dependent on the maximum power of the charging station. At home, a maximum charging power is assumed to be 11 kW (EV Charge Plus 2018), which can result in a full battery charge taking from 5-10 hours depending on the storage capacity of the battery. The maximum power in a public charging station is assumed to be 43 kW (EV Charge Plus 2018). Typically, these batteries are charged overnight at home, however this is often the time when less renewable energy is being produced.

FCEV

Fuel cell electric vehicles utilise a compressed hydrogen tank which supplies a fuel cell with hydrogen to create electricity and an electric motor for propulsion. The vehicle also contains a small battery; thus it can utilise regenerative braking to increase efficiency. The battery is mainly used in start-up periods when the fuel cell is cold, as they typically take several minutes to come to temperature and produce electricity, and to balance the response rate of the fuel cell. Through the use of the battery, the power output of the fuel cell can be decoupled from the required power fluctuations and can therefore operate at a higher efficiency. A H_2 tank compressed at 700 bar is required. As opposed to a BEV, this tank can be recharged quickly at around 0.8 kg of hydrogen per minute (Hofer 2014), resulting in a full tank charging

in around 5 minutes. In addition, the range of a FCEV is typically as long as the range for an ICEV due to the high energy density of the compressed fuel. The fuel cell, however, is a costly item that has a lower efficiency than the BEV on discharge, but a higher efficiency than an internal combustion engine. Charging infrastructure for hydrogen is currently limited in Switzerland, although there are future plans to create a network of hydrogen charging stations (H2 Energy 2018). To charge FCEVs in this simulation, a hydrogen charging station with an electrolyser, a compressor, and a hydrogen storage tank are included at an additional cost. Since these technologies are already quite expensive on their own, this represents an additional cost.

5.2.4.1   *Vehicle Efficiencies*

The efficiencies for all vehicles described in the previous section are determined using the WLTP, which has been the current standard for laboratory testing of vehicle efficiencies since September 2015 (Mock et al. 2014). The WLTP cycle contains four different segments, which include a low or urban cycle, a medium cycle with higher speed city routes, a high cycle which represents major connecting roads, and an extra-high cycle which is designed to reflect highway driving. The WLTP driving cycle velocity and acceleration are shown in Fig. 5.6. In this Figure, it can be seen that the low driving cycle includes more acceleration and deceleration than the other cycles, although the average speed is the lowest. This is due to the large amount of braking that is required with city driving due to the stop and start nature of driving in traffic. The least amount of acceleration and deceleration is found in the extra-high cycle, which has the highest velocities, but the least amount of braking. This results in a lower potential for energy recuperation due to regenerative braking.

The resulting efficiencies of the mid-size version of these vehicle powertrains were simulated in the work of Hofer (2014). Hofer assessed the status of these vehicles for the years of 2012, 2035, and 2050. To
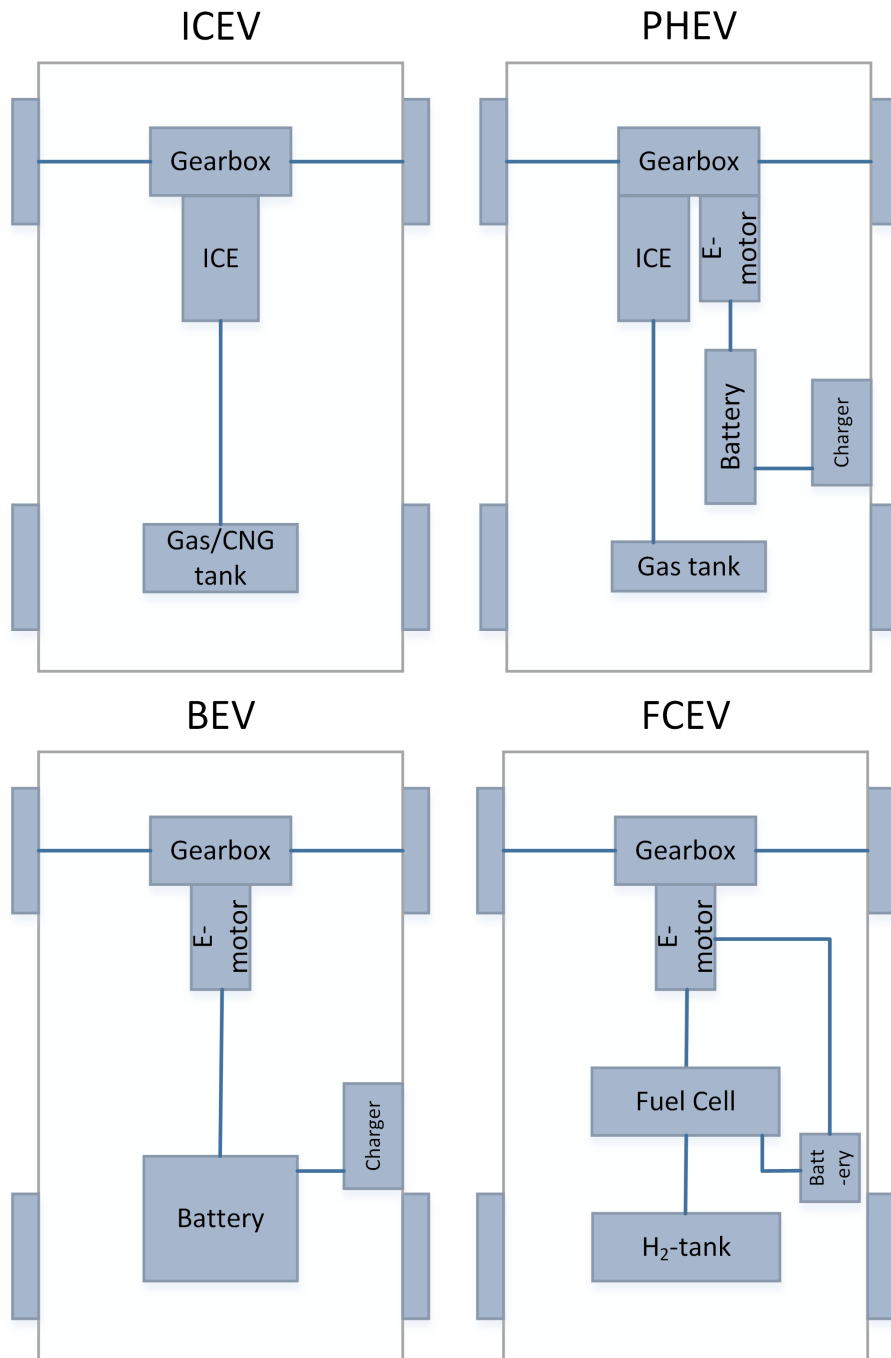
Figure 5.5.: Schematic diagrams for individual vehicles with different powertrains.
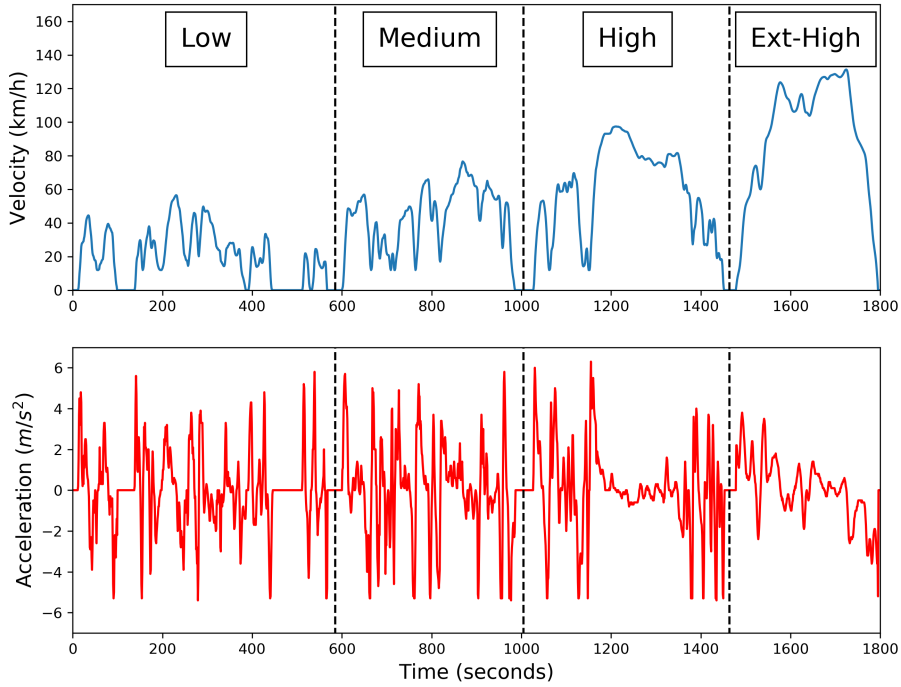
Figure 5.6.: The velocity and acceleration of the entire WLTP driving cycle used for testing the efficiencies of vehicles.

calculate the energy consumption from propulsion at different driving cycles, Eq. (5.1) and (5.2) are used.

$$
EC_{v,d} = \frac{1}{\eta_{trac}} \cdot ((A_{v,d} \cdot c_{ar} \cdot A_f + B_{v,d} \cdot c_r \cdot m_v + C_{v,d} \cdot m_v) +
$$

$$
\eta_{regen} \cdot \kappa \cdot (A'_{v,d} \cdot c_d \cdot A_f + B'_{v,d} \cdot c_r \cdot m + C'_{v,d} \cdot m_v)) \ \forall \, v \in V, \ d \in D
$$

$$
\tag{5.1}
$$

$$
m_v = m_{gl} + \chi \cdot (m_v^{pt} + m_{es}) \ \forall \, v \in V \tag{5.2}
$$

In Eq. (5.1) and (5.2) V is the index that describes the selection of vehicle technologies (ICEV-g, ICEV-cng, FCEV, PHEV, and BEV), and D represents the set of driving cycles used in this analysis (urban, highway, and average). In addition, $EC_{v,d}$ refers to the energy consumption of a vehicle type while operating in a particular driving cycle, η_{trac} is the traction efficiency, η_{regen} is the regeneration efficiency, c_d is the area of the front windshield, c_{ar} is the aerodynamic resistance, c_r is the rolling

resistance, A_f is the frontal area of the vehicle, κ is the fraction of regenerative versus friction braking, and m_v is the total mass of the vehicle. In Eq. (5.2), m_{gl} represents the vehicle's glider mass (i.e., the vehicles mass without the powertrain or fuel tanks), which is assumed to be 950 kg for mid-sized vehicles in 2015 and is reduced 0.5% per year, χ is a factor introduced to account for additional structural support of the powertrain and energy storage beyond the glider baseline and is assumed to be 1.3. m_v^{pt} is the mass of the powertrain for each vehicle types, and m_{es} is the mass of the energy storage system installed. The masses for the energy storage and for the powertrain are found in Hofer (2014).

$A_{v,d}$, $B_{v,d}$, $C_{v,d}$, $A'_{v,d}$, $B'_{v,d}$, $C'_{v,d}$ are parametrisation constants used to calculate the contributions to mechanical energy demand required for propulsion in kJ per 100 km. These are defined for the different driving cycles. Coefficients A, B, and C are used to calculate the traction energy of the vehicle and coefficients A', B', and C' are used to calculate the regeneration energy of the vehicle. These coefficients are also related to Equations (5.3) to (5.5). The coefficients for the WLTP driving test are shown in Table 5.2 and are taken from Hofer (2014).

$$A + A' = const \tag{5.3}$$

$$B + B' = const \tag{5.4}$$

$$C + C' = 0 \tag{5.5}$$

Table 5.2.: Parametrisation coefficients used to calculate vehicle energy consumption in kJ per 100 km.

Coefficient	Unit	WLTP				
		Avg	Low	Mid	High	Ext-High
A	$kg/m-s^2$	27,072	3,410	10,079	23,314	48,992
B	m/s^2	744	586	716	819	839
C	m/s^2	12.6	19.7	18.3	10.5	8.4
A'	$kg/m-s^2$	3,692	2,065	3,068	2,350	5,826
B'	m/s^2	207	395	265	162	142
C'	m/s^2	-12.6	-19.7	-18.3	-10.5	-8.4

In addition, c_d is assumed to be 0.31 m^2 in 2015, 0.28 m^2 in 2035, and 0.26 m^2 in 2050. c_r is assumed to be 0.01 in 2015, 0.0092 in 2035,

and 0.0083 in 2050. A_f is assumed to be 2.2 m^2. κ is assumed to be zero for ICEVs since there is no battery for regenerative braking, and is assumed to be 0.6 for PHEVs, FCEVs, and BEVs. These assumptions are made for mid-size vehicles according to Hofer (2014).

From these results, the efficiencies for the year of 2015 were interpolated assessed for three different drive cycles: the urban or low WLTP drive cycle, the highway or extra-high drive cycle, and the average of the full WLTP drive cycle (including low, medium, high and extra-high). The resulting efficiencies for the vehicle technologies in different drive cycles and years are shown in Figure 5.7. These efficiencies include not only the energy required for propulsion, but also the auxiliary power consumption of the vehicles. Auxiliary power includes the heating, cooling, and the electric consumption of the safety and entertainment systems of the vehicle. The heating loads for vehicles with an Internal Combustion Engine (ICE) are generally much lower since the waste heat from the engine can be used for heating. In BEVs, a heat pump can be used instead. As a result, BEVs generally have higher energy demands in the winter due to the energy required to heat the vehicle with a heat pump. For more details on the calculation, please refer to Hofer (2014).

For the years of 2035 and 2050, it is assumed that the weight of the
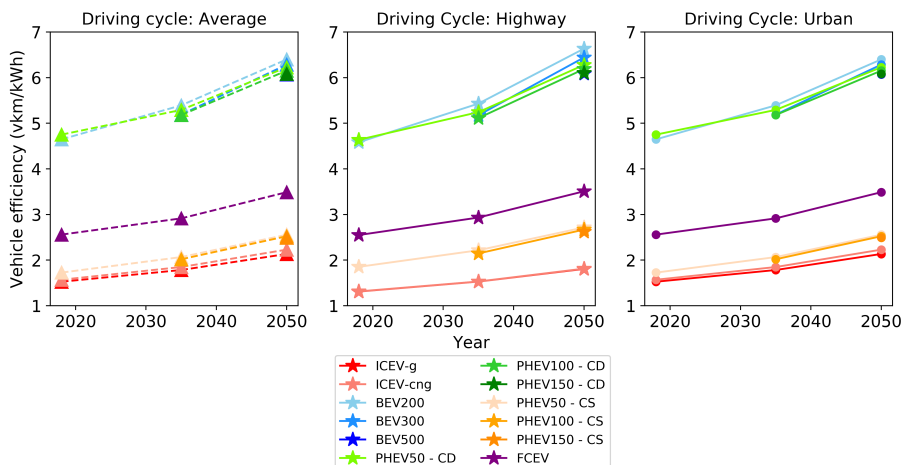
Figure 5.7.: Vehicle technology efficiencies in different driving cycles from 2015 to 2050 in kWh of propulsion energy per vehicle kilometre.

glider mass decreases over time, thus the efficiency of all vehicles improve due to lower mass. In addition, improvements in the efficiencies of batteries and fuel cells are considered. Due to these increases in efficiencies, the mass of batteries and fuel cells decrease over time, thus further increasing the vehicle efficiency. Since the vehicle range is kept constant, the capacity of the storage for all vehicles are adjusted for the same range with the WLTP average cycle, thus the mass of stored fuel is also decreased, which also increases the efficiency. These improvements result in the efficiency improvements observed in Fig. 5.7.

5.2.4.2 *Vehicle Storage and Range*

The range of the vehicles (in kilometres) is based on both the efficiency of the vehicle's propulsion and the storage within the vehicles. The storage energy in the vehicles is calculated vy the range of vehicles and the average efficiencies of the vehicles through Eq. (5.6).

$$E_v^{vcap} = \frac{Range_v^{km}}{\eta_{v,avg}^{WLTP}} \ \forall \ v \in V \tag{5.6}$$

Here, E_v^{vcap} is the vehicle's energy storage capacity, $Range_v^{km}$ is the range of the vehicle as defined in Table 5.3, and $\eta_{v,avg}^{WLTP}$ is the efficiency of the vehicle over the whole WLTP driving cycle. The assumed ranges of the vehicles in the different years of consideration are shown in Table 5.3.

As is seen in Table 5.3, there are several different battery size options for the years of 2035 and 2050. The specific battery range for PHEV and BEVs will be referred to with the battery range in kilometres after the vehicle's powertrain. This means that PHEVs will be referred to as PHEV50, PHEV100, and PHEV150 for the range of 50, 100 and 150 kilometre batteries respectively. BEV200, BEV300, and BEV500 refer to BEVs with ranges of 200, 300, and 500 kilometres respectively.

The storage capacity in kWh or kg (for H_2) of the vehicle is calculated with the average performance of the WLTP cycle, producing the vehicle kilometre ranges found in Table 5.3.

5.2.5 *Mobility Optimisation*

In Section 3.4 an optimisation model was built that included the descriptions of conversion technologies, storage technologies, and the description of multi-objective optimisation. This optimisation model

Table 5.3.: Vehicle Ranges from 2015-2050 in vehicle kilometres (vkm).

Vehicle	Year	Gasoline (vkm)	Battery (vkm)	H₂ tank (vkm)
ICEV	2015	700	-	-
	2035	700	-	-
	2050	700	-	-
PHEV	2015	400	50	-
	2035	600	50, 100	-
	2050	600	50, 100, 150	-
BEV	2015	-	200	-
	2035	-	200, 300	-
	2050	-	200, 300, 500	-
FCEV	2015	-	-	500
	2035	-	-	700
	2050	-	-	700

is now extended to include the selection, operation, and charging of vehicles within the Zuchwil case study. The 77 vehicles owned by building occupants will now be optimised to operate with either ICEVs, PHEVs, BEVs, or FCEVs and the charging of the vehicles is now considered a demand within the case study that must be met. This can be demonstrated in Fig. 5.8. In this Figure, the driving demand, which has been described in Section 5.2.3, must be met through electricity, hydrogen, natural gas, or gasoline. Electricity and hydrogen can either be created on-site or electricity, natural gas, and gasoline can be purchased. The technologies located in Fig. 5.8 can be installed on two different levels: either on the building level, or on the district level. These two technologies levels are shown further in Fig. 5.9. Since the buildings are connected by the electricity grid and the natural gas grid, the battery, electrolysers, fuel cells, hydrogen storage, and the catalytic methanisation reactor are, if selected, installed on the district level. PVs are installed on the building level because they are located on rooftops and heat pumps and gas boilers are installed on the building level as there is no heating grid. Charging stations for electric vehicles are located on the building level, and charging stations for hydrogen, gasoline, and CNG are located on the district level.
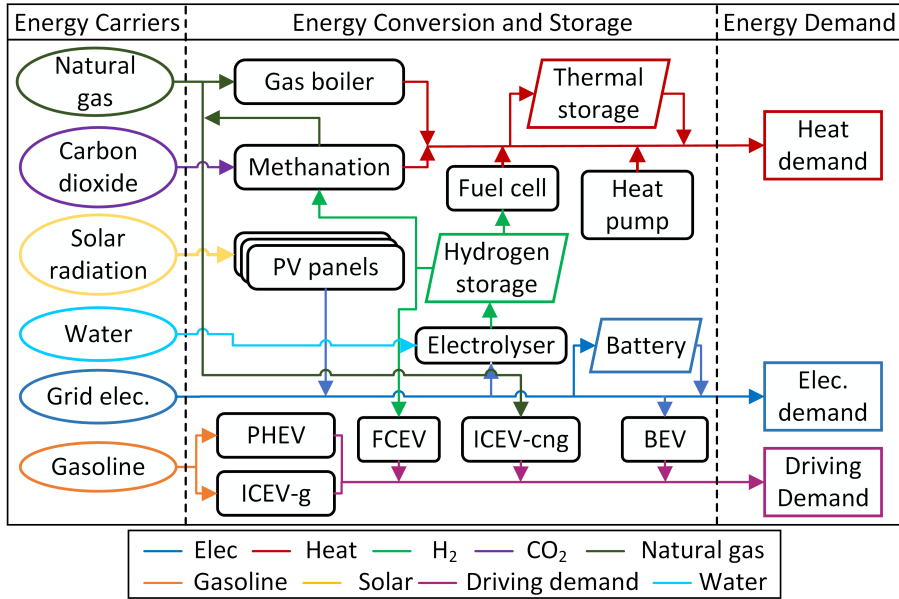
Figure 5.8.: The multi-energy system simulated in this work, including energy carriers, conversion technologies, storage technologies, vehicle technologies, and energy demands.
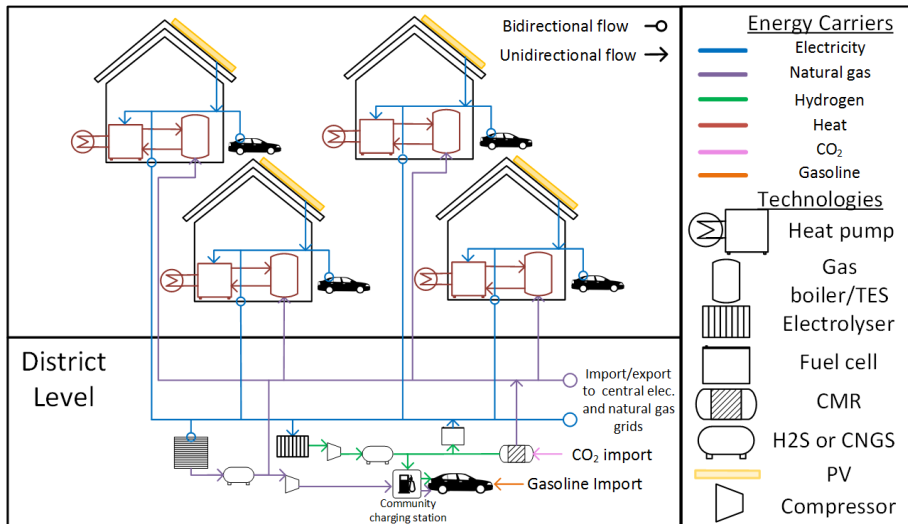
Figure 5.9.: Schematic diagram representing the grids and the installation location of components on both the building and district levels.

5.2.5.1 *Export Constraints*

The system is connected to both the centralised electricity grid and to the centralised natural gas grid, thus both these energy carriers can be exported for a profit. Since PV is produced on the building level, it can be exported from the buildings to the microgrid (Eq. (5.7)). This energy can then be used by another consumer within this community, or it can be exported to the centralised grid. To limit the exports to only PV production, Eq. (5.8) constraints the exported electricity to the sum of the PV energy exported from the buildings. The exports are limited to only renewable production, as exported energy receives the feed-in tariff, which must only be given to renewable energy production sold back to the grid.

$$P_{elec,b,h}^{building,export} \leq P_{PV,elec,b,h}^{out} \ \forall \ f \in F, \ b \in B, \ h \in H \tag{5.7}$$

$$P_{elec,h}^{district,export} \leq \sum_{b}^{B} P_{elec,b,h}^{buildings,export} \tag{5.8}$$

Since SNG can be produced via methanation within the Decentralised Energy Systems (DES), Eq. (5.9) limits the exported SNG to the methane production on site.

$$P_{CH4,h}^{district,export} \leq P_{CMR,CH4,h}^{out} \tag{5.9}$$

Both electricity from PV and SNG can be exported for a profit per kWh sold. The prices of these energy carriers are summarised in Table D.1.

5.2.5.2 *Storage Constraints*

There are four different storage technologies considered in this work: battery electric storage, thermal hot water storage (TES), H2S, and Compressed Natural Gas Storage (CNGS). The total energy capacity of these technologies is limited below the maximum capacity with Eq. 5.10.

$$E_f^{cap} \leq E_f^{max} \ \forall \ f \in Elec, \ Heat, \ H_2, \ CH_4 \tag{5.10}$$

The total energy stored in each time step, $E_{f,h}^{SOC}$, is constrained below the installed capacity, E_f^{cap} in Eq. 5.11.

$$E_f^{cap} \geq E_{f,h}^{SOC} \ \forall \ h \in H, \ f \in \ Elec, \ Heat, \ H_2, \ CH_4 \tag{5.11}$$

A container storage model is used for the optimisation of the storages. In this model, the storage is defined by a charging efficiency (η_f^{ch}), a discharging efficiency (η_f^{dch}), and a loss of stored energy per hour (η_f^{loss}). This is defined in Eq. 5.12. Eq. 5.13 defines the energy that can be charged or discharged from the storage as a function of the percent of the total installed capacity. Lastly, Eq. 5.14 defines that the storage level in the first and last hour of the simulation must be equivalent.

$$E_{f,i}^{SOC} = E_{f,i-1}^{SOC} \cdot \eta_f^{decay} + \eta_f^{ch} \cdot P_{f,h[i]}^{ch} \Delta T - (1/\eta_f^{dch}) \cdot P_{f,h[i]}^{dch} \Delta T$$
$$\forall\, i \in I,\, f \in Elec,\, Heat,\, H_2,\, CH_4 \tag{5.12}$$

$$P_{f,h}^{ch/dch} \leq P_f^{cap} \cdot \eta_f^{ch/dch} \,\forall\, h \in H \tag{5.13}$$

$$E_{0,f}^{SOC} = E_{8760,f}^{SOC} \,\forall\, f \in F \tag{5.14}$$

To consider long-term storage, the decision variable of the energy level in the storages uses a full horizon, or 8760 hours. The charging and discharging profiles are repeated for the number of days they represent. We have chosen 12 representative days a year with each month assigned a representative day. The representative days are repeated for the number of days in that month. Peak days represent a single day. In order to translate the reduced time horizon for charging and discharging to the full time horizon for storage, the term $h[i]$ is used, which indexes the hour in the full horizon (i, which ranges from 0-8760 hours) to the corresponding hour in the representative day (h, which ranges from 0-360) in the short-time horizon. This indexing allows the charging and discharging schedules of the representative days to be repeated and linked to establish a full storage horizon. Using this method, the net charge and discharge over 24 hours does not need to be equal to zero, although the net charge and discharge over one year still needs to equal zero.

5.2.5.3   Vehicle Constraints

The vehicles all contain on-board storage that is controlled in a similar fashion to the stationary storage, except that the size of the storage is fixed when a particular vehicle is selected. The storage size for installed technologies is then enforced using the constraint in Eq. (5.15).

$$E_{c,v,f}^{vcap} = E_{storage,v,f}^{vcap} \cdot \delta_{c,v}^{vehicle} \,\forall\, c \in C,\, v \in V,\, f \in F \tag{5.15}$$

Here, C is the index that describes the 77 vehicles owned by the households in the community, as determined in Section 5.2.2. In addition, $E_{v,f}^{vcap}$ is the vehicle storage capacity described in Eq. (5.6), $\delta_{c,v}$ is the binary variable that symbolises whether a vehicle technology was installed, and $E_{c,v,f}^{vcap}$ is the installed vehicle storage capacity. To ensure that only one vehicle type is installed per vehicle assigned, Eq. (5.16) is used.

$$\sum_{v}^{V} \delta_{c,v} = 1 \, \forall \, c \in C \tag{5.16}$$

The storage level is then managed similarly to the stationary storage technologies with Eq. (5.17) to (5.19). Eq. (5.19) ensures that the storage level at the beginning and end of each day is equal to each other. In addition, Eq. (5.12) is a constraint that enforces that the level of charge in the vehicle's storages must carry over from day to day. Long-term storage is not necessary for the vehicle storages.

$$E_{c,v,f,h}^{SOC} \leq E_{c,v,f}^{vcap} \, \forall \, c \in C, \, v \in V, \, f \in F, \, h \in H \tag{5.17}$$

$$E_{c,v,f,h}^{SOC} = E_{c,v,f,h-1}^{SOC} \cdot \eta_f^{loss} + \eta_{v,f}^{vch} \cdot P_{c,v,f,h}^{vch,home} + \eta_{v,f}^{vch} \cdot P_{c,v,f,h}^{vch,public} -$$
$$\sum_{d}^{D} P_{c,v,f,d,h}^{vdriving} - P_{c,v,f,h}^{vdch} \, \forall \, i \in I, \, f \in F \tag{5.18}$$

$$E_{c,v,f,h}^{SOC} = E_{c,v,f,h+24}^{SOC} \, \forall h \in H \, if \, mod \, (h/24) = 0 \tag{5.19}$$

Here, $E_{c,v,f,h}^{SOC}$ is the hourly energy capacity within the storage, $\eta_{v,f}^{vch}$ is the vehicle charging efficiency, $P_{c,v,f,h}^{vch,home}$ is the charging power at home, $P_{c,v,f,h}^{vch,home}$ is charging at a public charging station, $P_{c,v,f,d,h}^{vdriving}$ is the discharging energy for propulsion at each driving cycle within a timestep, and $P_{c,v,f,h}^{vdch}$ is the discharging energy enabled by bidirectional charging from the vehicle batteries back to the buildings that is enabled with bidirectional charging when vehicles are at home.

Vehicles can be charged either at a public charging location or at home. At home, they can be charged either with PV produced on the rooftops, by the fuel cell, the battery discharge, or by electricity purchased from the grid. In public locations, the electricity used for charging is assumed to be the grid mix of CO_2 and a surplus for the electricity is assumed based on the current cost of charging in public stations in Switzerland (0.45 CHF/kWh) (Motion 2019). The efficiency of each individual car technology with their corresponding driving

cycle efficiencies is constrained with Eq. (5.20). This constraint ensures that the vehicle demand (in vkm) in each driving cycle is met. In addition, the availability of electric charging at home is limited to the times in which the vehicle is located at home, thus the binary variable representing whether a vehicle is at home or not (which was defined in Section 5.2.3) can be used to enforce this with Eq. (5.21). Similarly, times at which electric vehicles are available for public charging are limited to times when the vehicle is underway or in transit, but has less than 40 km of driving within the hour. The availability of public charging is then limited with Eq. (5.22). The availability of hydrogen charging is limited to times when the vehicles are either departing or returning home. Lastly, the time of gasoline charging is limited to any time when the vehicles are in transit.

$$P_{c,v,f,d,h}^{vdch} \cdot \eta_{v,f,d} = P_{c,d,h}^{vdemand} \ \forall \ c \in C, \ v \in V, \ f \in F, \ d \in D, \ h \in H \quad (5.20)$$

$$P_{c,v,f,h}^{vch_{home}} \leq \delta_{c,h}^{home} \cdot P_{v,f}^{max} \cdot \delta_{c,v}^{vehicle} \ \forall \ c \in C, \ v \in V, \ f \in F, \ h \in H \quad (5.21)$$

$$P_{c,v,f,h}^{vch_{public}} \leq \delta_{c,h}^{transit} \cdot P_{v,f}^{max} \cdot \delta_{c,v}^{vehicle} \ \forall \ c \in C, \ v \in V, \ f \in F, \ h \in H \quad (5.22)$$

Here, $\eta_{v,f,d}$ is the efficiency of each vehicle in each driving cycle (as indicated in Fig. 5.7), $P_{c,d,h}^{vdemand}$ is the vehicle driving demand in units of vehicle kilometres (vkm) which is taken from the driving profiles demonstrated in Fig. 5.3 and 5.4. In addition, $\delta_{c,h}$ is the charging binary variable that represents whether charging is available for the vehicle and $P_{v,f}^{max}$ is the maximum charge available in an hour, which is limited to 11 kW for at home charging and 22 kW for public station charging. The maximum charging potential is 295 kWh/min for ICEVs and 0.8 kg H_2/min for FCEVs.

To ensure that the bi-directional charging from BEVs back to the building and the grid is only available when the vehicles are at home, Eq. (5.23) is used. The $P_{v,f}^{max}$ limit for this discharge is also set to 11 kW.

$$P_{c,v,f,h}^{vdch} \leq \delta_{c,h}^{home} \cdot P_{v,f}^{max} \cdot \delta_{c,v}^{vehicle} \ \forall \ c \in C, v \in V, f \in F, h \in H \quad (5.23)$$

Please note that vehicles discharging back to the building (V2B) is only available for the electrical energy carrier.

5.2.6 *Energy Balances*

To meet the demands within the buildings for electricity, heat, and vehicle charging, production has to be balanced with imports, exports,

and storages. These balances are performed both on the individual building level, as well as on the district level. Since PV is installed on the individual building level, it can produce electricity ($P^{out}_{t,f,b,h}$) for the buildings' local demands, or the electricity can be exported ($P^{export}_{f,b,h}$) to the community microgrid. In addition, electricity can be imported ($P^{import}_{f,b,h}$) from the community microgrid to meet the building electricity demand ($P^{l}_{f,b,h}$), the heat pump energy consumption, or the electric vehicle charging demand ($P^{vch}_{c,v,f,h}$). The building energy demand is met with Eq. (5.24).

$$
P^{import}_{f,b,h} - P^{export}_{f,b,h} + \sum_{t}^{T} P^{out}_{t,f,b,h} + \sum_{c}^{C \in b} \sum_{v}^{V} P^{vdch}_{c,v,f,h} =
$$
$$
P^{demand}_{f,b,h} + \sum_{c}^{C \in b} \sum_{v}^{V} P^{vch}_{c,v,f,h} \ \forall \ f \in F, \ b \in B, \ h \in H
$$

(5.24)

It is noted in Eq. (5.24) that heat, hydrogen, CO_2, water, and gasoline cannot be exported on the building level and heat, gasoline, CO_2 and water cannot be imported. In addition to the energy balance on the building level, there is also a limit of power imported or exported to the local grid, which is based on a 16 Amp current limit for most households and apartments (Tan et al. 2016). Similarly, an energy balance is then performed on the district, as shown in Eq. (5.25). Since the stationary storage technologies are located on the district level (so they can be shared between the buildings) the storage charging and discharging energy is also included.

$$
P^{import}_{f,h} - P^{export}_{f,h} + \sum_{b}^{B} P^{export}_{f,b,h} + \sum_{t}^{T} P^{out}_{t,f} +
$$
$$
P^{dch}_{f,h} - P^{ch}_{f,h} = \sum_{b}^{B} P^{import}_{f,b,h} \ \forall \ f \in F, \ h \in H
$$

(5.25)

5.2.6.1 *Objective Functions*

There are two objective functions used in this analysis, both of which are minimised using the epsilon-constraint method, which was described in Section 3.5.2. The epsilon-constraint method minimises a first objective while reducing the second objective below a particular value with the use of Eq. (3.45) and (3.46). This epsilon-value can be increased or

reduced to provide a variety of Pareto optimal points. In this Chapter, the calculation of costs are modified to include vehicle capital and operational costs. The new net annual cost objective is calculated with Eq. (5.26).

$$Cost_{total} = C_{inv}^{district} + C_{inv}^{buildings} + C_{inv}^{vehicles} + C_{OMF} + C_{OMV} + C_{Carriers}$$
(5.26)

Here, $Cost_{total}$ is the total cost of the system per year, $Cost_{inv}^{district}$ is the investment cost of technologies on the district level, $Cost_{inv}^{buildings}$ is the investment cost of the technologies on the building level, $C_{inv}^{vehicles}$ is the investment cost of the vehicles, C_{OMF} is the fixed operation and maintenance cost, C_{OMV} is the variable operation and maintenance cost, and $C_{Carriers}$ is cost of importing and exporting of energy carriers. The district technology, building technology, and vehicle technology investment costs are shown in Eq. (5.27), (5.28), and (5.29) respectively.

$$Cost_{inv}^{district} = \sum_{t}^{T}[(\delta_t \cdot Cost_t^{fixed} + P_t^{cap} \cdot Cost_t^{linear}) \cdot CRF_t] +$$
$$\sum_{s}^{S}[(\delta_s \cdot Cost_s^{fixed} + P_s^{cap} \cdot Cost_s^{linear}) \cdot CRF_s]$$
(5.27)

$$Cost_{inv}^{buildings} = \sum_{b}^{B}[(\delta_{t,b} \cdot Cost_t^{fixed} + P_{t,b}^{cap} \cdot Cost_t^{linear}) \cdot CRF_t]$$
(5.28)

$$Cost_{inv}^{vehicles} = \sum_{v}^{V}[\sum_{c}^{C}(\delta_{c,v}) \cdot Cost_v^{fixed} \cdot CRF_v]$$
(5.29)

In these three equations, δ is the binary variable that indicates whether or not a technology is installed, $Cost^{fixed}$ represents the fixed capital costs, P^{cap} is the installed capacity (in kW for conversion technologies and kWh for storage technologies), $Cost^{linear}$ is the linear capital costs, and CRF is the capital recovery factor which is further defined in Eq. (5.30). The costs of the vehicles with the different powertrains from 2015-2050 are shown in Table D.3

$$CRF_{t,f,v} = \frac{r}{[1 - \frac{1}{(1+r)^{Lifetime_{c,s,v}}}]} \quad \forall\, t \in T,\, f \in F\, v \in V$$
(5.30)

Here, $Lifetime_{c,s}$ represents the lifetime of the conversion technologies, storages, and vehicles in years. For the vehicle technologies, the lifetime is 200,000 vehicle kilometres (Dun et al. 2015). The lifetime in years

calculated by dividing the vehicle kilometres lifetime from the annual driving demand of the households based on the Swiss mobility micro census data (Bundesamt für Statistik 2015). The technology operation and maintenance costs are calculated with Eq. (5.31) and (5.32).

$$Cost_{OMF} = \sum_t^T P_t^{cap} \cdot Cost_t^{OMF} + \sum_t^T \sum_b^B P_{b,t}^{cap} \cdot Cost_t^{OMF} + \sum_v^V \sum_c^C \quad (5.31)$$

$$Cost_{OMV} = \sum_t^T \sum_f^F \sum_h^H P_{t,f,h}^{Out} \cdot Days_h^{rep} \cdot Cost_{t,f}^{OMV} +$$
$$\sum_c^C \sum_d^d \sum_h^H (P_{c,d,h}^{vdemand} \delta_{c,v} \cdot Days_h^{rep} \cdot Cost_v^{OMV}) \quad (5.32)$$

Here, $Cost^{OMF}$ is the fixed operating costs which are based annually on capacity and $Cost^{OMV}$ are the variable operating costs which are based on kWh of output annually for each technology. In addition, $Days_h^{rep}$ is the typical days factor, which is derived from Section 5.2.1. This factor describes how many other days within the year that the typical day is meant to represent, thus it must be used to reflect a full year of operation. The energy carrier costs are calculated with Eq. (5.33).

$$Cost_{carriers} = \sum_i^I \sum_h^H P_{import,f,h}^{district} \cdot Price_f^{Purchase} \cdot Days_h^{rep} -$$
$$\sum_i^I \sum_h^H P_{export,f,h}^{district} \cdot Price_f^{sell} \cdot Days_h^{rep} \quad (5.33)$$

Here, $P_{import,f,h}^{district}$ refers to energy carriers imported into the district and $P_{export,f,h}^{district}$ is the exported energy carriers. In this case, only natural gas and electricity can be exported from the district to the centralised natural gas and electricity grids respectively, and heat and H_2 cannot be purchased or imported into the district as they must be locally produced. $Price_f^{Purchase}$ describes the cost of purchasing energy carriers per kWh and $Price_f^{sell}$ is the cost of selling produced energy back to the centralised grids.

The total carbon emissions is the second objective function, which is constrained in the multi-objective function. In contrast to Chapter 3 and 4, embodied emissions, or the emissions that are involved in the production, manufacturing and transport of the conversion, storage,

and vehicle technologies are included in this calculation. The total CO_2 is calculated with Eq. (5.34).

$$CO2_{total} = CO2_{EE}^{District} + CO2_{EE}^{Buildings} + CO2_{EE}^{Vehicles} + CO2_{Carriers} \quad (5.34)$$

In this equation, $CO2_{EE}$ denotes the embodied emissions for conversion and storage technologies on the district and building level as well as the vehicles. In addition, $CO2_{Carriers}$ is the total operational CO_2 emissions. The embodied emissions for district technologies, building technologies, and vehicles are described with Eq. (5.35), (5.36), and (5.37) respectively.

$$CO2_{EE}^{district} = \sum_t^T [(\delta_t \cdot CO2_{EE,t}^{fixed} + P_t^{cap} \cdot Cost_{EE,t}^{linear}) / Lifetime_t] \quad (5.35)$$

$$CO2_{EE}^{buildings} = \sum_t^T \sum_b^B [(\delta_b \cdot CO2_{EE,t}^{fixed} + P_{t,b}^{cap} \cdot Cost_{EE,t}^{linear}) / Lifetime_t] \quad (5.36)$$

$$CO2_{EE}^{vehicles} = \sum_v^V [\sum_c^C (\delta_{c,v}) \cdot CO2_{EE,v}^{fixed} / Lifetime_{c,v}] \quad (5.37)$$

Here, $CO2_{EE}^{fixed}$ are the fixed embodied emissions and $Cost_{EE}^{linear}$ are the variable embodied emissions that increase with capacity and $Lifetime$ is the lifetime of the technologies in years. The total emissions of all energy carriers are calculated with Eq. (5.38).

$$CO2_{Carriers} = \sum_f^F \sum_h^H (P_{Import,t,h}^{District} \cdot CF_f^{Import} \cdot Day_h^{Rep}) \quad (5.38)$$

The capital costs, operating and maintenance costs, and embodied emissions are listed with references in Table D.2 for the conversion technologies, Table D.4 for storage technologies, and Table D.3 for the vehicle technologies. The prices for imports, exports, and the CO_2 values of purchased energy carriers are shown in Table D.1.

5.3   2000 WATT SOCIETY TARGETS

The emissions targets used in Chapter 3 and 4 were established exclusively for buildings. Since building energy and transport are separate sectors, they typically also have separate energy and emissions targets. Buildings typically assess their emissions targets on a per m^2 basis. For

vehicles, this is assessed this per vkm.

One alternative is the 2000 Watt Society Targets. In Switzerland, the 2000 Watt Society is an initiative, defined in 1998 by ETH Zürich (Board of Swiss Institutes of Technology (ETH-Rat) 1998), that attempts to reduce the energy consumption of citizens from developed countries to 2000 Watts or one ton of CO_2 per person per year without lowering the standard of living. The current level of energy consumption per person in Western Europe is calculated to be just above 6000 W/person/year, thus this concept requires an energy reduction of 66% (Blindenbacher 2019). This concept attempted not only to address household and personal energy usage, but also embodied emissions for the energy, building, and transport systems which represent a significant amount of emissions that are usually neglected from emissions calculations. Embodied emissions and embodied energy refer to the emissions or energy required to produce a particular good or service. This includes raw material extraction, manufacturing, and transport. It is frequently used to assess the energy for the entire life-cycle cost, emissions, or energy of a product rather than just the operational cost, emissions, or energy. When only operational emissions are reduced, the bigger picture of the actual amount of CO_2 being emitted into the atmosphere because of a particular energy system design decision is often miscalculated, particularly when a product is manufactured outside of the country.

The 2000 Watt society target includes life-cycle energy used in living and office spaces, electricity production, automobile travel, air travel, public transportation, and public infrastructure. To realise these strict targets, significant reductions in both building energy consumption and in transportation are required. With vehicle charging integrated into the community or into the buildings, energy and emission targets can be reduced simultaneously using locally produced energy and by exploiting the storage potential in the vehicle stock.

As an extension of the 2000 Watt Society energy targets (Bébié et al. 2009), the Swiss Society of Engineers and Architects (SIA) 2040 Standard for Energy Efficiency Pathways was developed in 2011 SIA 2011. Unlike the Swiss Energy Strategy targets used in Chapter 4 for buildings in Switzerland, the SIA 2040 standard includes embodied energy and emissions for buildings and transport. This standard only includes embodied emissions for infrastructure and consumer goods related to building materials and domestic transport. Other consumer

goods and food are not accounted for in this standard. SIA 2040 allocates 5 kg CO_2-eq/m^2/year for retrofitted building operation, 5 kg CO_2-eq/m^2/year for building retrofit materials and systems (mostly comprised of embodied emissions), and 5.5 kg CO_2-eq/m^2/year for mobility (including public transit)[1]. This represents a target of 900 kg CO_2-eq/person, using the standard living space per person specified in the standard itself. To meet 2050 targets, 450 kg CO_2-eq/person is required. Since the model developed in this Chapter includes both building and transport sectors, these targets are used for comparison in the next chapter. These targets also include operational and embodied emissions for public transit and embodied emissions for building materials. Although these two categories are not included in the optimisation model, they will be calculated on a per person basis in the following chapter and included in the analysis. This calculation per person can be further described with the Kaya identity, that was formally introduced only for buildings in Eq. (3.49). In Eq. (5.39), the Kaya identity is expanded to include buildings and transport.

$$CO2_{total} = (\frac{CO2_{buildings}}{E_{buildings}} \cdot \frac{E_{buildings}}{P_{buildings}} +$$
$$\frac{CO2_{transport}}{E_{transport}} \cdot \frac{E_{transport}}{vkm} \cdot \frac{vkm}{pkm} \cdot \frac{pkm}{P_{buildings}}) \cdot P_{buildings} \quad (5.39)$$

Here, $CO2_{buildings}$ is the CO_2 emissions from the buildings sector, $CO2_{transport}$ are the emissions in the transport sector, and $CO2_{total}$ are the combined emissions. $E_{buildings}$ is the energy consumption for both electricity and heating and $E_{vehicles}$ is the energy used to propel vehicles per vehicle kilometre (vkm). $\frac{pkm}{vkm}$ represents the number of passenger kilometres (pkm) per vehicle kilometre. This can be calculated by multiplying the number of passengers in the mode of transportation by the vehicle kilometres travelled. Lastly, $P_{buildings}$ is the population of occupants in the buildings.

5.4 SUMMARY

In this chapter, we have extended the model developed in Chapter 3 to include the personal vehicle transport. To do this, the number of

---

1 Please note that new buildings have the targets of 8.5 kg/m^3 for building materials and 2.5 kg/m3 for operation. The mobility targets remain the same at 5.5 kg/m^3

vehicles owned by the inhabitants must be known. Since the data for the majority of the buildings in Switzerland is lacking precise data in this regard, mobility census data from 2015 was used to train a random forest model to predict vehicle ownership per household based on the location of the household, the size of the municipality, the number of adults and children in the household, the income, the household type, and the building type. Driving profiles are then assigned to these vehicles to specify when and on which roads drivers are using their vehicles. Five types of vehicles with different powertrains are then established and their efficiencies are determined for three different driving cycles.

Within the optimisation model, a series of constraints are defined to specify the installation of the vehicles, the limitations of charging, and the driving cycles. The objective functions are then updated from Section 3.5.2 to include vehicle related costs and operating emissions and also to include embodied emissions for all technologies into the CO_2 emission calculations. Finally, new energy targets are established based on SIA 2040 that includes both personal transport and building demand with embodied emissions related to the necessary infrastructure required in both sectors.

The updated model in this Section will be applied to the case study of Zuchwil in Chapter 6 to demonstrate its implementation from 2015 to 2050 and compare the results to Chapter 4.

APPLICATION OF MES OPTIMISATION FOR POWER-TO-MOBILITY

The optimisation model developed in the previous chapter is built and designed to investigate the interactions of buildings and vehicle charging systems for personal transport demands within a community. The model allows for a holistic outlook of the future decarbonisation of our homes and our personal transport. The optimal vehicle selection is presented and discussed, as well as the relationship between driving distance and vehicle selection. The building technologies chosen to meet the building's loads and support the vehicle charging are then presented. The operation of the storage systems over a one-year period along with the operation of the conversion technologies are also assessed and discussed. Then, the objective functions, with a full breakdown of emissions and costs are shown and compared to the energy targets. Lastly, the self-sufficiency of the community is presented.

6.1 BACKGROUND AND CONTEXT

Typically, the energy consumption of buildings and mobility are analysed with separate models since the emissions lie in different energy sectors. Models that simulate the diffusion of alternative fuel vehicles into the vehicle stock often neglect to include charging infrastructure and rarely include the simulation of the energy system providing the vehicles' charging energy. Unlike other work where vehicle diffusion rates are an input into the simulation, this work uses optimisation to select the best diffusion rates over time. In addition, models that include the energy system and charging infrastructure for vehicle typically only consider the electrical energy carrier for battery electric vehicles. However, with the recent improvements in alternative vehicle technologies and the increasing cost of fossil fuels, AFVs and their charging and discharging potentials are widely recognised to be an essential part of the energy transition.

Since the charging for these vehicles is anticipated to be performed either in the district or in the home, it is essential to optimise the vehicle charging within the energy system, since it is likely to become a sig-

nificant household load. The energy supply for charging must also be decarbonised to ensure that energy targets are met. Our optimisation model allows for PV installations and energy storage installations inside the district to allow for reduction of emissions in the energy supply for vehicle charging and building demands.

In this chapter, ICEVs, BEVs, PHEVs, and FCEVs are optimally selected for a vehicle fleet within a group of buildings. Zuchwil, a case study of 52 buildings and 77 cars owned by vehicle occupants, is selected to demonstrate the model. In addition, the conversion technologies for heating and electricity for the 52 buildings are simultaneously selected. Bi-directional charging of the electric vehicles is also allowed within the community microgrid, including the costs of charging stations for the chosen vehicles.

For each vehicle, a driving profile has been generated which includes details of the driving cycle of the vehicle, at which times driving is conducted, and the distances driven. Since PV is also installed on the roofs of each of the homes, this PV energy can be used to charge the BEV or FCEVs in the community. The powertrain efficiencies for each type of vehicle are also calculated in specific WLTP driving cycles.

6.2 BUILDING ENERGY DEMANDS

To calculate the building demands for Zuchwil, the same methodology that was used in Section 3.2.1 is applied. Since three years of analysis are simulated, namely 2015, 2035, and 2050, the current situation of the building stock in 2015 is modelled and then retrofits of the building stock are considered for 2035 to 2050. Retrofits are then assigned based on the construction age of the building and the year of consideration according to the Swiss Energy Strategy 2050 'New Energy Policy' scenario (Prognos AG 2013). These retrofit rates were found in Table 3.1. Buildings within each age class are then stochastically selected based on these assumed retrofit rates and the building age.

The retrofit rates applied to the building stock in 2035 and 2050 are summarised in Table 3.1 using the New Energy Policy scenario (Prognos AG 2013).

Buildings selected for retrofit are then simulated using 7 different retrofit options: roof, ground, facade, window, window and wall, window and roof, and all components retrofitted. Insulation is added to the

existing building construction of the retrofit tool until the U-value of
the retrofitted construction reaches the target value set by the SIA 380/1
(Schweizerischer Ingenieur und Architektenverein 2019) for thermal
energy usage in construction. The selected solution is then the lowest
cost option that meets the Minergie P-standard for retrofitted buildings
of less than 60 $kWh/m^2/year$ (Minergie Schweiz 2019). Please note that
the costs and embodied emissions of the building materials included in
these retrofits are listed in Appendix B.

Out of the 52 buildings, 1.67% are built in 1981-1985, 50% are built in
1986-1990, 35% are built in 1991-1995, and 13.3% are built in 1996-2000.
When a building has been chosen to be retrofitted, the applied partial
retrofit option is then selected as the lowest cost option that achieves an
annual heating energy intensity less than 60 kWh/m^2/year as specified
in Minergie-P Standard (Minergie Schweiz 2019). The applied retrofit
options using this method are shown in Fig. 6.1 for 2035 and 2050.
The costs of these retrofits are then multiplied by the *CRF* (see Eq.
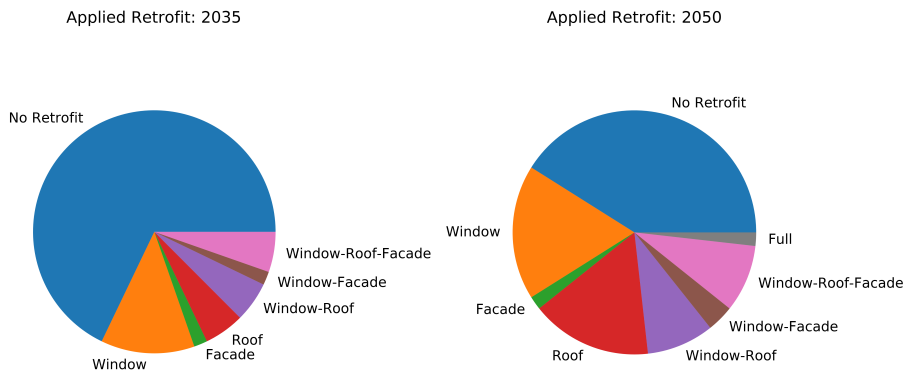
Figure 6.1.: Retrofits applied to the building stock in the years of 2035
and 2050.

5.30), assuming a lifetime of 40 years for retrofit materials according
to Jakob et al. (2014). The embodied emissions are divided by this
lifetime. This results in total costs of 170 CHF/person/year for 2035
and 307 CHF/person/year for 2050. The cost of retrofit is higher in
2050 than in 2035, because the costs are cumulative and increase over
time as more buildings are retrofitted. The total embodied emissions
are calculated to be 14 kg CO_2-eq/person/year for 2035 and 28.5 kg

CO_2-eq/person/year. These costs and emissions are calculated, because the SIA 2040 targets that were outlined in Section 5.3 include building materials and will thus be later added on to the optimisation total costs and emissions to compare these emissions with the target.

In addition to retrofitting of the existing buildings, improvements in electrical appliances and lighting are also considered. Standard reductions for lighting and household appliances are reduced according to the percentages set by the Swiss Energy Strategy 2050 (Prognos AG 2013). The resulting electricity and heating demand in 2015, 2035, and 2050 are shown in Figure 6.2.

In this Figure, it is seen that the electricity demands are approx-
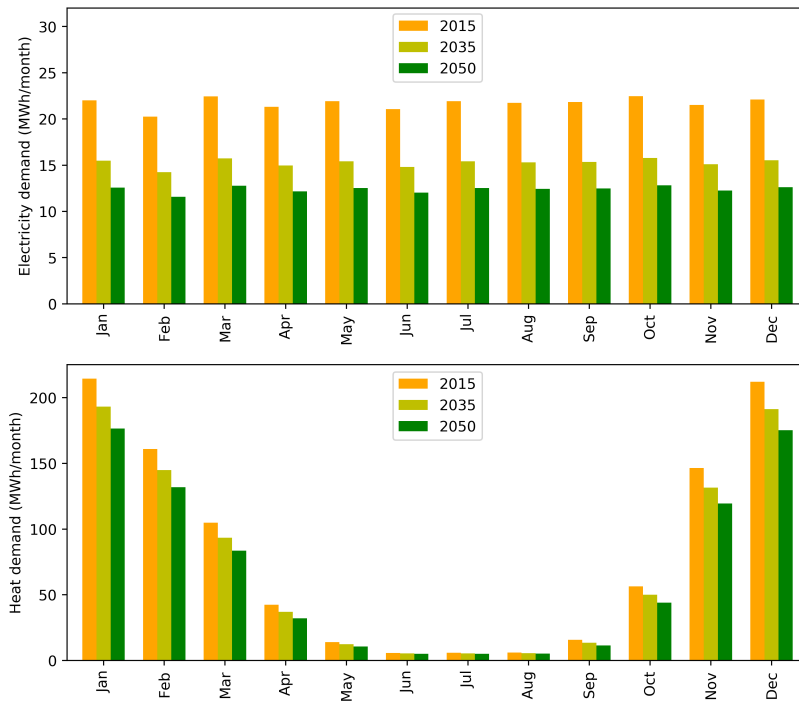
Figure 6.2.: Electricity and heating demand for 52 buildings over the years of 2015, 2035, and 2050. Please note that the buildings in this case study are all significantly newer (all built after 1980) than in the Altstetten and Zernez cases, therefore the drop in heating demand is significantly less previously observed.

imately the same from month to month with an annual total of 0.26

GWh in 2015. The electricity demand is predicted to decrease by 30% and 43% from 2015 to 2035 and 2050 respectively. The heating demand includes both the domestic hot water and the heating demand. The heating demand totals 0.98 GWh annually and peaks in January. This heating decreases to only domestic hot water demand in the summer months. The heating demand is predicted to decrease 11% and 19% from 2015 to 2035 and 2050 respectively. The heating demand is predicted to be lower since the buildings are new in this district and are retrofitted at a low rate according to Table 3.1.

6.3 EMISSIONS FOR PUBLIC TRANSIT

In addition to the emissions for building materials, the public transport emissions are included even though these emissions are not included in the model. Since our model only handles personal vehicles, yet the targets include all domestic travel, the other domestic travel of the users must be included to be consistent with the SIA 2040 standard. This public transport is based on the Swiss Micro Census Mobility data from 2015 (Bundesamt für Statistik 2015), which defines the total passenger kilometres (Passenger kilometre (pkm)) for each transit type per person. Since the population in the case study is known to be 168, the average annual public transit per person can be approximated. This is shown in Fig. 6.3. The emissions for these public transport types are assumed from the SBB transport calculator (Tuchschmid et al. 2011), which includes embodied energy. In addition, embodied and operation emission data for motorbikes and e-bikes are assumed from Eco-Invent studies (Leuenberger et al. 2010). Using the values in this Table, the total passenger kilometres per person are defined and the total cost and CO_2 emissions for public transit can be accounted for. Similar to the building retrofit emissions, these emissions will also be added on to the optimisations total emissions when comparing total emissions to the targets.

6.4 SOLAR POTENTIAL

The solar potential on the rooftop is calculated with the information from the Sonnendach data set for each buildings' surfaces (Eidgenössisches Departement für Umwelt 2019). This dataset has analysed the

Table 6.1.: Embodied and operational emissions per passenger kilometre (pkm) for the most commonly used public transport types.

Transport Type	Embodied Emissions (g CO_2-eq/ pkm)	Operation emissions (g CO_2-eq / pkm)	pkm/ day /person 2015	pkm/ day/ person 2035	pkm/ day/ person 2050
Train	7.5	0.7	7.5	8.76	8.96
ICE Bus	8.5	92	1.5	0.88	0
Electric bus	31	5.1	0	0.88	1.79
Motorbike	42	84	0.5	0.58	0.60
E-bike	16	0.5	0.13	0.15	0.17
Bicycle	12	0	0.77	0.90	0.92
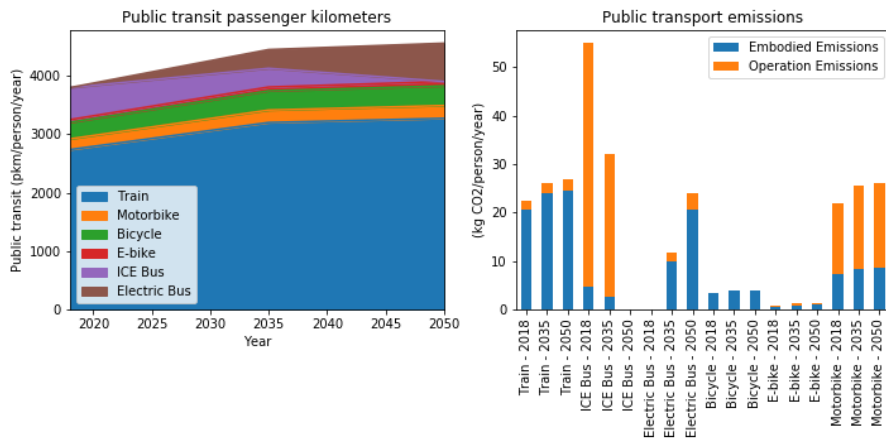
Figure 6.3.: Left: Annual passenger kilometres per person in Switzerland from 2015-2050, Right: Emissions per public transit passenger kilometre for each type of travel from 2015-2050.

annual solar incidence and available rooftop area for all buildings in Switzerland using a GIS analysis and LiDAR data. Using this method, the maximum area available on each rooftop that is suitable for solar (i.e., south facing) is calculated. A reduction factor of 40% of this maximum area is then deducted to account for objects on roofs that make certain areas not suitable for solar panel installation (Mavromatidis, Orehounig, and Carmeliet 2015). The dataset also provides the rooftop slope and the surface azimuth for the rooftop surfaces. To calculate hourly incidence on each eligible rooftop surface in the case study, the TRNSYS (University of Wisconsin - Madison 1975) solar module for calculating incident solar radiation on a sloped surface is combined with the local weather file to calculate the solar incident radiation on the sloped surface. The JEplus tool is then used to solve for the solar incidence for each rooftop's unique surface azimuth and slope for one-year at hourly intervals (Yi Zhang et al. 2009).

6.5 OPTIMISATION RESULTS

6.5.1 *Vehicle Selection*

Figure 6.4 shows the selection of the vehicle technologies for each of 77 vehicles, the years of consideration, the 10 Pareto optimal solutions, and the reference case. On the x-axis of this Figure, these ten Pareto optimal solutions are referred to with number 1 representing a fully cost optimal solution and number 10 representing a fully CO_2 optimal solution. Solutions 2-9 represent intermediate solutions that provide a spectrum of Pareto optimal options between fully cost optimal and fully CO_2 optimal.

In this Figure, the cost optimal solution in 2015 begins with a combination of Internal combustion engine gasoline vehicle (ICEV-g) and Internal combustion engine compressed natural gas vehicle (ICEV-cng) solutions. As emissions are reduced in solutions 4-9, the ICEVs are replaced with PHEV50 and BEV200s as their fuel supply is decarbonised. In the fully CO_2 optimal solution, all BEV200s are recommended.

For the year of 2035, the cost optimal solution recommends that more of the vehicle fleet should be BEV200s, with the remainder being a mix of ICEV-cngs and ICEV-gs. This indicates that, according to the assumptions of this thesis, that for most of the drivers it will be cost optimal to drive a BEV vehicle by 2035. In Pareto solution 8 in 2035, all of
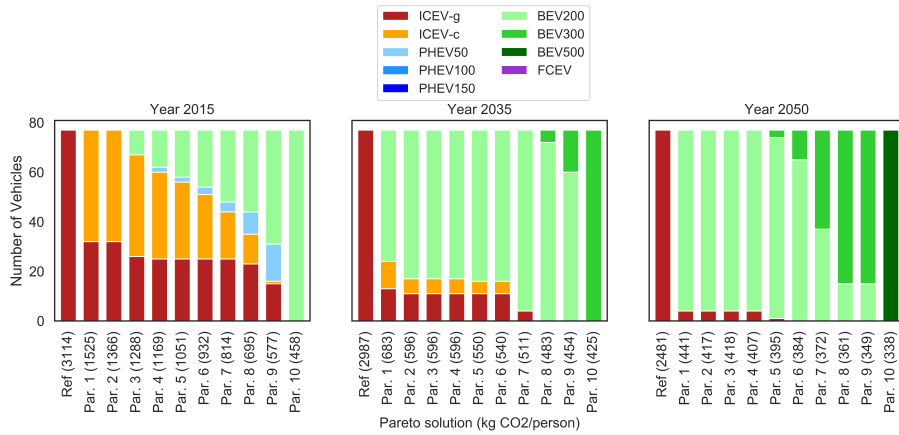
Figure 6.4.: Optimal vehicle selection in 2015, 2035, and 2050 for Pareto solutions 1-10. The number on the x-axis represents to total emissions in kg CO_2-eq/person. The total number of vehicles is 77.

the ICEVs have been replaced with BEVs. From solution number 1 until 7, the smallest range BEV200s are recommended, but from solution 7-9, BEV300s are increasingly recommended. In solution 10, only BEV300s are recommended. In 2050, the cost optimal solution recommends over 90% of the vehicles to be BEV200s. From Pareto solution 4-7, BEV300s replace BEV200s as the dominant vehicle technology and finally in the CO_2 optimal solution, only BEV500s are recommended. Since the optimisation only acts in terms of the benefits for the two objectives (cost and emissions), the optimisation does not always choose the vehicle selection that would be chosen by the consumer. In reality, the decision of which vehicles the consumers choose depends largely on other factors, such as the convenience of quick or less frequent charging, a desired range, or simply preferring one vehicle over another. BEV300 or 500 vehicles provide convenience from a larger battery since they do not have to be charged as frequently. However, they are not selected since they have higher capital costs and public charging is available when the vehicles are underway. Similarly, ICEV and PHEVs are more convenient than BEVs since they require much less time to charge, but they have higher emissions and are most costly when fossil fuel prices increase after 2015.

It is noted that FCEVs are not installed in any case due to both their

high cost and high embodied emissions, thus they are not preferred for either objective. It was predicted that the FCEVs may be a good technology for vehicles with high annual driving ranges or which require quick and frequent charging, but the optimisation did not select FCEVs, since the results indicate that the cost and emissions are lower to simply recharge a BEVs more frequently. Again, this selection is due to the BEVs lower cost and emissions compared to an FCEV rather than the preferences of the consumer.

Although the model in 2015 and 2035 recommends installing ICEV-cngs in cost optimal solutions, this is unlikely to be the case in reality since the cars will likely only be cost optimal until 2035 at the latest due to the increasing cost of natural gas and decreasing cost of BEVs. Most drivers already have ICEV-gs, which they will likely keep until BEVs become affordable. Thus although ICEV-cngs are recommended due to the low costs of the vehicles and of natural gas, the current vehicle ownership will likely change the outcome of this result.

The selection of vehicles is also directly related to the total number of kilometres driven per vehicle. The relationship between driving distance and the selection of the vehicle is shown in Fig. 6.5.

In Fig. 6.5, the columns from left to right represent Pareto solution 1, 5, and 10 respectively and the rows represent years 2015, 2035, and 2050 respectively. In 2015, Pareto solution 1 shows that ICEV-g vehicles are chosen for driving demands less than 10,000 km/year and ICEV-cng vehicles for demands more than 10,000 km. Since the ICEV-g have the lowest embodied emissions of all available vehicles, they are recommended for vehicles that drive the least and thus have lower operational emissions. For Pareto solution 5, the vehicles with the highest annual distances are replaced with BEV200s and several of those with driving distances less than 20,000 kilometres per year select PHEV50s, particularly if these vehicles drive for the majority of the time in urban settings. For Pareto solution 10, only BEV200s are selected, and we can see that the average cost per vehicle has increased while the average emissions have strongly decreased. In 2035 and 2050 in Pareto solution 1, it is seen that only a few vehicles with low annual kilometres remain as ICEV-g vehicles, however almost all vehicles with larger driving distances kilometres prefer BEV200s. In 2050, in solution 5, vehicles with high driving ranges optimally prefer BEV300s. In the CO_2 minimal case, BEV500s are chosen for all vehicles. This indicates that larger batteries are still recommended for minimal emissions, despite the increased embodied
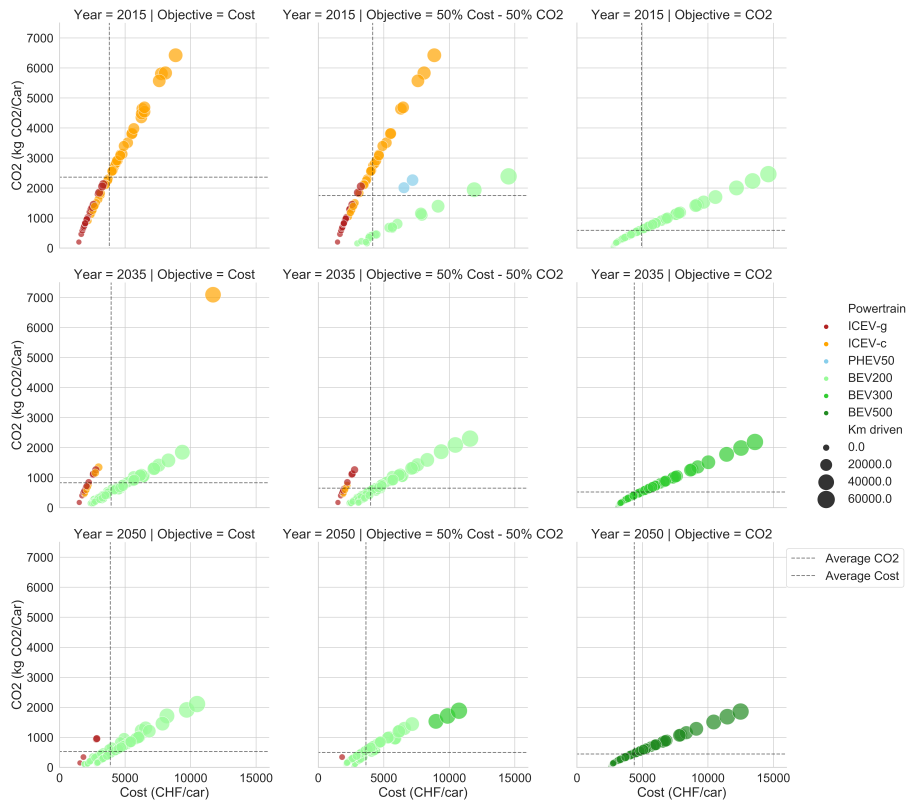
Figure 6.5.: Vehicle selection plotted by the cost and emissions of the individual cars. The size of the points represents their annual kilometres. The average vehicle cost and emissions are plotted in dashed lines for each year and objective.

emissions of the vehicles since they can be charged less frequently and only when renewable electricity is available.

The electric vehicles also have the option of either charging at home or using public charging stations. Figure 6.6 shows the fraction of the total energy used to charge electric vehicles that is supplied by public charging stations. In this work, public charging stations are assumed to
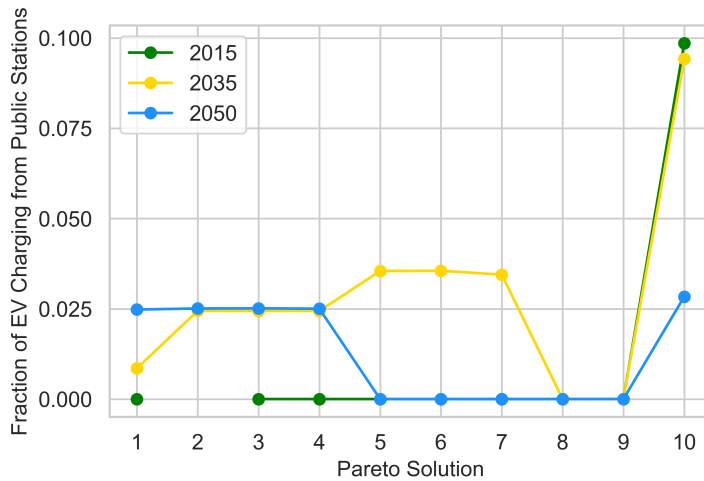
Figure 6.6.: Fraction of the electrical energy used to charge either BEVs or the battery of PHEVs in public charging stations vs. at home.

use electricity from the centralised grid and thus use the grid CO_2 mix. Although this is predicted to decrease to 0.060 kg CO_2/kWh by 2050, it is still quite high at 0.102 kg CO_2/kWh in 2015, thus charging is mostly done at home where low emission PV electricity can be used. The cost of EV charging in public stations (0.45 CHF/kWh) is also much higher than electricity used at home (0.20-0.25 CHF/kWh from the grid). Only in Pareto solution 10 in 2015, where only BEV200s are chosen, is public charging used for 10% of the EV charging demands. This is due to high demand vehicles that require faster charging times and public charging stations when away from home. In 2035, BEV200s are used in most cases and public charging is used for 1% of the charging energy in Pareto solution 1. As larger range BEV300s are installed with lower carbon targets, this increases to 2.5% in solution 4, 3.5% in solution 6, and 9.4% in solution 10. In 2050, a high percentage of BEVs are used in all cases. In cost optimal solutions, public charging is used for 2.5%

of the loads. This decreases to 0 in solution 5, with the installation of larger BEV300 batteries, and rises again to 2.5% in Pareto solution 3.

Overall, the results show that the public charging was not used more than 10% of the time in any case from 2015-2050 due to both the higher cost and higher emissions when compared with charging at home with the microgrid PV and battery system. For public EV charging to become more optimal, it will have to become cheaper or renewables will have to be integrated directly into the electricity supply.

6.5.2 *Building and Storage Technologies*

The conversion and storage technologies, are also selected by the optimisation, and their selection is shown in Fig. 6.7. This Figure shows installation of PV in all cases until the maximum available roof area, indicating that it is both cost and CO_2 optimal. For the heating system, it is shown that a heat pump is optimal for the majority of buildings in most cases. Several buildings still use gas boilers in 2015 in the cost optimal cases, but these are phased out by 2035 and 2050 in most cases. Due to the PV installed, the excess of electricity makes the electricity supply for the heat pump cheaper than the natural gas for the boiler would be. This is especially true in 2035 and 2050, since the natural gas costs are assumed to increase in the future (please refer to Table D.1 for details). Thermal storage is installed in all scenarios, due to its ability to store heat produced by the heat pump and its low cost. Battery storage is only used in the CO_2 optimal solutions in 2015, but is installed in solutions 2-10 for 2035 and 2050. In Pareto solution 2 in 2035, it is installed in a capacity of less than 100 kWh. This capacity increases as CO_2 is reduced in optimal solutions with its maximum recommended capacity being just over 600 kWh. Hydrogen storage is also an option that is utilised in some of the scenarios favouring deep decarbonisation. Hydrogen storage was intended to be installed in conjunction with FCEVs, however it is used in conjunction with the PEMFC, which acts as a CHP and provides both electricity and heat for the multi-family houses. Hydrogen is used in this case over battery or thermal storage due to its long-term storage potential. This can be observed in Fig. 6.8. This Figure demonstrates the use of the storages over the one-year simulation period. It is shown that the battery storage is used as a diurnal storage to shift excess daily PV production to evening electricity demands (including heat pumps and vehicle charging). The thermal
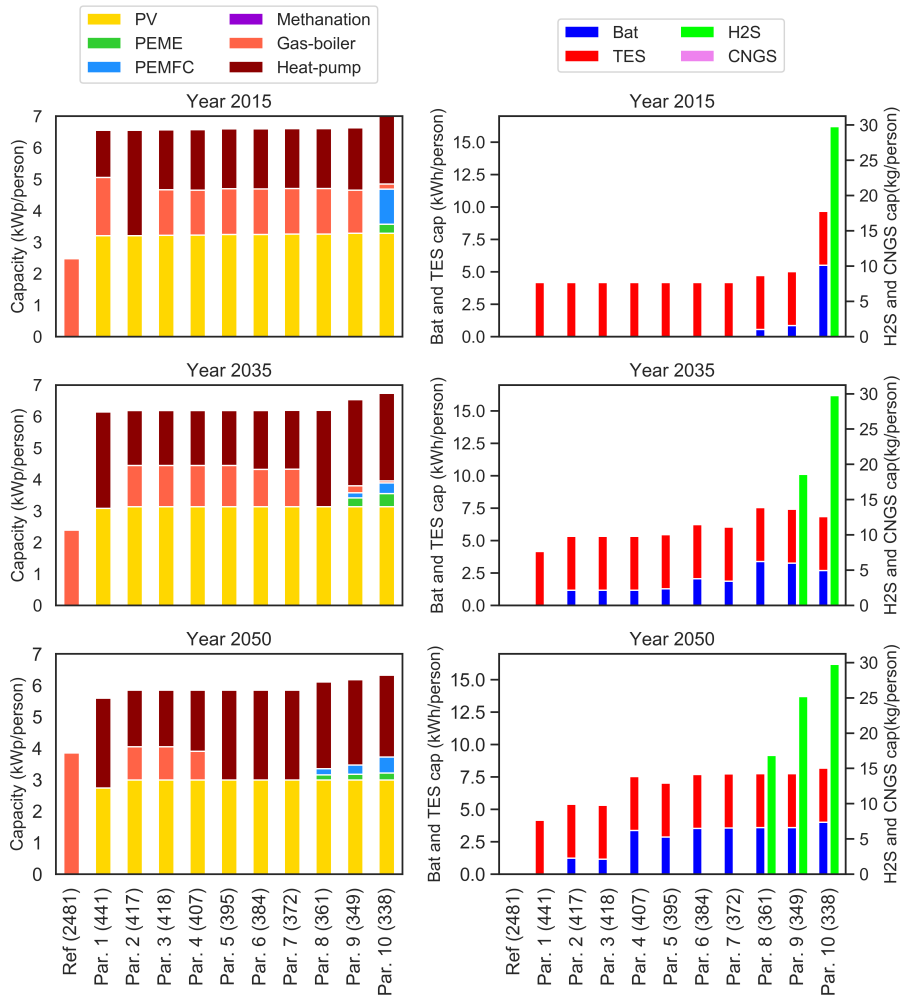
Figure 6.7.: Conversion (shown on the top) and storage (shown on the bottom) technologies selected in 2015, 2035, and 2050.
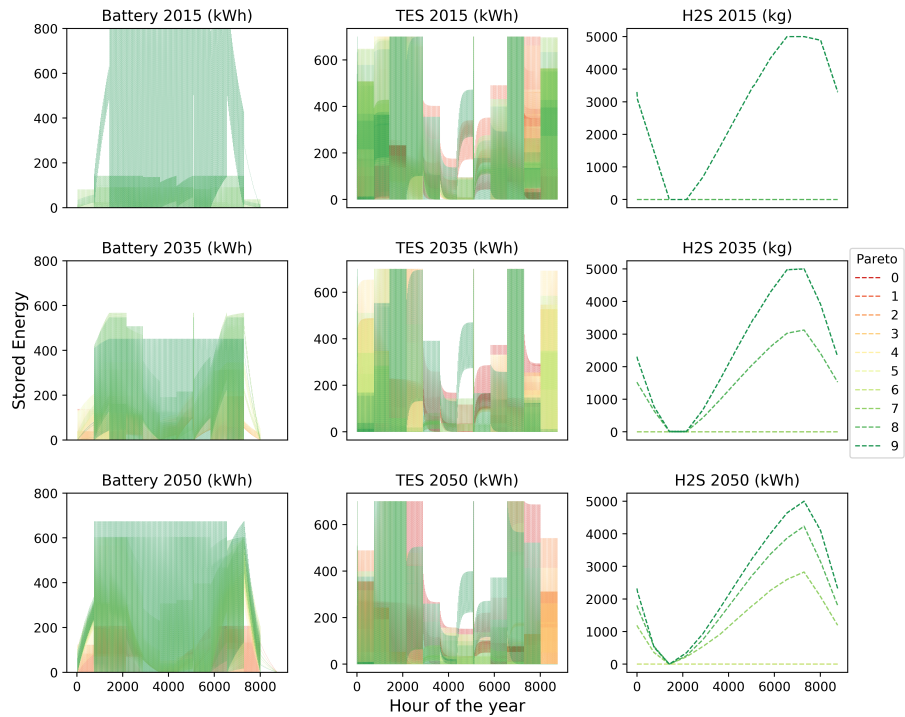
Figure 6.8.: Annual storage level of the three storage systems, demonstrating the charging and discharging profiles of the storages.

storage is used in a daily manner, similar to the battery, however more significantly in the winter months than in the summer months.

The most important outcome is the hydrogen storage, which is used as a seasonal storage when deep decarbonisation is required. These results are consistent with those found in Chapter 4. A Power-to-CHP seasonal storage is only used in the CO_2 optimal solution in 2015, which is an extreme case. However, a long-term Power-to-CHP system is used solutions 9-10 in 2035 and 8-10 in 2050. This indicates that a seasonal storage is useful for a deep decarbonisation when a high self-sufficiency fraction is desired, or if the grid CO_2 level is high. The produced hydrogen can be stored until winter and then used to create both heat and electricity. Although this large storage is expensive in relation to its decrease in CO_2 in comparison to the previous solutions, it would be more attractive for isolated communities that require high self-sufficiency levels due to the expense and difficulty of importing energy.

6.5.3 *Total Cost and Emissions*

The two objective functions, cost and CO_2 emissions, are displayed with their full breakdowns by cost and emission type in Fig. 6.9. Please note that the building retrofit and public transport cost and emissions have been included in this Figure, as was previously discussed in Section 6.2 and 6.3. Please note that the reference case is re-simulated in 2035 and 2050 with the same technology selection but updated costs and emissions, thus the cost and emissions of the reference case change over time.

In the reference case, it can be observed that the gasoline and natural gas purchases cause the majority of the CO_2 emissions. In addition, they comprise approximately 30% of the reference case costs. Although the amount of fuel purchased is estimated to decrease over time due to improved efficiencies, the costs are also anticipated to rise for the fossil fuels. In the cost optimal case, the vehicle investment and conversion technology investment costs dominate the total cost. These costs increase and emissions decrease with the switch to BEVs. In the cases in which a seasonal storage is used, the storage investment costs also represent a large portion of the total cost, but it is the vehicles that are the major deciding factor in the optimisation, since they represent
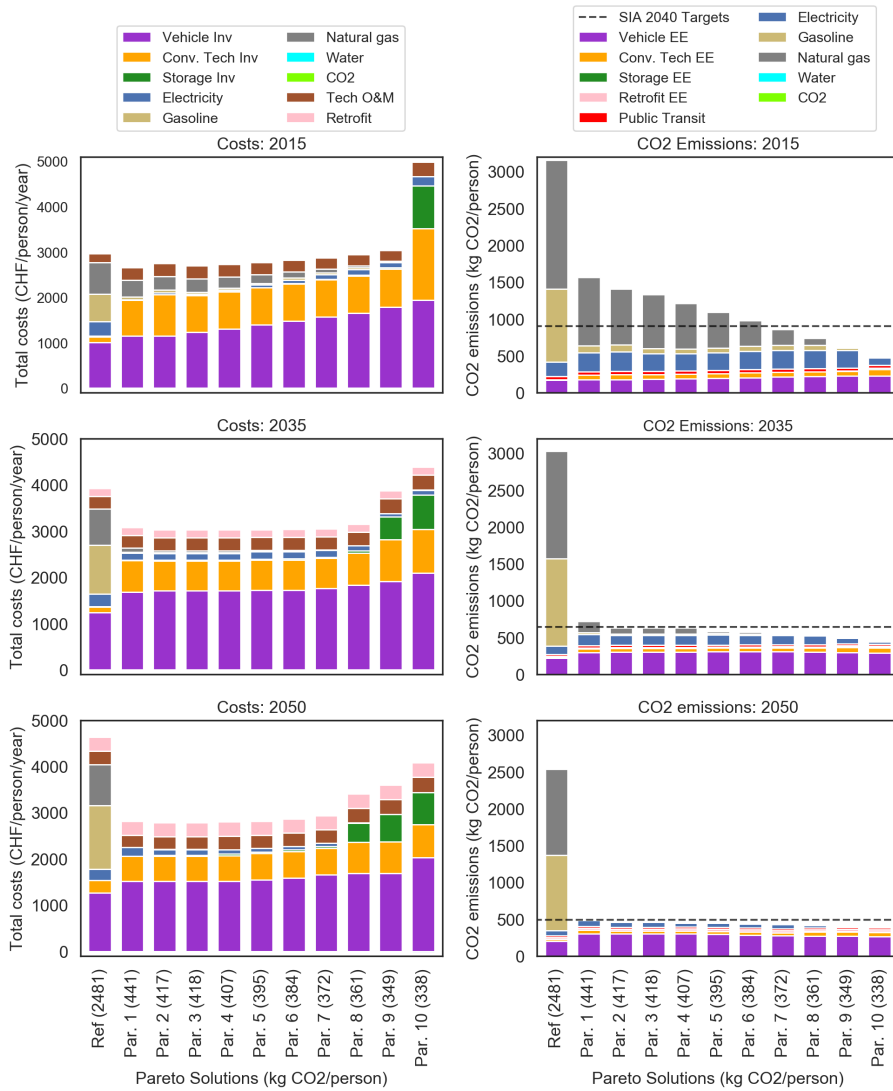
Figure 6.9.: Costs and total CO_2 emissions of both objective functions broken down by type. The energy targets referred to in Section 5.3 are also displayed in dashed lines.

the majority of the costs and a large portion of the emissions. As of 2050, it can be seen that the embodied emissions of the vehicles is the largest contributor to CO_2 emissions and cost, as the manufacturing and extraction emissions are significant and the charging is no longer reliant on fossil fuels. This indicates that switching to heat pumps (compared to the reference case) and to BEVs are the two most influential factors required to decarbonise the community. To further decarbonise, vehicles would have to be replaced with other transit methods, such as public transit or car sharing services. Buildings can also be further decarbonised by increasing the retrofit rate above the rates assumed in the NEP scenario.

6.5.4 *Annual Operation*

To predict the operation of these systems, we have plotted the optimal energy production and consumption of the model over the year. This operation is shown in Fig. 6.10 for Pareto solution 8. Solution 8 is chosen to represent the operation with seasonal storage. The corresponding plots for Pareto solutions 1 (cost minimal), Pareto solutions 5 (50% cost minimisation - 50% CO_2 minimisation), and Pareto solution 10 (CO_2 minimisation) are shown in Appendix E.

 This figure shows the production and consumption (or export) of each energy carrier over the one-year period simulated. We observe that the majority of the annual electricity production comes from PV production in summer and that much of the produced PV is exported. Electricity imports from the grid mainly occur in winter due to the reduced PV production. In summer, the PV surplus, combined with the battery usage, is enough to meet the buildings' electricity demands, vehicle electric charging, and electricity consumption of the heat pump required to meet heating demands. The electricity imported from the grid and the electricity exported to the grid decreases in 2035, and further in 2050. This is due to the lower electricity demands due to lighting and appliance retrofits that occur over time and the increased use of storage respectively. The heating demand is also lower due to the envelope retrofits in the buildings. This decrease is also observed in the plots for the heating energy carrier, where the heating demands decrease over time, thus the use of the heat pump and the thermal storage also decreases. The electricity demand due to vehicle charging increases in 2035 due to the increase number of BEVs (21 in 2015 vs.
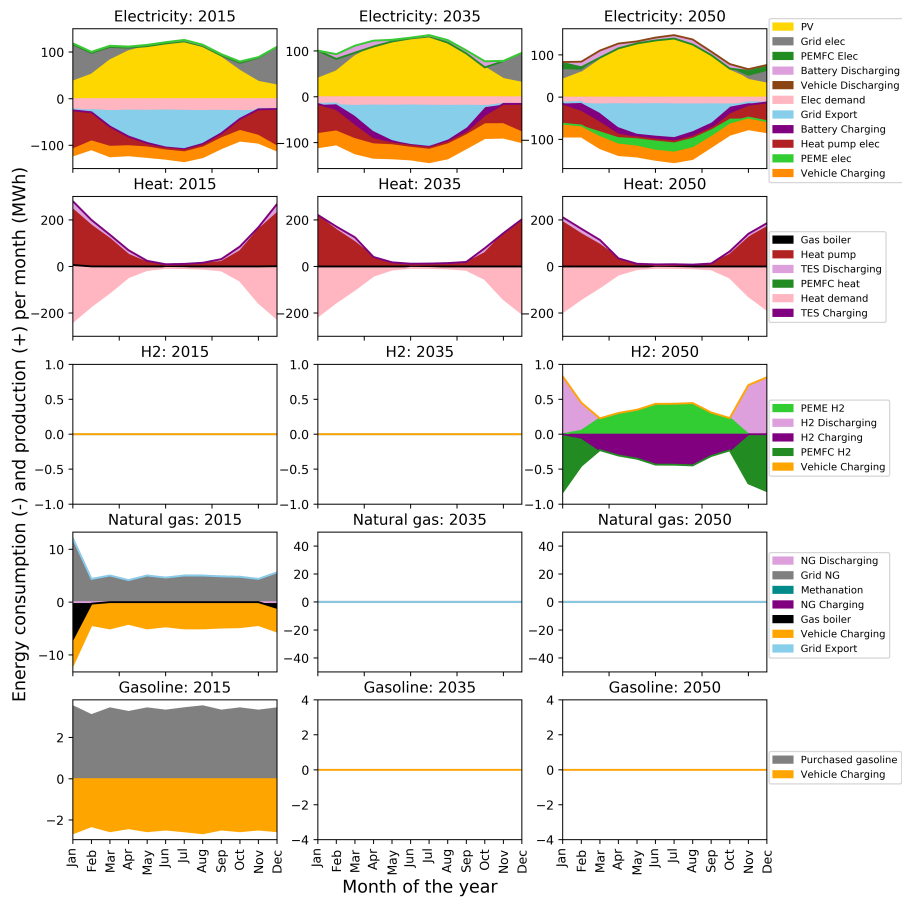
Figure 6.10.: Monthly energy consumption (negative) and production (positive) separated by energy carrier for Pareto Solution 8.

74 in 2035 and 77 in 2050). This vehicle charging demand decreases in 2050 due to the increased efficiency of the BEVs.

In 2050, it is also observed that the PEM electrolyser runs in the summer months to produce hydrogen. This is also observed in the plots of the hydrogen energy carrier in 2050. Here, the H_2 storage tank is charged during the summer months and is discharged in winter to operate the PEMFC, which demonstrates the use of a seasonal storage. It was expected that FCEV charging may play a role in 2050, but the vehicle costs are too significant and it is cheaper to implement a fuel cell as a CHP engine. Although seasonal hydrogen storage is exploited in this Pareto solution, it is only used in the scenarios where a deep decarbonisation is required, and significantly increases the cost of the system for a marginal decrease in the emissions. In winter, this is discharged via the PEMFC to produce both electricity and heat. Since the PV produced in summer is in excess of the demand, most of this energy is exported to the grid, however the level of export decreases over time due to the increasing use of storages and BEVs.

It is also noted that the natural gas and gasoline energy carriers still play a role in 2015, however this is nearly completely phased out in 2035 by the switch to BEVs and away from gas boilers. If FCEV technology would become cheaper, it could be possible for hydrogen storage to be further exploited, however the lower cost and increase in efficiency of BEVs shows that FCEVs are unlikely to be competitive for personal transport in these cases. The main advantage of FCEVs, a fast charging time and a longer kilometre range, are not predicted to be able to compete with the larger BEV capacities and the availability of public electric charging stations. It is possible that certain consumers could have a preference for FCEVs, due to their longer ranges, however due to their higher costs and limited charging infrastructure, this is unlikely to represent a large fraction of the vehicle stock.

6.5.5 *Self-Sufficiency*

With the use of heat pumps for heating and electric vehicles for transport, the electricity produced from PVs can be used to provide the heating, electric, and personal transport demand for the buildings. As was shown in Fig. 6.10, much of the PV production is exported to the centralised grid and not used locally. As the CO_2 emissions de-

crease through the Pareto solutions, less of the PV energy is exported, more BEVs are installed, and storage systems (especially batteries) are included to utilise more of the local PV production. This increase in self-sufficiency can be observed in Fig. 6.11.

For the cost optimal solution in 2015, the self-sufficiency ratio lies
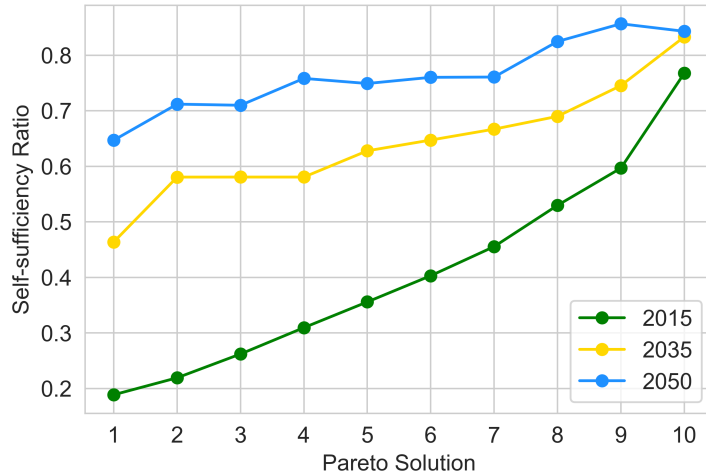
Figure 6.11.: Self-sufficiency ratio for Pareto solutions 1-10 for 2015, 2035, and 2050.

just above 15%, however this can be increased to as high as 78% in the CO_2 optimal case with the use of seasonal hydrogen storage. The cost optimal CO_2 case increases to 42% in 2035 and 63% in 2050, although the CO_2 optimal case only increases to 80% in 2035 and 82% in 2050. This is because of the higher fuel costs in 2035 and 2050 and the lower reimbursement rate for PV exported to the centralised grid in the future. This allows for a higher investment in BEVs and in batteries or H2S stationary storage which allows more PV energy to be used for local demand. The use of BEVs has a profound effect on the use of local electricity. Since public charging uses the Swiss CO_2 energy mix, local PV allows the electricity used for charging at home to be lower CO_2 intensity per kWh than the electricity from public charging stations. Although the CO_2 in the energy mix is assumed to decrease in the future, lower emission electricity can still be achieved at home due to the surplus of PV electricity. BEV charging is also a load that remains high in the summer, when PV is at its peak and the excess electricity would otherwise be exported or curtailed.

For case studies, such as Altstetten, where the renewable potential of the community is very low, there would be less of an advantage for most people to charge BEVs at home. Due to the lower renewable potential, it is unlikely that there would be enough renewable energy available for people to charge their vehicles, thus relying on the grid. However, one advantage of urban case studies with multi-family homes is that people are far less likely to own as many vehicles and are far more likely to use public transit, thus keeping mobility emissions low. In rural case studies, such as Zernez, residents are much more likely to own vehicles due to limited public transit infrastructure. People are also more likely to drive longer distances annually. In this case study, charging at home is likely to be far more important that it would be in urban or suburban cases due to more limited infrastructure. An advantage is that renewable potential is likely to be high enough to support the charging demands in rural cases, as long as storage systems are utilised.

6.6 DISCUSSION

The Pareto optimal solutions indicate that there are two important factors that contribute to the decarbonisation of the community. The first factor is a switch from ICEVs to BEVs. BEVs have clearly been chosen to be the preferred low emissions choice of alternative vehicle technologies for all vehicles and in all years. The higher efficiency of BEVs over FCEVs and PHEVs combined with decreasing capital costs and increasing fossil fuel costs indicate that it is the best option to decarbonise the community.

Referring back to the papers reviewed in Section 2.4, the lack of installation of the FCEVs is in contrast to the predictions of both Dodds and McDowall (2014), Shafiei et al. (2015), and X. Zhang et al. (2015) who strongly recommended FCEVs for decarbonising the mobility sector. However the recommendation of BEVs is in line with predictions from Onat et al. (2014), Contestabile et al. (2011), and Hofer (2014). If the cost of the hydrogen technologies, such as FCEVs, PEMEs or PEMFCs could be reduced more than is predicted in this work, it is possible that hydrogen could play a larger role as an energy carrier at a lower cost to the users.

Although P2H was used in scenarios that required deep decarbonisation, its cost relative to the amount of emissions it reduces is significant.

Seasonal storage requires very large storage sizes, and the payback period for such a storage is exceedingly long since they only obtain one charge and discharge cycle per year. This means that the costs for storage would have to be exceptionally low for it to be economical to implement. This type of storage may be more attractive in isolated communities where the cost of imported energy is higher.

The optimisation also showed that BEV200 vehicles are sufficient to reduce the majority of emissions and to meet the majority of peoples' driving needs at a lower cost due to the smaller battery, however longer range vehicles appeal to consumers due to the increased convenience of charging the vehicle less frequently. From the perspective of the two objectives considered, purchasing a smaller battery vehicle and frequently recharging is a lower cost method that is still able to meet the user's needs and ensures that the CO_2 emissions are still reduced. One solution that can be implemented in this model is to use penalties that are applied whenever a vehicle is charged. These penalties could disincentive frequent charging by applying a penalty in the objective function to represent the opportunity cost of time wasted while charging vehicles. Since the objective function wants to minimise these penalties, frequent charging will be deterred. This can be implemented with Lagrangian Relaxation methods (Fisher 1981).

Since our model is also of a particular group of buildings and their energy system, the network of public or work charging stations outside of our case study are not optimised for and thus is difficult to realistically model or predict in the future. The availability of public charging stations along the users routes could be assessed in more detail. The routes of the vehicle owners extend all throughout the country, thus it would be a significant challenge to predict the availability of public or work charging stations on each of these routes today or in the future. It is currently assumed that vehicle charging is available within a few kilometres of the assigned routes, and that it uses the average Swiss CO_2 mix, thus it is more environmental to charge at home, resulting with the maximum public charging rates of between 5-10%. It is possible that some of these public charging stations could be directly connected to their own decentralised renewable installations, thus making them attractive for emissions reductions. We also do not know if the users have access to charging stations at work, or at what price the electricity would be at these work located charging stations. Since data specifying the owners work type and charging station availability are not available

to us, and it is currently not the norm in Switzerland to charge vehicles at work, we have not yet considered this third option for EV charging. An analysis for this would have to model user decision behaviour, possibly with an agent based simulation, rather than considering the details of the energy supply system design and focusing on emissions reduction as is done in this work.

It was also noted that vehicles with higher annual ranges are the first vehicles selected for a transition from ICEV to BEVs. In cost optimal solutions, the lower range BEV200 is chosen and in CO_2 minimisation cases, the longer range BEV300 or BEV500s are chosen. Although longer range vehicles are more convenient, they are more expensive for the user and the embodied emissions of the vehicle are higher due to the larger batteries.

The second major improvement is the switch from gas boilers to heat pumps and PV. A heat pump and the maximum PV size allowed were chosen in every solution, indicating that it is both cheaper and more environmentally friendly in all years of consideration and with both objectives. The use of a heat pump greatly increases the electricity demand in the community. This is managed both by using Power-to-Heat (with the heat pump and thermal storage tank) and the battery to manage the fluctuations in the grid.

As was mentioned in Section 5.2.4, only mid-sized C-Segment vehicles were used in this analysis. In reality, the top sales classes include: small, medium, multi-purpose vehicles, sports utility vehicles, and luxury vehicles. Although C-Segment or medium vehicles have approximately 24% of the market share (Thiel et al. 2014), small cars, large cars, and multi-purpose cars also represent a significant percentage of the market. These other classes could be less likely to switch to BEVs. Small cars might have difficulty incorporating a battery with a sufficient range for most people due to lack of space. Larger vehicles typically have large fuel tanks which would also be difficult to replace with a battery. FCEVs or PHEVs might be more attractive for these classes. The next step of modelling should try to include the small, large, and multi-purpose vehicle segments by using a fleet of vehicles with known vehicle classes and the calculated efficiencies of the driving cycles in all vehicle classes considered. Although FCEVs are not recommended in this work for mid-sized vehicles in Switzerland, this might not be true for larger vehicles classes, for overland shipping, or for car sharing services.

A similar criticism is also the lack of consideration of the use of vehicle sharing services, such as Uber or Mobility, which are likely to expand in the future. Currently, Uber only exists in the major cities in Switzerland, and Zuchwil is not located in one of these areas, however expansion of service areas is planned in the future. Consideration of ride sharing would also require simulation of consumer behaviour and another level of transport user decision making, which is beyond the scope of this work.

The major limitation of this study is the lack of uncertainty considered in this process. The input cost and CO_2 emission assumptions are based on multiple sources for each parameter, however future predictions also result in a great deal of uncertainty. The next step for this model is to conduct an uncertainty and sensitivity analysis based on uncertain input parameters to determine how sensitive the model decisions are to these changes, which will be done in the next Chapter.

This work is also limited to the scope of the case study used. A larger group of buildings could allow the charging stations to get more use, thus resulting in lower costs, however the optimisation in this model is quite computationally intensive. A larger case study would have significantly more decision variables and be even more difficult to compute. The current run time for a single Pareto front with 10 solutions takes over two days to compute with all vehicle technologies. Since it was our intention to conduct a sensitivity analysis in the future, we limited the size of the case study to keep the model's run time model short. Since the location of the case study is also in Switzerland, technology costs are frequently higher than they may be in other countries. The Swiss energy mix CO_2 is also relatively low due to the use of hydroelectricity and nuclear power, but it is not as low in emissions or as inexpensive as places that would have almost 100% renewable energy such as Quebec or Norway. In these countries, there would be little difference between charging in public or at home and little incentive to install PV since the CO_2 emissions in the grid are already low. Many countries that use significant amounts of coal or natural gas for power generation would have significantly higher emissions in the grid, thus BEVs might be less attractive in comparison to ICEV in these cases.

When comparing the results of Chapter 4 and Chapter 6, there are many similarities and several key differences. The main similarities are the selections of the conversion and storage technologies. Similar to both Altstetten and Zernez, heat pumps and thermal storage (Power-

to-Heat) were preferred over gas boilers, especially after the costs of natural gas increase and the costs of heat pumps decrease. It is also noted that PV is installed in all case studies close to the maximum potential, even when embodied emissions are considered. Even though the embodied emissions of PV are high, the renewable potential is used to offset a significant amount of fossil fuels in the Zuchwil case, therefore they are always optimal in all Pareto solutions.

Lastly, Power-to-CHP systems are still installed for long-term storage in the CO_2 minimisation cases, as they are still able to increase the utilisation of renewables. It is noted that the recommended hydrogen storage capacity in this chapter is much lower than in Zernez in Chapter 3, particularly due to lower renewable potential available and due to the consideration of embodied emissions of the storage system. The major differences between the results of Chapter 4 and 6 are that the emissions due to mobility dominate the total emissions objective, especially in later years when the emissions due to gasoline and natural gas are eliminated. This drastically changes the optimisation problem, as now decarbonising a vehicle stock based on fossil fuels is now the optimisation's priority. This comparison may be quite different when looking at Altstetten and Zernez. Altstetten is likely to have lower vehicle ownership, but has very energy intensive buildings. Since the targets with operation emissions were not achieved, the mobility energy usage must be very low for the targets to be achieved for the energy target metric used (SIA 2040). Zernez is likely to have even more vehicle ownership and demand. We can see in this case study that the emissions targets are reached in 2035 and 2050 without difficulty. The same should be tested for the other case studies in their different municipalities.

6.7 SUMMARY AND OUTLOOK

In this Chapter, Zuchwil was chosen as a case study to test the methodology developed in Chapter 5. The case study's system currently consists of ICEV-g, gas boilers, and no PV. This reference case is shown to have both significantly higher emissions and costs in each year of consideration, when compared to the optimal solutions. The main findings indicate that:

1. BEVs with a range of 200 kilometres are sufficient and low cost way of meeting energy targets for the mobility sector, although longer range vehicles can achieve lower emissions at a higher cost.

2. FCEVs result in higher emissions and higher costs due to expensive charging infrastructure, higher embodied emissions, and lower efficiencies than BEVs. This work strongly recommends the use of BEVs over FCEVs for use as personal vehicles, due to the large cost of hydrogen infrastructure and the lack of a necessity for quick charging times and ranges over 500 kilometres.

3. Heat pumps and BEVs can be used together in households, with the assistance of community batteries and Power-to-Heat for balancing the demands.

4. Vehicles with the lowest number of annual kilometres should be the last to change to AFVs, due to their lower operating emissions relative to the vehicles embodied emissions.

5. For deep decarbonisation targets, Power-to-CHP can be used. Power-to-Methane was not considered optimal.

6. With a 100% BEV diffusion rate, public charging was used 10% of the time at maximum, but this is highly dependent on the CO_2 intensity of the electricity used.

7. For this community, a self-sufficiency ratio of 45% and 65% are predicted for solutions reaching the SIA 2040 (SIA 2011) targets in 2035 and 2050 respectively.

As was mentioned in the discussion, the optimisation model's results change vastly depending on the input conditions used. There are many parameters assumed in this section that are highly uncertain, especially in the future. Since we do not know the final costs, emissions factors, and performances of so many of the variables, an uncertainty analysis is used in the next section to assess the variance of solutions depending on the uncertain inputs. A sensitivity analysis will then assess under which conditions certain P2X pathways are optimal to give a deeper insight into the major parameters that are influencing the utilisation of certain P2X pathways. This will be addressed in the next Chapter when an uncertainty and sensitivity analysis are performed on the exact model and case study that was used in this Chapter.

7

UNCERTAINTY AND SENSITIVITY ANALYSIS

In this Chapter, the model developed in Chapter 5 and applied deterministically in Chapter 6, will now be used for an uncertainty and sensitivity analysis. A Monte Carlo simulation with Latin Hypercube Sampling is used for the uncertainty analysis to solve for 500 stochastic Pareto fronts. Uncertainty characterisation is first performed for each uncertain parameter to define the probability distribution function. Next, the results of the Monte Carlo stochastic objective values and technology selection are shown. A regional sensitivity analysis using Monte Carlo Filtering is described and then conducted to identify the most sensitive input parameters resulting in the installation of each P2X pathway of interest. The stochastic Pareto solutions that meet the energy targets are then identified as the most significant P2X pathways.

7.1 BACKGROUND AND CONTEXT

Up until this point in this thesis, only deterministic optimisation has been performed. This means that the input parameters assumed in the model are determined to be certain and without variance. In reality, many of these parameters vary from year to year or even from hour to hour. Some of these inputs vary for obvious reasons, such as weather patterns affecting solar radiation and influencing building heating demand, or depending on occupant behaviour for building electricity demand. Other parameters, such as investment costs, can seem more certain. However, when trying to predict these values for the future, we cannot be certain of their exact value and thus we should not assume that a single deterministic value for a cost in the future is guaranteed to be realised.

When trying to create a model that makes predictions until 2050, not considering the uncertainty in these input parameters can lead to large modelling errors and suboptimal decisions due to the failure to look at the full picture of the decision space. We have seen from the future scenarios analysis in Chapter 4 and the different years of consideration in Chapter 6 that the optimal results are highly sensitive to the assumed input parameters. However, the scenario analysis previously conducted

in Chapter 4 only shows us that the output varies, and does not allow us to quantify this uncertainty or to identify the parameters that make the model uncertain.

When investigating the optimal pathways of P2X, the most influential parameters that make certain pathways optimal would be of interest to determine, in order to identify the conditions which could benefit certain pathways. As we are mainly trying to predict future outcomes from 2020 to 2050, a well performed sensitivity analysis could act as guidelines for the future conditions which could benefit certain pathways if they are realised or to identify the outcomes that are the most probable.

The stochastic optimisation shown in this Chapter is based on the exact optimisation model developed in Chapter 5 and the Zuchwil case study applied in Chapter 6.

7.2   UNCERTAINTY ANALYSIS

Uncertainty analysis is the process of quantifying how uncertain the solutions of the model are depending on the uncertainty of the inputs. The considered outputs can be either the objective values being optimised or the range of other decision variables in optimal cases.

The most popular method of conducting an uncertainty analysis on an optimisation model is to run Monte carlo (MC) simulations on the deterministic optimisation model. MC simulations consist of running many random samples of the uncertain input parameters using the deterministic model. First, probability density functions (Probability density functions (PDFs)) representing the uncertainty in each parameter must be established. These distributions are then sampled randomly and the random samples for each distribution are input into the deterministic optimisation model. This process is then repeated, typically for several thousand samples. The output solutions of these samples can then be evaluated and the uncertainty in the output can be quantified. For a complex optimisation problem, this typically requires a massive amount of computational time.

MC often uses a random sampling technique to select the outputs for each case, but different sampling techniques are also available. Since random sampling can allow for repetition of similar values, it generally requires many runs to get a full representation of a PDF. Other sampling techniques attempt to try to reduce the number of runs required

to fully represent a distribution, thus requiring much computational time. Since the model developed in Chapter 5 is a complex model with over 2 million decision variables, typically taking between 1-3 hours for a single run, reducing the computational intensity is of high importance.

One such technique that requires less samples is Latin Hypercube Sampling (LHS). This technique was first used by McKay et al. (1979) and was found to reduce the required number of simulations compared to random sampling. This type of sampling is commonly performed in uncertainty analysis, as was done in the work of Shi et al. (2008) and Jirutitijaroen et al. (2008). Some other popular sampling techniques include Halton's low discrepancy sequences and Sobol's sequence. The efficiency of these sampling sequences has been evaluated by Dige (2016) who found that LHS was better for dimensions of variables less than 100 and the Sobol's sequence was better for higher dimensions. Since the number of variables analysed in this work is under 100 LHS was chosen over the other sampling techniques in this thesis.

7.2.1 *Latin Hypercube Sampling*

Latin hypercube sampling method attempts to stratify the Cumulative distribution function (CDF) to more efficiently distribute samples across the Probability density function (PDF). The CDF is a function that returns the cumulative probability associated with the PDF. As opposed to random sampling, in which all samples are selected independently of the selection of previous samples, LHS divides the CDF into even stratified intervals and then allocates a sample in each stratification interval. This is demonstrated in Fig. 7.1 for a normal, a beta, and a uniform distribution. In this Figure, we can see that, regardless of the shape of the PDF, even samples can be determined through the use of the CDF. Normal, beta, and uniform distributions are the types most commonly used in uncertainty characterisation in this thesis, therefore the calculations of the PDFs will be defined. The PDF and CDF of a normal distribution are shown in Eq: 7.1 and 7.2.

$$f(x|\mu,\sigma^2) = \frac{1}{\sqrt{2\pi\sigma^2}}e^{-\frac{(x-\mu)^2}{2\sigma^2}} \tag{7.1}$$

$$\Phi(x) = \frac{1}{2}[1 + erf(\frac{x-\mu}{\sigma\sqrt{2}})] \tag{7.2}$$
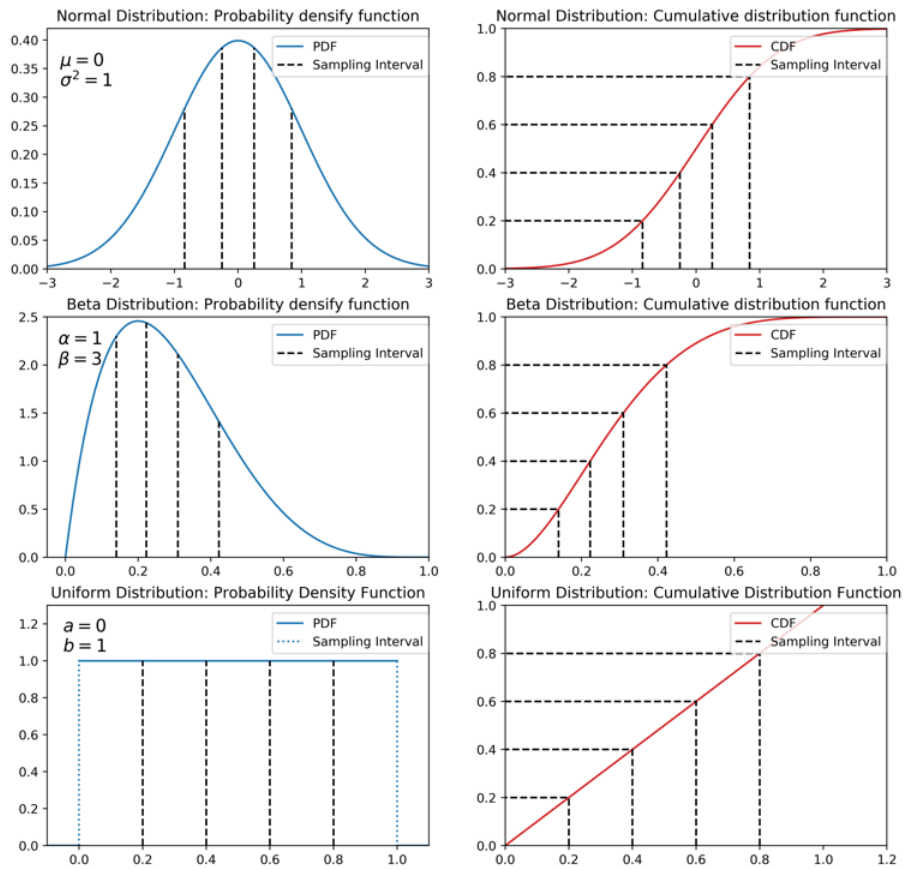
Figure 7.1.: Latin hypercube sampling is demonstrated with a sample size of 5 for a normal, beta, and uniform distribution. The PDF is shown on the left and CDF on the right.

Here, μ is the mean of the distribution σ is the standard deviation, and σ^2 is the variance. Φ is the CDF for a normal distribution and $erf(x)$ is the error function, which is further defined in Eq: 7.3.

$$erf(x) = \frac{2}{\sqrt{\pi}} \int_0^{\text{inf}} e^{-t^2} dt \qquad (7.3)$$

The normal distribution relationship is later denoted using the format $N(\mu, \sigma)$. The PDF and CDF of a beta distribution are shown in Eq: 7.4 and 7.5.

$$f(x|\alpha, \beta) = \frac{x^{\alpha-1}(1-x)^{\beta-1}}{B(\alpha, \beta)}$$
$$B(\alpha, \beta) = \frac{\Gamma(\alpha)\Gamma\beta}{\Gamma(\alpha + \beta)} \qquad (7.4)$$

$$\Phi(x|\alpha, \beta) = \frac{B(x|\alpha, \beta)}{B(\alpha, \beta)} = I_x(\alpha, \beta) \qquad (7.5)$$

Here, α and β are both shape parameters for the distribution. $B(\alpha, \beta)$ is the beta function, and Γ is the gamma function. The beta distribution is later denoted using the format $B(\alpha, \beta, a, b)$. Here, a and b represent the lower and upper bounds of the distribution respectively.

The PDF and CDF of a uniform distribution are shown in Eq: 7.6 and 7.7.

$$f(x) = \begin{cases} \frac{1}{b-a} & for\ x \in [a, b] \\ 0 & otherwise \end{cases} \qquad (7.6)$$

$$\Phi(x) = \begin{cases} 0 & for\ x < a \\ \frac{x-a}{b-a} & a \le x \le b \\ 1 & for\ x > b \end{cases} \qquad (7.7)$$

Similar to the beta distribution, a here is the lower bound of the distribution and b is the upper bound of the distribution. The uniform distribution is later denoted with the form $U(a, b)$. With these functions defined, we can then proceed with defining the individual PDFs for each uncertain parameter. This is often called uncertainty characterisation. Uncertainty characterisation for each of these factors will be reviewed in the following sections.

7.3   UNCERTAINTY CHARACTERISATION

The purpose of uncertainty characterisation is to define a PDF that defines the uncertainty of a particular parameter. These density functions should ideally come from recorded or observed data of a particular parameter over numerous real life samples. A distribution and the shape parameters can then be assigned based on the best fit to the real distribution samples. This is easy to do for several parameters, such as electricity costs which are well recorded, however this can be difficult for other parameters such as embodied emissions of technologies, where information on uncertainty is difficult to find. In cases where little data is known, a distribution is defined based on assumptions using the information that is known. To do this, groups of similar parameters are characterised in the following section.

Many of the input parameters that have been introduced in both Chapter 3 and in Chapter 5 are uncertain, particularly when assigning values for the future. To cover the uncertainty for all of these variables, they have been sorted into categories:

1. Building energy demands (e.g., electricity, heat)

2. Vehicle driving demands

3. Solar radiation

4. Energy carrier prices (e.g., electricity, natural gas, gasoline, CO_2, water)

5. Carbon factors (e.g., electricity, natural gas, gasoline, CO_2, water)

6. Investment costs

7. Embodied emissions

8. Efficiencies

7.3.1   *Building Energy Demands*

Building energy demand for all buildings in the Zuchwil case study were simulated using a building stock EnergyPlus model (see Section 3.2.2). Uncertainty regarding these models can be influenced by many uncertain input parameters.

The uncertainty for single-family and multi-family homes using EnergyPlus has already been assessed in the work of Mavromatidis (2017). In this thesis, an UA was performed on 24 multi and single-family houses for Swiss buildings in Zürich. The resulting uncertainty in the demands from this analysis was divided into four distributions: heating demand for multi-family homes, electrical demand for multi-family homes, heating demand for single-family homes, and electrical demand for single-family homes.

Heating demand is highly influenced by weather, especially including outdoor temperatures. Due to climate change impacts, we can assume that the outdoor temperature in the future will be higher than it is today. For the determination of the distribution, future weather files including climate change (Remund et al. 2010) were used in the simulation so that the temperature distributions are based on future conditions rather than on the weather of 2015. The weather files are therefore biased towards higher temperatures, and thus lower the heating demand. Some of the other uncertainties considered in building energy models include occupancy, thermostat schedules, set-point temperatures, human activity, metabolic rates, installed lighting capacity, installed electrical capacity, hot water demand, material properties, infiltration, and ventilation rates. These uncertainties have been accounted for in the uncertainty analysis of the building energy models in Mavromatidis (2017) and the resulting output uncertainty distributions have been adopted in this work. They are shown in Table 7.1.

7.3.2 *Mobility Energy Demands*

The mobility demands that are generated using the methodology in Chapter 5 are based on stochastic sampling of profiles from real world census data. We do not know the scheduling error in this census data, based on the times that people go to work, but the census data does record the total annual vehicle kilometres for 72,719 vehicles in Switzerland in 2015 (Bundesamt für Statistik 2015). This is shown in Fig. 7.2.

The data taken from the census data is user reported, which is clear due to the significantly higher rate of samples recorded that are rounded off to the nearest 5000 kilometres. Although self-reported user data is not the most ideal source of driving demand probability, the high number
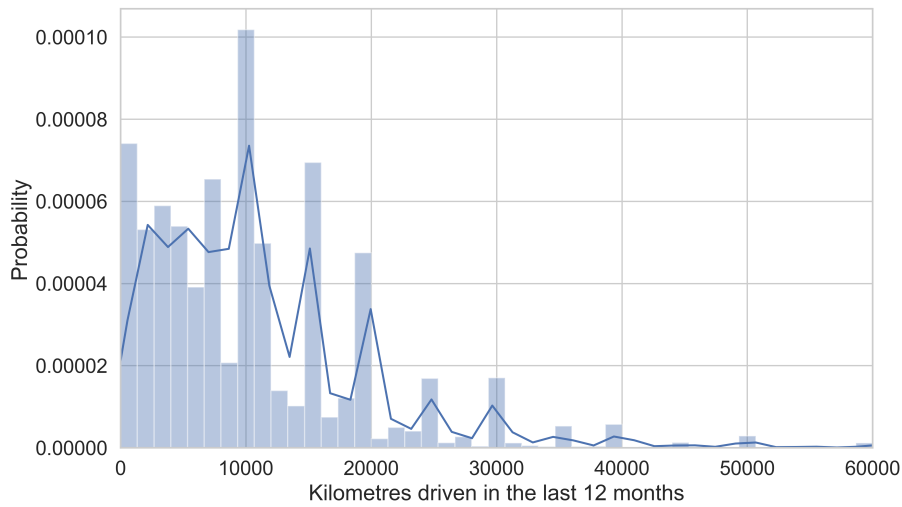
Figure 7.2.: Histogram of the user reported driven kilometres of vehicles in the last 12 months from the mobility census data (Bundesamt für Statistik 2015). This data was taken in 2015 for a sample size of 72,719 vehicles.

of samples and use of the same data set for driving profiles gives a good indication of the variance of total kilometres driven annually. With this considered, the distribution is best modelled as a beta distribution with an α of 2 and a β of 5.

7.3.3 *Solar Radiation*

To simulate the solar radiation in this work, the slope and surface azimuth angle are derived from the GIS methods identified in Section 3.1. These GIS models use solar radiation data from weather files to calculate the hourly solar radiation. The uncertainty in this solar radiation was also evaluated in the thesis of Mavromatidis (2017) when he characterised the uncertainty in weather files. The same PDF that he used for solar radiation in his work is adopted in this work.

The exact PDFs used for the building demands, the mobility demands, and the solar radiation can be found in Table 7.1.

Table 7.1.: Probability density functions for the building demands, mobility demands, and solar radiation.

UNCERTAIN PARAMETER	DISTRIBUTION	UNIT
SFH Elec	$N(0.937, 0.077) * Demand$	kW
SFH Heat	$N(0.923, 0.12) * Demand$	kW
MFH Elec	$N(0.925, 0.047) * Demand$	kW
MFH Heat	$N(0.935, 0.097) * Demand$	kW
Mobility Demand	$B(2, 5, 0.85, 1.5) * Demand$	vkm
Solar radiation	$N(1.072, 0.0674) * Demand$	kW$/m^2$

7.3.4 *Energy carrier prices*

The prices for energy carriers can be assessed on an individual basis for all parameters that can be purchased (imported) or sold (exported) into or out of a MES. These include electricity prices, feed-in tariffs, natural gas prices, SNG export prices, gasoline prices, CO_2 prices, and water prices.

ELECTRICITY, NATURAL GAS, AND GASOLINE PRICES

Electricity prices, natural gas prices and gasoline prices have all been reviewed in the Swiss Energy Strategy 2050 (Prognos AG 2013). The strategy makes predictions for these prices in two scenarios, the Business as usual (BAU) and the New energy policy (NEP). The predictions for these prices from 2020 until 2050 are shown in Fig. 7.3. The NEP prices in 2050 give us an upper bound for our distribution. The lower bound is set as the prices in 2015. Since we do not have any information on how probable it is for one scenario to occur over the other, a uniform distribution is used.

FEED-IN TARIFFS

The renumeration rates for distributed renewable generation in Switzerland have gone through several changes in the last decade. The feed-in tariff in 2018 for rooftop systems less than 30 kW was found to be 0.136 CHF/kWh (SwissGrid 2015), however these have decreased to 0.11 CHF/kWh at present. They are predicted to further decrease in the future and will likely go to zero before 2050, thus zero is determined to be the lower bound for this distribution.
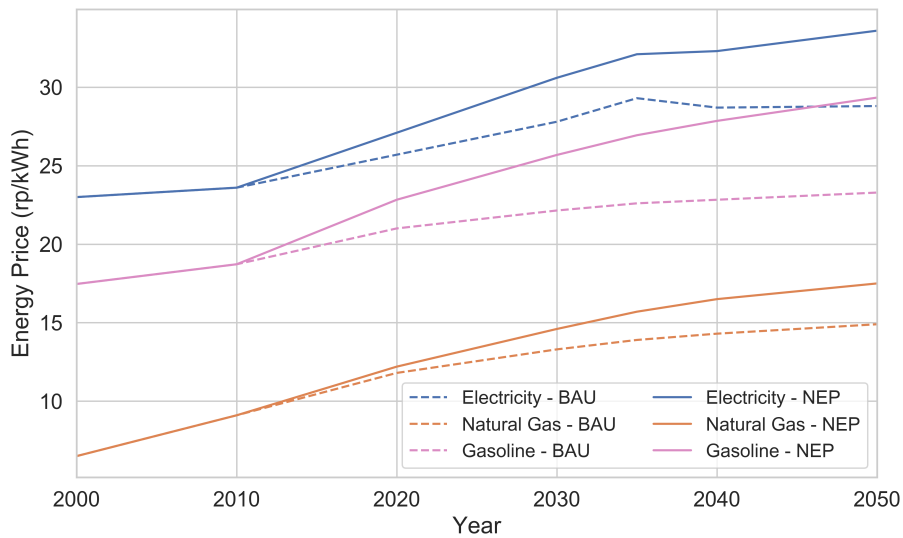
Figure 7.3.: Swiss Energy Strategy 2010-2050 energy price predictions for the BAU and NEP scenarios.

Generally, non-renewable energy sold back to the grid can also be given a rate between 0.04-0.08 CHF/kWh, although generally this must be sold on the spot market and must provide grid services, such as ancillary services. It is unclear at this time which rate PV in the future may sell for, but it is clear that the range is likely to be between the value at present (0.136 CHF/kWh), and the minimum value, which is zero.

CARBON DIOXIDE PRICE

The carbon dioxide price is one of the most uncertain parameters with the widest range of inputs. This is because carbon dioxide can be sourced for P2X from a variety different sources, all which vary significantly in their costs. Carbon dioxide can be sourced from the outputs of several different industrial processes. Some of these include extraction from the exhaust of cement production, chemical industry processes, and steel and iron furnaces. The cost of extraction varies for these from 33-70 CHF/ton for cement production to 16-41 CHF/ton for steel production (Kuramochi et al. 2012). Another source of CO_2 is the treatment of biogas or bioethanol. This pathway has the lowest predicted cost, with the average cost being as low as 8 CHF/ton (Ku-

ramochi et al. 2012). It is not known how much of the CO_2 available for extraction can come from each of these carriers in each country with certainty, but the potential of extraction of these industrial processes is high. A more direct route is to capture CO_2 directly from the atmosphere. These direct capture plants are beginning to be deployed by companies such as Climeworks (*Climeworks – Capturing CO2 from Air* 2019) in Switzerland and Carbon Engineering in Canada (*Carbon Engineering* 2019). This technology is currently still expensive in comparison to industrial extraction, typically about 80-280 CHF/ton (Kober et al. 2019). Since the demand for carbon dioxide is not yet very high, it is not known from which sources CO_2 might come if P2M is implemented on the larger scale. In light of this uncertainty, a uniform distribution with a minimum of 8 CHF/ton and a maximum of 280 CHF/ton is used in this work.

WATER PRICE

The water price is a parameter which does not seem to vary significantly, especially since its costs are significantly lower than that of the other imports and exports. The current price of water in Switzerland is around 4 CHF/m^3 OECD 2017, although some cities state that the price could be as high as 9 CHF/m^3 OECD 2017. Although it can be predicted that fresh water will become an increasingly scarce resource in the future, it is not predicted to become an extremely scarce resource in Switzerland. As a result, a uniform distribution with the price ranging from 4 to 9 CHF/m^3 is used. The exact PDFs for all distributions for energy carriers are shown in Table 7.2.

Table 7.2.: Probability density functions for the energy carrier prices.

UNCERTAIN PARAMETER	DISTRIBUTION	UNIT
Purchase Price		
Electricity	$U(0.18, 0.27)$	CHF/kWh
Natural Gas	$U(0.08, 0.17)$	CHF/kWh
Gasoline	$U(0.16, 0.29)$	CHF/kWh
CO_2	$U(8.00, 280)$	CHF/kg
Wate	$U(0.004, 0.0.009)$	CHF/kg
Selling Price		
Feed-in tariff	$U(0.00, 0.136)$	CHF/kWh

7.3.5   *Carbon factors*

The carbon factors for many of the imported energy carriers can be a major factor influencing the CO_2 prices in the model. Please note that the CO_2 emissions values used in Chapter 6 are for life-cycle emissions, therefore the CO_2 factors analysed in the scenarios of the Swiss Energy Strategy 2050 (Prognos AG 2013) and many other papers cannot be used if they do not use a life-cycle method for calculating emissions. We instead source our values from other publications that calculate carbon factors using the life-cycle methodology.

ELECTRIC GRID CO2 INTENSITY

There is a significant amount of data for the carbon factors in the grid without embodied emissions, but grid factors with life-cycle emissions are more limited. One work that reviews this is Itten et al. (2014), who published that the Swiss grid mix value was estimated to be 0.135 kg CO_2-eq/kWh in 2008. Wyss et al. (2013) investigated the life-cycle CO_2 mix values of the Swiss Energy mix until 2050 for the different scenarios of the Swiss energy strategy. The maximum value was predicted to be the BAU scenario that includes trade with other countries, which was 0.250 kg CO_2/kWh. This is used as the upper bound in the PDF for the electricity grid carbon factor in this work. The lowest value observed was the NEP scenario without trade, which was estimated to be 0.061 kg CO_2/kWh. This was used as the lower bound in the PDF. Similar to the electricity cost, a uniform distribution will be used for the electricity carbon factor as it is not known what which value is more likely occur in the future.

NATURAL GAS GRID EMISSIONS

Although natural gas is a fuel that has a constant carbon emission factor under combustion, the natural gas in the grid contains a current mix of imported natural gas, imported biogas, and local biogas. This biogas currently represents around 3.8% of the gas in the grid (Scarlat et al. 2018), but this percentage is predicted to increase in the future. The Swiss Energy Strategy's NEP scenario states that biogas and SNG usage should have a target of 10% (Prognos AG 2013), thus decreasing the emissions intensity from the natural gas grid. The LCA value for biogas in Switzerland is approximately 0.098 kg CO_2-eq/kWh (Wernet et al. 2016). The LCA value for natural gas is predicted to be between 0.225

and 0.30 kg CO_2-eq/kWh, thus the best case scenario (assuming 10% biogas by volume) for these emissions is estimated to be approximately 0.21 kg CO_2/kWh and the worst case scenario assuming no biogas is 0.3 kg CO_2-eq/kWh. With these upper bounds and lower bounds set, a uniform distribution is used.

GASOLINE EMISSIONS

The carbon factor of gasoline was not considered to be an uncertain value. It was fixed at the a value for Switzerland of 0.32 kg CO_2-eq/kWh (Eggimann et al. 2016).

CO2 PROCESSING EMISSIONS

The LCA value of extracted CO_2 for methanation also varies greatly depending on the method of extraction. Direct capture from the air is quite an energy intensive method of supplying CO_2, as the sequestration process requires significant heating and electric energy. The process can be improved if waste heat is utilised from an industrial facility. Its value is estimated to be 0.71 kg CO_2-eq/kg CO_2 (Wernet et al. 2016). This value is positive, because although CO_2 is being sequestered from the atmosphere, it will be combusted as methane again, thus making the process CO_2 neutral. A less energy intensive method, as was previously discussed, is to capture from the exhaust of an industrial facility or coal plant. From coal sources, this LCA value is predicted to be 0.3 (Assen et al. 2014). Although these values represent the current operation, there are few predictions about the future LCA values, thus the range from 0.3 to 0.71 is used in this work. A uniform distribution is also assumed for this parameter.

WATER PROCESSING EMISSIONS

This value was taken assuming the life cycle CO_2 emission values for processing 1 kg of water. The value used in Table D.1 was taken from Ecoinvent (Wernet et al. 2016) at 0.0003, however some other publications have shown higher values up to 0.0013 kg CO_2/kg, which was calculated for Denmark (Godskesen et al. 2013). Higher values can be associated with countries with scarce water supplies. A uniform distribution was also used for this CO_2 factor.

The PDFs defined for the carbon factors are shown in Fig. 7.3.

Table 7.3.: Probability density functions for the energy carrier carbon factors.

UNCERTAIN PARAMETER	DISTRIBUTION	UNIT
Carbon Factor		
Electricity	$U(0.061, 0.250)$	kg CO_2-eq/kWh
Natural Gas	$U(0.21, 0.3)$	kg CO_2-eq/kWh
Gasoline	0.32	kg CO_2-eq/kWh
CO_2	$U(0.3, 0.74)$	kg CO_2-eq/kg CO_2
Water	$U(0.0003, 0.0013)$	kg CO_2-eq/kg water

7.3.6 *Investment costs*

When considering investment costs, the technologies are split into two categories: technologies that are considered technologically mature, and technologies that are not yet mature. These maturity ratings are often demonstrated through technological learning curves, that show the decrease in costs per unit as demand for a technology increases. This is demonstrated in the technological learning curve shown in Fig. 7.4. As a technology matures and its sales in the market become saturated, the drop in cost per additional units flattens out. At this stage, it is unlikely that a technologies cost will decrease in the future relative to its price today. These technologies that have reached their maturity will be represented using normal distributions. Normal distributions are used for mature technologies with the mean set to the nominal value of the cost. They are symmetrical, thus are not biased towards either increasing or decreasing costs. Technologies that still have potential to expand and decrease in costs will be represented using beta distributions and the maturity of the distribution can be adjusted by changing the α and β values. Beta distributions are non-symmetrical, thus they are biased towards increasing when is α is larger than β and are biased towards decreasing if α is smaller than β. a is used to represent the lowest anticipated cost for the technology and b is used to represent the highest anticipated cost for a technology. These are then multiplied by the nominal value to achieve the final cost.

With this learning curve established, the technological learning rates for these technologies can be used to define the shape of the PDFs. The
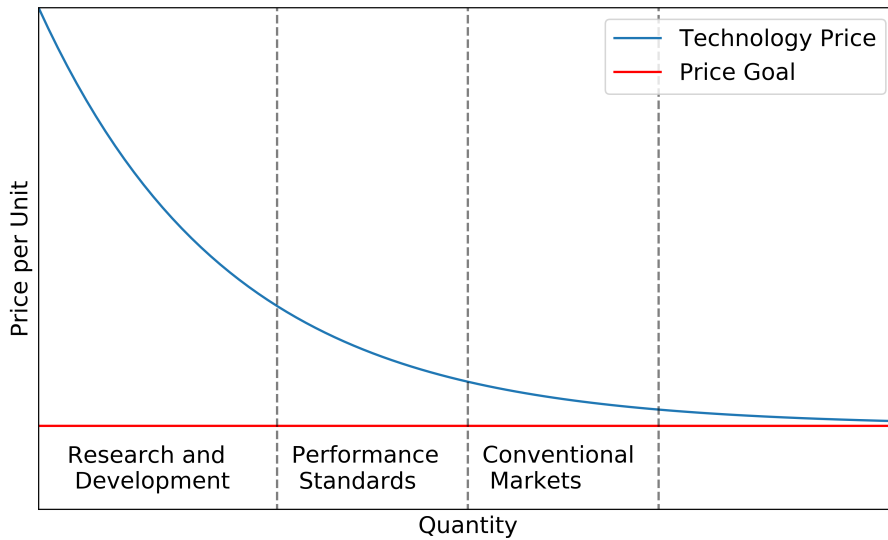
Figure 7.4.: Example of a technological learning curve with its stages of development.

technological learning rates for the technologies assessed in this study are shown in Table 7.4.

Referring to Table 7.4, it is clear that the technologies that are fossil

Table 7.4.: Technological learning rates for the assessed technologies.

TECHNOLOGY	LEARNING RATE	SOURCE
Solar PV (systems)	18.6%	Louwen et al. (2018)
PEME	20%	Grosspietsch et al. (2018)
Heat pumps	10%	Louwen et al. (2018)
Gas boiler	2.2%	Louwen et al. (2018)
Methanation	No data found	Böhm et al (2018)
PEMFC	18.0%	Grosspietsch et al. (2018)
Residential Li-ion battery	12.5%	Louwen et al. (2018)
Thermal storage	8%	Breyer et al (2017)
Hydrogen Storage Tanks	10%	Grosspietsch et al. (2018)
Natural Gas Storage	10%	Grosspietsch et al. (2018)
ICEV	8%	Ruffini et al. (2018)
BEV	15.2%	Weiss et al. (2012)
PHEV	10.8%	Weiss et al. (2012)
FCEV	18.0%	Ruffini et al. (2018)

fuel based are generally the more mature technologies, as they have

generally all been on the market for at least 50 years and the market for these technologies is already saturated, therefore their costs are unlikely to decrease in the future. These technologies include gas boilers and thermal storage for the heating demands and ICEVs for transportation.

Many of the most popular renewable technologies, such as PV, Li-ion batteries, PHEVs, and BEVs have already decreased significantly in costs over the past decade, although there is still potential for improvement. Other technologies, such as the electrolysers, fuel cells, and hydrogen storage, are still continuously being improved and have a low market share since they are still in the research and development phase. The market for these technologies is expected to expand between now and 2050, therefore it is likely that they could have a significant decrease in cost (Körner et al. 2015). As a result, hydrogen based technologies are framed for more significant future cost reductions. To set the distributions, several sources for predictions of the future costs of each technology are chosen, which the distributions are then based on. These variables were used for creating the scenario data in Chapter 4. The minimum cost for all technologies in 2050 is set as the lower bound for the distribution and the maximum current cost was set at the upper bound. The resulting predicted distributions are shown in Table 7.5. Please note that since investment costs in Chapter 5 were calculated with both a fixed and linear portion ($Cost_{t/s}^{linear}$ and $Cost_{t/s}^{fixed}$), the same distribution and LHS sampling interval in the CDF are applied to both costs. The actual PDFs applied for the technology investment costs are shown in Table 7.5.

7.3.7 *Embodied emissions*

Embodied emissions of the technologies are one of the factors in this work that has the least amount of data available in current research. Although there are a series of publications that perform uncertainty analyses for LCAs, information on some of the specific technologies considered in this work, such as catalytic methane reactors, is scarce. Although the data is lacking, the embodied emissions are also represented on a per unit basis, which means that they are also impacted by technological learning curves similar to cost. This method of applying technological learning curves to LCAs was used by Arvidsson et al. (2018) to predict the reduction in material usage while conducting

Table 7.5.: Probability density functions for the technology investment costs.

INVESTMENT COST	NOMINAL VALUE	DISTRIBUTION
Conversion Tech.	**Fixed/Linear**	**PDF · Nominal**
	(CHF)/(CHF/kW)	
Gas boiler	12,500/607	$N(1, 0.03)$
Heat pump	9,625/993	$B(18, 4, 0.12, 1.12)$
PV	1,143/206	$B(10, 4, 0.3, 1.3)$
PEMFC	7,500/1,750	$B(6, 4, 0.4, 1.9)$
PEME	5700/29,189	$B(6, 4, 0.4, 1.4)$
CMR	6500/350	$B(10, 4, 0.2, 1.8)$
Storage Tech.	**Fixed/Linear**	**PDF · Nominal**
	(CHF)/(CHF/kWh)	
Batteries	3000/250	$B(6, 4, 0.3, 1.7)$
TES	1685/12.6	$N(1, 0.03)$
H2S	40,000/275	$B(8, 4, 0.6, 1.2)$
CNGS	675/4.4	$N(18, 4, 0.2, 1.2)$
Vehicle Tech.	**Fixed**	**PDF · Nominal**
	(CHF/vehicle)	
ICEV-g	22,380	$N(1, 0.03)$
ICEV-cng	26,510	$N(1, 0.03)$
PHEV50	32,100	$B(8, 4, 0.6, 1.25)$
BEV200	33,000	$B(6, 4, 0.5, 1.4)$
BEV300	38,000	$B(6, 4, 0.5, 1.4)$
BEV500	42,000	$B(6, 4, 0.5, 1.4)$
FCEV	42,160	$B(6, 5, 0.3, 1.7)$

LCAs. Since material usage is directly correlated to the embodied emissions, it is assumed in this work that the shape of the PDF for embodied emissions follows that of the investment costs. The PDFs defined for the embodied emissions are shown in Table 7.6.

7.3.8 *Technology efficiencies*

The efficiencies of the technologies assessed also follow the same trend of technological learning curves as embodied emissions and costs are assumed to apply. The relationship between technological learning and

Table 7.6.: Probability density functions for the technology embodied emissions.

EMBODIED EMISSIONS	NOMINAL VALUE	DISTRIBUTION
Conv. Tech.	**Fixed/Linear**	**PDF · Nominal**
	$(kg\ CO_2)/(kg\ CO_2/kW)$	
Gas boiler	0/51	$N(1, 0.03)$
Heat pump	2150/70	$B(18, 4, 0.12, 1.12)$
PV	210/40	$B(10, 4, 0.3, 1.3)$
PEMFC	480/20	$B(6, 4, 0.4, 1.9)$
PEME	800/1,400	$B(6, 4, 0.4, 1.4)$
CMR	10/6.67	$B(10, 4, 0.2, 1.8)$
Storage Tech.	**Fixed/Linear**	**PDF · Nominal**
	$(kg\ CO_2)/(kg\ CO_2/kW)$	
Batteries	116/25	$B(6, 4, 0.3, 1.7)$
TES	31/4.7	$N(1, 0.03)$
H2S	660/5.8	$B(8, 4, 0.6, 1.2)$
CNGS	58/0.65	$N(18, 4, 0.2, 1.2)$
Vehicle Tech.	**Fixed**	**PDF · Nominal**
	$(kg\ CO_2)/vehicle$	
ICEV-g	6,104	$N(1, 0.03)$
ICEV-cng	6,424	$N(1, 0.03)$
PHEV50	7,272	$B(8, 4, 0.6, 1.25)$
BEV200	8,215	$B(6, 4, 0.5, 1.4)$
BEV300	8,513	$B(6, 4, 0.5, 1.4)$
BEV500	9,076	$B(6, 4, 0.5, 1.4)$
FCEV	9,000	$B(6, 5, 0.3, 1.7)$

performance was also noted by Arvidsson et al. (2018), except that while the investment costs of such technologies usually decrease with quantity produced, the efficiency of these technologies usually increases. As a result, the technologies that are flagged as immature are represented by the reverse beta distributions (swapping the α and β values). Similar to the future investment cost data, the future efficiency data for the years of 2020, 2035, and 2050 that was used for the scenarios in Chapter 4 are taken and applied as upper and lower bounds of the distribution. The PDFs defined for the technology efficiencies are shown in Table 7.7.

Table 7.7.: Probability density functions for the technology efficiencies.

TECHNOLOGY EFF.	NOMINAL VALUE	DISTRIBUTION
Conv. Tech.	**Efficiency**	**PDF · Nominal**
Gas boiler	89%	$N(1, 0.03)$
Heat pump	4.2%	$B(4, 12, 0.7, 1.4)$
PV	17%	$B(4, 10, 0.82, 1.82)$
PEMFC	19 kWh Elec./kg H_2	$B(4, 6, 0.75, 1.9)$
PEME	0.195 kg H_2/kW Elec.	$B(4, 6, 0.8, 1.4)$
CMR	26.3 kWh CH_4/kg H_2	$B(4, 10, 0.95, 1.2)$
Storage Tech.	**Fixed/Linear**	**PDF · Nominal**
Batteries	92%	$B(4, 6, 0.3, 1.7)$
TES	90%	$N(1, 0.03)$
Vehicle Tech.	**Hwy/Avg/Urb**	**PDF · Nominal**
ICEV-g	1.81/1.78/1.53 (vkm/kWh)	$N(1, 0.03)$
ICEV-cng	1.86/1.85/1.53 (vkm/kWh)	$N(1, 0.03)$
PHEV50 CD	4.67/5.29/5.24 (vkm/kWh)	$B(4, 8, 0.9, 1.3)$
PHEV50 CS	1.74/2.07/2.15 (vkm/kWh)	$B(4, 8, 0.9, 1.5)$
BEV200	4.65/5.38/5.44 (vkm/kWh)	$B(4, 6, 0.9, 1.3)$
BEV300	4.37/5.19/5.17 (vkm/kWh)	$B(4, 6, 0.9, 1.3)$
BEV500	4.25/4.97/4.82 (vkm/kWh)	$B(4, 6, 0.9, 1.3)$
FCEV	93/97.15/97.8 (vkm/kg H_2)	$B(4, 6, 0.8, 1.3)$

7.3.9 *Uncertainty Analysis Results*

The sample size chosen for LHS is 500. For each sample of input data, five Pareto points are solved, which represents 17,500 Pareto optimal

simulations. Due to the long run time of the model (typically between 1-3 hours per Pareto point), this represents a significant amount of computational time which was performed on the Hypatia cluster at Empa over two months. Monte Carlo simulations can often be performed using several thousands of runs, but due to the computational time of the model this was not possible.

These 500 Pareto fronts can be seen in Fig. 7.5 and are compared against the deterministic Pareto curves that were solved for 2015, 2035, and 2050 in Chapter 6.
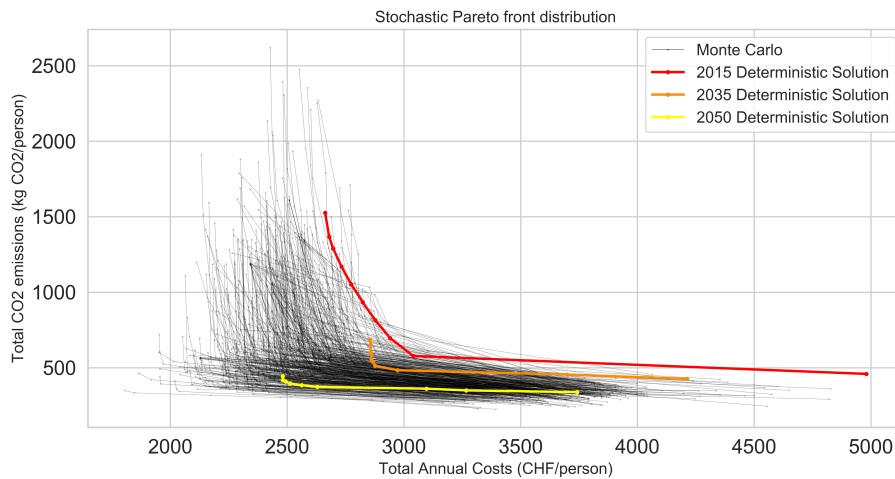
Figure 7.5.: Deterministic Pareto fronts for 2015, 2035, and 2050 plotted against the Pareto fronts for 500 stochastic multi-objective Monte Carlo runs.

In this Figure, it is clear that the uncertainty results of the Monte Carlo runs vary significantly from the deterministic values. It is particularly obvious that the 2015 case will likely have been too pessimistic for future decision making, and the variables assumed for the 2050 case are likely too optimistic. Similar to the Pareto fronts observed in Chapter 4 and Chapter 6, the Pareto fronts are shown to have initially low costs and high emissions in the cost optimal objective, but these emissions decrease sharply for a marginal increase in costs as CO_2 is reduced in the multi-objective cases.

The CO_2 optimal cases are also observed again to represent a very high cost for a very small increase in emissions between Pareto solution

4 and 5 (the CO_2 optimal point). This is again associated with large seasonal storage cases which are required for deep decarbonisation, however this comes at a very high cost for a marginal decrease in emissions for all stochastic cases.

7.3.9.1 *Vehicle Selection*

To investigate the variance of the preferred vehicle types, the fraction of total vehicles per type is calculated by dividing the number of vehicles selected for each type by the total number of vehicles, which is 77. This fraction of total vehicles for each type is plotted against the total CO_2 emissions in Fig. 7.6. The colour of each point in this plot represents the total cost, with red being the cheapest and blue being the most expensive. The black markers represent the deterministic solutions. In this Figure, we are able to see a trend that demonstrates the relationship of vehicles selected with the CO_2 emissions. Although the total emissions in the study include both building emissions (which aren't influenced by the vehicle selection), as well as the mobility emissions, there is a clear trend between type of vehicle selected and total emissions. Both the ICEVs show the trend where the fraction installed decreases with decreasing CO_2 emissions. This is more pronounced with ICEV-g vehicles than ICEV-cng vehicles. ICEV-cng vehicles are used more in stochastic optimisation cases than in deterministic cases. ICEV-g vehicles are used less frequently in stochastic cases than deterministic cases.

For the PHEVs, there is a large amount of usage within the 500-1000 kg CO_2/person range, but there are few cases that have either very low or very high emissions and the average emission is generally higher than it is for BEVs. Stochastic cases also have a much higher preference for PHEVs than the deterministic cases do. This is most likely due to the lower anticipated costs and embodied emissions relative to BEVs.

There is a clear trend that higher percentages of BEVs represent the majority of the lowest emission cases. Most of these vehicles are BEV200s vehicles, as the larger capacity vehicles always have larger embodied emissions, but there are a series of scenarios where BEV300 and BEV500 vehicles are used for 5-10% of the stock. Smaller battery vehicles that can be frequently recharged are always selected by the optimiser over the convenience of larger batteries for the user, as the
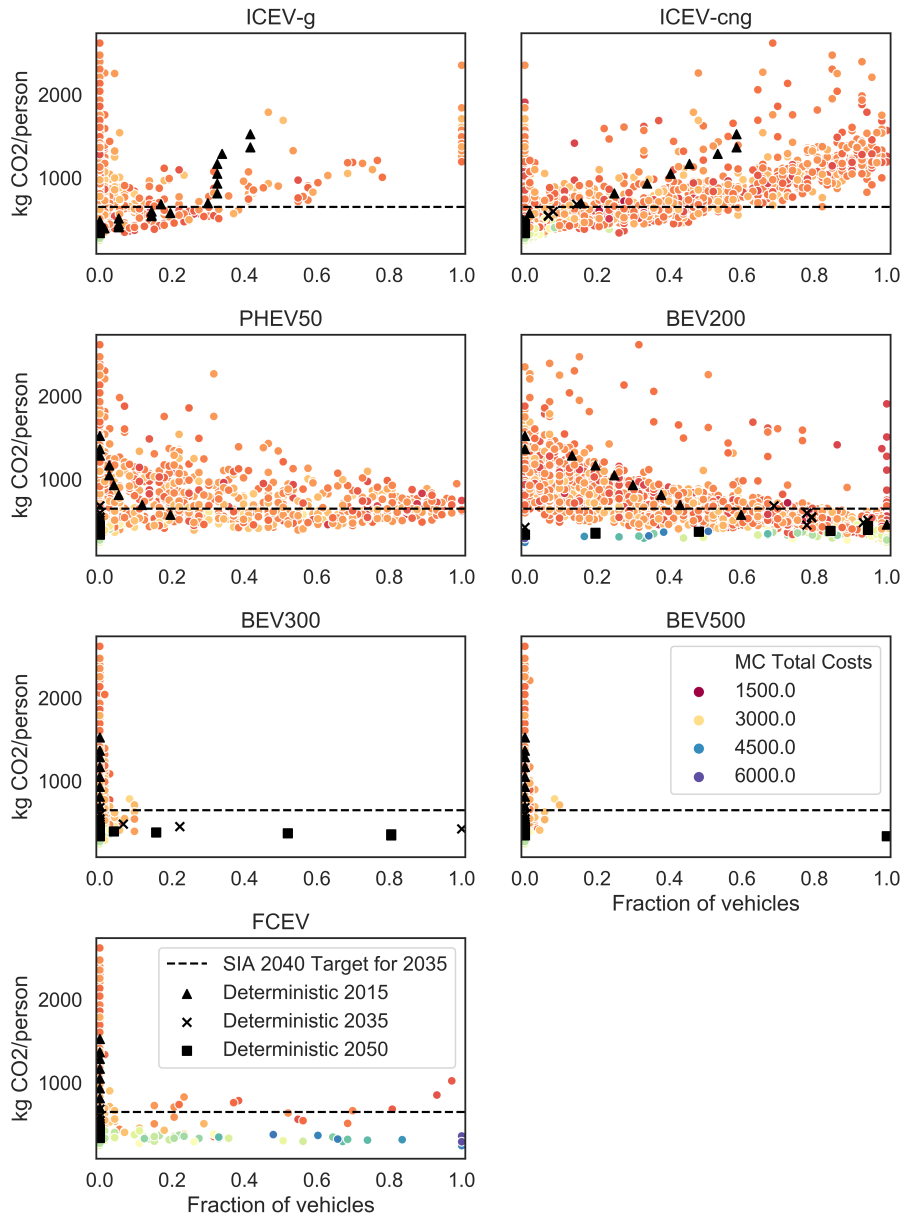
Figure 7.6.: CO₂ emissions per person vs. the optimal fraction of the vehicle stock for 500 stochastic Monte Carlo runs. The colour represents the total cost in CHF/person for the stochastic solutions. The deterministic solutions are shown in black.

objectives does not account for user preference. In the deterministic cases, there was occasionally a selection of a BEV300 or BEV500 in CO_2 minimisation cases, however this is not the case for the stochastic results. This is most likely due to the overly optimistic cost and emission decrease predictions in the deterministic results.

Lastly, FCEVs are the least popular choice of vehicle, but they are used in small number of the low emission cases. In the deterministic cases, the FCEVs were never used, which indicates that there are certain areas in the decision space including uncertainty where they are optimal. To further investigate these solutions, the parameters that influence FCEVs installation will be focused on in Section 7.4.3 in the sensitivity analysis.

7.3.9.2 *Conversion and Storage Technology Selection*

In this Section, the preference of conversion and storage technologies is evaluated. The CO_2 emissions per vehicle are plotted against the total installed capacity for each conversion technology in Fig. 7.7 and each storage technology in Fig. 7.8.

Here, gas boilers are typically in lower capacities than heat pumps. Heat pumps tend to be selected in higher capacities in lower emissions scenarios. The reverse is true for gas boilers, which are installed in their largest capacities in the highest emission cases. These trends are observed for both heat pumps and gas boilers in both the deterministic and the stochastic solutions.

PV was used in capacities greater than 450 kWp in the deterministic cases, however it is seen that there are scenarios where it is used in smaller capacities. Due to the high embodied emissions of PV, it is often installed in lower capacities when the embodied emissions are high.

PEMEs are almost only installed in emission cases that are less than 1000 kg CO_2/m2. In the lower cost cases, it is only installed in small capacities. Electrolysers are only installed in capacities larger than 50 kW in the lowest emission cases. Fuel cells, similarly, are installed in capacities less than 20 kW in cost effective solutions. Methanation is not often installed, but when it is, it is preferred in the CO_2 minimisation cases. In the deterministic cases, methanation was never selected. Since there are certain stochastic cases that do use methanation, the
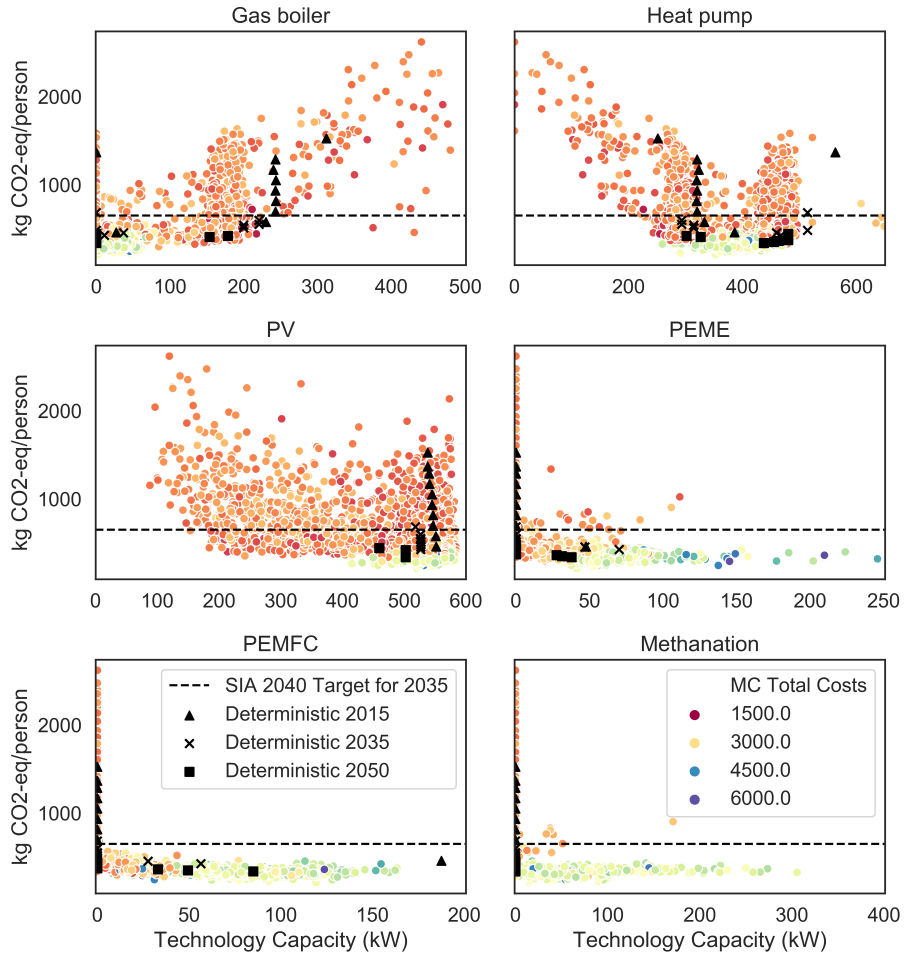
Figure 7.7.: CO_2 emissions per person vs. the installed conversion technology capacity for 500 stochastic Monte Carlo runs. The colour represents the total cost in CHF/person for the stochastic solutions. The deterministic solutions are shown in black.

parameters that influence this selection will be investigated in greater detail in Section 7.4.3 in the sensitivity analysis.
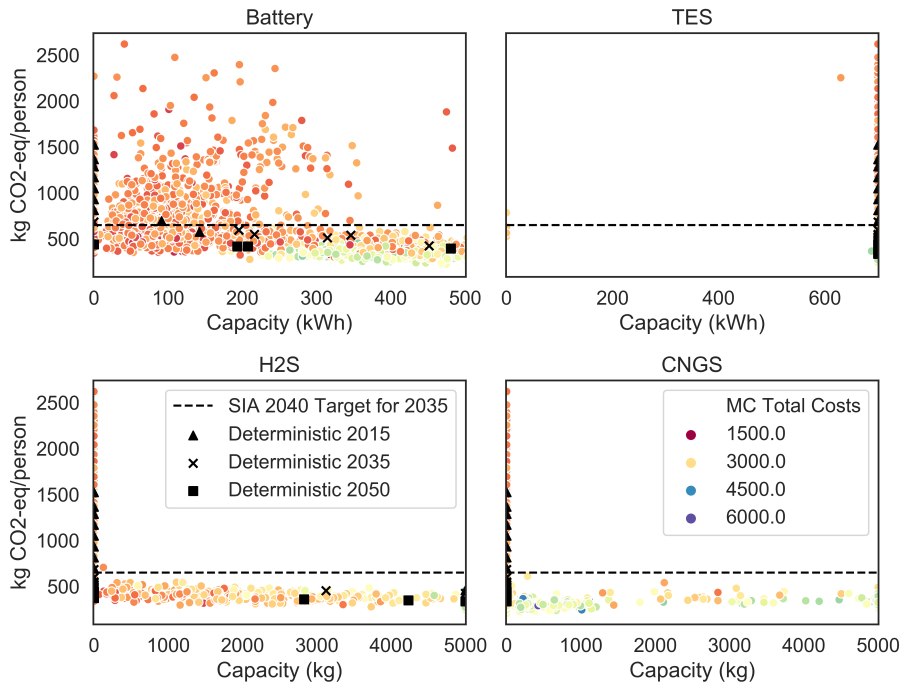
Figure 7.8.: CO_2 emissions per person vs. the installed storage technology capacity for 500 stochastic Monte Carlo runs. The colour represents the total cost in CHF/person for the stochastic solutions. The deterministic solutions are shown in black.

For the storage systems, the battery is installed in many of the future scenarios in capacities ranging from 10-500 kWh, although capacities larger than 200 kWh are only required for very low emission cases. In the deterministic cases, batteries are only used in cases where the emissions are lower than 670 kg CO_2/person, however the stochastic simulations show several cases where batteries are installed with higher emissions.

The thermal storage is nearly always installed to its maximum allowable limit, regardless of the emission target. This is observed in both deterministic and stochastic cases. An upper limit was established in the model to represent the largest thermal storage that is allowed in

households, however perhaps a district system could exploit Power-to-Heat to a larger extent.

H2S is reserved exclusively for cases where the emissions are lower than 550 kg CO_2-eq/person, indicating that it is a strategy that is only exploited for deep decarbonisation. It is noted that the deterministic cases often include higher capacities for H2S when it is optimal, while stochastic cases prefer smaller hydrogen storage sizes. This is likely because the assumptions for costs and embodied emissions of H2S were overly optimistic for 2035 and 2050 deterministic cases. Lastly, the CNGS storage is used less frequently than the H2S storage and when it is used, the associated costs are generally much higher than they are for the H2S solutions, due to the need for methanation. CNGS is never used in the deterministic solutions, similar to how methanation was never used in deterministic cases. Further investigation is needed to identify the parameters that prefer methanation and CNGS in Section 7.4.3.

7.3.9.3 *Objective Functions*

The prediction of the total cost and particularly the emissions can also vary vastly from the deterministic assumptions. To better demonstrate this variance, the total cost and emissions per Pareto solution are shown in Fig. 7.9.
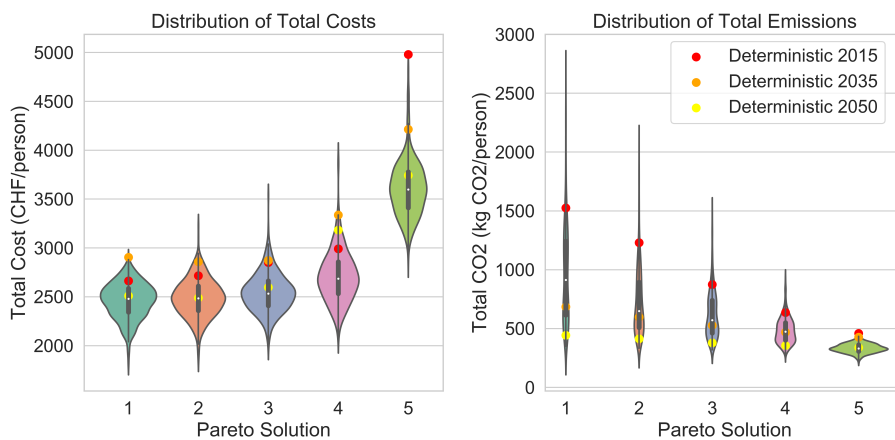
Figure 7.9.: Distributions of the resulting costs and emissions for all MC Pareto points.

In this Figure, it becomes clear that the variance for the CO_2 emissions in the cost optimal case shows the largest variance, which indicates that much of the uncertainty is due to the assumed CO_2 values. As the restriction on CO_2 emissions decreases (i.e., the epsilon constraint), the variance in the emissions decreases and the variance in the costs increases. This is due to the CO_2 limit restricting the solutions to a narrow range of values, thus the variation is low. In general, it can be assumed that when one objective is favoured in multi-objective optimisation, the variance in the secondary objective is more uncertain. To investigate the variance in the individual costs, they are separated further into their individual costs. This is demonstrated in Fig. 7.10 for net annual costs and Fig. 7.11 for net annual emissions.

In this Figure, it is observed that the most significant costs are typically associated with the capital costs of the vehicles. Specifically, the most popular vehicle choice, BEV200s typically holds the highest fractions of the overall annual costs. In certain cases, FCEVs, and ICEVs hold the majority of the costs, but the number of solutions where these vehicles represent the majority of the costs are generally outliers.

In terms of conversion technologies, it is clear that PV panels represent the majority of these costs, followed by heat pumps. Although the electrolysers, fuel cells, and batteries are generally thought to be expensive technologies, they are installed in much smaller capacities. The widest range in this graph is clearly demonstrated by the hydrogen storage, which can vary from low costs to the most significant cost. It has been demonstrated that long-term storage is generally very expensive. Since the size of this storage can range from very small, to a massive seasonal storage, it currently represents a huge uncertainty. Please note that the largest H2S installations are always associated with CO_2 minimisation solutions. While these solutions show us the theoretical maximum reduction emissions using the assumptions for this case study, it is noted that these solutions would not be accepted in reality due to their high costs. They are shown here to demonstrate extremes of the decision space.

In terms of energy carrier costs, electricity represents the largest uncertainty, followed by natural gas, and gasoline. Although it was predicted that CO_2 costs could be hugely uncertain, P2M is not exploited enough in this model for CO_2 to play a major role in the uncertainty in the decision space. Between the three major costs (i.e., vehicles,

Figure 7.10.: The uncertainty variation observed in the various optimisation annual costs emissions for 500 stochastic Monte Carlo samples.

conversion and storage technologies, and energy carriers) it is clear that vehicle costs play the most signifiant role overall.

When looking at the breakdown of emissions, we can see that embodied emissions of the vehicles play a major role, particularly BEV200 and ICEV-cng, which are the two most popular choices. For conversion technologies, PV clearly plays the most significant role, however these emissions are still much lower than for the embodied emissions of BEVs. Although the embodied emissions of PV are still quite high, they are nevertheless exploited heavily in every case investigated. Since they are the only source of renewable energy in the community, their role in supplying carbon free renewable operational energy is crucial to supply energy to the heating and transport energy carriers. The embodied emissions of the remaining conversion technologies are insignificant in comparison to the embodied emissions of vehicles.

Lastly, in terms of energy carriers, it can be observed that in extreme cases, the CO_2 emissions of natural gas and gasoline can be very high. In most cases, these emissions are prevented with the use of BEVs and heat pumps, but there are still cases where ICEV-g, PHEV, and ICEV-cng vehicles are used significantly. It becomes very difficult to completely get rid of natural gas, because some of the more heating intensive buildings remain reliant on gas boilers throughout the simulation. This is because there is not enough renewable energy available to completely cover the entire heating load with heat pumps, the building electricity load, and the transportation load with BEVs. Since gas boilers remain the most efficient non-renewable technology, they are still relied upon.

Electricity emissions from the grid are also a source of uncertainty that is second only to vehicle embodied emissions and natural gas. Electricity grid emissions cannot be prevented since the community is not able to achieve 100% self-sufficiency from the production of the PV arrays, therefore it must rely to a certain degree on the centralised electricity grid.

7.3.10 *Usage of P2X pathways*

When applying the Monte Carlo simulation technique, we can think of several important groups of solutions that we want to investigate in more detail. Since the focus of this thesis is on P2X pathways, we want to investigate the occurrences of the following outcomes of Power-to-
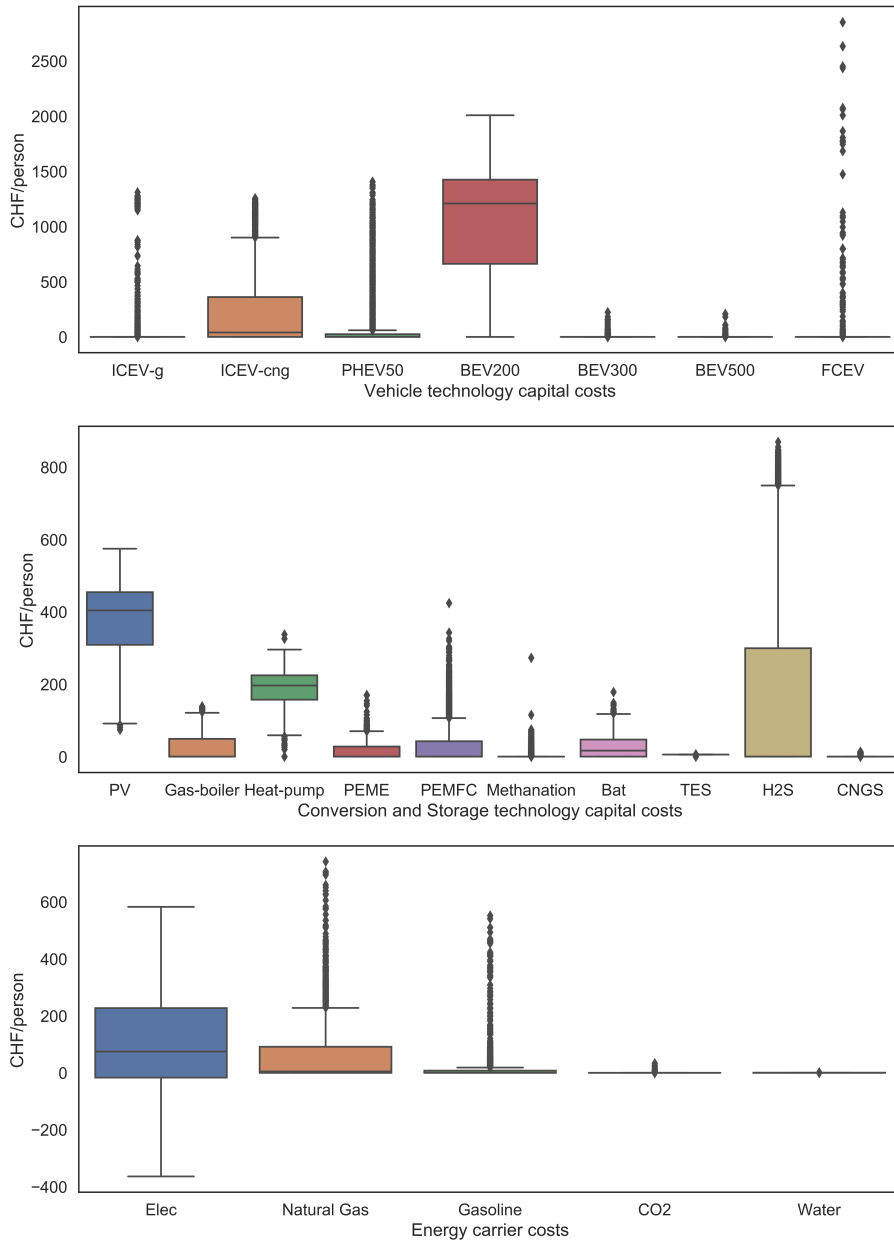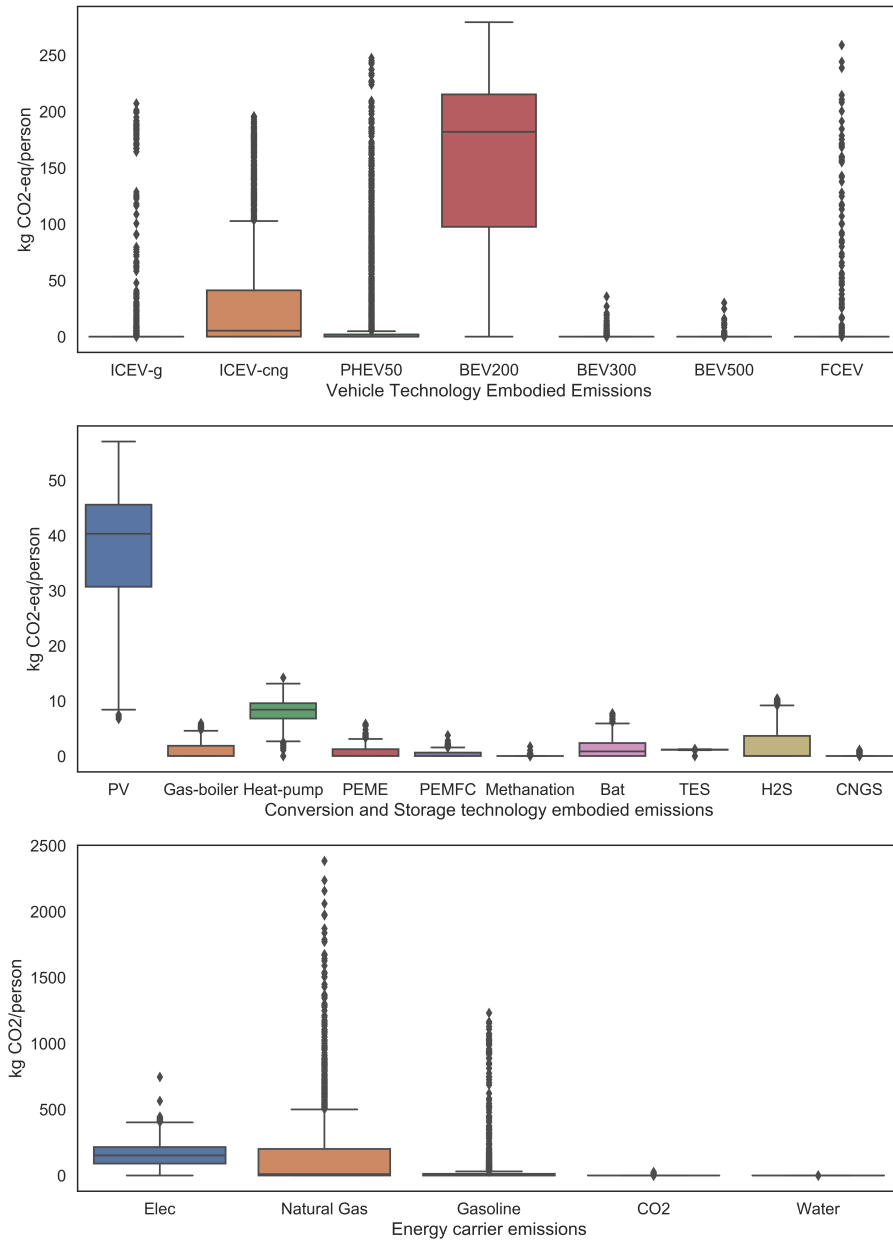
Figure 7.11.: The uncertainty variation observed in the various opti- misation annual CO_2 emissions for 500 stochastic Monte Carlo samples.

Hydrogen, Power-to-Methane, Power-to-CHP, Power-to-Mobility with BEVs, Power-to-Mobility with FCEVs, and Power-to-Mobility with ICEV-cngs.

To evaluate this, the Pareto solution on each curve that corresponds to the carbon target of 475 kg CO_2-eq/person are selected. This target is taken by subtracting the 2035-2050 retrofit emissions (21 kg CO2-eq/person/year) and public transit emissions (54 kg CO2-eq/person/year) from the average target between 2035 and 2050 from Section 5.3 (which is 550 kg CO_2-eq/person target), which results in a target of 475 kg CO_2-eq/kg. Although the uncertainty in public transit and retrofit material emissions has not been accounted for in this work, 475 kg CO_2/person is between the 650 target for 2035 and the 450 target for 2050, and is also a point that is achievable for most of the Pareto fronts observed in Fig. 7.5 before there is a sharp increase in costs. The epsilon-constraint is then set to 475 kg CO_2-eq/person as a target and the Pareto point that reaches this emissions level along each of the Pareto curves is computed. The Pareto solutions are then sorted according to the P2X pathways that are used in each solution. This is shown in Table 7.8.

Table 7.8.: Percent of the Monte Carlo solutions under 475 kg CO_2/kg that utilise P2X pathways Battery storage is also included, although it is technically not a P2X pathway.

P2X Pathway	Percent of the Solutions
Power-to-Mobility (BEV)	100%
Power-to-Heat (TES+HP)	100%
Batteries	84%
Power-to-Hydrogen (PEME)	22.6%
Power-to-CHP (PEME+H2S+PEMFC)	19.2%
Power-to-Methane (CMR+CNGS)	5.6%
Power-to-Mobility (PEME+CMR+ICEV-cng)	5.6%
Power-to-Mobility (PEME+H2S+FCEV)	2%

In this Table, we can see that Power-to-Mobility with BEVs and Power-to-Heat are included for a percentage of the vehicles in every solution observed. The next most popular method of storage is Power-to-Hydrogen, which is used in 22.6% of cases. Although not a P2X pathway, batteries are still an important storage technology and are used in 84% of overall cases. It is noted that batteries are installed

in 96% of cases where Power-to-Hydrogen is used. It was found in Chapter 4 that batteries are an important technology to be used with P2H, as one is responsible for short-term shifts in demand and the other for long-term storage.

The P2H solutions can be further separated into 19.2% of cases using Power-to-CHP (fuel cells) and 5.6% using Power-to-Methane. It is also noted that in every case where methanation is used, there is also a significant percentage of ICEV-cng vehicles installed. Power-to-Mobility with FCEVs is the least used pathway at 2%. From these results, it is clear that a combination of pathways is included in most solutions. In addition, a combination of vehicles is also used in most cases. It is rare for 100% of the cars to be the same vehicle type, although BEV200 vehicles are by far the most common. This is followed by ICEV-cngs, PHEV50s, ICEV-g, and lastly FCEVs. This trend shows us that one single solution is not likely to be the answer to solve our climate problems, but rather combinations of solutions and P2X pathways are the best solutions. The coupling of both long-term and short-term technologies into a hybrid storage system is a necessity for implementing long-term storage in order to keep the costs low and the efficiency high.

7.3.11   *Discussion of the UA Results*

Our departure from deterministic optimisation has shown us that the true decision space varies significantly from the results shown in Chapter 4 and 6. In particular the scenario analysis previously conducted in Chapter 4 shows vastly less information regarding uncertainty than the results in this Section. The scenario results only showed three potential cases, for four years of consideration, and these deterministic solutions have been shown to be either universally optimistically biased or universally pessimistically biased, depending on the year of analysis considered. The real decision space lies in between the optimistic and pessimistic assumptions. The scenario analysis also gives no indication of the likelihood off one outcome over another, where in a UA, the frequency of solutions can be collected to identify robust solutions.

Although the development of the PDFs are a modelling decision and an assumption in themselves, not considering the variation of these inputs is likely to result in overly optimistic cost and emissions reductions when assigning values for the future, and overly pessimistic costs

and emissions when assuming present values. The scenario analysis, in comparison, contained just as many assumptions regarding model inputs as is done in this section with uncertainty characterisation and the assumptions are far less forgiving when variance is ignored. It is also clear that the overall CO_2 emissions are the more uncertain objective in this work when optimising for a minimum cost. When stricter CO_2 emission targets are set, the decision space converges to a set of technologies which are used in most cases. These include PV, heat pumps, thermal storage, batteries, and BEVs. These solutions represent a large portion of the reduction in emissions that is required to meet the targets. Very large capacities of BEVs and PV are used. Even though the embodied emissions of these technologies are high, they both offset such significant amounts of fossil fuels that they are relied upon in each stochastic case. Once these technologies are installed and the CO_2 emissions from gasoline and natural gas are offset, the embodied emissions of these technologies become the major source of emissions in the optimisation.

Although the technologies listed above are able to reduce the majority of the emissions, there is a competition among the remaining P2X technologies to increase the utilisation of renewables. These include Power-to-CHP, Power-to-Methane, Power-to-Mobility with FCEVs, and Power-to-Mobility with ICEV-cngs, as was observed in Table 7.8. Out of these options, Power-to-CHP was used the most frequently, although this usually requires the use of long-term storage which can also be associated with very high costs. Limiting the size of this storage to a reasonable level is important, because the cost of utilising 100% of the renewable energy onsite is very high for a small reduction in the emissions and large storage systems require a significant amount of space. Power-to-Methane is only used in cases that use a large percentage of ICEV-cng vehicles, which indicates that the solutions for P2M coincide with Power-to-Mobility for ICEV-cng vehicles. This pathway is rarely used, as additional natural gas from the grid must always be supplemented with produced SNG to meet the ICEV-cng vehicle charging and gas boiler fuel demand. This is more likely to be implemented if the costs for natural gas are low and the embodied emissions and costs in the electricity grid are high. Unfortunately, the results of the UA are not able to quantify which of these input parameters are driving the decisions to make particular P2X pathways optimal. Therefore, in the

next section, we conduct a sensitivity analysis to rank the importance of these input parameters.

7.4   SENSITIVITY ANALYSIS

7.4.1   *Background*

In the UA section, we observed the frequency with which certain P2X pathways occur, but we are not yet able to tell how the uncertainty in the outputs drives these different outputs of the mode. To find what drives the model to certain pathways, sensitivity analysis is used.

There are two main types of sensitivity analysis: global and local sensitivity analysis. Local sensitivity analysis is a method where perturbations in a single input parameter are varied individually to investigate the effect of the input on the output. One example of this is investigating the effect of varying the outdoor temperature in a building simulation and observing the effect this has on the change of the heating demand of a building. Local sensitivity analysis is, by far, the most common type of sensitivity analysis, mostly because it is the simplest to conduct and requires the least computational time. In many cases, a set of input parameters that are deemed important are selected, the inputs are varied individually, and the effect of this variation on the output is determined. Although this method is straightforward and not computationally intensive, the selection of these parameters is only a partial look at the total effect of uncertainty that can occur in a mode, as was evaluated in the UA. In addition, second order effects of varying several input parameters at once cannot be investigated. An example of these second order effects could be that reducing the costs of both electricity and heat pumps could promote the installation of heat pumps more than only reducing the costs of heat pumps would. The lack of considering these second order effects is one of the biggest drawbacks of local sensitivity analysis.

The second type of sensitivity analysis is the global sensitivity analysis. This method analyses the decision space by varying all input parameters simultaneously, to look at the effect of uncertainty in the whole decision space. Many of the most common methods of sensitivity analysis, such as the Method of Morris (Morris 1991) or Sobol Sensitivity Analysis (Nossent et al. 2011), are available and are able to search the whole decision space for relations between input and output

parameters (first order sensitivities) and even relations between input parameters (second order sensitivities). Although a global sensitivity analysis gives a more complete picture of the decision space, it requires a very large number of computational runs to properly calculate these first and second order interactions. The number of runs is typically recommended to be $N(2k + 2)$ where k is the number of parameters, and N is typically recommended to be at least 500 and up to 1500 (Mavromatidis 2017). Since we investigate 63 parameters, this would indicate that over 60,000 runs would need to be performed, which is far too many for a model that takes between 1-3 hours to solve for a full set of uncertain parameters.

In light of this limitation, a regional sensitivity analysis can also be used (Pianosi et al. 2016). A regional sensitivity analysis is a method that tries to identify regions of the input space that correspond to particular outcomes of the model. As opposed to a local sensitivity analysis, a regional sensitivity analysis looks at all inputs of the optimisation, but focuses on the effect of specific model outputs. This differs from other variance based global sensitivity analysis, that looks at the sensitivity effects of the entire input vector on the entire output vector.

7.4.2 *Monte Carlo Filtering*

The most common form of regional sensitivity analysis is Monte Carlo filtering. Using this method, the results of a Monte Carlo simulation, which was already computed for the UA in Section 7.3.9, can be used. This method involves filtering the MC runs into two subsets: a 'behavioural' and 'non-behavioural' subset. This devision is based on a particular model output parameter that is of interest for a 'regional' assessment. This is often done by selecting an output variable of importance and splitting the subset into values higher and lower than a particular value of interest. An example of this would be to split the UA cost optimal Pareto solutions into a subset of data where the CO_2 emissions per person are lower than the 650 kg CO_2/person/year emission target as the 'behavioural' or Y_b subset of size n and solutions that have higher emissions than the target are grouped into the 'non-behavioural' or $Y_{\bar{b}}$ subset of size $\bar{n}$. The division for this example can be shown in Fig. 7.12. According to the division $n + \bar{n}$ must equal the total number

of MC runs.
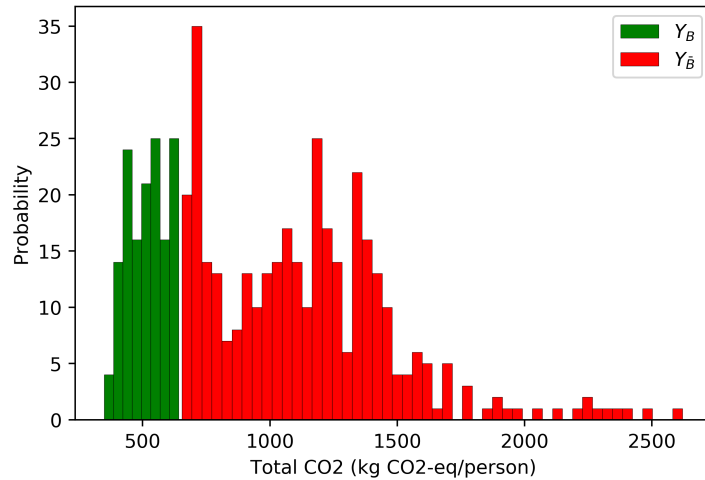
Figure 7.12.: The 'behavioural' subset of Y_b (green) of values less than 650 kg CO_2/person/year and the 'non-behavioural' subset $Y_{\bar{b}}$ of values over 650. The data set is taken from the cost optimal solutions (not the CO_2 or multi-objective solutions).

Once the data is divided into these subsets, the CDFs of the input parameters can be reviewed. $F_{x_i|y_b}$ denotes the CDF for the 'behavioural' subset of data and $F_{x_i|y_{\bar{b}}}$ denotes the 'non-behavioural' subset's CDF. x_i refers to each input parameter. For each x_i, the CDFs can be compared using the two-sample Kolmogorov-Smirnov (K-S) test (Wu et al. 2017). This test is a hypothesis test in which the null hypothesis predicts that the two CDFs are taken from the same distribution. If the two subsets' CDFs for a particular input value are shown to be taken from the same distribution, the null hypothesis is accepted. If this null hypothesis is rejected, then the two CDFs are taken from different distributions. If the CDFs are taken from the same distribution, then any value of the input parameter is equally likely to be found in either subset, thus the parameter is insignificant to the division of the subsets. On the other hand, if the null hypothesis is rejected and the CDFs are deemed different, then it is likely that the input parameter, x_i, has an effect on whether the output lies in subset Y_b or $Y_{\bar{b}}$. The K-S test has two outputs that allow us to quantify the difference between the CDFs and

whether or not the null hypothesis should be rejected. These outputs are the D-statistic ($d_{n,\bar{n}}$) and the P-value. The D-statistic represents the maximum vertical difference between $F_{x_i|Y_b}$ and $F_{x_i|Y_{\bar{b}}}$. The larger the D-statistic is, the more dissimilar the CDFs are and the more significant the parameter is. This is demonstrated in Fig. 7.13.
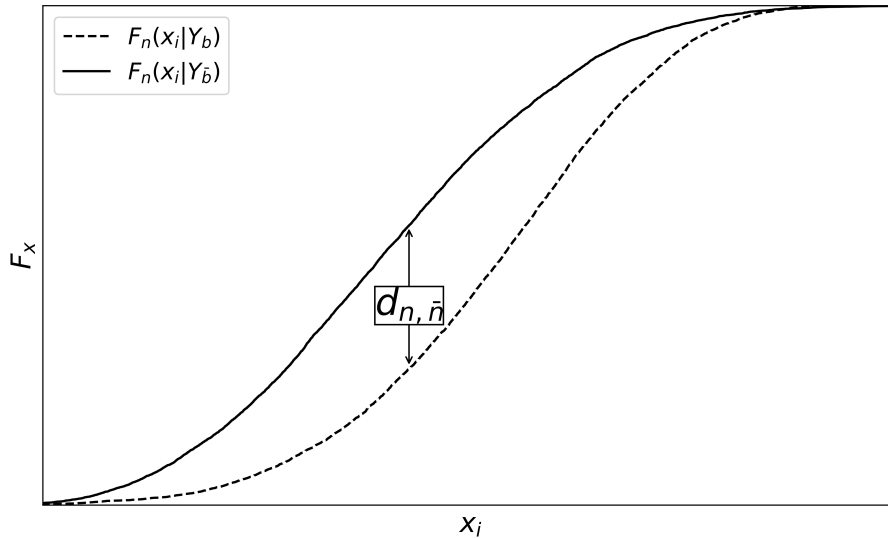
Figure 7.13.: Comparison of two CDFs, showing the maximum distance or $d_{n,\bar{n}}$ between CDFs. The larger this difference, the more dissimilar the distribution sets are.

Here, we can see the CDFs of the two subsets are different, since there is a large distance between them. The larger this distance is, the more significant the parameter is. Here, we are able to specifically see that the behavioural subset $F_{x_i|y_b}$, includes lower values of x_i than $F_{x_i|y_{\bar{b}}}$.

The P-value also indicates how significant the differences between the CDFs are. The smaller the P-value, the more significant the difference is. As a general guideline, a P-value greater than 0.1 indicates that the input parameter is insignificant. If the P-value is between 0.01 and 0.1, then the input parameter is important. If the P-value is less than 0.01, then the input parameter is critical.

An advantage of this method of CDF comparison used by Monte Carlo filtering has been indicated by Pianosi et al. (2016) as being able to *provide a robust approximation of the underlying distribution, even if computed over small samples.*

Another advantage of Monte Carlo Filtering is that the subset can be divided, not only for objective functions (i.e., net annual CO_2 emissions and costs), but for any output. This means that the subset can be divided by the selection of different P2X technologies of interest, such as electrolysers (Power-to-Hydrogen), fuel cells (Power-to-CHP), methanation reactors (Power-to-Methane), FCEVs (Power-to-Mobility with FCEVs), and ICEV-cng with methanation (Power-to-Mobility with ICEV-cngs). Since these pathways are of more interest to us than the rest of the decision space, Monte Carlo Filtering is chosen to investigate the input parameters that effect the decision of P2X pathways.

7.4.3 *Sensitivity Analysis Results*

In this Section, the Monte Carlo Filtering technique is applied to the section of 500 solutions used in Section 7.3.10 along the Pareto curves that use the epsilon-constraint value of 475 kg CO_2-eq/person. There are four particular 'regions' of the outputs that are focused on in this Regional Sensitivity analysis:

1. Solutions where Power-to-CHP is selected

2. Solutions where Power-to-Methane and ICEV-cngs are selected (these are combined since all solutions that contain P2M also include ICEV-cngs)

3. Solutions where Power-to-Mobility with FCEVs is selected

4. Solutions where the total costs lie under 2500 CHF/person

Please note that Power-to-Heat and Power-to-Mobility with BEVs are not analysed as they are selected in all cases, regardless of the uncertainty. Power-to-Hydrogen, or solutions that include electrolysers and hydrogen storage, is further subdivided into Power-to-CHP and Power-to-Methane, since there are no cases where only electrolysers and H2S are used.

DRIVERS FOR SOLUTIONS SELECTING POWER-TO-CHP

Using Monte Carlo Filtering (MCF), the set of 500 solutions is divided into solutions where electrolysers, H2S, and fuel cells are selected, and solutions where they are not. As was shown in Table 7.8 19.2% of this subset used Power-to-CHP. Once both the input and output

vectors are divided into Y_b or the subset with Power-to-CHP and $Y_{\bar{b}}$ or the subset without Power-to-CHP, all of the input parameters in both subsets are compared using the two-sided K-S test. As was previously mentioned, an input parameter is considered significant if its P-value is less than 0.01, important if the parameter is between 0.01 and 0.1, and insignificant if the P-value is over 0.1. All input parameters where the P-value is less than 0.1 are shown in Fig. 7.14 and the input parameter CDFs for both subsets are compared for the 5 most important parameters.

In this Figure, it is observed that the most significant parameter effecting the selection of P2H is the CO_2 emission intensity in the electricity grid. This is obvious, because the electrolyser must run off of electricity to produce H_2. This electricity must come either from the PV panels or from the electricity grid. Since P2H systems are meant to be a storage for renewable energy, high emission electricity from the grid is not of interest to use to run the electrolyser. If emissions must be kept below the 475 kg CO_2/person limit, it is in the interest to store all renewable energy on site, which means that P2H is more likely to be installed when CO_2 grid electricity is high. We can observe from the first subplot that Power-to-CHP is not used unless electricity in the grid is above the level of 0.150 kg CO_2/kWh.

The second most important parameter is the embodied emissions of BEV200 vehicles. Although it is not obvious why it would affect the selection of Power-to-CHP, it is noted that BEV200 vehicles are usually the largest source of emissions overall for these 500 solutions. Since emissions are reduced significantly in the solutions used here, BEVs are only installed in high quantities when the embodied emissions are lower. When fewer BEVs are installed, there is more renewable energy from the PV available to run the electrolyser. The importance of this parameter lies solely with the availability of renewable electricity with which the electrolyser can be run. As a result, when BEV embodied emissions are higher than 6100 kg CO_2-eq, P2H is more likely to be chosen.

The third most important parameter is solar radiation. It is indicated that lower solar radiation occurs more in the solutions that select Power-to-CHP. Solar radiation is directly tied to the output of PV. The two technologies in this analysis that produce electricity are fuel cells and PV panels. These two technologies are in competition, especially in the winter when fuel cells are mostly used, to provide electricity for the

Figure 7.14.: The K-S test results for the solutions that select Power-to-CHP pathways. Subplots 1-5 show the comparisons of the CDFs for the five most significant parameters. Subplot 6 shows the distance and *P*-value for all input parameters with *P*-values lower than 0.1 (lower is more significant). The identified significant parameters are the electricity grid CO_2 intensity, BEV embodied emission, solar radiation, heat pump COP, and PV efficiency.

case study. Due to this competition, lower solar radiation incentives fuel cells and thus Power-to-CHP since renewable electricity demand in winter is in even higher demand than normal. This can indicate that seasonal storage is even more important at higher latitudes, since the discrepancy between summer solar radiation and winter solar radiation is even more significant.

The fourth most important parameter is the efficiency of the heat pump. Fuel cells are a CHP technology; thus they are able to provide heat. As a result, fuel cells are directly in competition with heat pumps as a heating technology. The lower the efficiency of the heat pumps, the more likely fuel cells will be chosen.

The last parameter with a *P*-value less than 0.01 is the PV efficiency. Lower PV efficiency is more likely to result in an installation of Power-to-CHP. The rational for this is similar to the reason why lower solar radiation is preferable for Power-to-CHP. Since Power-to-CHP and PV are both the only technologies that produce local electricity, they are in competition with each other. The lower the PV efficiency, the more reliant the system is on the electricity from the fuel cell, which is where Power-to-CHP is best suited. This is especially true in winter, since there is generally enough solar radiation in summer to meet demands with some surplus. If PV output in winter is lower, there will be a higher preference for fuel cells producing electricity and heat.

The final subplot shows the ranking of the importance of the parameters. This shows that the critical parameters, or those with *P*-values less than 0.01, are the CO_2 grid intensity, the embodied emissions of BEV200 vehicles, the solar radiation, the heat pump COP, and the PV efficiency. Some other important parameters include the price of water, which is used in water electrolysis, the embodied emissions of ICEV-g vehicles, and the electricity demand.

DRIVERS FOR SOLUTIONS SELECTING POWER-TO-METHANE

In this Section, the 500 MC solutions are split into a subset that includes methanation (Y_b) and a subset that does not ($Y_{\bar{b}}$). It is noted that all solutions that include P2M also include ICEV-cngs. The same process, with the two-sided K-S test and sorting the input parameters into groups that have a *P*-value less than 0.1, that was applied in the previous section is applied here. The resulting significant input parameter set is shown in Fig. 7.15.
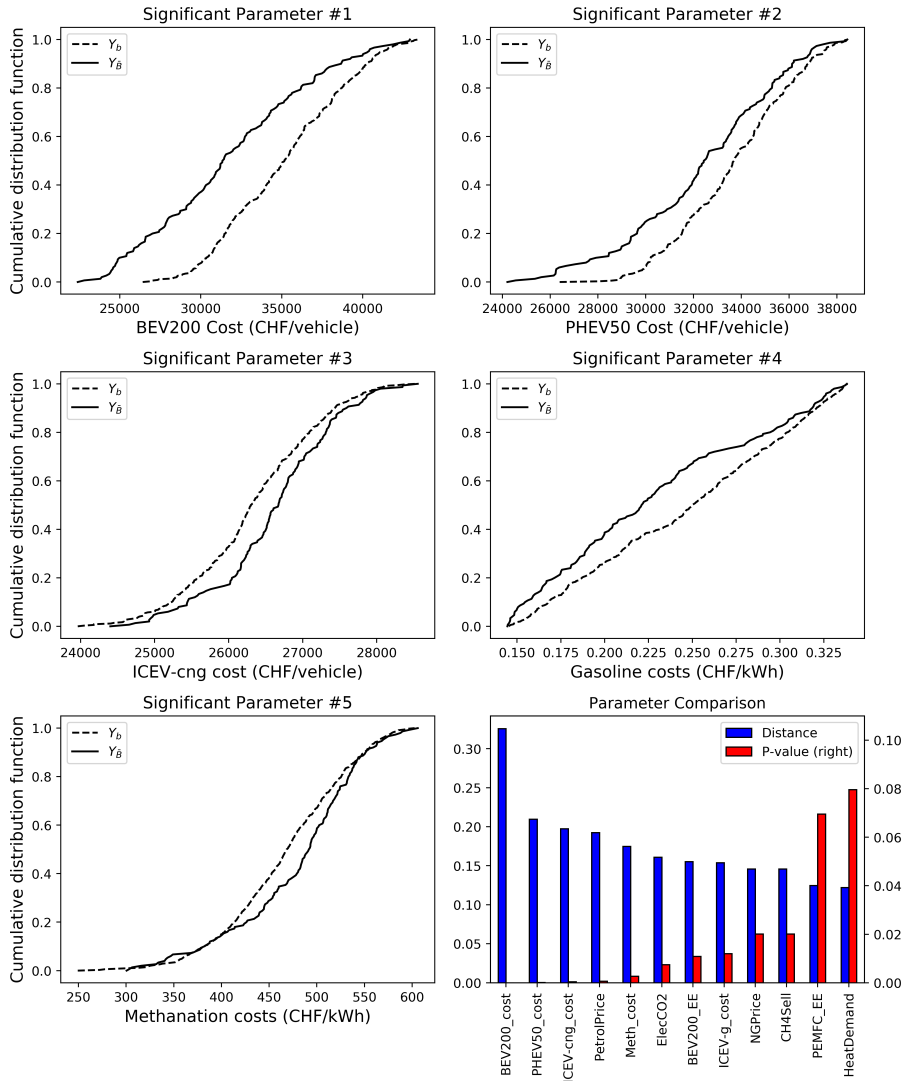
Figure 7.15.: The K-S test results for the solutions that select P2M and ICEV-cng vehicles. Subplots 1-5 show the comparisons of the CDFs for the five most significant parameters. Subplot 6 shows the distance and P-value for all input parameters with P-values lower than 0.1 (lower is more significant). The most significant parameters are identified to be BEV costs, PHEV costs, gasoline costs, and the costs of methanation.
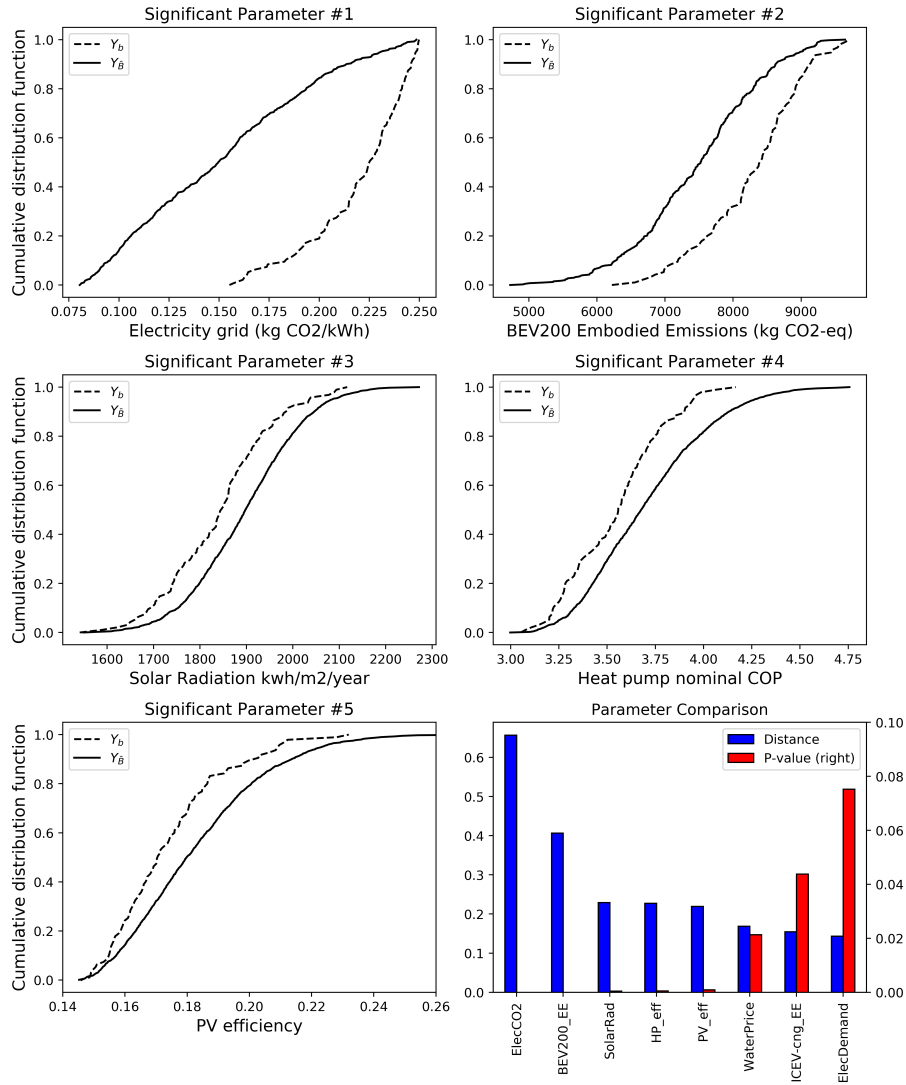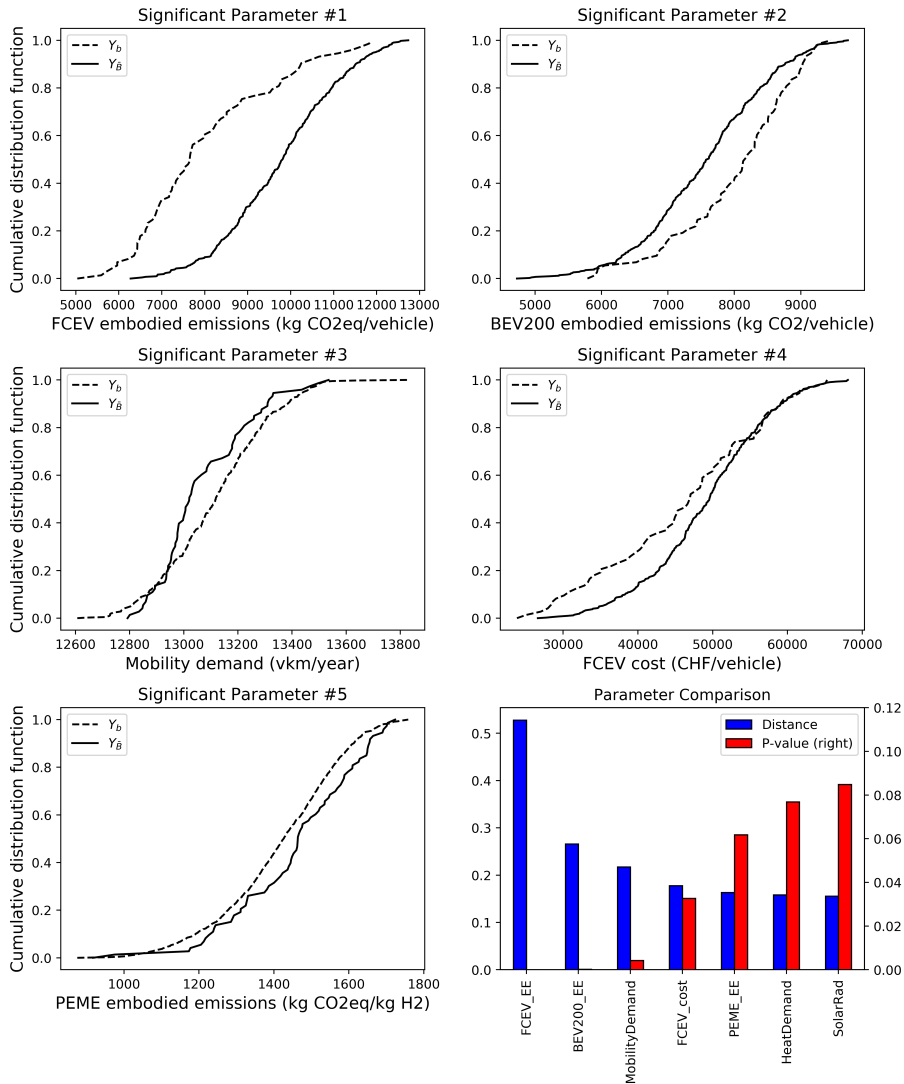
Figure 7.16.: The K-S test results for the solutions that select FCEVs. Subplots 1-5 show the comparisons of the CDFs for the five most significant parameters. Subplot 6 shows the distance and *P*-value for all input parameters with *P*-values lower than 0.1 (lower is more significant). The most significant costs are shown to be the embodied emissions of FCEVs, the embodied emissions of BEVs, the mobility demand, the FCEV costs, and lastly the embodied emissions of the electrolyser.

Here, it can be seen that the two most significant parameters represent the costs of alternative vehicles to ICEV-cng vehicles. It is observed that higher BEV and PHEV costs correspond to the use of P2M, since they are in direct competition with ICEV-cng vehicles. The third most significant parameter is the cost of the ICEV-cng itself. Obviously, P2M and ICEV-cngs are more likely to be chosen when ICEV-cng costs are low. This is followed by the price of gasoline, where higher costs indicate that P2M is likely to be selected. This is because ICEV-cng vehicles are also in direct competition with ICEV-g vehicles. The last significant parameter is the cost of the methanation itself, where it is observed that lower methanation costs correlate to a higher usage of P2M. It is clear in this case that using SNG to charge vehicles is the driving force installing P2M. Selling natural gas back to the grid did not play a role in this case as the selling cost is too low compared to the costs of methanation and there is no environmental benefit to the system itself if it is injected into the natural gas grid. Although this pathway was initially thought to be very inefficient, it is slightly more attractive than Power-to-Mobility with FCEVs due to the lower costs of vehicles and the option to also use SNG for gas boilers.

The final subplot in Fig. 7.15 ranks the importance of these parameters. It is found that the critical parameters with P-values less than 0.01 are the costs of BEV200 vehicles, the costs of PHEV50 vehicles, the costs of ICEV-cng vehicles, the price of gasoline, the investment cost of methanation, and the CO_2 intensity in the electricity grid. Other important parameters are the embodied emissions of BEV200 vehicles, the costs of ICEV-g vehicles, the price of natural gas, the selling cost of SNG, the embodied emissions of fuel cells, and the heating demand.

DRIVERS FOR SOLUTIONS SELECTING FCEVS

The subset of solutions where FCEVs are used can now be separated from the remaining subset of data. Many these cases indicate that FCEVs are only installed for the vehicles that drive the most per day. The most significant parameters observed for this selection are shown in Fig. 7.16.

The most important parameter in the selection of FCEVs is identified to be the embodied emissions of the vehicles themselves. The lower the embodied emissions of the vehicles, the more likely they are to be installed, especially since FCEVs typically have the highest embodied emissions. The second most important parameter is the embodied emis-

sions of BEVs. Since BEVs are generally the most selected technology, higher BEV embodied emissions would likely result in a preference for FCEVs.

Mobility demand is identified as the next important parameter. This is because of the longer ranges of FCEVs relative to BEVs as compressed hydrogen is more energy dense than Li-ion batteries. FCEV costs are then the fourth most significant input parameter for the selection of FCEVs, where lower costs are associated with a higher selection of FCEVs. Lastly, the embodied emissions of the electrolyser are identified. The installed capacities of electrolysers are much higher for FCEV applications than for Power-to-CHP or long-term storage applications. This is due to the fact that the charging period for hydrogen storage can be quite long with Power-to-CHP. FCEV charging demand, on the other hand, requires quicker charge and discharge rates due to the constant daily demand of hydrogen which is high at all times in the year. When a larger electrolyser is required to supply this hydrogen, lower embodied emissions play an important role.

The ranking of the parameters in the final subplot of Fig. 7.16 indicate that the only three critical parameters are the embodied emissions of FCEVs, the embodied emissions of BEV200 vehicles, and the mobility demand. The cost of FCEVs, the embodied emissions of PEMEs, the heating demand, and the solar radiation are considered important parameters.

DRIVERS FOR SOLUTIONS WITH ANNUAL COSTS LOWER THAN 2500 CHF/PERSON

In this last regional investigation, we depart from looking at P2X pathways of interest and look into the economic viability of the overall MES system. In this section, we ask the question 'which input assumptions play the biggest role in achieving the emission targets for under 2500 CHF/person?' To do this, the data set is split into a subset where the costs lie under 2500 CHF/person and a subset where the costs are higher than 2500 CHF/person. This split is shown in the PDF in Fig. 7.17. From these subsets, the K-S test is again applied on all input parameters, and the inputs with the P-values lower than 0.01 are identified as significant. These are shown in Fig. 7.18. Here, it is clear that the costs for BEVs is the most important parameter for both meeting our emissions targets and having our costs lower than 2500 CHF/person/year. Since BEVs are the technology used in every
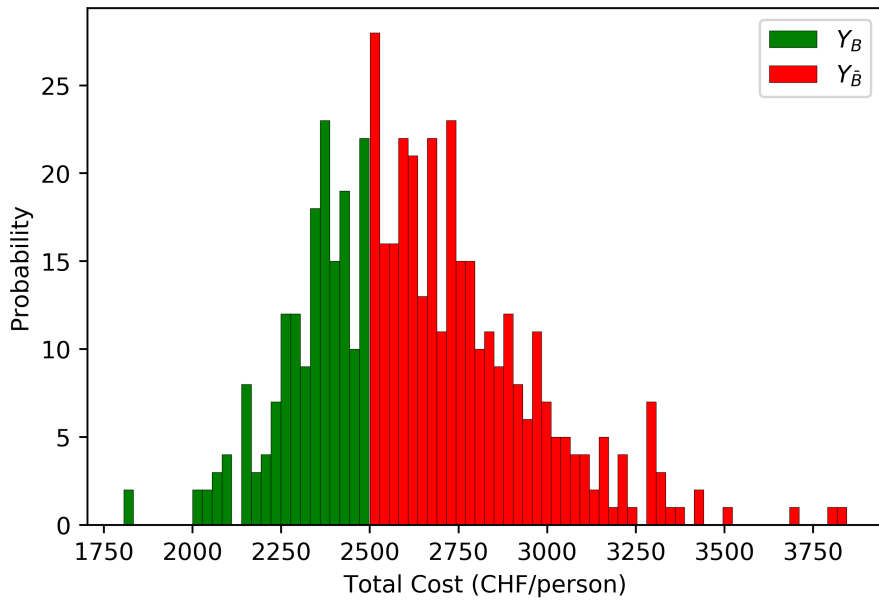
Figure 7.17.: The 'behavioural' subset of Y_b (green) of values less than 2500 CHF/person/year and the 'non-behavioural' subset $Y_{\bar{b}}$ of values over 2500.
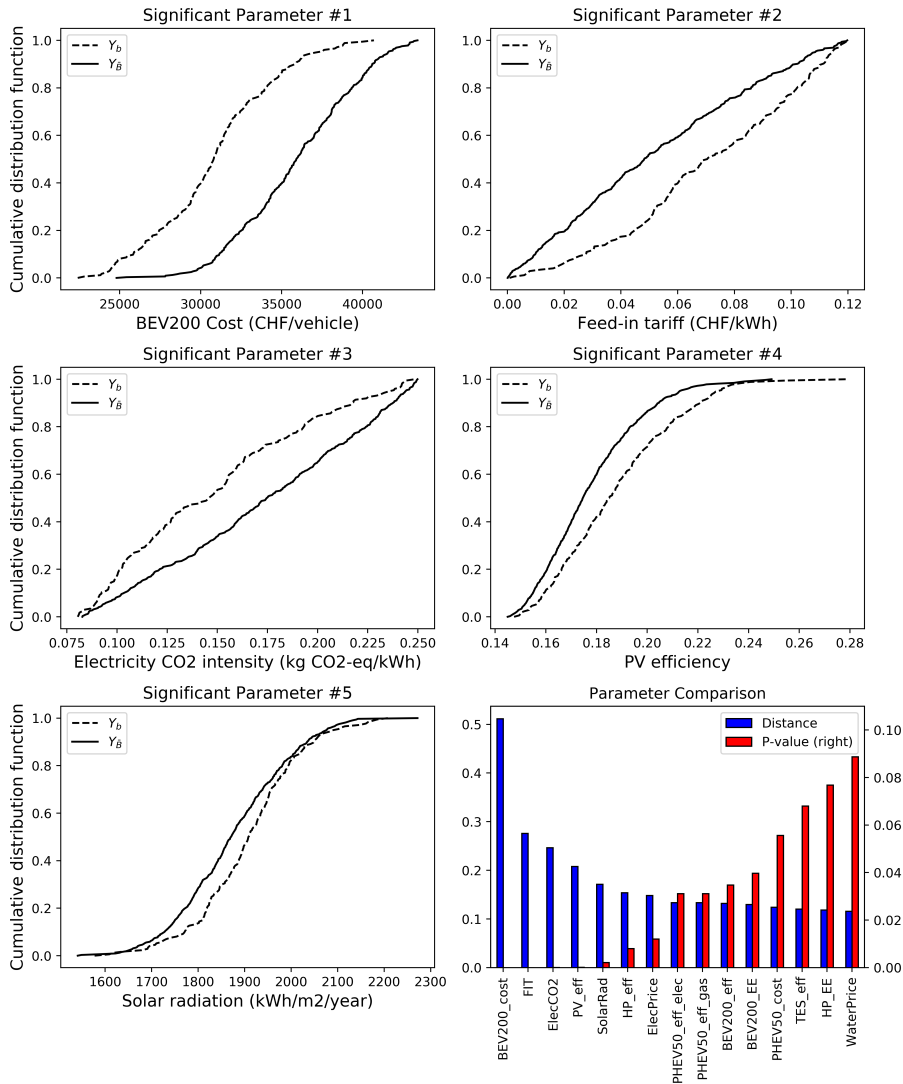
Figure 7.18.: The K-S test results for the solutions where the costs are lower than 2500 CHF/person/year. Subplots 1-5 show the comparisons of the CDFs for the five most significant parameters. Subplot 6 shows the distance and *P*-value for all input parameters with *P*-values lower than 0.1 (lower is more significant). The most significant parameters are shown to be the cost of BEV200 vehicles, the feed-in tariff, the CO_2 intensity of the centralised grid, the PV efficiency, and the solar radiation.

scenario that meets the targets, and often make up large percentages of the vehicle stock in the majority of solutions, they are the most influential factor since they represent the most significant cost and embodied energy in the system.

Secondly, the feed-in tariff or renumeration rate plays a large role. Higher feed in tariffs are generally accepted to contribute to lower costs. This is clear since the surplus electricity could be a source of profit in many cases, rather than being curtailed or used in large and expensive storage systems.

The electricity intensity of the grid is also a major factor. With strict CO_2 targets in place, lower CO_2 levels in the electricity grid mean that more electricity can be purchased from the grid. Purchasing electricity from the grid during times of non-production from the PV panels is much lower cost than implementing large storage solutions.

The last two important factors are the PV efficiency and solar radiation. Higher efficiency and solar radiation levels both result in more renewable energy available for the MES. In this case, we can see that even slight increases in the solar radiation and the PV efficiency have a large effect on the system.

7.4.4 *Discussion of Sensitivity Analysis*

This Section investigated the effects of the input parameters on the selection of several different P2X pathways. Monte Carlo Filtering was chosen as a method of sensitivity analysis, as it is able to use the simulation results of the UA analysis, which eliminates the requirement for further simulations. In addition, it is stated in literature as being a robust method of SA to use, even when samples sizes of the data are small. Since our model in this work is quite computationally intensive, we were not able to afford the high number of runs required with many of the variance based global sensitivity analysis methods. Using Monte Carlo Filtering, we were also able to identify the sensitivity in regions of the decision space that are of particular interest to us; namely those where P2X pathways are selected. The specific P2X pathways that were investigated were Power-to-CHP, Power-to-Methane, and Power-to-Mobility with FCEVs.

When filtering for solutions where Power-to-CHP was chosen, we are able to conclude that high CO_2 intensity in the electricity grid is the most influential parameter for installing Power-to-CHP. This is due to

the high reliability on local renewable potential that must be utilised onsite to decarbonise when grid emissions are high. It was specifically noted that Power-to-CHP was only used when electricity grid emissions are higher than 0.15 kg CO_2-eq/kWh. The other important parameters for the selection of Power-to-CHP include the embodied emissions of BEVs, the solar radiation, the heat pump COP, and the PV efficiency. Fuel cells are in direct competition with both heat pumps for supplying heating demand and PV panels for supplying electricity demand, therefore lower production efficiencies from both of these cause a preference for fuel cells, especially in the winter when renewable potential and heat pump efficiency is low.

Power-to-Methane is only viable when it is able to produce SNG for ICEV-cng vehicles and gas boilers. As a result, high costs for BEVs and PHEVs and low costs for ICEV-cng vehicles cause ICEV-cng vehicles to be preferred. When renewable potential is high and ICEV-cng vehicles are selected, Power-to-Methane becomes a viable solution. High gasoline costs and low methanation costs also have a significant effect promoting the use of Power-to-Methane and Power-to-Mobility with ICEV-cng vehicles.

Power-to-Mobility with FCEVs is the least frequently used P2X pathway. When FCEVs are selected, the most influential uncertain parameters were determined to be the embodied emissions and costs of FCEVs themselves. When these embodied emissions and costs are on the low end of their distributions, they are often installed in a small percentages of the vehicle stock. It is also observed that higher than normal BEV embodied emissions correspond with a higher selection of FCEVs. It is also observed that higher mobility demand coincides with selection of FCEVs, as they have longer ranges than BEVs. Lastly, the embodied emissions of PEMEs was determined to be an important parameter. Larger electrolysers are required to support FCEVs charging than are required for Power-to-CHP. This is due to the high demand of hydrogen that must be produced to support FCEV charging, thus the embodied emissions of PEMEs are an influential factor.

Lastly, the output sample set was filtered for solutions that were able to meet the CO_2 targets, while still keeping costs low. It was found that the heavy dependence on BEVs resulted in the costs of these vehicles having the largest effects. Other important factors were the feed-in tariff, the CO_2 intensity in the grid, the PV efficiency, and the solar radiation.

The large costs and embodied emissions in the results that are directly related to the vehicles indicate a that replacing a large percentage of the vehicles in the vehicle stock represents both significant investment costs and embodied emissions due to the purchase and manufacturing of a large number of vehicles. Due to the high embodied emissions, the current ICEV-g vehicle stock should be used until their end-of-life to reduce these embodied emissions as much as possible when transitioning to BEVs. In addition, using used vehicles and extending the lifetime of vehicles as much as possible is also important to reduce these embodied emissions and extend costs.

Using this analysis, we are able to determine the most sensitive parameters for each pathway using a small sample set. Although only four regions of the output decision space are evaluated, Monte Carlo Filtering can be a very useful tool for answering other specific questions that either policy makers or engineers have regarding system design. It can even be used to target specific input parameter ranges that are required for specific model outcomes. One limitation of this model, is that we are not able to quantify second order effects. Using variance based methods, such as a Sobol analysis, first and second order relations can be quantified. This allows for the identification and quantification of relationships between input parameters. This is a limitation of Monte Carlo Filtering, however accurate calculation of these second order parameters requires very large sample sizes, which can be difficult or impossible to obtain for computationally intensive models. This study had access to cluster computing to obtain these results, however this is not always available to all researchers or model users. In addition, researchers should be aware that increasingly complex models are not always more beneficial, if it means that the model can only be deterministically assessed. This is especially true, when trying to model with input parameters that are known to be uncertain. Reducing model complexity in favour of a through UA and SA can often be more informative for real applications.

Another limitation of this study is that the UA and SA were only performed for one of the case studies, therefore the results here are case study specific. The same analysis should be applied to the other two case studies of Zernez and Altstetten to see if the uncertainty is in the same range and if the significant parameters for each pathway were determined to be the same. Zuchwil was chosen as a case study, due to its size, high ownership of vehicles, and proximity to the natural gas

and water grids. Zernez had a very high renewable potential, which is not available for most case studies. Altstetten was a restrictive case study due to its low renewable potential. Applying the methods in this section to the other two case studies could help to identify the most appropriate municipal context for the application of decentralised MESs.

7.5 SUMMARY AND OUTLOOK

In this Chapter, we have performed both a Uncertainty Analysis (UA) and Sensitivity Analysis (SA). To perform a UA, a Monte Carlo simulation with Latin Hypercube sampling was selected. After this, the uncertainty characterisation to define the PDFs for each input parameter were individually defined for all 63 uncertain input parameters. The results of the UA were then presented, showing the deviation of the stochastic results from the deterministic results. The deterministic cases are shown to be too optimistic while setting parameters for the future, and too pessimistic when setting parameters for the current condition. In addition, the results show significantly more information about the uncertainty decisions space than the scenario analysis did, which was performed in Chapter 4. Upon review of the results in both Chapter 4 and 6, it is concluded that scenario analysis is an insufficient method to properly address uncertainty in a model as it does not show likelihood of a particular scenario's solution occurring. Although the process uncertainty characterisation is full of assumptions, scenario building and parameter setting is even more arbitrary, contains more assumptions, and ultimately cannot address the issue of uncertainty adequately.

From the results of the UA, it was identified that the uncertainty in the objective values was much higher for the CO_2 emissions than for the costs. When broken down by cost type, it was noted that the investment costs for vehicles and the cost of long-term storage played a significant role. For CO_2 emissions, the most significant effects are the embodied emissions of the vehicles, the PV embodied emissions, and the emissions from purchased electricity and natural gas. Due to the significant costs and embodied emissions of vehicles, it is not recommended to replace vehicles until they are at their end-of-life.

When investigating the specific P2X pathways, it was noted that Power-to-Mobility with BEVs and Power-to-Heat (Heat pumps + ther-

mal storage) are used in every MC case that meets the targets, while Power-to-CHP (which is used as a long-term storage) was used in 19.2% of cases that met the emissions targets. This storage system operates off of on-site renewable energy to utilise more of the local resources, thus it is used more when the CO_2 emissions in the grid are high. Power-to-Methane is only used in cases were ICEV-cng was used, and this is only representative of 5.6% of cases. Power-to-Mobility with FCEVs is even less attractive at only 2% of cases that met the target. It is a possibility that ICEV-cngs could play a role in meeting our future personal transport needs, however it is unlikely that FCEVs will play a role, since they cannot compete with BEVs for consumer vehicles. Since FCEVs are more attractive at higher mobility ranges, they should be considered in a sector, such as trucking or heavy shipping, where high vehicle ranges and quick charging demands are required. The costs and embodied emissions are still limiting factors, so these will have to be further reduced if FCEVs want to be competitive with ICEV-cngs, ICEV-gs, and PHEVs, which can also handle long ranges and quick charge times.

Monte Carlo Filtering was found to be a robust sensitivity analysis technique for computationally intensive models that are only able to compute a low sample size in a reasonable amount of time. It is considered to be one of the most accurate methods for small sample sizes, although the accuracy will increase with larger sample sizes. It is a superior method to local sensitivity analysis, since it allows for the accounting of second order effects in the UA itself, even if these second order effect are difficult to quantify from the results. The ability to use the same sample set from the UA for the SA analysis was another time saving advantage.

There are many papers that look only at local sensitivity analysis due to the computational complexity of a model, but this method has severe limitations for addressing the true uncertainty and sensitivity in a model decision space. Monte Carlo Filtering shows a robust SA alternative for computationally intensive models that other researchers should consider in the future for their sensitivity analyses. It is particularly useful when trying to investigate under what conditions a certain outcome of interest are optimal. Engineers and policy makers often make their decisions by looking at key performance indicators, therefore this technique is able to address the sensitivity for whether these specific indicators, are above or below a particular threshold.

The major limitation of this method is that it can only look at certain regions of the output space, therefore is only effective if there are certain outputs of the model that are of particular interest. For a more general global overlook of the entire uncertainty vector of a model, variance based global sensitivity analysis is required.

In the context of MES optimisation, this method has allowed us to investigate the particular conditions required for use of P2X pathways, which can be useful to engineers, policy makers, and decision makers alike when trying to investigate the applications of P2X. Although the results in this model are specific to the case study used here, the technique developed in this work is widely applicable to different communities in Switzerland and abroad. It can be used for analysis of charging stations in workplaces or even for vehicle fleets within a community. Currently, many P2X projects are installed due to biases towards one technology vs. another (i.e., methanation vs. fuel cells), but project leaders should take a neutral approach towards the selection of different P2X pathways and conduct a thorough analysis of their MES, including uncertainty, before making a pathway selection.

CONCLUSION AND OUTLOOK

In this Chapter, the content of the thesis is first summarised including major findings. Secondly, the major contributions of this work to the field of MES analysis are then listed. A section on the limitations of the thesis and areas for improvement, are then reflected upon and discussed. These critical reflections are then used to advise the directions for further research in this area. Lastly, the most important conclusions of this research for society and the environment are presented.

8.1 SYNTHESIS

The aim of this thesis is to investigate the application of different P2X pathways in decentralised multi-energy systems. With the increasing deployment of decentralised renewable energy sources, such as rooftop PV, these P2X technologies are investigated for their potentials to shift renewable energy surpluses to later building energy demand, not only over short time horizons but over long durations. Several P2X pathways, such as Power-to-Hydrogen, Power-to-Heat, Power-to-Methane, Power-to-CHP, and Power-to-Mobility have been investigated in this thesis for their potential to store energy in urban MESs and to see if these pathways can contribute to meeting the emissions targets in not only the building sector, but also the personal transport sector.

With the objective of the thesis defined, a review of the state of the art research was performed in Chapter 2. This Chapter was dedicated to reviewing the status of the current literature applying Power-to-X technology in MESs. The review began with an evaluation of the state of the art in electrolysis, fuel cells, and methanation. This review compared the different technologies available for each process and discussed the advantages and disadvantages for application in the context of a MES. The review is then is divided into papers looking at Power-to-Hydrogen (Section 2.2), Power-to-Methane (Section 2.3), Power-to-Mobility (Section 2.4), Power-to-Heat (Section 2.5), papers that compare P2X pathways (Section 2.6) and other storages, and the status of uncertainty analysis in the reviewed papers. It was concluded

from the review that there was a lack of focus on studies that combined both vehicle charging and building demands in a MES and that most papers do not consider long-term decentralised storage systems. The level of uncertainty and sensitivity analysis in the investigated papers was limited to local sensitivity analysis. It was therefore proposed to build a MES optimisation model that can investigate long-term energy storage, considers both buildings and personal transport demands, is applied to decentralised cases, and includes a through uncertainty and sensitivity analysis.

Chapter 3 built the framework of the P2X optimisation model. This section described the modelling of the building energy demands, building retrofits, the calculation of renewable potential (i.e., rooftop PV, small wind turbines, and small hydro), and the development of the optimisation framework. The optimisation framework includes the energy carriers, the conversion technologies (i.e., their part-load operation, minimum operating conditions, and start-up and shut-down behaviour), storage systems, direct injection into the natural gas grid, and the losses associated with district heating and electricity grids. The multi-objective optimisation using the epsilon-constraint method was described, including the calculations of the levelised cost of energy and emissions for the decentralised MES, which are used for comparison of systems of different sizes. Lastly, the energy targets for the Swiss Energy Strategy are proposed to rank the Pareto solutions. It is noted that only operational CO_2 emissions were accounted for in this Chapter, but this work set the way for later work that would use a full life-cycle approach to calculating emissions.

In Chapter 3 and 4, only operational CO_2 was used for the calculation of emissions, however this calculation was expanded to include embodied emissions in Chapters 5-7. In addition, the personal transport sector of emissions is not considered in this first model, thus Power-to-Mobility is neglected in Chapters 3 and 4, but this first model setsthe basis for the Power-to-Mobility model developed in Chapter 5.

In Chapter 4, the optimisation model built in Chapter 3 was tested with two case studies: Zernez, a rural village, and Altstetten, an urban neighbourhood. The future potential of P2X is tested by running the model for the years of 2015, 2020, 2035, and 2050. To consider the uncertainty in predicting economic, environmental, and performance parameters in the future, different scenarios were developed based on the Intergovernmental Panel on Climate Change's Special Report on

Emissions Scenarios. Three future scenarios were developed based on the A1, the B1, and the B2 scenarios from the report that correlate to the *Conventional Markets, Global Sustainable Development, and Regional Sustainable Development* scenarios. The Conventional Markets scenarios is a business as usual case where fossil fuels only increase moderately in price and renewable energy technologies do not decrease significantly in cost or increase in efficiency. The Global Sustainable Development scenario is a case with a strong focus on renewable energy, but in a centralised context rather than promoting decentralised energy systems. Costs for fossil fuels increase more significantly than in the Conventional Markets scenario, however the feed-in tariff remains high to feed renewable energy back to the centralised grid. Lastly, the Regional Sustainable Development scenario is similar to Global Sustainable Development scenario, however the focus is on decentralised renewable energy rather than centralised renewable energy. The building energy demands were calculated for both Zernez and Altstetten in 2015, the retrofit model was then used to calculate the demand in 2020, 2035, and 2050, and the renewable potentials were calculated for both case studies including the effects climate change through use of future weather files based on the IPCC scenarios.

The optimisation was then conducted to create Pareto fronts with 5 points in each scenario and future year of analysis. The results indicated that the energy targets could be met in Zernez, but Altstetten missed its targets in each year of consideration, even when optimising for a complete minimisation of CO_2. In other words, it was determined that it was not technically feasible in Altstetten to meet the energy targets without importing renewable energy into the district. This was mostly attributed to the old building stock and very low renewable potential coming from the PV systems on rooftops. Due to the lack of renewable production and the low efficiency of the buildings, the best advice for this case study to lower their environmental footprint is to retrofit the buildings at a higher rate than 2%. It was determined that seasonal storage using Power-to-CHP was used in the Pareto solutions that required a significant reduction in emissions. This is also known as deep decarbonisation. In the Global Sustainable Development case, which was associated with high feed-in-tariffs, the seasonal storage was exploited to a lower extent due to the profitability of selling renewable production back to the grid compared to storing it onsite. One consistent conclusion for all years of analysis and scenarios was that

both PV, heat pumps, and thermal storage were used in nearly all cases evaluated.

The analysis of the results in this Chapter also determined that it was difficult to draw conclusions about the system from the scenario analysis. It was noticed that the feed-in tariff, renewable potential, and the building energy demands had a high effect on the size of storage systems installed, but it was difficult to quantify the impact of individual input parameters on the selection of the technologies in the system. To give a more comprehensive analysis of the output of the optimisation model, a full uncertainty and sensitivity analysis was performed in Chapter 7, to make up for the shortcomings in the scenario analysis.

In the CO_2 minimisation cases, the optimisation tended to oversize most technologies, as there was no penalty for excessive storage sizes with this objective. This can be rectified by including embodied emissions to use a life-cycle approach to calculating emissions. Embodied emissions for installed technologies are usually a hidden factor that is not considered in the operation of a system. However, material extraction, processing, manufacturing, and transportation are a significant source of emissions into the atmosphere and should not be neglected.

In Chapter 5, the optimisation model developed in Chapter 3 was expanded to include personal transport demand and charging for Alternative fuel vehicles (AFV) in the MES. This included the development of several sub-models to analyse the current vehicle stock in MESs and to predict vehicle driving demand, including driving cycles that are based on road types. A set of five vehicle technologies are defined: a gasoline Internal Combustion Engine Vehicle (ICEV), a compressed natural gas Internal Combustion Engine Vehicle (ICEV), a Plug-in Hybrid Electric Vehicle (PHEV), a Battery Electric Vehicle (BEV), and a Fuel Cell Electric Vehicle (FCEV). The efficiencies for these technologies are then calculated in three driving cycles defined by the Worldwide Harmonised Light Vehicle Test Procedure (WLTP). In addition, a random forest car ownership sub-model was developed to predict the number of vehicles owned by occupants in the Zuchwil case study. Developments in the optimisation model were then made to select the vehicle types, model the onboard storage systems and driving cycles, incorporate charging stations and vehicle charging into the buildings and district, bi-directional vehicle charging, and to manage public charging stations. The multi-objective functions were then re-defined to include vehicle costs and emissions, and to include the embodied emissions of all tech-

nologies into the optimisation model. Lastly, a new set of energy targets were defined. The chosen energy targets are based on the 2000 Watt society concept applied in SIA 2040 (SIA 2011): a standard that includes embodied emissions and mobility demands in addition to operational building emissions.

The optimisation model built in Chapter 5 is then tested with the Zuchwil case study for the years of 2015, 2035, and 2050 in Chapter 6. The process first includes calculating the building energy demand and the retrofitted demands for 2035 and 2050. To compare results to the SIA 2040 targets (SIA 2011), mobility emissions from other sources (e.g., S-bahn, tram, biking, busses, and motorbikes) are calculated separately, as they are not considered in the optimisation model. To do this, the public transit emissions for each of the residents in the case study were quantified including embodied emissions. Secondly, the retrofit material emissions are also quantified. The optimisation results for the vehicle selection showed a strong preference towards ICEV-cng and ICEV-g vehicles in 2015 cost optimal cases, but this was shifted quickly to a preference for BEVs by 2035. It is also noted that BEV200 vehicles were preferred strongly over BEV300 and BEV500 vehicles due to their lower cost and embodied emissions. FCEVs were not used in any year or Pareto point. It was noted that the lowest range vehicles preferred to remain with ICEV-g vehicles due to the lower embodied emissions while ICEV-cng vehicles were preferred for higher driving demands. In terms of conversion technology selection, little was changed when compared to the results of Chapter 4. It was still found that gas boilers are phased out for heat pumps over the years, that PV is always installed to the maximum available capacity, and that a Power-to-CHP system was installed for long-term storage when deep decarbonisation is required. It was noticed that higher battery capacities are installed in more Pareto optimal solutions than before, most likely to provide grid balancing now that electricity demands are higher with BEVs charging at home. The self-sufficiency ratio was predicted to be as high as 80% with only PV produced on the rooftops, although it would be very expensive to reach levels higher than 70%.

The aim of Chapter 7 was to perform both an Uncertainty and Sensitivity analysis on the model built in Chapter 5 and case study tested in Chapter 6. For the UA, a Monte Carlo analysis using Latin Hypercube Sampling was chosen. To sample uncertain input parameters, uncertainty characterisation was performed on 63 input parameters. These

uncertain parameters include building energy demand, vehicle driving demand, solar radiation, the costs of energy carriers, the carbon factors of energy carriers, the technology investment costs, the embodied emissions of technologies, and the efficiencies of the technologies. With the probability distribution functions for each input defined, a MC analysis was performed for 500 Pareto fronts composed of 5 Pareto points each. These curves were compared to the deterministic Pareto fronts for 2015, 2035, and 2050 which were presented in Chapter 6. It was shown that the deterministic assumptions included in 2015 were too pessimistic and the assumptions in 2035 and 2050 were overly optimistic when trying to predict the cost and emissions. In addition, the range of solutions showed that the uncertainty in predicting the CO_2 emissions was very high in estimating the cost minimal solutions in the future.

For each LHS input sample set, the point on the Pareto front with emissions less than 476 kg CO_2/person was solved for. The solutions were grouped by Power-to-X pathways that were used in the optimal cases. Here, it was found that:

1. 100% of MC cases used BEV200 with the average utilisation being 77% of the vehicle stock. The second most popular powertrain was PHEV, followed by ICEV-cng, and then by ICEV-g vehicles. FCEVs were the least popular and were used in only 2% of cases.

2. Power-to-Methane was used in 5.6% of cases to supply SNG for ICEV-cng charging and methane for gas boilers. This methane was never sold and injected into the centralised grid. All produced SNG was used on-site.

3. BEV300 and 500 vehicles were rarely used in comparison to BEV200 vehicles due to their higher embodied emissions and costs. Since there were no constraints for frequent recharging, it was preferred to simply recharge the vehicles with smaller batteries more frequently. This may be unrealistic; as frequent recharging can be a large inconvenience for consumers. Nevertheless, it is clear that the embodied emissions of higher range vehicle batteries play a significant role in the overall emissions and it should be noted that bigger batteries usually result in higher emissions.

4. 100% of MC cases used Power-to-Heat (heat pumps + thermal storage)

5. 84% of the cases used batteries

6. 19.2% of the cases used Power-to-CHP

From these results, much can be understood about the different pathways. Power-to-Heat and Power-to-Mobility with battery vehicles were both strongly advocated by the papers reviewed in Section 2.5 and 2.4, and this work reiterates their claims. Power-to-Heat in particular was used to its maximum potential in Zernez, Altstetten, and in Zuchwil. FCEVs, on the other hand, were advocated very strongly by many researchers (see Dodds and McDowall (2014), Shafiei et al. (2015), or X. Zhang et al. (2015)). In the personal transport context modelled in this work, FCEVs are simply unable to compete with the efficiency, lower costs, and lower embodied emissions of BEVs. The fast charging capabilities and the longer ranges were not found to be critical factors in this work. These 2% of cases which chose FCEVs were the cases where the embodied emissions of BEVs were higher than normal and where the embodied emissions of FCEVs were lower than normal. Since the fast charging times and longer ranges were not determined to be critical for personal transport demands, different transportation sectors, such as shipping of goods via trucks, can be looked at. Long-haul trucks generally cover much longer distances and require quick charging times to be continually on the move, therefore this sector may be a better fit for FCEVs. This is already being investigated in Switzerland in collaboration with H2 Energy and Hyundai Motors (Pauchard 2019).

To identify the driving input parameters that determine the optimality of different pathways, regional sensitivity analysis using Monte Carlo Filtering was used in Section 7.4. Using Monte Carlo Filtering, the subset of solutions with an epsilon-constraint under 476 kg CO_2 were filtered into subsets that used particular pathways and subsets of the results that did not. It is to be noted that the results of the Monte Carlo Filtering analysis are specific to those solutions that meet this emissions target. Selection of another point along the Pareto curve is ultimately a different objective and would result in different findings.

The particular pathways investigated with Monte Carlo Filtering include Power-to-CHP, Power-to-Methane, and Power-to-Mobility with FCEVs. It was found that the most important uncertainties influencing the use of Power-to-CHP are the CO_2 intensity in the electricity grid, the embodied emissions of BEV200 vehicles, solar radiation, heat pump efficiency, and PV efficiency. The most important uncertainties

influencing the optimality of Power-to-Methane are the costs of BEV200 vehicles, the costs of PHEV50 vehicles, the costs of ICEV-cng vehicles, gasoline costs, and methanation costs. The use of Power-to-Methane was only determined to be feasible if ICEV-cngs are also used, therefore the vehicles completing with ICEV-cngs must have higher than normal costs in comparison to ICEV-cngs for P2M to be used. Lastly, FCEVs are selected when their own embodied emissions are low, the BEV embodied emissions are high, mobility demand is high, FCEV costs are low, and embodied emissions of the electrolysers are low.

In addition, solutions were also filtered by those where the costs were lower than 2500 CHF/person/year and solutions where the costs are over this level. It was found that the most significant parameters are the low cost of BEV vehicles, high feed-in tariffs, a low CO_2 intensity in the electricity grid, high PV efficiency, and high solar radiation. This point echos the importance of reducing the costs of BEVs, as they are shown to comprise the majority of the vehicle stock. The high feed-in tariffs would obviously benefit to lower costs, as energy can be sold for a profit rather than curtailed or stored onsite. The PV efficiency and solar radiation are both related to increasing the renewable energy potential in the community.

The UA analysis in this work was found to be significantly more informative in approach for analysing the uncertainty of the model compared to the scenario analysis that was performed in the Future Scenarios analysis in Chapter 4. The scenario analysis was initially performed as a method of dealing with the uncertainty of future parameters for a model that was considered too complicated to perform a UA. In retrospect, the scenario analysis required a significant amount of work to construct the scenario narratives and to set the parameters appropriately. The results of the future scenario analysis only showed three different system options and could not speak to the likelihood of these outcomes of the model or the drivers that lead to the different solutions. Scenario analysis is widely used in both the research community and in climate and energy reports that are done by organisations like the International Energy Agency or the Intergovernmental Panel on Climate change. In reality, a scenario analysis can show only a small window of the decision space, thus making it difficult for well informed decisions to be made.

Local sensitivity analysis is usually performed over global sensitivity analysis because of the computational time required to perform a full

global sensitivity analysis. This work was successful in performing a regional sensitivity analysis on the optimisation model, which allowed for direct identification of the most important input parameters and the ranges of these input parameters in which certain pathways are optimal. Few researchers who focus on the field of P2X analyse uncertainty with a more detailed approach than a local sensitivity analysis. However, the costs and uncertainties for P2X technologies are more uncertain than for other technologies, since most are in their early stages of commercialisation and are not yet widely deployed. If they are widely deployed between 2020 and 2050, their costs could rapidly drop, but it is not yet known to what extend hydrogen technology will be adopted. If costs for these technologies begin to reduce, we can use sensitivity analyses as guidelines to direct our decision making.

Lastly, the consideration of embodied emissions was an extremely important part of the analysis. Embodied emissions are not usually considered in the calculation of emissions of multi-energy systems. However, embodied emissions play a significant role in our energy systems, whether we realise it or not. There is significant criticism recently on the toxic byproducts of PV (Shellenberger 2018) and Li-ion battery (Eckart 2017) production and manufacturing, especially since their production has scaled up massively with increasing demand. Both of these technologies have large embodied emissions, therefore it is of importance that they are only being installed in settings where they will actually help to lower the CO_2 emissions and offset their own embodied emissions. Although these embodied emissions are predicted to decrease in the future, it will be very difficult to eliminate them. Nevertheless, lowering the embodied emissions should be encouraged by integration of renewable energy into the industrial energy supply chain. Large scale manufacturing problems could also occur with fuel cells and electrolysers if their production was scaled up rapidly. Both PEMFCs and PEMEs require platinum catalysts, although significant research is being done to reduce the amount required or to replace it due to its high costs. In this work, deep decarbonisation strategies often require very large capacities of storages for a very small reduction in emissions. These large capacities were often offset when embodied emissions of the systems were considered.

In Chapter 6 and 7, it was found that vehicle embodied emissions were the largest source of emissions in the solutions that met the targets. Replacing our vehicle stock will require a massive amount of material

and energy to produce. Our current vehicle stock should not transition too quickly, as it is of importance that all of our vehicles meet or exceed their current lifetimes to reduce embodied emissions related to vehicle manufacturing. This is especially true for countries where the life-cycle CO_2 intensity of grid electricity is very high. The development for energy and emissions targets with embodied energy and emissions already exists, but few researchers or policy makers are using these energy targets as they are much harder to meet than those that only consider operational emissions. In the vehicle sector, many look at "well-to-wheel" emissions, but these do not consider the embodied emissions of the vehicles themselves. In the building sector, few people look at the embodied energy in building materials, concrete, boilers, heat pumps, and other technologies. They are primarily concerned with the total annual operational energy demand. With the large amount of information available in life-cycle analyses, we should be able to extract these embodied emissions and take our own life-cycle approaches to our system analyses.

8.2   CONTRIBUTIONS TO THE FIELD

The main contributions to the scientific field can be detailed on a per Chapter basis as follows:

CHAPTER 2: POWER-TO-X IN MULTI-ENERGY SYSTEMS: STATE OF THE ART

- Review of the state of the art in commercially available technologies in electrolysis, fuel cells, and methanation.

- Comprehensive review of papers considering the modelling of Power-to-Hydrogen, Power-to-Methane, Power-to-Mobility, Power-to-Heat, and papers comparing different P2X and storage systems.

CHAPTER 3: MES OPTIMISATION WITH P2X TECHNOLOGY PATHWAYS

- A MES optimisation framework has been developed that is capable of analysing P2X pathways using both short-term and long-

term storage systems. Relevant technologies such as electrolysers, fuel cells, methanation, hydrogen storage, and natural gas storage have been included in this framework with guidelines.

- Establishment of the calculation of levelised cost of energy and CO_2 for decentralised energy system so that the economics and emissions of different decentralised systems can be compared.

Limitations: Mobility has not yet been implemented into the process and embodied emissions of the technologies have not yet been accounted for.

CHAPTER 4: FUTURE SCENARIOS IN P2X FOR TWO DECENTRALISED CASES

- Development of three scenarios from the IPCC's Special report on Emissions Scenarios to analyse the optimal design for MESs in two difference case studies from 2015-2050

- Demonstration of the use of P2X in two different municipal contexts and evaluation for meeting the energy targets.

CHAPTER 5: INCORPORATION OF MOBILITY IN THE OPTIMISATION

- Development of a random forest model to predict car ownership in Switzerland

- Optimisation model that can meet building energy demands and local personal transport demands in a single model, including vehicle selection and charging with several different energy carriers. Vehicles can also represent several different driving cycles.

CHAPTER 6: APPLICATION OF MES OPTIMISATION FOR POWER-TO-MOBILITY

- Application of the Power-to-Mobility optimisation model to a case study.

- Quantification of public transit embodied emissions and operational emissions is performed.

- An optimal profile of AFV diffusion recommendation for the years of 2035 and 2050 are presented.

- Application of set of emission targets for coupling building and mobility emissions.

CHAPTER 7: UNCERTAINTY AND SENSITIVITY ANALYSIS

- Uncertainty characterisation and analysis for P2X energy carrier costs and emissions as well as technology investment costs, embodied emissions, and efficiencies.

- Uncertainty analysis using latin hypercube sampling for evaluating uncertainty in the entire decision space for the model developed in Chapter 6.

- A sensitivity analysis methodology using Monte Carlo Filtering that can be used to assess regional sensitivities with fewer model runs than is required for variance based methods. This method allowed for the investigation of the most significant parameters for selecting certain P2X pathways.

8.3 CRITICAL REFLECTIONS

One major limitation in this work is the lack of consideration of the modelling of the electrical, heating, and natural gas grids. It was attempted several times in this work to incorporate the linearised power flow equations into the model the electricity grid (see B. Morvaj et al. (2016)), however the decision variables that are required for an optimal power flow optimisation were too complex in addition to the large number of variables that were already dedicated to P2X technologies. Power limits in the buildings and the district for imported and exported energy were set in the model, however the modelling of the active and reactive power in the grid was not considered. Considering the inclusion of BEVs, heat pumps, and electrolysers in the final model, modelling of the active and reactive power in the grid should be considered to see if the grid would require an upgrade to implement the

recommended system. If the grid requires an upgrade, it is possible that the costs for implementation are higher than is determined in this work. To include optimal power flow, the model in this work would have to be reduced to a very small case study (most likely under 10 buildings) or many of the technologies and their dynamic operating parameters would need to be removed.

A heating grid was assumed for the case studies in Chapter 4, however we were only able to linearly approximate the heat losses and electricity required for pumping based on the length of piping and the heat delivered. This is a very simplistic way of modelling a heating grid, however district heating modelling was not the focus of this work, therefore the heating grid was removed entirely in Chapter 6, and the heating technologies are installed directly in buildings.

Although a certain amount of hydrogen directly injected into the natural gas grid was considered, a detailed model of the gas flow and limitations was not considered due to the limited potential of direct injection. Since we were only considering decentralised cases, a 2-4% limitation by volume meant that direct injection was not a large energy sink. On the centralised level, direct injection would be much more effective but it is not recommended for decentralised cases and thus a detailed method of modelling direct injection in the gas grid was not developed.

When considering hydrogen and methane storage, it was difficult to decide what the upper limit for storage sizes should be in this work. In reality, an upper limit on the space available for storage should be made by project developers familiar with the urban site. The optimisation can then have a constraint for the upper limit of area available for storage systems. This was not set in this work due to lack of information, however the very large hydrogen storage systems shown in the CO_2 minimisation cases are modelling extreme cases of deep decarbonisation and are not recommended for implementation.

In the context of mobility, one significant limitation is the assumption that the number of vehicles owned by occupants will not change over time. It is predicted that the number vehicles owned by people may reduce in the future and will be replaced with car sharing services such as Mobility or by ride sharing services such as Uber. Although the case study of Zuchwil, which was used for the mobility case, does not currently have Uber services, this will likely change in the future. The driving behaviour of users, which is the basis of our mobility demand

predictions taken from 2015 census data, is likely to change in the future but these changes have not been considered in this work. It is predicted by Raubel et al. (2017) that vehicle kilometres are predicted to increase in the future as much as 10% relative to 2017, but it is not known how this should be integrated into the driving profiles (i.e., whether this increase represents more vehicle trips or simply longer trips in general). Due to lack of information, this increase was not considered in this work.

Charging in the workplace was also an element of the mobility optimisation that was not included in this work. This element can be included in the optimisation without a large amount of difficulty if three pieces of information are known. Firstly, the availability of charging stations at each person's workplace must be known. Secondly, the price of charging at the workplace must be known. Thirdly, the life-cycle value of the CO_2 emissions at each workplace must be known, although the grid CO_2 intensity value can be assumed if this data is not known.

Another limitation of this work is that only mid-sized C-segment vehicles were considered for the vehicle stock. In reality, the vehicles should represent other classes of vehicles (e.g., luxury, multi-purpose vehicles, small, large, etc.). In future work, the model should be modified to include all major vehicle classes for to the stock and the efficiencies of each class of vehicle, each powertrain, and each driving cycle should be included. It is highly likely that vehicles in different classes will have different preferences for AFVs. This was not included in this work due to the extra decision variables that it would require in the optimisation and also due to lack of information regarding the ownership of different vehicle classes, but it would not take a large amount of effort to extend the optimisation model of Chapter 5 to include these different vehicle classes. The most difficult part of this assumption will be to predict the change in ownership in different vehicle classes in the future.

Due to the computational intensity of the optimisation model in Chapter 5, the uncertainty and sensitivity analysis in Chapter 7 was only applied to the Zuchwil case study. A comprehensive analysis would also include the Zernez and the Altstetten cases to draw conclusions about different municipalities. Nevertheless, the results of MES optimisations will always be specific to the case study used to a certain extent, but by trying to apply the model to typical districts in Switzerland, we attempted to draw comprehensive conclusions about rural, urban, and suburban cases, but were only able to do so for the

suburban case. Including Power-to-Mobility in the last two case studies would be helpful to identify which municipal contexts are best suited for decentralised MESs and which case studies should remain reliant on the centralised grids. From the results of Chapter 4, we have predicted that the rural cases are much more attractive for decentralised MESs and that urban cases are less attractive, however these conclusions should be re-evaluated with personal transport included.

Lastly, this work assumed constant annual values for the CO_2 intensity of the electricity grid and the electricity price in the grid. In reality, these values are time resolved. The CO_2 intensity in the grid changes hourly depending on which sources of generation are producing in the hour and how much trade in between different countries is ongoing in each hour. This data is available for the present day, but it is difficult to predict the hourly trade between nations in the future, especially if renewable generation technologies are widely deployed between now and 2050. If these time resolved values could be predicted in a reliable way, they should be included. The night time intensity of CO_2 is usually much higher than in the daytime, which would act as an incentive to either charge vehicles in the daytime at home or at work. The optimisation results currently assume a significant amount of charging at night, which could be more CO_2 intensive than is assumed in this work if the time-resolved values were accounted for.

8.4 DIRECTIONS FOR FUTURE RESEARCH

In the field of urban energy systems, P2X technology currently plays a small role. It is typically the aspects of Power-to-Chemicals, Power-to-Mobility, and Power-to-Gas for centralised applications on the national scale that receive the most attention in this field. This is mostly due to the current expense of the hydrogen technologies, but if the costs of the technologies are strongly reduced, P2X can also play a valuable role in decentralised cases. In fact, Power-to-Heat and Power-to-Mobility with BEVs were determined to be some of the most cost effective and robust solutions for meeting the energy targets in case studies analysed in this work. Other pathways, such as Power-to-Hydrogen, Power-to-CHP, and Power-to-Methane could also be beneficial for communities that have high electricity and fossil fuel costs, high renewable potential, and are relatively isolated.

Three of the major outcomes of this thesis are the strong support for heat pumps, PV, and BEVs. As was mentioned in Chapter 8.3, the installation of all of these technologies simultaneously could put severe stress on the electricity grid. This stress was not evaluated in this work, but there are other researchers that are conducting this work (see Boran Morvaj et al. (2016)). The cost of upgrading the grid to accommodate increased electrification should be a second step that is added onto this analysis. It could be that FCEVs and ICEV-cngs are more attractive than is portrayed in this work due to the fact that they have less of an impact on the centralised electricity grid than EVs, especially with a high concentration of EVs charging in a small vicinity.

Another improvement that can be made is to implement an optimisation approach where decision making for the system is made at different time intervals (i.e., every 5 years as is done in the MARKAL/TIMES model (Dodds and McDowall 2014)). In this thesis, the consideration of sunken assets from previous decision periods are not considered. In reality, people who just purchased a new ICEV-g will be unlikely to turnover and buy a BEV right away. The same is true for new gas boilers that may be recently installed. In addition, system improvements may be built and installed over decades, therefore assuming the purchase of all the equipment at once is also unrealistic.

The major problem with models that have several decision making periods over decades is that they usually overly simplify the operation of the technologies. This is because the larger number of decision periods mean that many years must be modelled, thus few representative days per year are included so that decades of operation can be considered. When using so few representative days a year, it becomes impossible to properly consider the design and impact of long-term storage systems. These models also rarely include uncertainty analysis in the costs and emissions over time and usually opt for a scenario based approach to modelling the future (see Yazdanie et al. (2017)). Strategies for considering multiple decision making intervals and optimising over several years, but with a more detailed consideration of each year's operation, can be further developed to consider the best of both model types.

Lastly, the change in mobility demand in the future is also something that should be considered. This change refers not only to the increase in vehicle kilometres driven, but also behavioural changes in the types of transport used. This includes people who might switch from owning vehicles to opting for only mobility sharing services or ride sharing.

People may also switch to public transit or e-bikes in the future. This also may include in people switching to owning to larger or smaller vehicle classes in the future. These predictions will not be based on the optimal solution, but rather on user driven behaviour and preferences which are inherently difficult to predict. Behavioural changes, such as transport mode switching (Daly et al. 2012), can be further investigated for application in our models, but it will be difficult to validate these models without investigating real consumer behaviour. In this work, transport modelling was avoided by using census data, however transport demand models such as MatSIM (Horni et al. 2016) are being developed with agent based modelling techniques to try and predict transport behaviour including mode switching in the future, as is done in Erath et al. (2012). The downside of this method is that large amounts of data on many users is required. It is also possible that machine learning meta-models would be a particularly attractive application for these large vehicle demand models to reduce the cost of computation.

8.5 RELEVANCE FOR SOCIETY AND THE ENVIRONMENT

One of the major conclusions of this thesis is the prediction that we can meet the majority of our emissions reductions with technologies that are already commercially available and are becoming cost effective. There are a few simple solutions that are strongly advocated from the results of this work. These are listed as follows:

1. Gas boilers should be replaced with heat pumps and larger thermal storages.

2. Rooftop PV should be deployed on all eligible south facing rooftop surfaces.

3. Old buildings should be retrofitted at higher rates, especially in urban areas.

4. Most of the vehicle stock for personal transport should be replaced with battery electric vehicles but only after the current vehicle stock reaches their end of life. This especially includes vehicles that drive mostly in urban conditions.

5. Shared batteries should be deployed in neighbourhoods with high amounts of PV on rooftops.

These solutions are shown to be both low emissions and cost effective in the majority of cases that meet the emissions targets. Since there is strong indication that these solutions should be deployed universally, policy makers should implement extra subsidies for these technologies to motivate people to adopt them sooner.

The solutions listed above may go a long way towards meeting our emissions targets, however they alone will not be able reach deep decarbonisation targets. There has been a recent trend in literature for researchers to advocate for the feasibility and design of 100% renewable energy systems. In these papers, P2X, and hydrogen for long-term storage in particular, is a popular technology. Since 2004, there have been over 180 articles published that look exclusively into designing 100% renewable energy systems for all sectors (Hansen et al. 2019). Due to the flexible nature of renewables, this goal is under debate for whether it is a reasonable target to set, or whether it is even feasible. The 2015 study by Jacobson et al. (2015) proposed a 100% renewable energy system for the entire United States. This paper drew a large amount of attention in the public media with the claim that it would be possible to go to 100% renewable energy in the entire United States by 2050, but the paper also drew a large amount of criticism (see Clack et al. (2017)) from other researchers regarding the assumptions and modelling methods used. One of these criticisms is that the original paper assumes a 100,000% expansion in hydrogen energy as long-term storage, which is likely both infeasible and extremely expensive. Despite the academic criticism on these 100% renewable energy papers, the concept of 100% renewable energy has been adopted by the media, companies, and politicians alike, many of who are now advocating strongly for extending national energy targets to 100% renewable energy. So far, 9 cities and hundreds of companies globally have advocated for 100% renewable energy targets (Hansen et al. 2019). In the United States, proponents of the Green New Deal are recently advocating for 100% renewable energy by 2035. The UK government has already advocated to put a 100% net zero emissions law into government. The politicians that advocate for these targets operate under the incorrect assumption that it will be as easy to go from 80% to 100% renewable energy as it is to go from 60% to 80% renewable energy. Unless there is a large amount

of hydropower available, it is very difficult to reach 100% renewable energy. In this thesis, it was observed that the difference between achieving 90% emissions reductions and 95% emissions reductions often causes the costs of the entire system to double. Although these results are specific to decentralised systems, the same will likely be true of the whole energy system. When looking at the costs of Power-to-Hydrogen and other Power-to-X pathways in these 100% renewable energy systems, one may argue that seasonal or long-term storage systems are not worth the expense. In this case, I would argue that the *'perfect is the enemy of the good'*. This is to say that in pursuit of 100% renewable energy, we may begin to undermine or disregard solutions that are economically attractive and may get us the majority of the way to our goal to pursue something that is not feasible, affordable, or realistic.

The neglect of considering embodied emissions and energy in these targets is also a massive fault of this research and the policy makers that advocate for net zero emissions or 100% renewable energy targets. Targets that advocate for net zero emissions or 100% renewable energy do not include embodied energy. Considering the massive amount of new renewable technology required to support 100% renewable energy systems, ignoring embodied emissions is a massive oversight. Many companies and plans simply advocate for carbon capture while neglecting to take a life-cycle approach to emissions. These energy targets are both misleading to the public and allow for suboptimal environmental decisions to be made by not looking at the whole picture. Researchers in this field should be held responsible for overly optimistic claims of 100% renewable energy targets without properly assessing the life-cycle emissions and the total costs of such plans, as it is clear that misinformed policy tends to get developed based on overly optimistic research projections.

Nevertheless, it is clear from the research that has been performed in deep decarbonisation that P2X pathways are essential to maximise the utilisation of renewable energy in our systems. Still, not all P2X pathways are equal. This thesis has shown that most of the short-term storage pathways (i.e., batteries, Power-to-Heat, and Power-to-Mobility with BEVs) are a good idea in several urban contexts, while long-term storage pathways, such as Power-to-CHP or Power-to-Methane are usually not optimal unless deep decarbonisation targets are required. When they are used, they are best implemented when coupled with

short-term storage technologies and should only be implemented in systems with sufficient levels of renewable generation. In the future, when the costs for electrolysis, fuel cells, and methanation decrease, system designers should take an unbiased approach to investigating which pathways are best suited for their system demands and renewable potentials. The level of deployment of these pathways will be highly dependent on how much decentralised renewable generation we are able to implement and how many consumers will switch to alternative fuel vehicles between now and 2050. Implementation of a carbon tax is a necessary policy push to incentivise the switch to AFVs and motivate to deployment of more rooftop PV systems, but it is likely that further subsidies will be required to speed up these processes. Only when these changes are made will these decentralised long-term P2X systems be optimal.

A

CASE STUDY BUILDING DETAILS

A.1 CONSTRUCTION AGE

The construction year of the buildings in Zernez (308 buildings), Altstetten (77 buildings), and Zuchwil (52 buildings), that are described in Section 1.7.2, are shown in Fig. A.1. These construction years assign the building constructions in EnergyPlus that are further described in Appendix B. This data is provided by the municipality of Zernez and the Building and Apartment Registry (Bundesamt für Statistik 2012).
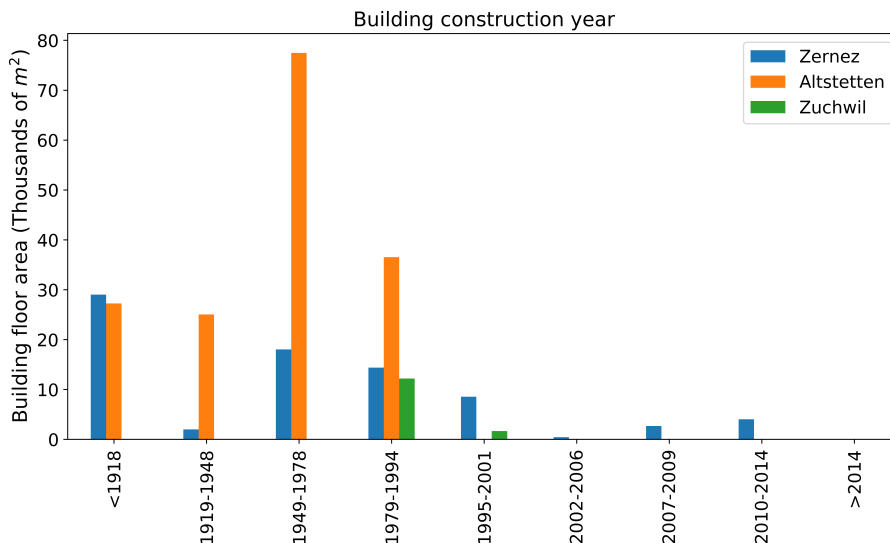
Figure A.1.: Total building floor area in each case study according to the range of construction years.

Here, we can see that the Zernez case study has a large amount of building floor area built before 1918 and also between 1949-2001. There are also some buildings that have been built since 2007, but these comprise a small fraction of the total floor area. In Altstetten, the building stock is all built before 1994, with a large portion before 1978.

This building stock is quite outdated at present and the total floor area is much higher than the other case studies, despite a lower number of buildings than Zernez. This is due to larger buildings with more floors. Lastly, Zuchwil is the smallest case study with all buildings being built after 1979. This represents the newest building stock.

The building types in the model are also shown for each case study according to total floor area in Fig. A.2.
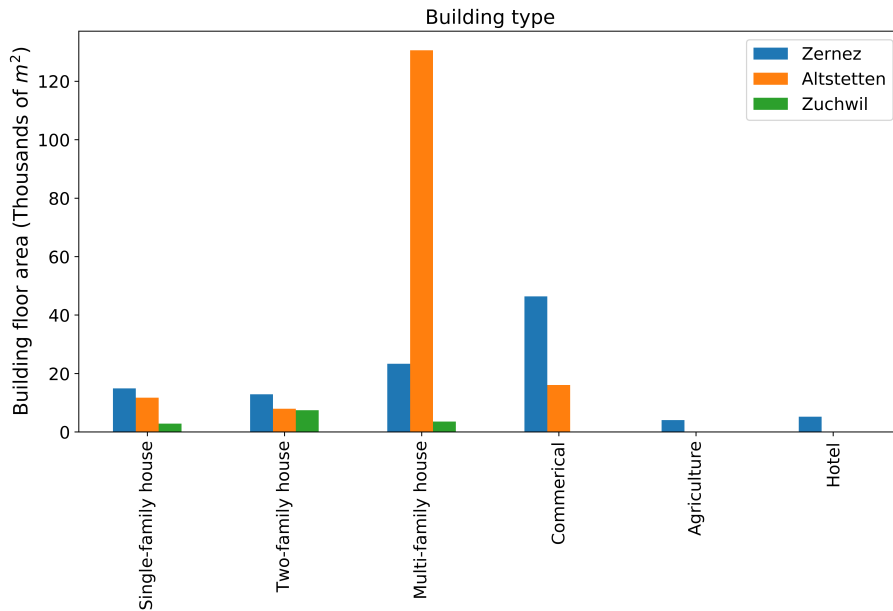
Figure A.2.: Total building floor area in each case study according to the building types.

In Zernez, there is a greater diversity of building types than in the other two case studies. These include an even fraction of single-family, two-family, and multi-family houses. There are commercial buildings, agriculture buildings, and hotels. This gives an even mix of both residential and commercial buildings. Altstetten is composed mostly of residential buildings, especially multi-family homes. There is also a significant fraction of commercial buildings. Lastly, Zuchwil is composed of mostly attached two-family homes with smaller fractions of both single and multi-family houses. There are no non-residential buildings in this district.

RETROFIT COSTS AND EMBODIED EMISSIONS

In Table B.1, the U-value of the building materials assigned in the building stock model from Section 3.2.1 are shown.

Table B.1.: U-value (W/m2-K) assigned to EnergyPlus buildings depending on construction period.

		Construction Period								
		$\leq$ 1918	1919-1948	1949-1978	1979-1994	1995-2001	2002-2006	2007-2009	2010-2014	$>$ 2014
Walls	Min	1.202	0.814	0.814	0.456	0.261	0.209	0.189	0.153	0.113
	Max	1.912	3.060	1.710	0.814	0.352	0.237	0.210	0.183	0.153
	Nom	1.592	1.592	1.371	0.490	0.318	0.222	0.202	0.160	0.137
Roofs	Min	0.734	0.727	0.513	0.325	0.287	0.220	0.188	0.151	0.117
	Max	1.243	1.237	1.629	0.546	0.301	0.243	0.204	0.184	0.139
	Nom	0.847	0.947	0.880	0.387	0.301	0.243	0.204	0.184	0.139
Floor	Min	0.711	0.578	0.578	0.661	0.283	0.267	0.246	0.181	0.128
	Max	0.839	1.163	1.163	1.098	0.325	0.283	0.248	0.227	0.174
	Nom	0.839	0.821	0.821	1.098	0.325	0.283	0.248	0.227	0.153
Windows	Min	5.660	5.660	2.549	1.272	1.237	1.199	1.062	0.929	0.788
	Max	5.660	5.660	3.134	2.455	1.660	1.412	1.176	1.176	1.143
	Nom	5.660	5.660	2.797	1.677	1.367	1.237	1.176	1.176	1.143

In order to calculate the retrofit costs and embodied emissions that are included in the assessment in Section 6.2, the embodied energy and materials for different insulation materials for different costs are required. These insulations are assigned in order to specify the mini-

mum U-value in SIA 380/1, thus older buildings often require thicker insulation and thus are more expensive per m^2. The minimum required U-value for the targets listed in SIA 380/1 are 0.20 W/m2-K for roofs, facades, floors or basements, and 1.2 W/m2-K for windows. In the model, the insulation is chosen to be Rockwool, and the thickness and embodied emissions per centimetre of thickness are assigned. These costs and emissions can be found in Table B.2. Please note that to calculate the *CRF* (Eq. (5.30)) costs and emissions on an annual basis, the lifetime of the materials is required. This lifetime is assumed to be 40 years (Jakob et al. 2014).

Table B.2.: Retrofit costs and embodied emissions by retrofit component. Please note that the insulation thickness refers to the total amount of insulation added for the retrofit rather than the total insulation, which may include insulation from the previous construction. Costs are taken from Jakob et al. (2014) and embodied emissions are taken from Ecoinvent (Wernet et al. 2016).

Construction age	Retrofit Component	Insulation	Costs (CHF/m^2)	Embodied Emissions (kg CO2 - eq/m^2)
≤ 1918	Facade	14 cm	290	15.5
	Roof	12 cm	150	13.6
	Basement	12 cm	100	8.80
1919 - 1948	Facade	12 cm	270	15.5
	Roof	10 cm	150	14.6
	Basement	10 cm	100	8.80
1949-1978	Facade	12 cm	270	15.5
	Roof	10 cm	150	39.9
	Basement	10 cm	100	8.80
1979-1994	Facade	10 cm	240	13.3
	Roof	10 cm	134	35.5
	Basement	8 cm	90	7.91
1995-2001	Facade	9 cm	220	7.92
	Roof	8 cm	123	31.2
	Basement	9 cm	27	2.26
2002-2006	Facade	6 cm	226	9.05
	Roof	6 cm	134	35.6
	Basement	6 cm	53	9.04
>2007	Facade	10 cm	223	26.4
	Roof	5 cm	150	32.4
	Basement	10 cm	53	6.78
All ages	Windows	1.143 W/m2-K	850	32.2

C

FUTURE SCENARIO (CHAPTER 4) INPUT PARAMETERS

The parameters used in the optimisation in Chapter 4 are listed in this section with references. Table C.1 lists the economic and market parameters, Table C.2 lists the renewable technology costs, Table C.3 lists the heating technology costs, Table C.4 lists the hydrogen technology costs, and Table C.5 lists the technology efficiencies.

Table C.1.: Economic and market parameters used for the scenarios (CM, GSD, and RSD) in Chapter 4.

Parameter	Scenario	2015	2020	2035	2050
Electricity price (CHF/kWh)	CM	0.198	0.206	0.235	0.231
	GSD	0.198	0.212	0.251	0.262
	RSD	0.198	0.212	0.251	0.262
	Source	WBF 2015	Prognos AG 2013	Prognos AG 2013	Prognos AG 2013
Natural gas price (CHF/kWh)	CM	0.067	0.037	0.052	0.061
	GSD	0.067	0.095	0.129	0.148
	RSD	0.067	0.193	0.270	0.305
	Source	WBF 2015	Prognos AG 2013	Prognos AG 2013	Prognos AG 2013
Feed-in Tariff (CHF/kWh)	CM	0.176	0.087	0.00	0.00
	GSD	0.176	0.176	0.176	0.176
	RSD	0.176	0.087	0.00	0.00
	Source	SwissGrid 2015	SwissGrid 2015	SwissGrid 2015	SwissGrid 2015
Grid CO_2 (kg CO2-eq /kWh)	CM	0.124	0.150	0.150	0.150
	GSD	0.124	0.100	0.100	0.072
	RSD	0.124	0.100	0.100	0.072
	Source	Itten et al. 2014	Itten et al. 2014	Itten et al. 2014	Itten et al. 2014
Discount rate (%)	CM	6.0	6.0	6.0	6.0
	GSD	6.0	6.0	6.0	6.0
	RSD	6.0	6.0	6.0	6.0
	Source	Sixth Northwest Power 2010	Sixth Northwest Power 2010	Sixth Northwest Power 2010	Sixth Northwest Power 2010

Table C.2.: Setting of parameters for the renewable technologies' investment costs, O&M costs, and efficiencies for the CM, GSD, and RSD scenarios.

Scenario	Year	Solar PV			Small-Hydro			Small-Wind	
		Capital (CHF /kW)	OMV (rp. /kWh)	Eff. (%)	Capital (CHF /kW)	OMF (% Cap.)	Eff. (%)	Capital (CHF /kW)	OMV (rp./ kWh)
Baseline	2015	2669	34	17	3478	3%	80	9645	14
	Source	Jakob et al. 2014	DEA 2016	Lang et al. 2015	IEA 2010	IEA 2010	Paish 2002	DEA 2016	Aventa 2018
CM	2020	2660	34	17	3478	3%	80	9645	14
	2035	2660	34	17	3478	3%	80	9645	14
	2050	2660	34	17	3478	3%	80	9645	14
	Source	Jakob et al. 2014	DEA 2016	Lang et al. 2015	IEA 2010	IEA 2010	Paish 2002	DEA 2016	Aventa 2018
GSD	2020	1285	25	17	3478	3%	80	9163	14
	2035	1087	19	17	3478	3%	80	8681	13
	2050	989	13	17	3478	3%	80	8198	12
	Source	DEA 2016	DEA 2016	Lang et al. 2015	IEA 2010	IEA 2010	Paish 2002	DEA 2016	Aventa 2018
RSD	2020	1285	25	17	3478	3%	80	9163	14
	2035	1087	19	17	3478	3%	80	8681	13
	2050	989	13	17	3478	3%	80	8198	12
	Source	DEA 2016	DEA 2016	Lang et al. 2015	IEA 2010	IEA 2010	Paish 2002	DEA 2016	Aventa 2018

Table C.3.: Setting of parameters for the heating technologies' investment costs, O&M costs, and efficiencies for the CM, GSD, and RSD scenarios.

Sce-nario	Year	Heat Pump			Gas boiler			MGT		
		Cap-ital (CHF /kW)	OMF (CHF /kW)	COP	Cap-ital (CHF /kW)	OMF (CHF /kW)	Eff. (%)	Cap-ital (CHF /kW)	OMV (rp./ kWh)	Eff. (%)
Base-line	2015	1977	5.4	3.2	260	3.7	85	900	13	25
	Source	Jakob et al. 2014	DEA 2016	San-ner 2003	Jakob et al. 2014	Jakob et al. 2014	DEA 2016	Nasci-mento et al. 2013	Nasci-mento et al. 2013	Nasci-mento et al. 2013
CM	2020	1977	5.4	3.2	260	3.7	85	750	13	28
	2035	1977	5.4	3.2	260	3.7	85	620	13	30
	2050	1977	5.4	3.2	260	3.7	85	500	13	32
	Source	Jakob et al. 2014	DEA 2016	San-ner 2003	Jakob et al. 2014	Jakob et al. 2014	DEA 2016	Nasci-mento et al. 2013	Nasci-mento et al. 2013	Nasci-mento et al. 2013
GSD	2020	1600	4.4	3.2	260	3.7	85	750	13	28
	2035	1500	4.1	3.2	260	3.7	85	620	13	30
	2050	1400	3.9	3.2	260	3.7	85	500	13	32
	Source	Jakob et al. 2014	DEA 2016	San-ner 2003	Jakob et al. 2014	Jakob et al. 2014	DEA 2016	Nasci-mento et al. 2013	Nasci-mento et al. 2013	Nasci-mento et al. 2013
RSD	2020	1600	4.4	3.2	260	3.7	85	750	13	28
	2035	1500	4.1	3.2	260	3.7	85	620	13	30
	2050	1400	3.9	3.2	260	3.7	85	500	13	32
	Source	Jakob et al. 2014	DEA 2016	San-ner 2003	Jakob et al. 2014	Jakob et al. 2014	DEA 2016	Nasci-mento et al. 2013	Nasci-mento et al. 2013	Nasci-mento et al. 2013

Table C.4.: The setting of parameters for hydrogen conversion technologies for the CM, GSD, and RSD scenarios.

| Scenario | Year | PEMFC | | | | PEME | | |
		Capital (CHF/kW)	OMV (CHF/kWh)	Elec. Eff. (%)	Thermal Eff. (%)	Capital (CHF/kW)	OMV (CHF/kWh)	Eff. (kWh/m^3)
Baseline	2015	6252	0.025	50	48	2650	0.025	6.0
	Source	Körner et al. 2015	Amos 1998	C. Wang et al. 2005	C. Wang et al. 2005	Körner et al. 2015	Lehner et al. 2014	Körner et al. 2015
CM	2020	2886	0.025	55	43	2200	0.025	5.5
	2035	1443	0.025	58	37	1500	5	5.0
	2050	962	0.025	60	35	760	5	4.5
	Source	Körner et al. 2015	Amos 1998	Schoots et al. 2010	Dodds, Staffell, et al. 2015	Körner et al. 2015	Lehner et al. 2014	Körner et al. 2015
GSD	2020	2886	0.025	55	43	2200	0.025	5.5
	2035	1443	0.025	58	37	1500	0.025	5.0
	2050	962	0.025	60	35	760	0.025	4.5
	Source	Körner et al. 2015	Amos 1998	Schoots et al. 2010	Dodds, Staffell, et al. 2015	Körner et al. 2015	Lehner et al. 2014	Körner et al. 2015
RSD	2020	2886	0.025	55	43	2200	0.025	5.5
	2035	1443	0.025	58	37	1500	0.025	5.0
	2050	962	0.025	60	35	760	0.025	4.5
	Source	Körner et al. 2015	Amos 1998	Schoots et al. 2010	Dodds, Staffell, et al. 2015	Körner et al. 2015	Lehner et al. 2014	Körner et al. 2015

Table C.5.: Setting of parameters for the storage technologies' investment costs, O&M costs, and efficiencies for the CM, GSD, and RSD scenarios.

Sce-nario	Year	Li-ion Battery			Thermal Storage		H2S	
		Capital (CHF/kWh)	OMF (CHF/kWh)	Eff. (%)	Capital (CHF/kWh)	Eff. (%)	Capital (CHF/kWh)	Eff. (%)
Baseline	2015	674	25	92.5	650	90	950	99
	Source	Lott et al. 2014	Rastler 2010	Battke et al. 2013	Jakob et al. 2014	Stadler et al. 2008	Amos 1998	Körner et al. 2015
CM	2020	578	25	92.5	650	90	680	99
	2035	482	25	95.5	650	90	510	99
	2050	385	25	92.5	650	90	460	99
	Source	Lott et al. 2014	Rastler 2010	Battke et al. 2013	Jakob et al. 2014	Stadler et al. 2008	Körner et al. 2015	Körner et al. 2015
GSD	2020	260	25	92.5	650	90	680	99
	2035	260	25	92.5	650	90	510	99
	2050	260	25	92.5	650	90	460	99
	Source	Lott et al. 2014	Rastler 2010	Battke et al. 2013	Jakob et al. 2014	Stadler et al. 2008	Körner et al. 2015	Körner et al. 2015
RSD	2020	260	25	92.5	650	90	680	99
	2035	260	25	92.5	650	90	510	99
	2050	260	25	92.5	650	90	460	99
	Source	Lott et al. 2014	Rastler 2010	Battke et al. 2013	Jakob et al. 2014	Stadler et al. 2008	Körner et al. 2015	Körner et al. 2015

MOBILITY OPTIMISATION (CHAPTER 5) INPUT PARAMETERS

In this Section, the major economic, environmental, and performance assumptions in Chapter 5 and 6 are outlined with references. Firstly, the energy carrier costs, selling price, and life-cycle emissions factors are listed in Table D.1. The capital costs, O&M costs, and the embodied emissions for the conversion technologies are listed in Table D.2, the vehicles in Table D.3, and the storage technologies in Table D.4.

Table D.1.: Energy Carrier Economic and Emission Parameters. Please note that emissions parameters here are LCA values to account for embodied emissions.

	Years	Elec. (kWh)	H_2 (kWh)	Gaso-line (kWh)	Natural gas (kWh)	CO_2 (kg)	Water (kg)
Purchase Cost (CHF/ Unit)	2015	0.2	N/A	0.164	0.0934	0.14	0.004
	2035	0.23	N/A	0.246	0.121	0.12	0.006
	2050	0.25	N/A	0.375	0.154	0.1	0.009
	Source	Elektriz-ität-skom-mission 2017		Prognos AG 2013	Prognos AG 2013	Parra et al. 2017	OECD 2017
Selling price (CHF/ Unit)	2015	0.10	0.0934	N/A	0.0934	N/A	N/A
	2035	0.065	0.121	N/A	0.121	N/A	N/A
	2050	0.035	0.154	N/A	0.154	N/A	N/A
	Source	Swiss-Grid 2015	EIA 2015		EIA 2015		
Emissions (kg CO_2/ Unit)	2015	0.1	0	0.278	0.235	0.2	0.0003
	2035	0.085	0	0.278	0.224	0.1	0.0003
	2050	0.065	0	0.278	0.202	0.05	0.0003
	Source	Itten et al. 2014		Eggi-mann et al. 2016	Eggi-mann et al. 2016	Wernet et al. 2016	Wer-net et al. 2016

Table D.2.: Conversion technology parameters for Chapter 5 mobility optimisation model.

Conv. Tech	Year	Capital Costs		O & M		Embodied Emissions		Efficiency
		Fixed (CHF)	Var. (CHF/kW)	Fixed (CHF/kW)	Var. (CHF/kWh)	Fixed (kg CO_2)	Var. (kg CO_2/kW)	-
Gas boiler	2015	12,582	608	5	0	0	75	0.9
	2035	12,582	608	5	0	0	75	0.9
	2050	12,582	608	5	0	0	75	0.9
	Source	Jakob et al. 2014	Jakob et al. 2014	DEA 2016			Eggimann et al. 2016	SIA 2011
Heat pump	2015	11000	1335	0	0.015	2329	75	3
	2035	9625	993	0	0.015	1996	64	3.5
	2050	8250	851	0	0.015	1747	56	4
	Source	DEA 2016	DEA 2016		DEA 2016	Eggimann et al. 2016	Eggimann et al. 2016	SIA 2011
PEMFC	2015	15,000	3,500	0	0.034	528	51.2	0.5 (Elec)/ 0.4 (Heat)
	2035	7500	1750	0	0.034	480	24.2	0.55 (Elec)/ 0.35 (Heat)
	2050	5000	1167	0	0.034	440	22.2	0.6 (Elec)/ 0.3 (Heat)
	Source	Körner et al. 2015	Körner et al. 2015		Körner et al. 2015	Wernet et al. 2016	Wernet et al. 2016	Körner et al. 2015

PEME	2015	8400	1286	0	0.034	928	47	0.6
	2035	5700	877	0	0.034	856	33	0.65
	2050	2888	444	0	0.034	796	30	0.7
	Source	Körner et al. 2015	Körner et al. 2015		Körner et al. 2015	Wernet et al. 2016	Wernet et al. 2016	Körner et al. 2015
CMR	2015	11,212	603	20	0	10	6.7	0.8
	2035	7475	402	20	0	10	6.7	0.8
	2050	3737	201	20	0	10	6.7	0.8
	Source	Lehner et al. 2014	Lehner et al. 2014	Parra et al. 2017		Wernet et al. 2016	Wernet et al. 2016	Lehner et al. 2014
PV	2015	10 888	1960	24	0	1960	398	0.17
	2035	9144	1648	24	0	1568	318	0.19
	2050	8328	1432	24	0	1200	449	0.21
	Source	Denholm et al. 2014	Denholm et al. 2014	DEA 2016		Eggimann et al. 2016	Eggimann et al. 2016	Mayer et al. 2015

Table D.3.: Vehicle technology capital costs and embodied emissions.

Vehicle	Capital Costs (CHF)			Embodied Emissions (kg CO$_2$-eq)			OMV (CHF/km)
	2015	2035	2050	2015	2035	2050	All years
ICEV-g	22,285	22,379	22,663	6,529	6,104	5,467	0.035
ICEV-cng	26,396	26,509	26,845	6,871	6,424	5,754	0.035
PHEV50	37,302	32,011	29,032	8,848	8,827	8,692	0.030
PHEV100	N/A	34,227	30,875	N/A	8,216	7,969	0.03
PHEV150	N/A	N/A	31,445	N/A	N/A	7,054	0.03
BEV200	42,681	32,011	27,200	8,777	8,513	8,076	0.023
BEV300	N/A	37,788	30,415	N/A	7,967	7,272	0.023
BEV500	N/A	N/A	36,260	N/A	N/A	7,126	0.023
FCEV	68,083	48,158	31,444	10,978	9,562	7,812	0.028
Source	Hofer 2014	Hofer 2014	Hofer 2014	Hofer 2014	Hofer 2014	Hofer 2014	Reis 2010

Table D.4.: Storage technology parameters for capital costs and embodied emissions.

| Stor-age | Year | Capital Costs | | O & M | | Embodied Emissions | | Effi-ciency |
		Fixed (CHF)	Vari-able (CHF/kWh)	Fixed (CHF/kWh)	Vari-able (CHF/kWh)	Fixed (kg CO_2)	Vari-able (kg CO_2/kWh)	%
Battery	2015	6,167	343	10	0	156	41	92.5
	2035	2,250	143	10	0	117	25	92.5
	2050	1,500	120	10	0	87	16	92.5
	Source	Hofer 2014	Hofer 2014	Hofer 2014		Hofer 2014	Hofer 2014	Battke et al. 2013
TES	2015	1,685	12.6	0	0	0.31	4.68	90
	2035	1,685	12.6	0	0	0.31	4.68	90
	2050	1,685	12.6	0	0	0.31	4.68	90
	Source	Jakob et al. 2014	Jakob et al. 2014			Jakob et al. 2014	Jakob et al. 2014	Stadler et al. 2008
H_2 Tank	2015	1,400	22.3	0	0	22	0.2	99
	2035	1,150	8	0	0	20	0.17	99
	2050	1,000	7.3	0	0	17	0.15	99
	Source	Hofer 2014	Hofer 2014			Hofer 2014	Hofer 2014	Amos 1998
CNG Tank	2015	766	4.8	0	0	64	0.64	99
	2035	675	4.4	0	0	55	0.605	99
	2050	600	4	0	0	52	0.55	99
	Source	Hofer 2014	Hofer 2014			Hofer 2014	Hofer 2014	Amos 1998

POWER-TO-MOBILITY OPTIMISATION OPERATION

In Chapter 6, Fig. 6.10, the optimal operation of the Power-to-Mobility optimisation model was shown over a one-year period for Pareto solution 8. Solution 8 was chosen as it demonstrated the lowest cost solution that still used long-term storage. In this Section, we show the same plot for Pareto solutions 1, 5, and 10. These represent the cost optimal, the 50% cost minimisation - 50% CO_2 optimisation, and the CO_2 optimal solutions. They are shown in Fig. E.1, Fig. E.2, and Fig. E.3 respectively.
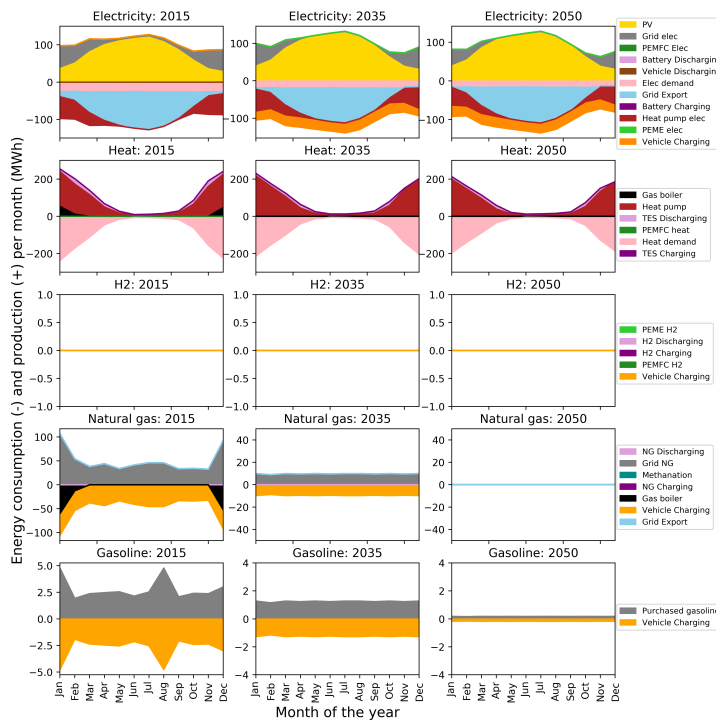
Figure E.1.: Monthly energy consumption (negative) and production (positive) divided by energy carrier for Pareto Solution 1.
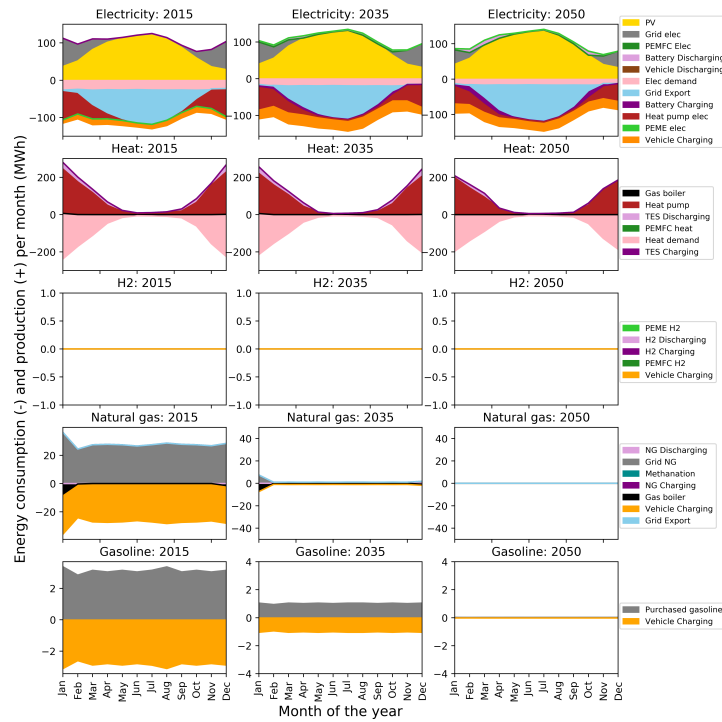
Figure E.2.: Monthly energy consumption (negative) and production (positive) divided by energy carrier for Pareto Solution 5.
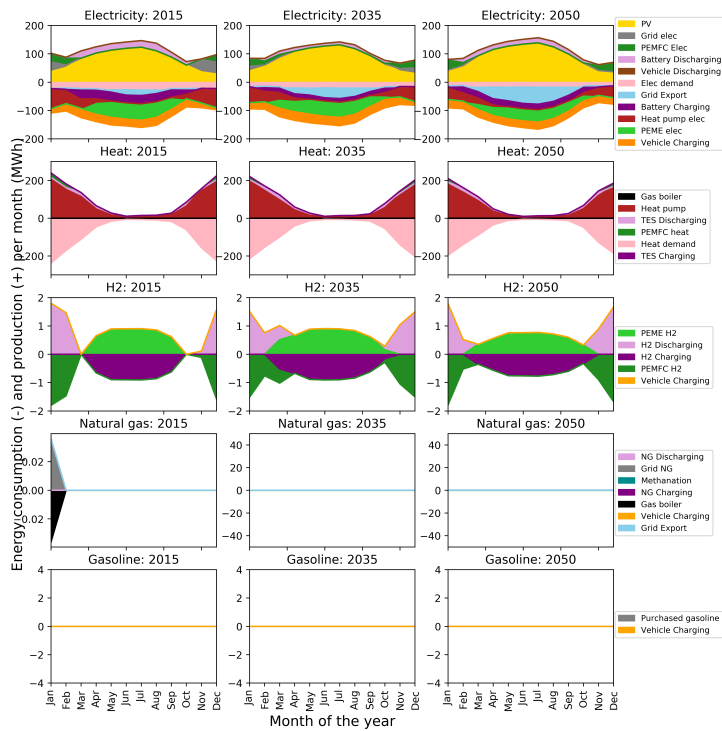
Figure E.3.: Monthly energy consumption (negative) and production (positive) divided by energy carrier for Pareto Solution 10.

BIBLIOGRAPHY

Allen, Robert C. (2009). *The British Industrial Revolution in Global Perspective*. Cambridge University Press.

Altfeld, Klaus et al. (2013). *Admissible Hydrogen Concentration in Natural Gas Systems*. Tech. rep. The European Gas Research Group. URL: http://gerg.eu/public/uploads/files/publications/GERGpapers/HIPS_-_the_paper_-_FINAL.pdf (visited on 11/20/2016).

Amos, Wade A. (1998). *Costs of Storing and Transporting Hydrogen. National Renewable Energy Laboratory*. Ed. by National Renewable Energy Laboratory. Tech. rep. Golden, Colorado. URL: https://www.nrel.gov/docs/fy99osti/25106.pdf (visited on 01/04/2018).

Arvidsson, Rickard et al. (2018). "Environmental Assessment of Emerging Technologies: Recommendations for Prospective LCA." In: *Journal of Industrial Ecology* 22.6, pp. 1286–1294. ISSN: 1530-9290. DOI: 10.1111/jiec.12690. URL: https://onlinelibrary.wiley.com/doi/abs/10.1111/jiec.12690 (visited on 10/06/2019).

Assen, Niklas von der et al. (2014). "Life cycle assessment of CO2 capture and utilization: a tutorial review." In: *Chemical Society Reviews* 43.23, pp. 7982–7994. ISSN: 1460-4744. DOI: 10.1039/C3CS60373C. URL: https://pubs.rsc.org/en/content/articlelanding/2014/cs/c3cs60373c (visited on 10/05/2019).

Assouline, Dan et al. (2017). "Quantifying rooftop photovoltaic solar energy potential: A machine learning approach." In: *Solar Energy* 141, pp. 278–296. ISSN: 0038-092X. DOI: 10.1016/j.solener.2016.11.045. URL: http://www.sciencedirect.com/science/article/pii/S0038092X16305850 (visited on 08/15/2019).

Aventa (2018). *LoWind Turbine AV-7*. URL: http://aventa.ch/en/leichtwindanlage-av-7.html (visited on 01/25/2018).

Battke, Benedikt et al. (2013). "A review of probabilistic model of life-cycle costs and stationary batteries in multiple applications." In: *Renewable and Sustainable Energy Reviews* 25, pp. 240–250. ISSN: 1364-0321. DOI: 10.1016/j.rser.2015.11.085. URL: http://www.sciencedirect.com/science/article/pii/S1364032115013520 (visited on 11/19/2016).

Bébié, Bruno et al. (2009). *Grundlagen für ein Umsetzungskonzept der 2000-Watt-Gesellschaft am Beispiel der Stadt Zürich*. Tech. rep. LSP4. Stadt Zürich: Novatlantis. URL: https://www.novatlantis.ch/wp-content/uploads/2014/10/PRZH_2kW_Methodikpapier_20090528.pdf (visited on 07/18/2019).

Bee, Elena et al. (2019). "Air-source heat pump and photovoltaic systems for residential heating and cooling: Potential of self-consumption in different European climates." In: *Building Simulation* 12.3, pp. 453–463. ISSN: 1996-8744. DOI: 10.1007/s12273-018-0501-5. URL: https://doi.org/10.1007/s12273-018-0501-5 (visited on 09/10/2019).

Bernal-Agustín, José L. et al. (2010). "Techno-economical optimization of the production of hydrogen from PV-Wind systems connected to the electrical grid." In: *Renewable Energy* 35.4, pp. 747–758. ISSN: 0960-1481. DOI: 10.1016/j.renene.2009.10.004. URL: http://www.sciencedirect.com/science/article/pii/S0960148109004303 (visited on 12/12/2017).

Blanco, Herib et al. (2018). "Potential for hydrogen and Power-to-Liquid in a low-carbon EU energy system using cost optimization." In: *Applied Energy* 232, pp. 617–639. ISSN: 0306-2619. DOI: 10.1016/j.apenergy.2018.09.216. URL: http://www.sciencedirect.com/science/article/pii/S0306261918315368 (visited on 10/04/2019).

Blindenbacher, Thomas (2019). *2000-Watt society and 2000-Watt Site*. 2000-Watt-Areale. URL: https://www.2000watt.swiss/english.html (visited on 05/22/2019).

Bloess, Andreas (2019). "Impacts of heat sector transformation on Germany's power system through increased use of power-to-heat." In: *Applied Energy* 239, pp. 560–580. ISSN: 0306-2619. DOI: 10.1016/j.apenergy.2019.01.101. URL: http://www.sciencedirect.com/science/article/pii/S0306261919301023 (visited on 09/10/2019).

Bloess, Andreas et al. (2018). "Power-to-heat for renewable energy integration: A review of technologies, modeling approaches, and flexibility potentials." In: *Applied Energy* 212, pp. 1611–1626. ISSN: 0306-2619. DOI: 10.1016/j.apenergy.2017.12.073. URL: http://www.sciencedirect.com/science/article/pii/S0306261917317889 (visited on 08/31/2019).

Blok, Kornelis et al. (2016). *Introduction to Energy Analysis*. 2nd Edition. Routledge. 310 pp. ISBN: 978-1-138-67115-7. URL: https://www.crcpress.com/Introduction-to-Energy-Analysis/Blok-Nieuwlaar/p/book/9781138671157 (visited on 03/03/2020).

Board of Swiss Institutes of Technology (ETH-Rat) (1998). *2000 Watt Society - Model Switzerland Sustainability Strategy within the Institutes of Technology (in german)*. Wirtschaftsplatform ETH Zürich.

Borbely, Anne-Marie et al. (2019). *Distributed Generation: The Power Paradigm for the New Millennium*. CRC Press. CRC Press. ISBN: ISBN 9780367397197. URL: https://www.crcpress.com/Distributed-Generation-The-Power-Paradigm-for-the-New-Millennium/Borbely-Kreider/p/book/9780367397197 (visited on 10/03/2019).

BP Statistical Review of World Energy (2019). BP global. URL: https://www.bp.com/en/global/corporate/energy-economics/statistical-review-of-world-energy.html (visited on 10/03/2019).

Brennan, John W. et al. (2016). *Battery Electric Vehicles vs. Internal Combustion Engine Vehicles: A United States-Based Comprehensive Assessment*. Tech. rep. Arthur D. Little. URL: http://www.adlittle.cn/sites/default/files/viewpoints/ADL_BEVs_vs_ICEVs_FINAL_November_292016.pdf (visited on 07/15/2019).

Bundesamt für Statistik (2012). *Statistisches Lexikon der Schweiz. GWS/GWR*. URL: https://www.bfs.admin.ch/bfs/de/home.html.

Bundesamt für Statistik (2015). *Mikrozensus Mobilität und Verkehr Daten*. Bern, Schweiz. URL: https://www.bfs.admin.ch/bfs/de/home/statistiken/mobilitaet-verkehr/erhebungen/mzmv.html.

Bundesamt für Statistik (2017). *Energiebereich: Heizsystem und Energieträger*. Bundesamt für Statistik. Ed. by Swiss Federal office for Energy. Swiss Federal Office of Energy. URL: https://www.bfs.admin.ch/bfs/de/home/statistiken/bau-wohnungswesen/gebaeude/energiebereich.html (visited on 07/15/2019).

Candanedo, Luis M. et al. (2017). "Data driven prediction models of energy use of appliances in a low-energy house." In: *Energy and Buildings* 140, pp. 81–97. ISSN: 0378-7788. DOI: 10.1016/j.enbuild.2017.01.083. URL: http://www.sciencedirect.com/science/article/pii/S0378778816308970 (visited on 09/30/2019).

Capstone Turbine Corporation (2017). *Products : Capstone Turbine Corporation (CPST)*. URL: https://www.capstoneturbine.com/products/ (visited on 12/13/2017).

Carbon Engineering (2019). *Carbon Engineering: CO2 capture and the synthesis of clean transportation fuels*. Carbon Engineering. URL: https://carbonengineering.com/ (visited on 10/07/2019).

Chaudhary, Anant (2017). "Predictive Modelling of Home Appliances Energy Consumption in Belgium." MA thesis. National College of Ireland, p. 27.

Clack, Christopher T. M. et al. (2017). "Evaluation of a proposal for reliable low-cost grid power with 100% wind, water, and solar." In: *Proceedings of the National Academy of Sciences* 114.26, pp. 6722–6727. ISSN: 0027-8424, 1091-6490. DOI: 10.1073/pnas.1610381114. URL: https://www.pnas.org/content/114/26/6722 (visited on 10/12/2019).

Clegg, S. et al. (2016). "Storing renewables in the gas network: modelling of power-to-gas seasonal storage flexibility in low-carbon power systems." In: *Transmission Distribution IET Generation* 10.3, pp. 566–575. DOI: 10.1049/iet-gtd.2015.0439.

Climeworks – Capturing CO2 from Air (2019). URL: https://www.climeworks.com/ (visited on 10/07/2019).

Collet, Pierre et al. (2017). "Techno-economic and Life Cycle Assessment of methane production via biogas upgrading and power to gas technology." In: *Applied Energy* 192, pp. 282–295. ISSN: 0306-2619. DOI: 10.1016/j.apenergy.2016.08.181. URL: http://www.sciencedirect.com/science/article/pii/S0306261916312909 (visited on 10/23/2019).

Contestabile, M. et al. (2011). "Battery electric vehicles, hydrogen fuel cells and biofuels. Which will be the winner?" In: *Energy & Environmental Science* 4.10, pp. 3754–3772. ISSN: 1754-5706. DOI: 10.1039/C1EE01804C. URL: https://pubs.rsc.org/en/content/articlelanding/2011/ee/c1ee01804c (visited on 07/02/2019).

Daly, Hannah et al. (2012). *Modal choice in a TIMES model*. Cork, Ireland: IEA, p. 25. URL: https://iea-etsap.org/projects/Modelling%20Transport%20Modal%20Choice%20in%20a%20TIMES%20Model.pdf.

DEA (2016). *Technology Data for Energy Plants*. Tech. rep. Copenhagen, Denmark: Danish Energy Agency. URL: http://www.energinet.dk/SiteCollectionDocuments/Danske%20dokumenter/Forskning/Technology_data_for_energy_plants.pdf (visited on 08/01/2016).

Denholm, Paul et al. (2014). *Technology Roadmap: Solar Photovoltaic Energy*. Energy Technology Perspectives. Paris: International Energy Agency. URL: https://www.sccer-mobility.ch/export/sites/sccer-mobility/capacity-areas/dwn_capacity_areas/TowardsAnEnergyEfficientSwissTransportationSystem_Ver1.2.pdf (visited on 04/26/2019).

Devlin, Joseph et al. (2017). "A multi vector energy analysis for interconnected power and gas systems." In: *Applied Energy* 192, pp. 315–328. ISSN: 0306-2619. DOI: 10.1016/j.apenergy.2016.08.040. URL: http://www.sciencedirect.com/science/article/pii/S0306261916311278 (visited on 10/23/2019).

Dige, Nishant (2016). "Efficient Sampling Algorithm for Optimization Under Uncertainty." MA thesis. University of Pune.

Dodds, Paul E. and Will McDowall (2014). "Methodologies for representing the road transport sector in energy system models." In: *International Journal of Hydrogen Energy* 39.5, pp. 2345–2358. ISSN: 0360-3199. DOI: 10.1016/j.ijhydene.2013.11.021. URL: http://www.sciencedirect.com/science/article/pii/S0360319913027468 (visited on 07/02/2019).

Dodds, Paul E., Iain Staffell, et al. (2015). "Hydrogen and fuel cell technologies for heating: A review." In: *International Journal of Hydrogen Energy* 40.5, pp. 2065–2083. ISSN: 0360-3199. DOI: 10.1016/j.ijhydene.2014.11.059. URL: http://www.sciencedirect.com/science/article/pii/S0360319914031383 (visited on 07/31/2016).

Dufo-López, Rodolfo et al. (2008). "Multi-objective design of PV wind diesel hydrogen battery systems." In: *Renewable Energy* 33.12, pp. 2559–2572. ISSN: 0960-1481. DOI: 10.1016/j.renene.2008.02.027. (Visited on 12/12/2017).

Dufour, Javier et al. (2012). "Life cycle assessment of alternatives for hydrogen production from renewable and fossil sources." In: *International Journal of Hydrogen Energy*. 10th International Conference on Clean Energy 2010 37.2, pp. 1173–1183. ISSN: 0360-3199. DOI: 10.1016/j.ijhydene.2011.09.135. URL: http://www.sciencedirect.com/science/article/pii/S0360319911022828 (visited on 02/11/2019).

Dun, Craig et al. (2015). *Improvements to the definition of lifetime mileage of light duty vehicles. Report for the European Commissions*. Tech. rep. Ares (2014) 2298698. Ricardo AEA, p. 68. URL: https://ec.europa.eu/clima/sites/clima/files/transport/vehicles/docs/ldv_mileage_improvement_en.pdf.

Eckart, Jonathan (2017). *Batteries can be part of the fight against climate change - if we do these five things*. World Economic Forum. URL: https://www.weforum.org/agenda/2017/11/battery-batteries-electric-cars-carbon-sustainable-power-energy/ (visited on 10/12/2019).

Eggimann, Paul et al. (2016). *Ökobilanzdaten im Baubereich*. Tech. rep. Koordinationskonferenz der Bau- und Liegenschaftsorgane der öffentlichen Bauherren (KBOB), pp. 16–17. URL: https://www.kbob.admin.ch/kbob/de/home/publikationen/nachhaltiges-bauen/oekobilanzdaten_baubereich.html.

EIA (2015). *Annual Energy Outlook 2015 with projections to 2040. Washington*. Tech. rep. Washington: U.S. Department of Energy (DOE). URL: https://www.eia.gov/outlooks/aeo/pdf/0383(2015).pdf (visited on 12/12/2017).

Eidgenössisches Departement für Umwelt Verkehr, Energie und Kommunikation UVEK (2019). *Sonnendach.ch und Sonnenfassade.ch: Berechnung von Potenzialen in Gemeinden*. Comp. software. URL: http://www.sonnendach.ch (visited on 01/25/2018).

Elektrizitätskommission, Eidgenössische (2017). *Strompreis*. Eidgenössische Elektrizitätskommission. URL: https://www.strompreis.elcom.admin.ch/ (visited on 01/04/2018).

Erath, Alex et al. (2012). *Large-scale agent-based transport demand model for Singapore*. Singapore: Future Cities Laboratory.

EU Commission (2015). *Heating and cooling*. Energy - European Commission. URL: https://ec.europa.eu/energy/en/topics/energy-efficiency/heating-and-cooling (visited on 10/03/2019).

EV Charge Plus (2018). *EV charging cables types for electric vehicels users*. EV Charge +. URL: https://evchargeplus.com/ev-charging-cable-types/ (visited on 07/26/2019).

Fisher, Marshall L. (1981). "The Lagrangian Relaxation Method for Solving Integer Programming Problems." In: *Management Science* 27.1, pp. 1–18. ISSN: 0025-1909. DOI: 10.1287/mnsc.27.1.1. URL: https://pubsonline.informs.org/doi/abs/10.1287/mnsc.27.1.1 (visited on 10/16/2019).

Gabrielli, P., B. Flamm, et al. (2016). "Modeling for optimal operation of PEM fuel cells and electrolyzers." In: *2016 IEEE 16th International Conference on Environment and Electrical Engineering (EEEIC)*. 2016 IEEE 16th International Conference on Environment and Electrical Engineering (EEEIC), pp. 1–7. DOI: 10.1109/EEEIC.2016.7555707.

Gabrielli, P., Matteo Gazzani, et al. (2018). "Electrochemical conversion technologies for optimal design of decentralized multi-energy systems: Modeling framework and technology assessment." In: *Applied Energy* 221, pp. 557–575. ISSN: 0306-2619. DOI: 10.1016/j.apenergy.

2018.03.149. URL: http://www.sciencedirect.com/science/article/pii/S0306261918304872 (visited on 02/11/2019).

Gahleitner, Gerda (2013). "Hydrogen from renewable electricity: An international review of power-to-gas pilot plants for stationary applications." In: *International Journal of Hydrogen Energy* 38.5, pp. 2039–2061. ISSN: 0360-3199. DOI: 10.1016/j.ijhydene.2012.12.010. URL: http://www.sciencedirect.com/science/article/pii/S0360319912026481 (visited on 07/31/2016).

Gao, Liuhua et al. (2015). "A Review on Borehole Seasonal Solar Thermal Energy Storage." In: *Energy Procedia*. International Conference on Solar Heating and Cooling for Buildings and Industry, SHC 2014 70 (Supplement C), pp. 209–218. ISSN: 1876-6102. DOI: 10.1016/j.egypro.2015.02.117. URL: http://www.sciencedirect.com/science/article/pii/S1876610215002398 (visited on 12/06/2017).

Garmsiri, Shahryar et al. (2014). "Integration of Wind Energy, Hydrogen and Natural Gas Pipeline Systems to Meet Community and Transportation Energy Needs: A Parametric Study." In: *Sustainability* 6.5, pp. 2506–2526. DOI: 10.3390/su6052506. URL: https://www.mdpi.com/2071-1050/6/5/2506 (visited on 10/23/2019).

Geidl, Martin and Göran Andersson (2006). "Operational and structural optimization of multi-carrier energy systems." In: *European Transactions on Electrical Power* 16.5, pp. 463–477. ISSN: 1546-3109. DOI: 10.1002/etep.112. URL: http://onlinelibrary.wiley.com/doi/10.1002/etep.112/abstract (visited on 11/15/2016).

Geidl, Martin, Koeppel Gaudenz, et al. (2007). "The Energy Hub – A Powerful Concept for Future Energy Systems." In: *Third Annual Carnegie Mellon Conference on the Electricity Industry*. Third Annual Carnegie Mellon Conference on the Electricity Industry. URL: https://www.ece.cmu.edu/~electriconf/2007/2007%20Conf%20Papers/Andersson%20Paper%20final.pdf (visited on 08/03/2017).

Girod, Bastien et al. (2009). "The evolution of the IPCC's emissions scenarios." In: *Environmental Science & Policy* 12.2, pp. 103–118. ISSN: 1462-9011. DOI: 10.1016/j.envsci.2008.12.006. URL: http://www.sciencedirect.com/science/article/pii/S1462901108001378 (visited on 12/12/2017).

Gnann, Till et al. (2015). "A review of combined models for market diffusion of alternative fuel vehicles and their refueling infrastructure." In: *Renewable and Sustainable Energy Reviews* 47, pp. 783–793. ISSN: 1364-0321. DOI: 10.1016/j.rser.2015.03.022. URL: http://www.

sciencedirect.com/science/article/pii/S1364032115001756 (visited on 07/02/2019).

Godskesen, B. et al. (2013). "Life-cycle and freshwater withdrawal impact assessment of water supply technologies." In: *Water Research* 47.7, pp. 2363–2374. ISSN: 0043-1354. DOI: 10.1016/j.watres.2013.02.005. URL: http://www.sciencedirect.com/science/article/pii/S0043135413000961 (visited on 10/06/2019).

Gorner, Marine et al. (2019). *Electric vehicles*. Electric Vehicles. URL: https://www.iea.org/tcep/transport/electricvehicles/ (visited on 10/03/2019).

Götz, Manuel et al. (2016). "Renewable Power-to-Gas: A technological and economic review." In: *Renewable Energy* 85, pp. 1371–1390. ISSN: 0960-1481. DOI: 10.1016/j.renene.2015.07.066. URL: http://www.sciencedirect.com/science/article/pii/S0960148115301610 (visited on 08/02/2016).

Graf, Mario (2019). *Regio Energie Solothurn Forscht an Power-to-Gas*. energate. URL: https://www.energate-messenger.ch/news/189096/regio-energie-solothurn-forscht-an-power-to-gas (visited on 10/08/2019).

Grosspietsch, David et al. (2017). "Multi-Energy-Hubs in Quartieren: Simulation dezentraler Energiesysteme." In: *VSE Energie Bulletin*. URL: https://www.bulletin.ch/de/news-detail/multi-energy-hubs-in-quartieren.html.

H2 Energy (2018). *Major Swiss companies push hydrogen mobility*. H2 Energy. URL: https://h2energy.ch/en/major-swiss-companies-push-hydrogen-mobility/ (visited on 07/26/2019).

Hajimiragha, A. et al. (2007). "Optimal Energy Flow of Integrated Energy Systems with Hydrogen Economy Considerations." In: *iREP Symposium- Bulk Power System Dynamics and Control - VII, Revitalizing Operational Reliability*.

Han, Seulki et al. (2017). "Scenario-based approach for design and comparatively analysis of conventional and renewable energy systems." In: *Energy* 129.Supplement C, pp. 86–100. ISSN: 0360-5442. DOI: 10.1016/j.energy.2017.04.063. URL: http://www.sciencedirect.com/science/article/pii/S0360544217306291 (visited on 12/12/2017).

Hansen, Kenneth et al. (2019). "Status and perspectives on 100% renewable energy systems." In: *Energy* 175, pp. 471–480. ISSN: 0360-5442. DOI: 10.1016/j.energy.2019.03.092. URL: http://www.

`sciencedirect . com / science / article / pii / S0360544219304967`
(visited on 10/11/2019).

Hofer, Johannes (2014). "Sustainability assessment of passenger vehicles: Analysis of past trends and future impacts of electric powertrains." PhD thesis. ETH Zürich.

Horni, Andreas et al. (2016). "The Multi-Agent Transport Simulation MATSim." In: *Ubiquity Press Ltd.* DOI: `http://dx.doi.org/10.5334/baw`.

IEA (2010). *Renewable Energy Essentials: Hydropower*. Tech. rep. Paris, France: International Energy Agency. URL: `https://www.iea.org/publications/freepublications/publication/HydropowerEssentials.pdf`.

International Energy Agency (2018a). *Statistics: CO2 Emissions from Fuel Combustion*. Statistics. Paris. URL: `https://webstore.iea.org/co2-emissions-from-fuel-combustion-2018` (visited on 07/02/2019).

International Energy Agency (2018b). *World Energy Outlook 2018*. 978-92-64-30677-6. International Energy Agency OECD. URL: `https://www.iea.org/weo2018/scenarios/` (visited on 10/04/2019).

Itten, Rene et al. (2014). *Life Cycle Inventories of Electricity Mixes and Grid*. Research rep. Uster, Switzerland: Paul Scherrer Institut (PSI).

Jacobson, Mark Z. et al. (2015). "100% clean and renewable wind, water, and sunlight (WWS) all-sector energy roadmaps for the 50 United States." In: *Energy & Environmental Science* 8.7, pp. 2093–2117. ISSN: 1754-5706. DOI: `10.1039/C5EE01283J`. URL: `https://pubs.rsc.org/en/content/articlelanding/2015/ee/c5ee01283j` (visited on 10/11/2019).

Jakob, Martin et al. (2014). *Intergrated Strategies and Policy Insturments for Retrofitting Buildings to Reduce Primary Energy Use and GHG Emissions (INSPIRE)*. URL: `http://www.energieschweiz.ch/de-ch/wohnen/energierechner/inspire-tool.aspx` (visited on 08/02/2016).

Jirutitijaroen, P. et al. (2008). "Comparison of Simulation Methods for Power System Reliability Indexes and Their Distributions." In: *IEEE Transactions on Power Systems* 23.2, pp. 486–493. DOI: `10.1109/TPWRS.2008.919425`.

Jordan, Dirk C. et al. (2012). *Photovoltaic Degradation Rates - An Analytical Review*. Tech. rep. National Renewable Energy Laboratory.

Keirstead, James et al. (2012). "The impact of CHP (combined heat and power) planning restrictions on the efficiency of urban energy systems." In: *Energy*. 23rd International Conference on Efficiency,

Cost, Optimization, Simulation and Environmental Impact of Energy Systems, ECOS 2010 41.1, pp. 93–103. ISSN: 0360-5442. DOI: 10.1016/j.energy.2011.06.011. URL: http://www.sciencedirect.com/science/article/pii/S0360544211003884 (visited on 12/01/2016).

Kirkerud, Jon Gustav et al. (2017). "Power-to-heat as a flexibility measure for integration of renewable energy." In: *Energy* 128, pp. 776–784. ISSN: 0360-5442. DOI: 10.1016/j.energy.2017.03.153. URL: http://www.sciencedirect.com/science/article/pii/S0360544217305479 (visited on 09/10/2019).

Knopf, F. Carl (2011). *Modeling, Analysis and Optimization of Process and Energy Systems*. John Wiley & Sons. 428 pp. ISBN: 978-1-118-12114-6.

Kober, T et al. (2019). *Perspectives of Power-to-X in Switzerland: A White Paper*. 2nd Edition. Paul Scherrer Institut (PSI). URL: https://www.sccer-mobility.ch/Joint_Activities/Power-to-Gas/ (visited on 10/09/2019).

Körner, Alexander et al. (2015). *Hydrogen Technology Roadmap - Hydrogen and Fuel Cells*. Tech. rep. Paris, France: International Energy Agency. (Visited on 08/02/2016).

Korpas, M. et al. (2006). "Operation planning of hydrogen storage connected to wind power operating in a power market." In: *IEEE Transactions on Energy Conversion* 21.3, pp. 742–749. ISSN: 0885-8969. DOI: 10.1109/TEC.2006.878245.

Kuramochi, Takeshi et al. (2012). "Comparative assessment of CO2 capture technologies for carbon-intensive industrial processes." In: *Progress in Energy and Combustion Science* 38.1, pp. 87–112. ISSN: 0360-1285. DOI: 10.1016/j.pecs.2011.05.001. URL: http://www.sciencedirect.com/science/article/pii/S0360128511000293 (visited on 10/04/2019).

Lang, Tillmann et al. (2015). "Don't just follow the sun – A global assessment of economic performance for residential building photovoltaics." In: *Renewable and Sustainable Energy Reviews* 42.Supplement C, pp. 932–951. ISSN: 1364-0321. DOI: 10.1016/j.rser.2014.10.077. URL: http://www.sciencedirect.com/science/article/pii/S1364032114009022.

Lehner, Marcus et al. (2014). *Power-to-Gas: Technology and Business Models*. Springer. URL: http://www.springer.com/us/book/9783319039947 (visited on 08/01/2016).

Leuenberger, Marienne et al. (2010). *Life Cycle Assessment of Two Wheel Vehicles. Ecoinvent dataset Implemented in ecoinvent data v2.2 (2010)*. Tech.

rep. Uster: ESU-services Ltd. URL: Life%20Cycle%20Assessment%20of%20Two%20Wheel%20Vehicles%20-%20ESU-services%20Ltd.%20esu-services.ch/fileadmin/download/leuenberger-2010-TwoWheelVehicles.pdf.

Lewandowska-Bernat, Anna et al. (2018). "Opportunities of power-to-gas technology in different energy systems architectures." In: *Applied Energy* 228, pp. 57–67. ISSN: 0306-2619. DOI: 10.1016/j.apenergy.2018.06.001. URL: http://www.sciencedirect.com/science/article/pii/S0306261918308675 (visited on 09/10/2019).

Li, Bei et al. (2017). "Sizing of a stand-alone microgrid considering electric power, cooling/heating, hydrogen loads and hydrogen storage degradation." In: *Applied Energy* 205.Supplement C, pp. 1244–1259. ISSN: 0306-2619. DOI: 10.1016/j.apenergy.2017.08.142. URL: http://www.sciencedirect.com/science/article/pii/S0306261917311595 (visited on 12/12/2017).

Lott, Melissa et al. (2014). *Technology Roadmap - Energy Storage*. Tech. rep. Paris, France: International Energy Agency, Pg. 18–19. (Visited on 10/18/2017).

Loulou, R. et al. (2004). *Documentation for the MARKAL family of models. ETSAP - IEA*. Tech. rep. ETSAP. URL: https://iea-etsap.org/index.php/documentation.

Lunz, Benedikt et al. (2016). "Scenario-based comparative assessment of potential future electricity systems – A new methodological approach using Germany in 2050 as an example." In: *Applied Energy* 171.Supplement C, pp. 555–580. ISSN: 0306-2619. DOI: 10.1016/j.apenergy.2016.03.087. URL: http://www.sciencedirect.com/science/article/pii/S0306261916304135 (visited on 12/12/2017).

Mancarella, Pierluigi (2014). "MES (multi-energy systems): An overview of concepts and evaluation models." In: *Energy* 65, pp. 1–17. ISSN: 0360-5442. DOI: 10.1016/j.energy.2013.10.041. URL: http://www.sciencedirect.com/science/article/pii/S0360544213008931 (visited on 02/22/2017).

Maroufmashat, Azadeh and Michael Fowler (2017). "Transition of Future Energy System Infrastructure; through Power-to-Gas Pathways." In: *Energies* 10.8, p. 1089. DOI: 10.3390/en10081089. URL: https://www.mdpi.com/1996-1073/10/8/1089 (visited on 09/09/2019).

Maroufmashat, Azadeh, Michael Fowler, et al. (2016). "Mixed integer linear programing based approach for optimal planning and operation of a smart urban energy network to support the hydrogen

economy." In: *International Journal of Hydrogen Energy*. Special Issue on Progress in Hydrogen Production and Applications (ICH2P-2015), 3-6 May 2015, Oshawa, Ontario, Canada 41.19, pp. 7700–7716. ISSN: 0360-3199. DOI: 10.1016/j.ijhydene.2015.08.038. URL: http://www.sciencedirect.com/science/article/pii/S0360319915021278 (visited on 02/22/2017).

Marquant, Julien F. et al. (2015). "Reducing Computation Time with a Rolling Horizon Approach Applied to a MILP Formulation of Multiple Urban Energy Hub System." In: *Procedia Computer Science*. International Conference On Computational Science, ICCS 2015 51, pp. 2137–2146. ISSN: 1877-0509. DOI: 10.1016/j.procs.2015.05.486. URL: http://www.sciencedirect.com/science/article/pii/S1877050915012946 (visited on 05/15/2018).

Mathiesen, B. V. et al. (2015). "Smart Energy Systems for coherent 100% renewable energy and transport solutions." In: *Applied Energy* 145, pp. 139–154. ISSN: 0306-2619. DOI: 10.1016/j.apenergy.2015.01.075. URL: http://www.sciencedirect.com/science/article/pii/S0306261915001117 (visited on 09/10/2019).

Mavromatidis, Georgios (2017). "Model-based design of distributed urban energy systems under uncertainty." PhD thesis. Zürich: ETH Zürich. URL: https://www.research-collection.ethz.ch/handle/20.500.11850/182697.

Mavromatidis, Georgios, Kristina Orehounig, and Jan Carmeliet (2015). "Evaluation of photovoltaic integration potential in a village." In: *Solar Energy*. ISES Solar World Congress 2013 (SWC2013) Special Issue 121, pp. 152–168. ISSN: 0038-092X. DOI: 10.1016/j.solener.2015.03.044. URL: http://www.sciencedirect.com/science/article/pii/S0038092X15001711 (visited on 09/20/2016).

Mavromatidis, Georgios, Kristina Orehounig, Peter Richner, et al. (2016). "A strategy for reducing CO_2 emissions from buildings with the Kaya identity – A Swiss energy system analysis and a case study." In: *Energy Policy* 88.Supplement C, pp. 343–354. ISSN: 0301-4215. DOI: 10.1016/j.enpol.2015.10.037. URL: http://www.sciencedirect.com/science/article/pii/S0301421515301609 (visited on 11/21/2017).

Mayer, Johannes et al. (2015). *Current and Future Cost of Photovoltaics: Long-term Scenarios for Market Development, System Price, and LCOE of Utility-Scale PV Systems*. Tech. rep. 059/01-S-2015/EN. Berlin: Fraunhofer ISE. URL: https://www.ise.fraunhofer.de/content/dam/ise/de/documents/publications/studies/AgoraEnergiewende_

`Current_and_Future_Cost_of_PV_Feb2015_web.pdf` (visited on 07/26/2019).

McKay, M. D. et al. (1979). "A Comparison of Three Methods for Selecting Values of Input Variables in the Analysis of Output from a Computer Code." In: *Technometrics* 21.2, pp. 239–245. ISSN: 0040-1706. DOI: `10.2307/1268522`. URL: `https://www.jstor.org/stable/1268522` (visited on 10/03/2019).

McKenna, Russell et al. (2017). "Energy autonomy in residential buildings: A techno-economic model-based analysis of the scale effects." In: *Applied Energy* 189.Supplement C, pp. 800–815. ISSN: 0306-2619. DOI: `10.1016/j.apenergy.2016.03.062`. URL: `http://www.sciencedirect.com/science/article/pii/S0306261916303828` (visited on 12/12/2017).

Miglani, Somil et al. (2016). "Assessment of the ground source heat potential at the building level applied to a large urban case study." In: *Brenet Status-Seminar*. Zürich.

Minergie Schweiz (2019). *Produktreglement zu den Gebäudestandards Minergie-P und Minergie-A*. Ed. by Minergie Schweiz. URL: `https://www.minergie.ch/de/zertifizieren/minergie-p/`.

Mock, Peter et al. (2014). *The WLTP: How a new test procedure for cars will affect fuel consumption values in the EU*. Tech. rep. The International Council on Clean Transportation, p. 20. URL: `https://theicct.org/publications/wltp-how-new-test-procedure-cars-will-affect-fuel-consumption-values-eu`.

Morris, Max D. (1991). "Factorial Sampling Plans for Preliminary Computational Experiments." In: *Technometrics* 33.2, pp. 161–174. ISSN: 0040-1706. DOI: `10.2307/1269043`. URL: `https://www.jstor.org/stable/1269043` (visited on 10/23/2019).

Morvaj, Boran et al. (2016). "Integrating multi-domain distributed energy systems with electric vehicle PQ flexibility: Optimal design and operation scheduling for sustainable low-voltage distribution grids." In: *Sustainable Energy, Grids and Networks* 8, pp. 51–61. ISSN: 2352-4677. DOI: `10.1016/j.segan.2016.10.001`. URL: `http://www.sciencedirect.com/science/article/pii/S2352467716300996` (visited on 10/12/2019).

Morvaj, B. et al. (2016). "Impact of electrical storage and grid upgrade on the optimal design and operation of a microgrid." In: *2016 IEEE Power and Energy Society General Meeting (PESGM)*. 2016 IEEE Power and Energy Society General Meeting (PESGM), pp. 1–5. DOI: `10.1109/PESGM.2016.7741102`.

Moss, R.H. et al. (2010). "The next generation of scenarios for climate change research and assessment." In: *Nature* 463, pp. 747–56. URL: https://www.nature.com/articles/nature08823 (visited on 12/12/2017).

Motion, Green, ed. (2019). *EV Pass: Charge your vehicle easily throughout Switzerland and abroad*. https://www.evpass.ch/. URL: https://www.evpass.ch/ (visited on 07/17/2019).

Nagengast, Bernard (2001). *An Early History Of Comfort Heating*. URL: https://www.achrnews.com/articles/87035-an-early-history-of-comfort-heating (visited on 10/03/2019).

Nakicenovic, N. et al. (2000). *Special Report on Emissions Scenarios*. Tech. rep. Intergovernmental Panel on Climate Change: Cambridge University Press. URL: https://www.ipcc.ch/pdf/special-reports/emissions_scenarios.pdf (visited on 12/04/2017).

Nascimento, Marco Antônio Rosa do et al. (2013). *Micro Gas Turbine Engine: A Review*. Chapter 5: Progress in Gas Turbines. INTECH. DOI: 10.5772/54444. URL: http://www.intechopen.com/books/progress-in-gas-turbine-performance/micro-gas-turbine-engine-a-review (visited on 10/18/2017).

Nossent, Jiri et al. (2011). "Sobol' sensitivity analysis of a complex environmental model." In: *Environmental Modelling & Software* 26.12, pp. 1515–1525. ISSN: 1364-8152. DOI: 10.1016/j.envsoft.2011.08.010. URL: http://www.sciencedirect.com/science/article/pii/S1364815211001939 (visited on 10/23/2019).

O'Connor, Peter A. et al. (2014). "U.S. Energy Transitions 1780–2010." In: *Energies* 7.12, pp. 1–39. URL: https://ideas.repec.org/a/gam/jeners/v7y2014i12p7955-7993d42829.html (visited on 10/03/2019).

OECD (2017). *OECD Environmental Performance Reviews: Switzerland 2017*. Google-Books-ID: V3BADwAAQBAJ. OECD Publishing. 219 pp. ISBN: 978-92-64-27967-4.

Offer, G.J. et al. (2010). "Comparative analysis of battery electric, hydrogen fuel cell and hybrid vehicles in a future sustainable road transport system." In: *Energy Policy* 38 (1), pp. 24–29. DOI: 10.1016/j.enpol.2009.08.040. URL: http://www.sciencedirect.com/science/article/pii/S0301421509006260.

Onat, Nuri Cihat et al. (2014). "Towards Life Cycle Sustainability Assessment of Alternative Passenger Vehicles." In: *Sustainability* 6.12, pp. 9305–9342. DOI: 10.3390/su6129305. URL: https://www.mdpi.com/2071-1050/6/12/9305 (visited on 07/02/2019).

Paish, Oliver (2002). "Small hydro power: technology and current status." In: *Renewable and Sustainable Energy Reviews* 6.6, pp. 537–556. ISSN: 1364-0321. DOI: 10.1016/S1364-0321(02)00006-0. URL: http://www.sciencedirect.com/science/article/pii/S1364032102000060 (visited on 11/29/2016).

Paredes, M. et al. (2017). "Machine learning or discrete choice models for car ownership demand estimation and prediction?" In: *5th IEEE International Conference on Models and Technologies for Intelligent Transportation Systems (MT-ITS)*. 2017 5th IEEE International Conference on Models and Technologies for Intelligent Transportation Systems (MT-ITS), pp. 780–785. DOI: 10.1109/MTITS.2017.8005618.

Parra, David et al. (2017). "An integrated techno-economic and life cycle environmental assessment of power-to-gas systems." In: *Applied Energy* 193, pp. 440–454. ISSN: 0306-2619. DOI: 10.1016/j.apenergy.2017.02.063. URL: http://www.sciencedirect.com/science/article/pii/S0306261917302064 (visited on 06/16/2017).

Pasaoglu, Guzay et al. (2012). "Potential vehicle fleet CO2 reductions and cost implications for various vehicle technology deployment scenarios in Europe." In: *Energy Policy*. Strategic Choices for Renewable Energy Investment 40, pp. 404–421. ISSN: 0301-4215. DOI: 10.1016/j.enpol.2011.10.025. URL: http://www.sciencedirect.com/science/article/pii/S0301421511008093 (visited on 07/02/2019).

Pauchard, Olivier (2019). *Hyundai to test hydrogen-powered trucks in Switzerland*. SWI swissinfo.ch. URL: https://www.swissinfo.ch/eng/business/cutting-pollution_hyundai-to-test-hydrogen-powered-trucks-in-switzerland/44416668 (visited on 10/12/2019).

Pedregosa, F. et al. (2012). *Sckit-learn: Machine Learning in Python*. URL: https://scikit-learn.org/stable/.

Petruschke, Philipp et al. (2014). "A hybrid approach for the efficient synthesis of renewable energy systems." In: *Applied Energy* 135, pp. 625–633. ISSN: 0306-2619. DOI: 10.1016/j.apenergy.2014.03.051. URL: http://www.sciencedirect.com/science/article/pii/S0306261914002827 (visited on 02/22/2017).

Pianosi, Francesca et al. (2016). "Sensitivity analysis of environmental models: A systematic review with practical workflow." In: *Environmental Modelling & Software* 79, pp. 214–232. ISSN: 1364-8152. DOI: 10.1016/j.envsoft.2016.02.008. URL: http://www.sciencedirect.com/science/article/pii/S1364815216300287 (visited on 10/07/2019).

Prognos AG (2013). *Erläuternder Bericht zur Energiestrategie 2050*. Tech. rep. www.energiestrategie2050.ch. Switzerland: Bundesamt für Energie. URL: www.energiestrategie2050.ch (visited on 11/19/2016).

Qadrdan, Meysam et al. (2015). "Role of power-to-gas in an integrated gas and electricity system in Great Britain." In: *International Journal of Hydrogen Energy* 40.17, pp. 5763–5775. ISSN: 0360-3199. DOI: 10.1016/j.ijhydene.2015.03.004. URL: http://www.sciencedirect.com/science/article/pii/S0360319915005418 (visited on 09/10/2019).

Rastler, D. (2010). *Electricity Energy Storage Technology Options: A White Paper Primer on Applications, Costs, and Benefits*. Tech. rep. 1020676. Electric Power Research Institute.

Raubel, M. et al. (2017). *Towards an Energy Efficient and Climate Compatible Future Swiss Transportation System*. URL: https://www.sccer-mobility.ch/.

Reis, Alexandra (2010). *A portfolio of power-trains for Europe: a fact-based analysis: The role of Battery Electric Vehicles, Plug-in Hybrids and Fuel Cell Electric Vehicles*. McKinsey & Company. URL: https://www.fch.europa.eu/sites/default/files/documents/Power_trains_for_Europe.pdf.

Reiter, Gerda et al. (2015). "Global warming potential of hydrogen and methane production from renewable electricity via power-to-gas technology." In: *The International Journal of Life Cycle Assessment* 20.4, pp. 477–489. ISSN: 1614-7502. DOI: 10.1007/s11367-015-0848-0. URL: https://doi.org/10.1007/s11367-015-0848-0 (visited on 10/23/2019).

Remund, J. et al. (2010). "The use of Meteonorm weather generator for climate change studies." In: *10th EMS Annual Meeting, 10th European Conference on Applications of Meteorology (ECAM)*, EMS2010–417. URL: http://adsabs.harvard.edu/abs/2010ems..confE.417R.

Ren, Hongbo et al. (2010). "A MILP model for integrated plan and evaluation of distributed energy systems." In: *Applied Energy* 87.3, pp. 1001–1014. ISSN: 0306-2619. DOI: 10.1016/j.apenergy.2009.09.023. URL: http://www.sciencedirect.com/science/article/pii/S0306261909004152 (visited on 07/24/2018).

Salpakari, Jyri et al. (2016). "Improved flexibility with large-scale variable renewable power in cities through optimal demand side management and power-to-heat conversion." In: *Energy Conversion and Management* 126, pp. 649–661. ISSN: 0196-8904. DOI: 10.1016/j.enconman.

2016.08.041. URL: http://www.sciencedirect.com/science/article/pii/S0196890416307154 (visited on 09/10/2019).

Sanner, Burkhard (2003). "Current status of ground source heat pumps in Europe." In: *Current status of ground source heat pumps in Europe*. Warsaw, Poland: Justus-Liebig-University. URL: http://www.buildingphysics.com/Futurestock%201.pdf (visited on 11/15/2016).

Scarlat, Nicolae et al. (2018). "Biogas: Developments and perspectives in Europe." In: *Renewable Energy* 129, pp. 457–472. ISSN: 0960-1481. DOI: 10.1016/j.renene.2018.03.006. URL: http://www.sciencedirect.com/science/article/pii/S096014811830301X (visited on 10/04/2019).

Schoots, K. et al. (2010). "Technology learning for fuel cells: An assessment of past and potential cost reductions." In: *Energy Policy*. The Role of Trust in Managing Uncertainties in the Transition to a Sustainable Energy Economy, Special Section with Regular Papers 38.6, pp. 2887–2897. ISSN: 0301-4215. DOI: 10.1016/j.enpol.2010.01.022. URL: http://www.sciencedirect.com/science/article/pii/S0301421510000285 (visited on 04/18/2018).

Schweizerischer Ingenieur und Architektenverein (2019). *SIA 380/1: Thermische Energie im Hochbau*. (Visited on 05/20/2019).

Sgobbi, Alessandra et al. (2016). "How far away is hydrogen? Its role in the medium and long-term decarbonisation of the European energy system." In: *International Journal of Hydrogen Energy* 41.1, pp. 19–35. ISSN: 0360-3199. DOI: 10.1016/j.ijhydene.2015.09.004. URL: http://www.sciencedirect.com/science/article/pii/S0360319915301889 (visited on 02/22/2017).

Shafiei, Ehsan et al. (2015). "Comparative analysis of hydrogen, biofuels and electricity transitional pathways to sustainable transport in a renewable-based energy system." In: *Energy* 83, pp. 614–627. ISSN: 0360-5442. DOI: 10.1016/j.energy.2015.02.071. URL: http://www.sciencedirect.com/science/article/pii/S0360544215002261 (visited on 07/02/2019).

Shellenberger, Michael (2018). *If Solar Panels Are So Clean, Why Do They Produce So Much Toxic Waste?* Forbes. URL: https://www.forbes.com/sites/michaelshellenberger/2018/05/23/if-solar-panels-are-so-clean-why-do-they-produce-so-much-toxic-waste/ (visited on 10/12/2019).

Shi, Jun-hai et al. (2008). "Robust design and optimization for autonomous PV-wind hybrid power systems." In: *Journal of Zhejiang*

University-SCIENCE A 9.3, pp. 401–409. ISSN: 1862-1775. DOI: 10.
1631/jzus.A071317. URL: https://doi.org/10.1631/jzus.A071317
(visited on 10/03/2019).

SIA (2011). *SIA 2040: Effizienzpfad Energie*. Zürich. URL: http://www.
sia.ch/de/themen/energie/effizienzpfad-energie/ (visited on
05/20/2019).

Simoes, Sofia et al. (2017). *The JRC-EU-TIMES model - Assessing the
long-term role of the SET Plan Energy technologies*. EUR - Scientific
and Technical Research Reports. Publications Office of the European
Union. DOI: 10.2790/97596. URL: https://ec.europa.eu/jrc/en/
publication/eur-scientific-and-technical-research-reports/
jrc-eu-times-model-assessing-long-term-role-set-plan-
energy-technologies.

Simonis, B. et al. (2017). "Sizing and operating power-to-gas systems
to absorb excess renewable electricity." In: *International Journal of Hy-
drogen Energy* 42.34, pp. 21635–21647. ISSN: 0360-3199. DOI: 10.1016/
j.ijhydene.2017.07.121. URL: http://www.sciencedirect.com/
science/article/pii/S0360319917329506 (visited on 10/23/2019).

Sixth Northwest Power (2010). *Sixth Northwest Conservation and Electric
Power Plan*. Tech. rep. Northwest Power and Conservation Council,
Appendix N: Financial assumptions and discount rate. URL: https://
www.nwcouncil.org/media/6332/SixthPowerPlan_Appendix_N.pdf
(visited on 11/20/2016).

Stadler, Michael et al. (2008). *Distributed Energy Resources On-Site Op-
timization for Commercial Buildings with Electric and Thermal Storage
Technologies*. Tech. rep. Berkeley, CA: Lawerence Berkeley National
Labs. URL: https://building-microgrid.lbl.gov/sites/all/
files/conference-paper-lbnl-293e.pdf (visited on 11/19/2016).

Sternberg, André et al. (2015). "Power-to-What? – Environmental assess-
ment of energy storage systems." In: *Energy & Environmental Science*
8.2, pp. 389–400. DOI: 10.1039/C4EE03051F. URL: https://pubs.rsc.
org/en/content/articlelanding/2015/ee/c4ee03051f (visited on
02/15/2019).

Sterner, Michael et al. (2014). *Energiespeicher - Bedarf, Technologien, Inte-
gration*. Springer Vieweg. ISBN: 978-3-642-37380-0. URL: https://www.
springer.com/de/book/9783642373800 (visited on 10/04/2019).

SwissGrid (2015). *KEV-EIV Vergtüngssätze gültig für neue Bescheide*. URL:
http://www.swissolar.ch/topthemen/kev-und-eiv/.

Swisstopo (2014). *swissBUILDINGS3D 2.0*. Federal Office of Topography. URL: https://shop.swisstopo.admin.ch/en/ (visited on 11/19/2016).

Tan, Kang Miao et al. (2016). "Integration of electric vehicles in smart grid: A review on vehicle to grid technologies and optimization techniques." In: *Renewable and Sustainable Energy Reviews* 53, pp. 720–732. ISSN: 1364-0321. DOI: 10.1016/j.rser.2015.09.012. URL: http://www.sciencedirect.com/science/article/pii/S136403211500982X (visited on 07/11/2019).

Tanguy, Kevin et al. (2016). "Optimization model and economic assessment of collaborative charging using Vehicle-to-Building." In: *Sustainable Cities and Society* 26, pp. 496–506. DOI: 10.1016/j.scs.2016.03.012. URL: http://www.sciencedirect.com/science/article/pii/S2210670716300439.

Thiel, Christian et al. (2014). "Cost and well-to-wheel implications of the vehicle fleet CO2 emission regulation in the European Union." In: *Transportation Research Part A: Policy and Practice* 63, pp. 25–42. ISSN: 0965-8564. DOI: 10.1016/j.tra.2014.02.018. URL: http://www.sciencedirect.com/science/article/pii/S0965856414000494 (visited on 07/23/2019).

Tuchschmid, Matthias et al. (2011). *SBB Ecocalculator: Background Report*. Ed. by SBB.

University of Wisconsin - Madison (1975). *TRNSYS, a Transient Simulation Program*. Ed. by Solar Energy Laboratory.

Vosen, S. R. et al. (1999). "Hybrid energy storage systems for stand-alone electric power systems: optimization of system performance and cost through control strategies." In: *International Journal of Hydrogen Energy* 24.12, pp. 1139–1156. ISSN: 0360-3199. DOI: 10.1016/S0360-3199(98)00175-X. URL: http://www.sciencedirect.com/science/article/pii/S036031999800175X (visited on 11/19/2016).

Vuuren, Detlef P. van et al. (2012). "Scenarios in Global Environmental Assessments: Key characteristics and lessons for future use." In: *Global Environmental Change* 22.4, pp. 884–895. ISSN: 0959-3780. DOI: 10.1016/j.gloenvcha.2012.06.001. URL: http://www.sciencedirect.com/science/article/pii/S0959378012000635 (visited on 12/12/2017).

Wang, Caisheng et al. (2005). "Dynamic models and model validation for PEM fuel cells using electrical circuits." In: *IEEE Transactions on Energy Conversion* 20.2, pp. 442–451. ISSN: 0885-8969. DOI: 10.1109/TEC.2004.842357.

Wang, Danhong et al. (2018). "CESAR: A bottom-up building stock modelling tool for Switzerland to address sustainable energy transformation strategies." In: *Energy and Buildings* 169, pp. 9–26. ISSN: 0378-7788. DOI: 10.1016/j.enbuild.2018.03.020. URL: http://www.sciencedirect.com/science/article/pii/S0378778817337696 (visited on 10/15/2019).

WBF (2015). *Der Website des Preisüberwachers zu den Gaspreisen*. URL: http://gaspreise.preisueberwacher.ch/web/index.asp (visited on 01/04/2018).

Weber, C. et al. (2011). "Optimisation based design of a district energy system for an eco-town in the United Kingdom." In: *Energy* 36.2, pp. 1292–1308. ISSN: 0360-5442. DOI: 10.1016/j.energy.2010.11.014. URL: http://www.sciencedirect.com/science/article/pii/S0360544210006407 (visited on 04/26/2017).

Wernet, G. et al. (2016). "The ecoinvent database version 3: overview and Methodology." In: *The International Journal of Life Cycle Assessment* 21.9, pp. 1218–130.

World Health Organisation (2014). *Indoor air pollution*. WHO. URL: https://www.who.int/features/qa/indoor-air-pollution/en/ (visited on 10/03/2019).

Wu, Zhong et al. (2017). "Application of Monte Carlo filtering method in regional sensitivity analysis of AASHTOWare Pavement ME design." In: *Journal of Traffic and Transportation Engineering (English Edition)*. SI: Advanced Transportation Infrastructure and Materials 4.2, pp. 185–197. ISSN: 2095-7564. DOI: 10.1016/j.jtte.2017.03.006. URL: http://www.sciencedirect.com/science/article/pii/S2095756417300934 (visited on 10/07/2019).

Wyss, Franziska et al. (2013). *Life Cycle Assessment of Electricity Mixes according to the Energy Strategy 2050*. Stadt Zürich, p. 42. URL: http://treeze.ch/fileadmin/user_upload/downloads/Publications/Case_Studies/Energy/472_ElectricityMixesEnergyStrategy2050_v3.0.pdf.

Yang, Hongming et al. (2016). "Optimal operation of DES/CCHP based regional multi-energy prosumer with demand response." In: *Applied Energy* 167, pp. 353–365. ISSN: 0306-2619. DOI: 10.1016/j.apenergy.2015.11.022. URL: http://www.sciencedirect.com/science/article/pii/S0306261915014634 (visited on 07/24/2018).

Yazdanie, Mashael et al. (2017). "Cost optimal urban energy systems planning in the context of national energy policies: A case study for

the city of Basel." In: *Energy Policy* 110.Supplement C, pp. 176–190. ISSN: 0301-4215. DOI: 10.1016/j.enpol.2017.08.009. URL: http://www.sciencedirect.com/science/article/pii/S0301421517305037 (visited on 12/12/2017).

Yilmaz, Hasan Ümitcan et al. (2018). "Analysis of the power-to-heat potential in the European energy system." In: *Energy Strategy Reviews* 20, pp. 6–19. ISSN: 2211-467X. DOI: 10.1016/j.esr.2017.12.009. URL: http://www.sciencedirect.com/science/article/pii/S2211467X17300871 (visited on 08/31/2019).

Zerrahn, Alexander et al. (2018). "On the economics of electrical storage for variable renewable energy sources." In: *European Economic Review* 108, pp. 259–279. ISSN: 0014-2921. DOI: 10.1016/j.euroecorev.2018.07.004. URL: http://www.sciencedirect.com/science/article/pii/S0014292118301107 (visited on 09/10/2019).

Zhang, Xiongwen et al. (2015). "Towards a smart energy network: The roles of fuel/electrolysis cells and technological perspectives." In: *International Journal of Hydrogen Energy* 40.21, pp. 6866–6919. ISSN: 0360-3199. DOI: 10.1016/j.ijhydene.2015.03.133. URL: http://www.sciencedirect.com/science/article/pii/S036031991500779X (visited on 07/02/2019).

Zhang, Yang et al. (2017). "Comparative study of hydrogen storage and battery storage in grid connected photovoltaic system: Storage sizing and rule-based operation." In: *Applied Energy* 201.Supplement C, pp. 397–411. ISSN: 0306-2619. DOI: 10.1016/j.apenergy.2017.03.123. URL: http://www.sciencedirect.com/science/article/pii/S0306261917303690 (visited on 12/12/2017).

Zhang, Yi et al. (2009). *JEPlus – An EnergyPlus simulation manager for parametrics*. Ed. by Energy Simulation Solutions Ltd. (UK). URL: http://www.jeplus.org/wiki/doku.php?id=start.

Zünd, Marianne (2019). *Electricity consumption down by 1.4% in 2018*. Electricity consumption down by 1.4% in 2018. URL: https://www.bfe.admin.ch/bfe/en/home/news-and-media/press-releases/mm-test.msg-id-74726.html (visited on 10/03/2019).

CURRICULUM VITAE

Portia Murray

Address: Schaffhauserstrasse 361, 8050 Zürich

Phone: +41 76 520 50 54

Email: murrayp@ethz.ch

Citizenship: Canada Date of Birth: August 25th 1990 (Vancouver, Canada)

EDUCATION

2016-2020	Doctor of Sciences, ETH Zürich, Switzerland
2013-2014	Master of Applied Sciences, Queen's University, Canada
2008-2013	Bachelor of Mechanical Engineering with Professional Internship (Honours), Queen's University, Canada

EMPLOYMENT

2016-2020	PhD Student/Research assistant, Empa, Switzerland
2014-2016	Research Assistant, Singapore-ETH Centre, Singapore
2012-2013	Research Assistant, Queen's Solar Calorimetry Laboratory, Queen's University, Canada
2011-2012	Component Engineering Intern, Ontario Power Generation, Darlington Nuclear, Bowmansville, Ontario, Canada
2010	Student Intern, Lafarge Inc., Richmond, BC, Canada
2009	Student Intern, Stemcell Technologies, Vancouver, BC, Canada

JOURNAL PUBLICATIONS

- Murray, Portia, Orehounig, Kristina, and Carmeliet, Jan. (2019). "Multi-objective Optimisation of Power-to-Mobility in Decentralised Energy Systems." *Resubmitted to Energy*.

- Murray, Portia, Marquant, Julien, Niffeler, Mathias, Mavromatidis, Georgios, and Orehounig, Kristina. (2020) "Optimal transformation strategies for buildings, neighbourhoods and districts to reach CO_2 emission reduction targets." *Energy and Buildings* 207, DOI: 10.1016/j.enbuild.2019.109569.

- Murray, Portia, Orehounig, Kristina, and Carmeliet, Jan (2019). "Uncertainty and Regional Sensitivity Analysis of Power-to-X Pathways in Multi-Energy Systems." *In Preparation.*

- Mavromatidis, Georgios, Orehounig, Kristina, Bollinger, L. Andrew, Hohmann, Marc, Marquant, Julien, Miglani, Somil, Morvaj, Boran, Murray, Portia, Waibel, Christoph, Wang, Danhong, and Carmeliet, Jan. (2019) "Ten questions concerning modelling of distributed multi-energy systems." *Building and Environment* 165, p. 106372. DOI: 10.1016/j.buildenv.2019.106372.

- Murray, Portia, Orehounig, Kristina, Grosspietsch, David, and Carmeliet, Jan. (2018) "A Comparison of Storage Systems in Neighbourhood Decentralised Energy System Applications from 2015 to 2050." *Applied Energy* 231, pp. 1285-1306. DOI: 10.1016/j.apenergy.2018.08.106.

CONFERENCE PUBLICATIONS

- Murray, Portia, Orehounig, Kristina, and Carmeliet, Jan. (2019). "Optimal Vehicle Selection in the Design of Urban Energy Systems: An Integration of the Private Transport and Building Energy Sectors." Building Simulation, Rome.

- Murray, Portia, Orehounig, Kristina, and Carmeliet, Jan. (2018). "Optimal Design of Multi Energy Systems at Different Degrees of Decentralisation." 10th International Conference on Applied Energy (ICAE 2018). Hong Kong.

- Murray, Portia, Omu, Akomeno, Orehounig, Kristina, and Carmeliet, Jan. "Impact of Renewable Energy Potential on the Feasibility of Power to Hydrogen in Different Municipal Contexts." International Conference on Efficiency, Cost, Optimisation, Simulation, and Environmental Impact of Energy Systems. Guimarães, Portugal, 2018.

- Gabrielli, Paolo, Fürer, Florian, Murray, Portia, Orehounig, Kristina, Carmeliet, Jan, Gazzini, Matteo, Mazzotti (2018). "A Time-series-based approach for robust design of multi-energy systems with energy storage." 28th European Symposium on Computer Aided Process Engineering. Graz, Austria.

- Murray, Portia, Omu, Akomeno, Orehounig, Kristina, and Carmeliet, Jan. (2017). "Power-to-Gas for Decentralised Energy Systems: Development of an Energy Hub Model for Hydrogen Storage." Building Simulation 2017. San Francisco, USA.

- Rysanek, Adam, Murray, Portia, Pantelic, Jovan, Mast, Matthias, Schlueter, Arno. (2015). "Simulation Analysis of a Low Exergy Decentralised Air-Conditioning System for Hot and Humid Climates: Towards a Pilot Implementation in Singapore." Building Simulation 2015. Hyderabad, 2015.

- Murray, Portia, Rysanek, Adam, Pantelic, Jovan, Mast, Matthias, Schlueter, Arno. (2015). "On Decentralised air-conditioning for hot and humid climates: Performance characterisation of a small capacity dedicated outdoor air system with built-in sensible and latent energy recovery wheels." International Building Physics Conference. Torino, 2015.

- Murray, Portia, Harrison, Stephen, Stinson, Ben and Johnson, Gary. (2014). "Experimental Evaluation of a Water Source CO2 Heat Pump Incorporating Novel Gas-Cooler Configuration," in ASME 8th International Conference on Energy Sustainability, Boston.

- Murray, Portia, Harrison, Stephen and Stinson, Ben. (2014). "Passive Gas Cooler Anti-Fouling for Carbon Dioxide Heat Pump Water Heaters," in American Society of Mechanical Engineers International Mechanical Engineering Congress and Exposition, Montreal.

OTHER PUBLICATIONS

- David Grosspietsch et al. (2017). "Multi-Energy-Hubs in Quartieren: Simulation dezentraler Energiesysteme." In: *VSE Energie Bulletin*. URL: https://www.bulletin.ch/de/news-detail/multi-energy-hubs-in-quartieren.html.